ROCK-SLOPE FAILURE IN PARTS OF THE SCOTTISH HIGHLANDS

GRAHAM HOLMES, B.Sc.

Ph.D.

University of Edinburgh

1984

DECLARATION

I certify that, in accordance with Regulation 2.4.15, this thesis is the result of my own work and has been composed by myself.

G. Holmes.

ABSTRACT

The deposits and scars of 432 rock-slope failures (RSFs), affecting over 74 km^2 of the Scottish Highlands, have been mapped from aerial photographs. Some 80% of the RSFs have formed in schists. Most RSFs lie within or close to the limits of the Loch Lomond Advance glaciation. RSFs usually occur midway up a slope often to where the upper surfaces of Advance glaciers reached. A spatial correlation has been established between RSF positions and the upper limits of the Advance.

Despite this correlation the RSFs were not, generally, triggered by glacial oversteepening. Mechanical analyses of 27 slopes prove that most would not have displaced unless some force augmented gravity. High cleft-water pressures, progressive-failure and earthquakes were probably the most important catalysts of slope failure.

A classification of RSFs into plane-sliding, wedge-sliding and toppling modes of failure provides a useful framework for the analysis of the smaller case studies. Large-scale RSFs (up to 112 million m^3), often displaying extensive obsequent-scarps, are an amalgam of various forms of failure and are more difficult to classify and analyse.

Assuming a constant frequency of rock-slope failure in the Scottish Highlands over the last 12,500 years (the generally accepted time of final Scottish ice sheet deglaciation), a rock-slope failure should have occurred on average every 29 years. However, field evidence suggests that a phase of high rock-slope failure incidence accompanied the deglaciation of the Loch Lomond Advance and perhaps other earlier readvances. The case study RSFs are thought to range in age from

greater than 11,000 years to c. 250-300 years old.

A probabilistic model, incorporating factors that are intrinsic and extrinsic to the rock-slope system, is advanced to explain the delayed response of some rock-slopes to deglaciation. An attempt is made to quantify the denudation achieved by RSFs.

CONTENTS

ACKNOWLEDGEMENTS

I am deeply grateful to my supervisor Dr. J.B. Sissons, who conceived of this project and provided much guidance, encouragement and stimulus throughout. Being the last of Brian Sissons' research students it falls to me to wish him and his wife Betty a long and happy retirement together.

The work was made possible by a Natural Environment Research Council Studentship for which I am very thankful.

I remain indebted to various colleagues who critised drafts of chapters. Professor J.N. Hutchinson (Imperial College) kindly commented upon Chapter 8 and I acknowledge early office discussion concerning this project and later valuable field discussion with him. Dr. D.G. Sutherland (Edinburgh) criticised Chapters 4 and 9 and offered much advice and encouragement throughout my stay at Edinburgh. I owe Mr. J.J. Jarvis (Imperial College) particular thanks for his penetrating criticisms of Chapters 6, 7 and 8 and for his field discussion and correspondence on engineering-geology matters.

My brothers, Geoffrey and Stephen, gave excellent field assistance and provided sorely needed company in the field. I apologise for inflicting my cooking on them in return for their toils. Timothy Hague gave excellent help, I would not have reached many of my field sites without his seemingly tireless load carrying.

Finally, I thank Allison for her support, perseverance and practical help over the last three years.

LIST OF SYMBOLS

A = area

B.P. = before present

b = breadth of a body

d = distance

F = factor-of-safety

H,h = height

i = roughness angle

RSF = rock-slope failure

S_i = shear strength intercept

U = water pressure

W = weight

Z_w = depth of water

α (alpha) = slope angle

γ (gamma) = unit weight of rock

γ_w = unit weight of water

ϵ (epsilon) = shear displacement

σ (sigma) = normal stress

τ (tau) = shear stress

θ (theta) = failure-plane angle

ϕ (phi) = angle of internal friction

ϕ_r = residual angle of internal friction

ϕ_u = friction angle of a smooth joint

ϕ' = effective friction angle

Figure 1.1: Rock-slope failure morphology.

1: INTRODUCTION

1.1 Definitions and nomenclature

A rock-slope failure (RSF) is a geomorphic event that results in the downslope and outward displacement of a rock-mass under the influence of gravity (cf. Terzaghi 1950). Ice and water may contribute to failure of the slope, by reducing its strength, but are not directly responsible for the movement of the rock-mass. The displacement may be abrupt but can occur in creep-like movements. To distinguish rock-slope failure from faulting, the plane or zone of movement must not be composed wholly of a fault-plane (Záruba and Mencl 1969).

Rock-slope failures are often referred to as a form of land-sliding. The term "landslide" however is a misnomer as displacement of a rock-mass need not occur by 'sliding' alone (Coates 1977). The definition of rock-slope failure avoids this difficulty and is also advantageous in that it describes the nature of the displaced material. Other terms used to identify RSF features are illustrated in Figure 1.1.

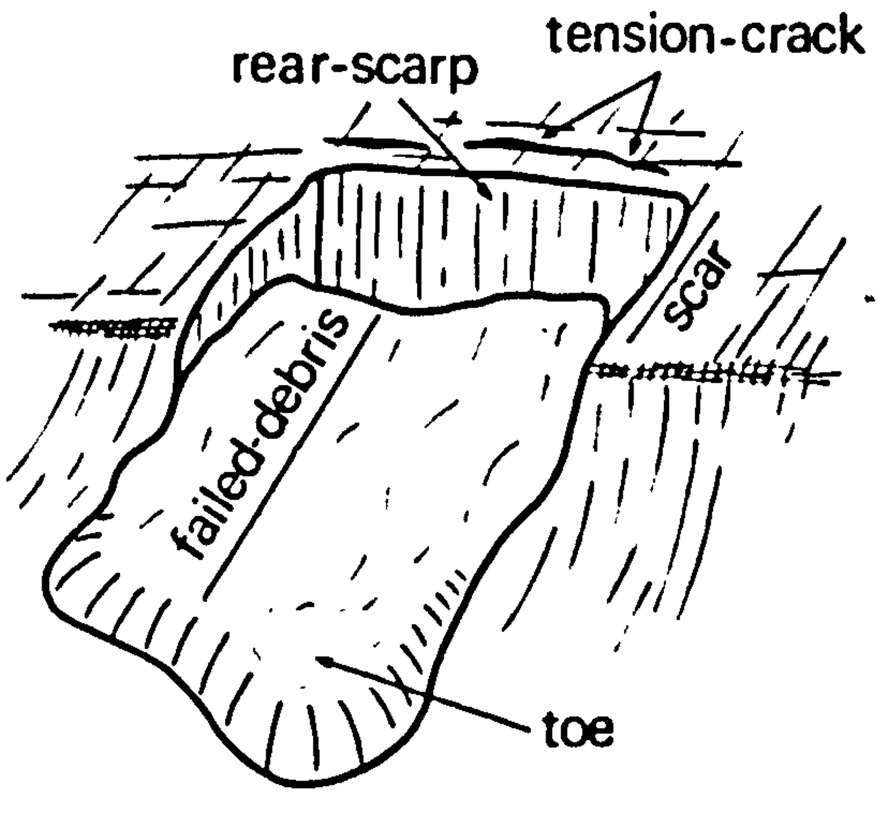

In this study a lower RSF size limit of c. 2,000 m^3 was imposed. This size limit lies within Whalley's (1974) 'cliff-fall' class of RSFs. A 'logical division' (cf. Harvey 1969) is used in this study to classify RSFs according to their mode and degree of displacement.

Figure 1.2: Formulation of the a priori model and hypothesis testing.

1.2 Research strategy

The research project utilises a deductive approach with an explanatory framework composed of five main research themes (Fig. 1.2). An a priori model was formulated from reading of the previous literature and a series of hypotheses followed logically from the model. These hypotheses were tested and organised under five research themes: (i) what is the spatial distribution of RSFs? (ii) what caused the slope failures to occur? (iii) what was their mode of failure? (iv) what is their temporal distribution? and (v) what are

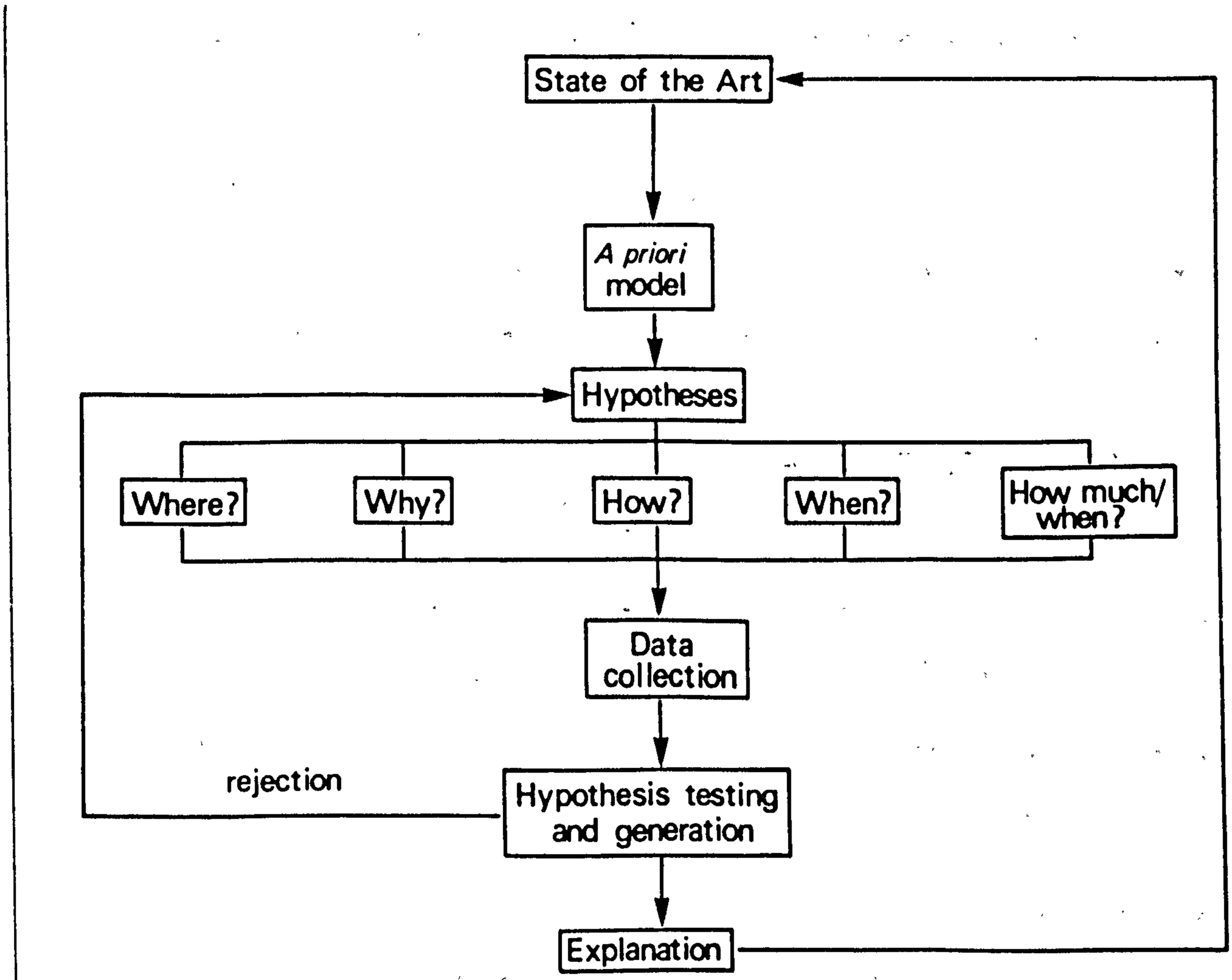

their magnitude frequency relationships? The research themes can be simplified into five questions: where? why? how? when? and how

much/when? These themes are retained throughout the thesis and are used to organise discussion of the research. Working hypotheses were constructed around the research aims and were generated by testing of the a priori model.

Following the formulation of hypotheses the data collection programme was planned. Data were collected at three geographic scales: (i) an inventory of RSFs within the main mountain areas of the Scottish Highlands, (ii) investigation of RSFs within four field areas and (iii) analysis of individual slope failures. The last, also smallest, scale of analysis investigates the basic 'system' within which various mechanical assumptions and geomorphic hypotheses can be tested.

The field-area approach is advantageous in that it minimises the variation in environmental factors such as climate and rock type. This technique was particularly important when attempts were made to date RSFs.

1.3 Organisation of the thesis

The thesis lay-out follows the organisation of the research programme itself, progressing from a review of the literature, compilation of an inventory of RSFs, field work and, finally, development of a rock-slope failure model for the Scottish Highlands.

The philosophy of the thesis, that an understanding of rock mechanics is a pre-requisite to investigation of RSF processes, is central to the discussion in Chapter 2. Given, as recently stated by Pitty (1982; p. 6), that rock mechanics is: "a fundamental

geomorphological property", Chapter 2 discusses rock-mass characteristics and the variations in the strengths of natural joints. An engineering-geology classification of modes of rock-slope failure is also presented in this chapter. The classification provides a framework for later analyses of slope failure process and form and is the basis of the logical division of RSF types.

A review of previous research into rock-slope failure in Scotland is provided in Chapter 3. Discussion of the literature is organised by the contributions made to each of the five research themes. The Scottish Lateglacial sequence is also summarised in Chapter 3 in preparation for later reference to the chronology of slope-failure. The a priori model of RSF is outlined in discussion of the previous literature and those research areas that demand attention are highlighted.

Chapter 4 discusses the RSF inventory which was compiled during the winters of 1981 and 1982. It examines the controls on the spatial distribution of RSFs, raising hypotheses that are tested later by detailed investigations of individual slopes. The RSF distribution data are listed in Appendix B of this thesis.

The criteria used in field area selection are given in Chapter 5, which also briefly introduces the physical background to the four field areas. The field techniques utilised to quantify rock-mass characteristics and determine the morphologies of RSFs are detailed in the second half of Chapter 5.

The core of the research work is presented in Chapters 6 to 9. These chapters are the product of field work undertaken over the

summers of 1982 and 1983. Chapters 6, 7 and 8 concern the modes and mechanisms of failure of 26 rock-slopes. These three chapters combine description of individual slope morphology with mechanical and geological interpretation of failure modes and processes.

The case studies are classified according to their mode of failure, following the engineering-geology scheme outlined in Chapter 2. The controls on failure at the individual level are examined using rock mechanics techniques. Ten examples, discussed in Chapter 6, exhibit simple sliding modes of failure. The ten examples examined in Chapter 7 are more complex, involving some component of forward rotation of layers (or toppling).

Much debate has centred upon the origin of extensive obsequent- (or uphill-facing) scarps on rock-slopes in high-mountain terrain. Extensive obsequent-scarps were observed during the aerial-photograph reconnaissance of Scottish RSFs. Subsequently, four large slope failures (some of which are massive even by world standards) which possess obsequent-scarps, were examined in the field and are discussed in Chapter 8. To do justice to the considerable literature on obsequent-scarp development, particularly that from N America, separate discussion is required of large-scale slope failures. Chapter 8 also examines evidence for a form of slope failure previously unrecognised in Britain, the so-called "sackung" or sagging of rock-slopes.

A major geomorphological problem is that of estimating the relative importance of high-magnitude RSFs in the denudation of mountain environments. It is therefore necessary to date RSFs to

establish their frequency. Chapter 9 examines the relative chronology of rock-slope failure in the four field areas as a precursor to discussion of the magnitude/frequency relationships. Rock-slope failure age data are organised by field area.

This thesis attends to different, but related, research themes at various scales of analysis. The concluding chapter attempts to provide a synthesis of these themes. It also gives an overview of the case studies and comments upon the magnitude-frequency relationships of RSFs in the field areas. The case study data are extrapolated to the inventory level and a speculative rock-slope failure model is detailed.

2: ROCK-MASS CHARACTERISTICS AND ROCK-SLOPE STABILITY

2.1 Introduction

The internal properties of a rock-slope may be conceptualized as intrinsic thresholds that must be exceeded to cause a geomorphic response. This threshold concept helps to explain why a widespread change in the environment may not produce an equally-distributed effect (Brunsden and Thornes 1979). Portions of a valley slope may fail, rather than the whole slope, because of inherent structural weaknesses and, therefore, lower intrinsic threshold values.

This chapter emphasises the internal properties of rock-slopes rather than the external processes that act upon them and is designed to illustrate the potential of an engineering-geology approach to rock-slope failure and to introduce fundamental properties of rock-masses.

Rock-masses are rendered discontinuous by faults, foliation planes, joints and other forms of geologic discontinuity, collectively termed 'joints' here regardless of their origin. Joints generally have much lower strengths than intact rock and cause rock-masses to be mechanically discontinuous. Foliation planes for instance, make schists, slates and other metamorphic rocks, highly directional (or anisotropic) in their mechanical properties (Goodman 1981).

The origins of geologic discontinuities are briefly discussed in Section 2.2 followed by an illustration of the stereonet method of summarising joint attitude data. Rock joint shear characteristics are reviewed in Section 2.4, where important concepts in rock mechanics

are also introduced. A variety of techniques have been used by engineering-geologists to determine rock-slope stability. Two techniques: limit-equilibrium modelling and kinematic testing are critically examined in Section 2.6. The theoretical implications of rock-mass shear behaviour are appraised in the Discussion, with particular reference to pre-failure displacements of rock-slopes.

2.2 Geologic discontinuities

Discontinuity orientations within a slope are a product of (i) the regional tectonic history, (ii) thermal stresses, and (iii) stress-relief processes (Chapman 1958). As an example of the first set of processes, the metamorphism of Pre-Cambrian sediments in the Scottish Highlands has formed foliation planes (a strong alignment of minerals within metamorphosed rock, reflecting the former presence of bedding planes) in the Moine rocks. The tectonic history of the Highlands with its associated folding, thrusting and faulting, has imposed complex jointing/foliation patterns on rock-slopes (Watters 1972).

Joints are thought to open by the interconnection of microscopic flaws or Griffith cracks in the rock-mass (Price 1966). Stresses tend to be high at the poles of the microscopic flaws and crack interconnection is caused by brittle failure of the material between the flaws. The nature of crack propagation is dependent upon the stresses acting on the rock-mass. In tension, crack lengthening will occur normal to the tensile stress. In compression, cracks tend to orientate themselves with the direction of principle stress, though crack propagation under compression is more complex than under

tension.

Stored elastic, energy inherited from the large loads imposed during earlier geological periods have been found to occur in many areas of the world (Brown and Hoek 1978). Relaxation of these horizontal stresses (stress-relief), activated by valley-deepening, may result in the formation of joints which trend parallel to the land surface. Price (1966) referred to such joints as "sheeting" or "mural" joints and Bjerrum and Jørstad (1968) termed them "valley joints". Since they are not confined to valleys the term 'stress-relief joint' is preferred here.

Several stress-relief joint sets may exist at varying depths within a rock-slope, the shallowest set, according to Bjerrum and Jørstad, usually occurs between 4 and 10-m-depth, normal to the slope face. They also stated that the distances between stress-relief joints increases with depth. Bjerrum and Jørstad inferred a connection between reductions in load, due to rock-slope failure in some instances (e.g. the Leon Slide, Norway), with the development of stress-relief joints.

2.3 Presentation of joint data

Discontinuity attitude data are usually plotted on lower-hemisphere equal-area stereonets (Goodman 1976, 1981 Hoek and Bray 1977) which provide a useful solution to the presentation of large volumes of joint survey data. Stereonets may also be utilised for graphical solutions of slope stability using kinematic analyses (p 20). As few geomorphological texts deal with stereonets, some

Figure 2.1: A lower-hemisphere stereonet projection of a joint pole and its great circle.

explanation of their use is considered appropriate.

Figure 2.1 shows the construction of a joint pole and its great circle on a stereonet. Their locations on the stereonet are a function of the dip angle and dip direction of the joint. Great circles on equatorial stereonets are equivalent to the lines of longitude on a map of the world. Small circles define the lines of latitude and calibrate the stereonet projection into 2° intervals.

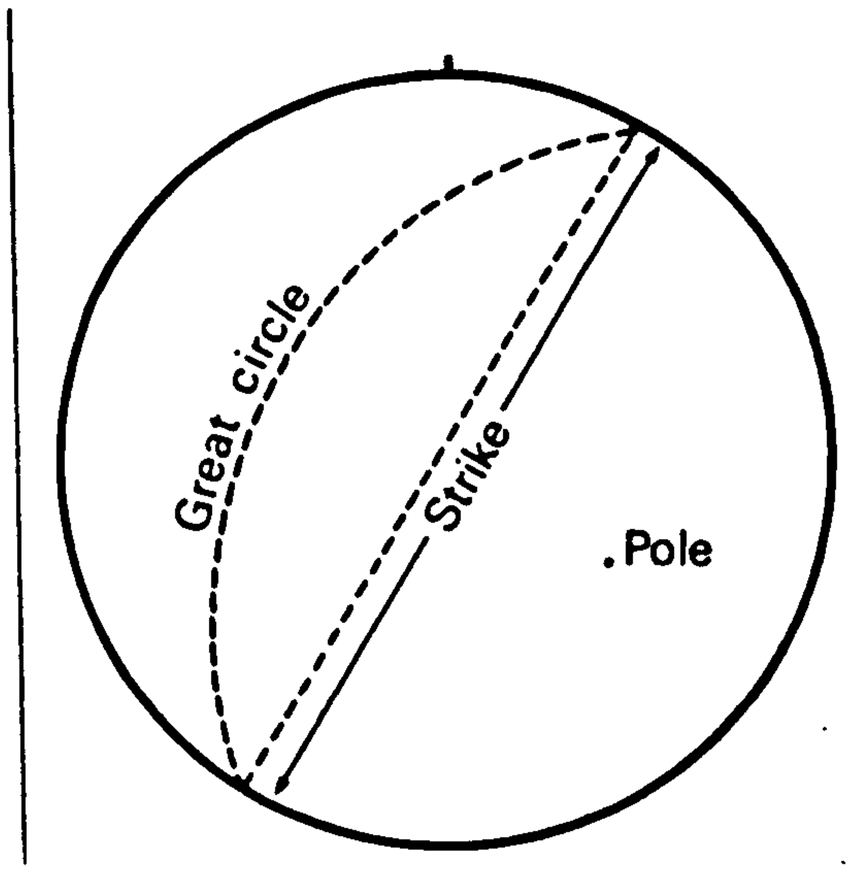

A joint pole can be plotted on a tracing by: (i) marking the dip direction (azimuth) of the joint on the circumference of the stereonet, ensuring that the N-points on the tracing and the stereonet are superimposed, (ii) rotating the tracing, keeping its centre-point over that of the stereonet, until the marked point lies above one of the stereonet axes (0, 90, 180 or 270°) and (iii) counting out the joint dip angle (along the stereonet small circles) from the stereonet centre in the direction opposite to the marked azimuth. The great circle of a joint lies 90° from the joint pole (Fig. 2.1) and will touch the stereonet circumference at two points, 180° apart. A line connecting the two points defines the strike of the joint plane. If two great circles (representing the attitudes of two joints) intersect on a stereonet, the point of intersection gives the azimuth and dip angle of the line of intersection of the joints.

All stereonets and joint attitude data in this study are related

Figure 2.2: The relationship between shear stress and normal stress for a smooth joint surface.

to true north and individual joints/joint sets are referred to by the convention of dip angle → azimuth (the joint in Figure 2.1 for example trends 45° → 300°). In discussion of joint data the terms 'positive' and 'negative' are used to indicate joints which dip valleywards and into a rock-slope respectively.

2.4 Rock mass shear characteristics

The graph below (Fig. 2.2) is typical of the results obtained when two blocks of rock are forced to slide along a common smooth joint or other discontinuity surface. Shear stress (τ) increases linearly with increasing normal stress (σ). The slope of the line determines the angle of friction (ϕ) of the joint, its cohesive strength (c) is given by the intercept with the Y-axis. Shear and normal stresses are therefore related in the following way:

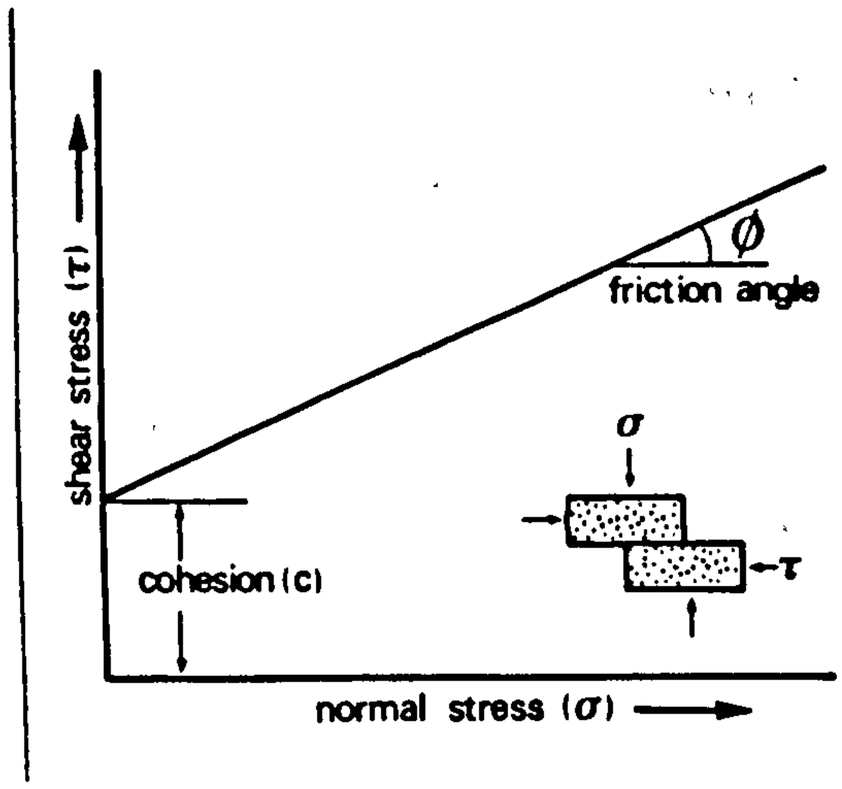

$$\tau = c + \sigma \, \mathrm{Tan}\phi \qquad 2.1$$

This is the Mohr-Coloumbe criterion. The cohesive strength (c) of unfilled smooth rock joints is generally assumed to be zero. Friction angles vary between rock types though Goodman (1981) has stated that most ϕ values lie between 21 and 40°.

The normal stress acting upon a joint may be reduced to the <u>effective stress</u> (σ-u) by water pressure (u). If water pressures are present then Equation 2.1 is modified to:

Figure 2.3: The effect of roughness on the shear behaviour of an idealised rough joint plane.

$$\tau = c + (\sigma - u)\ \mathrm{Tan}\phi \qquad 2.2$$

Unlike clays, the friction angles of hard rocks are not significantly altered by the presence of water. Any reduction in the shear strength of hard rocks, caused by the presence of water, is due almost entirely to the lowering of normal stress.

If the joint surface is rough the resulting shear strength curve will deviate from the linear relationship of Equation 2.1 (Patton 1966) as extra work is required to shear a rough joint surface. This concept is easily demonstrated. Assuming that: i equals the deviation of an asperity from the mean direction of shear along a joint plane, the friction angle of smooth joints in the same material equals ϕ_u and the joint surface has zero cohesion, at the instant of peak shear stress, the resultant (R) will be orientated at an angle of $90° + \phi_u$ from the joint surface on which displacement is about to occur (Fig. 2.3). As the asperity surface is inclined at an angle i from the mean direction of shear, the joint friction angle is given by: $\phi_u + i$. Goodman (1981) stated that the roughness angle i can be between 0 and 40°, or higher, at low normal stresses. Barton (1973) collated data showing that at normal stresses of between 1.47 and 3.43 kPa (kilopascals), i values for granite ranged between 40 and 50°. Selby (1982) suggested however that values for i of between 3 and 5° are typical for rock-slope exposures.

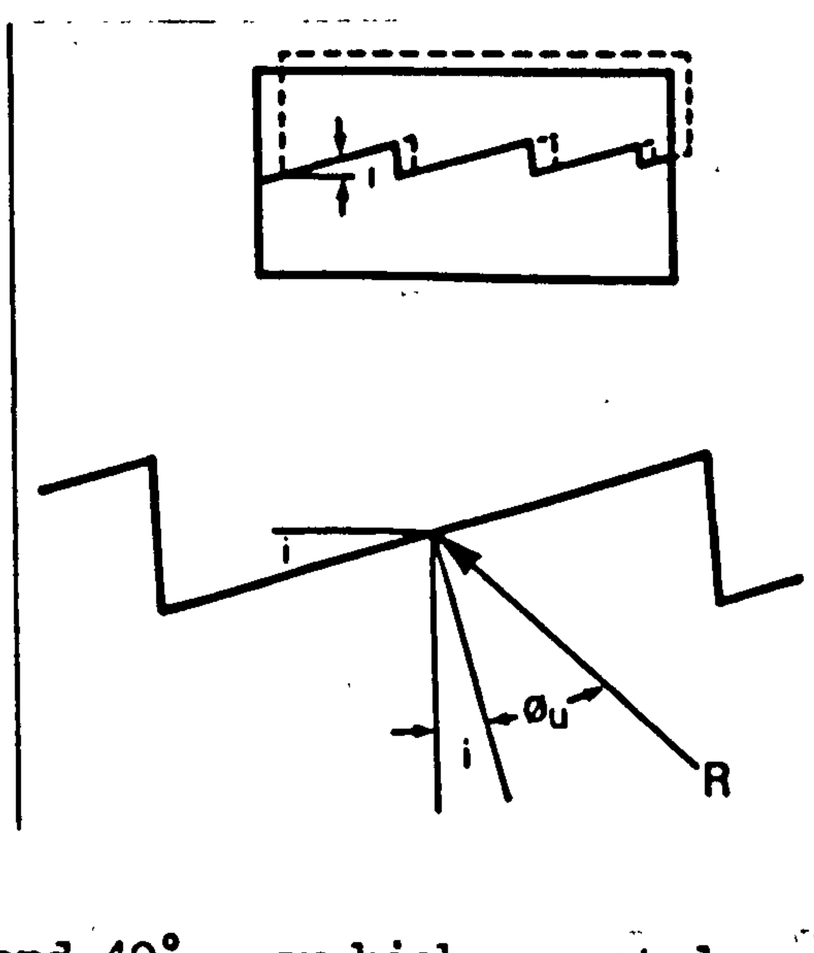

Figure 2.4: Shear strength/shear displacement curves for a hypothetical rough (A) and a smoother joint plane (B).

Figure 2.5: Shear strength/normal stress curve for a hypothetical rough joint. Note the stress dependence of the parameter S_i.

The friction angle of a joint is also sensitive to the degree of displacement it has suffered. Figure 2.4 shows the shear strength/shear displacement curve (A) of a theoretical rough joint, sheared at constant normal stress. With increasing shear displacement (ϵ) the shear strength (r) of the joint increases from zero to a peak corresponding to the instant of failure of the joint. Continued displacement beyond the peak in shear strength will reduce the strength to a residual level, as asperities are crushed. This form of shear behaviour is termed unstable and contrasts with the material exhibiting a stable strength/displacement curve (B in Fig. 2.4). The displacement along a joint surface required to mobilise peak shear strength determines the shear-stiffness of the joint. Failure of the joint or failure-surface in this study is assumed to have begun once shear displacement along the surface has occurred, this differs from the mechanical interpretation of failure of a material.

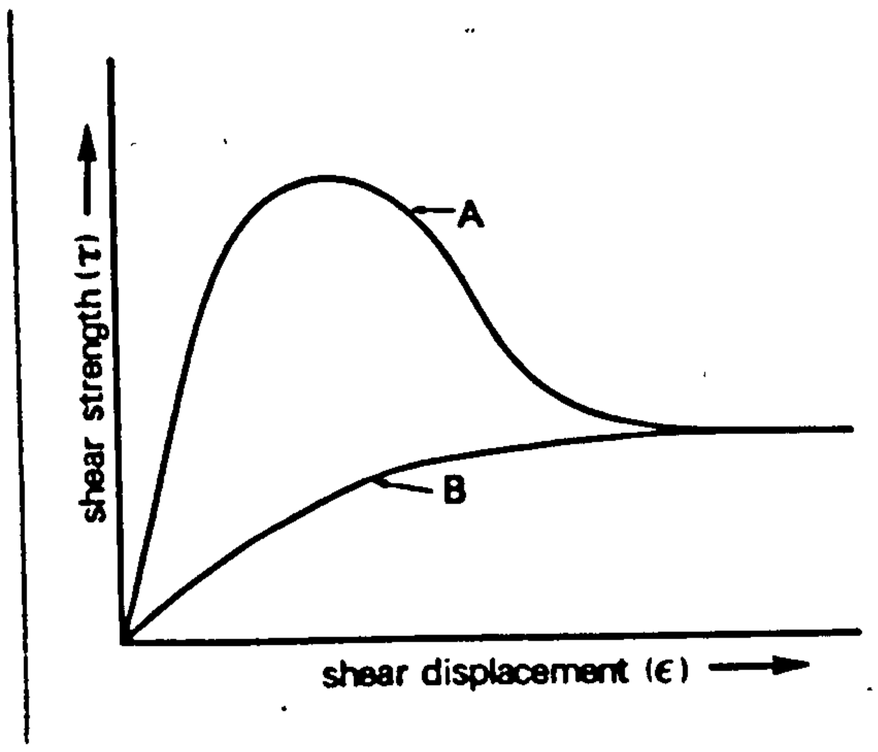

At high levels of normal stress, the work required to override asperities will exceed that required to shear through them, i will therefore tend towards zero with increasing normal stress. If the normal stresses acting on a joint are sufficiently high to cause failure through asperities, then a

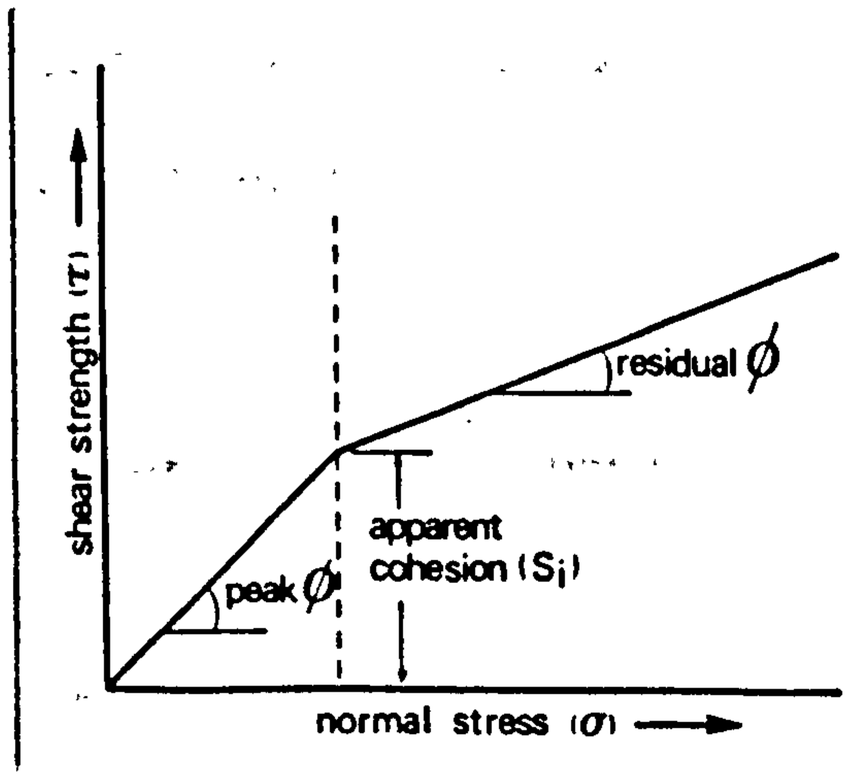

shear strength intercept (S_i) will be generated with a lower friction angle: due to crushing of asperities during shear (Fig. 2.5). Hence, convex upwards shear strength curves characterise the shear behaviour of rough joint surfaces (Patton 1966, Jaeger 1971).

In a series of shear tests made on rough-joint model material with zero cohesion, Barton (1971a) found that peak shear strength was mobilised after displacements of c.1% of the total joint length. A large increase in strength may therefore occur after relatively minute shear displacement along a rough joint (cf. Fig. 2.2). This may appear as a shear strength intercept, though in fact the strength at zero normal stress is itself zero. Barton and Choubey (1977) observed that the amount of shear displacement required to reach peak shear strength increases almost proportionally with joint length. Smoother joints were however found to require relatively greater shear displacement to reach peak shear strength than rough joints. Barton and Chaubey stated that the shear strength of a joint is both stress-dependent and scale-dependent.

In support of the scale-dependence of joint strength, Patton (1966) showed that the longer the length of joint considered the less steep the major asperities. Shear-stiffness may therefore be reduced, pre-failure displacements increased, as peak strength may not be reached until major and flatter asperities are in contact.

Riding up and over asperities by the upper block may occur during a shear test if the normal stress (σ) is low (cf. Fig. 2.3). This will cause dilation of the joint due to upward displacement of the upper block (Patton 1966, Bray 1967, Ladanyi and Archamboult 1969,

Figure 2.6: Forces acting on a block resting on an inclined plane.

Barton 1971a, Goodman and Dubois 1972). Monitoring of the vertical displacement (d) during shear permits investigation of the relationship between shear and dilation. Ladanyi and Archamboult (1969) found that the dilation rate ($\Delta d/\Delta \epsilon$) of sheared model joint surfaces is highest when peak shear strength is mobilised. They also found that beyond peak strength the dilation rate decreased. Joint roughness and normal stress therefore control both the shape of the shear strength/shear deformation curve and the rate and amount of dilation. The possible influences of dilation and shear-stiffness at the rock-slope scale will be returned to later.

2.5 Rock-slope stability

Figure 2.6. illustrates the forces acting upon a block resting upon a plane inclined at an angle Θ. Gravity is the only force acting upon the block so its weight (W) acts vertically downwards. A resolved part of W (W SinΘ) however acts parallel to the plane and attempts to cause sliding of the block. This force is opposed by a component of W (W CosΘ), acting normal to the plane, which seeks to stabilise the block. The normal

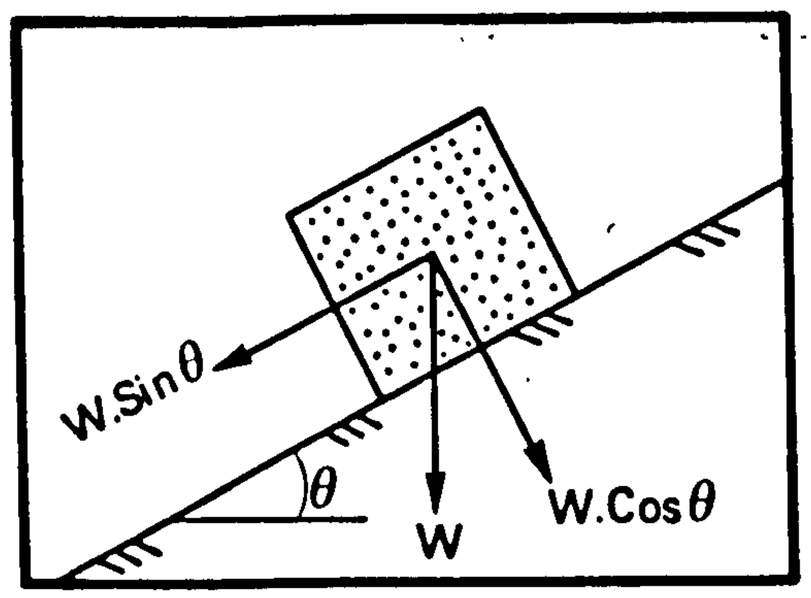

stress acting at any point along the plane is given by:

$$\sigma = (W \text{ Cos}\Theta) / A \qquad 2.3$$

where: A = the base area of the block.

If the Mohr-Coloumbe criterion is applicable to this problem,

then the shear force resisting sliding equals:

$$cA + W \cos\theta \cdot \tan\phi \qquad 2.4$$

Should the plane be tilted, then the block will slide when:

$$W \sin\theta = cA + W \cos\theta \cdot \tan\phi \qquad 2.5$$

If the cohesive force acting on the base of the block is zero, then sliding will occur when $\phi = \theta$.

Water pressures are now generally recognised by engineering-geologists as a major cause of rock-slope instability (e.g. Barton 1971a). Terzaghi (1962), like Muller (1964), considered that rock permeability is of prime importance in the stability of a rock-slope. Terzaghi distinguished between 'primary permeability' of rock (water within the voids of intact rock located between rock fissures) and 'secondary permeability' (the flow of water in open and discontinuous cracks: termed 'cleft-water' in this study). He considered that secondary permeability was the most significant destabilising process in rock-slopes.

Jaeger (1979) observed that primary permeability may be important for certain rock types. He cited the example of 50-70% reductions in the Young's modulus of elasticity of phyllite when soaked in water over a period of 3 days. Young's modulus (E) is defined as normal stress divided by normal strain: normal strain equals the amount of axial shortening of a rock sample, relative to its original length, when normal stress is applied to it.

Secondary permeability will reduce slope stability in two ways

Figure 2.7: Forces acting on a block resting on an inclined plane assuming cleft-water pressures.

(Terzaghi 1962, Muller 1964, Bjerrum and Jørstad 1968). First, by exerting an outward pressure on a potentially unstable block. According to Bjerrum and Jørstad, this pressure may be so large as to constitute a greater contribution to the shearing stresses than the weight of the block itself. The second effect is to counteract the normal stresses acting upon a potential failure-surface, thereby decreasing the shear strength of the surface (cf. Equation 2.2).

These concepts are most easily demonstrated by adapting the example of the block resting on an inclined plane. If the block is now assumed to be separated from other blocks by a tension-crack filled with water, an additional set of forces must be considered (Fig. 2.7). Cleft-water pressure within the tension-crack will increase linearly with depth. A total force V will act upon the rear of the block, adding to force (W Sinθ). If the tension-crack reaches to the inclined plane, allowing water to seep under the block to exit (at atmospheric pressure) at its outlet, then an uplift force U will reduce the normal stress. The condition for block-sliding in this case becomes:

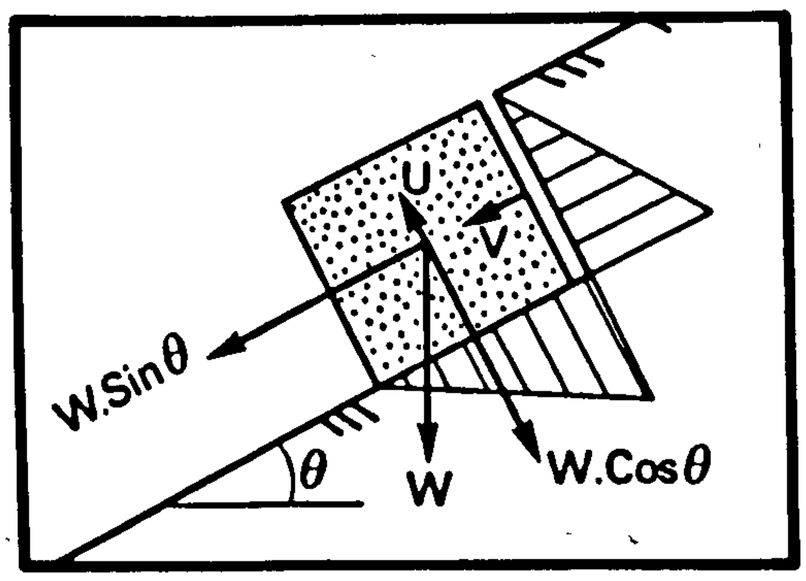

$$W \sin\theta + V = cA + (W \cos\theta - U) \tan\phi \qquad 2.6$$

The form of cleft-water pressure distribution described above is termed 'triangular'. A greater destabilising effect could be achieved by a 'static' cleft-water distribution which may be caused by complete impedence of drainage from a potential failure-plane. A static

Figure 2.8: Failure modes in rock (after Hoek and Bray 1976):

(a) plane-sliding

(b) wedge-sliding

(c) toppling

(d) circular

cleft-water pressure distribution could be induced by freezing of the outer layers of a rock-slope (Hoek and Bray 1977).

2.6 Classification and analyses of rock-slope failure

Modes of rock-slope failure have been classified in the engineering-geology literature according to the shape and attitude of displaced blocks, and their mode of deformation. Three rock-slope failure modes are most common (Varnes 1958, Hoek and Bray 1977):

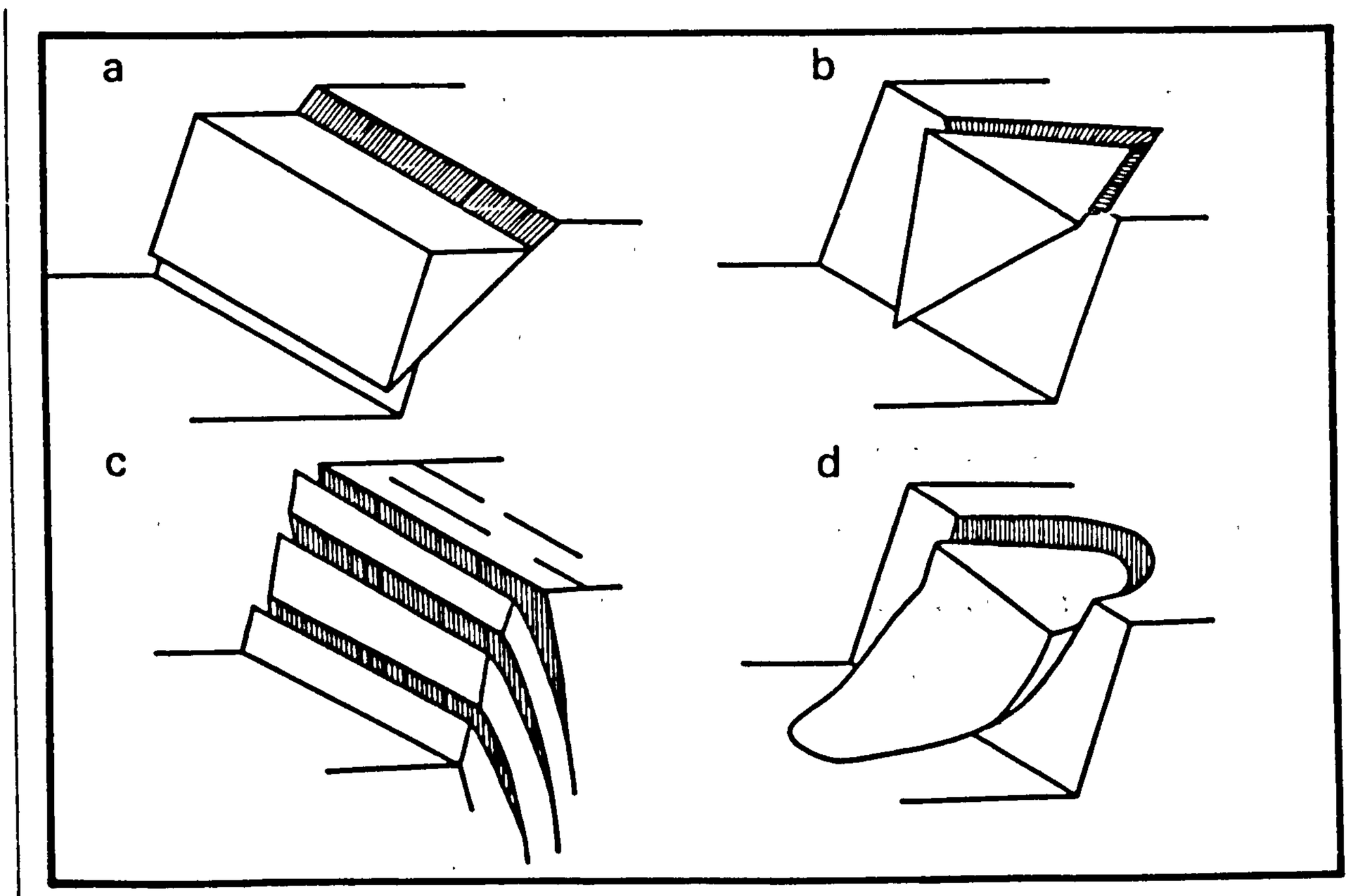

plane-sliding, wedge-sliding and toppling failure (Fig. 2.8). Circular failure, a common failure-mode in soils, may occur on rock-slopes with very closely-spaced joints, according to Hoek and Bray (1977). Addison (1981) however considered that circular failure of a rock-slope would be unlikely. The three-fold classification of failure modes has been successfully applied to many rock-slope

failures and will be used in this study. As natural rock-slopes often feature several joint patterns (Hoek and Bray 1977), the possibility of more complex modes of failure is increased. It is therefore unlikely that the three failure modes discussed above are exclusive of one another.

From earlier discussion it is clear that the block illustrated in Figure 2.7 will slide when the total force available to resist sliding is equalled by the total force seeking to induce it. The ratio of the two sets of forces, a measure of slope stability, is termed the factor-of-safety (F). The factor-of-safety of the block in Figure 2.7 is given by:

$$F = \frac{cA + (W\,\mathrm{Cos}\theta - U)\,\mathrm{Tan}\phi}{W\,\mathrm{Sin}\theta + V} \qquad 2.7$$

Two forms of analysis are generally used by engineering-geologists, and lately geomorphologists, to determine the stability of a slope: (i) limit-equilibrium models and (ii) kinematic tests. The assumptions which they make and their application are discussed below.

Limit-equilibrium models

Equation 2.7 is an example of a limit-equilibrium model, though modifications are required to model the geometry of more complex block shapes and different forms of cleft-water pressure distribution. Limit-equilibrium models may be used to back-analyse RSF case studies and estimate the disturbing and resisting forces acting on a failure-surface at the instant of failure. Such post-mortem studies have the advantage of being, in effect, large-scale shear tests and have

assisted slope-engineers in the design of slopes (e.g. Barton 1971b). Limit-equilibrium models have also been used by geomorphologists to infer formerly high piezometric levels, particularly in surficial deposits (e.g. Richards and Anderson 1978).

Limit-equilibrium models are available for plane-sliding, wedge-sliding and toppling modes of failure (e.g. Goodman and Bray 1976, Hoek and Bray 1977). The Goodman and Bray (1976) limit-equilibrium model for toppling is only applicable to slopes with very simple geometries (the model assumes toppling of retangular blocks on a stepped-base) and is not used in this study. Detailed descriptions of the limit-equilibrium models used for plane and wedge-sliding are given in Appendix A.

Slope stability analyses are only used in this study for small-scale slope failures, as accurate definition of the geometry of massive RSFs cannot be made. The application of back-analyses to large-scale RSFs raises the danger of using questionable assumptions and data to compute a calibrated (but erroneous) result (Tavenas et al. 1980).

Kinematic tests

Kinematics is the study of the motion of bodies without reference to the forces that move them. Kinematic tests may be used to assess whether a particular failure mode is feasible given the slope face orientation and the attitudes of discontinuities. This form of analysis is advantageous in that inputs can be varied easily and solutions made quickly. The main data required for kinematic testing

Figure 2.9: (a) Kinematic test for plane-sliding

(b) Kinematic test for wedge-sliding

are the attitudes of the slope face/discontinuities and the friction angle for the rock. The assumptions and use of kinematic tests for plane-sliding, wedge-sliding and toppling failure are discussed below.

Plane-sliding is possible when the great circle of a potential failure-surface falls inside the shaded area in Figure 2.9a. This is the graphical equivalent of: the slope angle being steeper than the failure-surface which is, in turn, steeper than the friction angle.

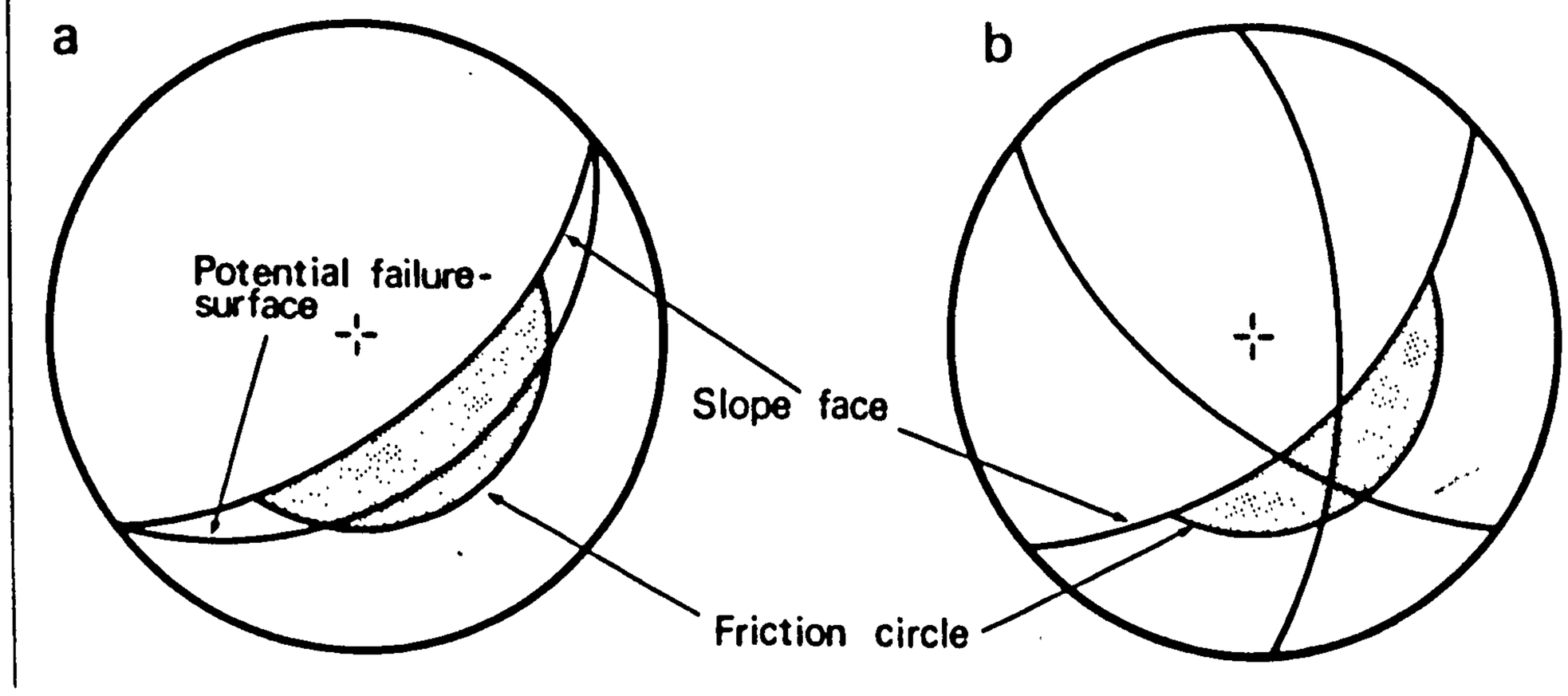

Similarly, wedge-sliding is possible when the intersection of two great circles (representing potential failure-surfaces) falls within the shaded region of Figure 2.9b. It should be noted however that if a potential failure-plane crops out into the slope face, failure is kinematically possible even if the plane is inclined less than the friction angle (cf. Equation 2.7). The effects of cohesion are not directly modelled in the kinematic tests.

Ashby (1971) developed a simple criterion for toppling of a single slab resting on an inclined plane. He demonstrated that toppling will occur when: $\tan \theta > b/H$ (where: θ = the inclination of the surface upon which the block rests, b = the width of the block and H its height). More simply, toppling will occur when a perpendicular

Figure 2.10: (a) Section through a potential topple

(b) Kinematic criterion for toppling

from a block centroid falls outside its base (Ashby 1971). Ashby's criterion for toppling is not always suitable for the analysis of field examples however as it takes no account of the slope-face angle and assumes that blocks are rectangular-shaped. Complex joint configurations often produce trapezoidal-shaped blocks (cf. Brown 1982), imposing a major constraint upon the practical use of Ashby's criterion.

Goodman and Bray (1976) have provided a kinematic test for toppling that utilises the interlayer slip between blocks before large deformations occur and imposes no restriction on block shape. If the discontinuities shown in Figure 2.10a have an angle of friction ϕ then Goodman and Bray have shown that the condition for interlayer slip is:

$$\theta > \phi + \alpha \text{ and } \alpha > \phi$$

in

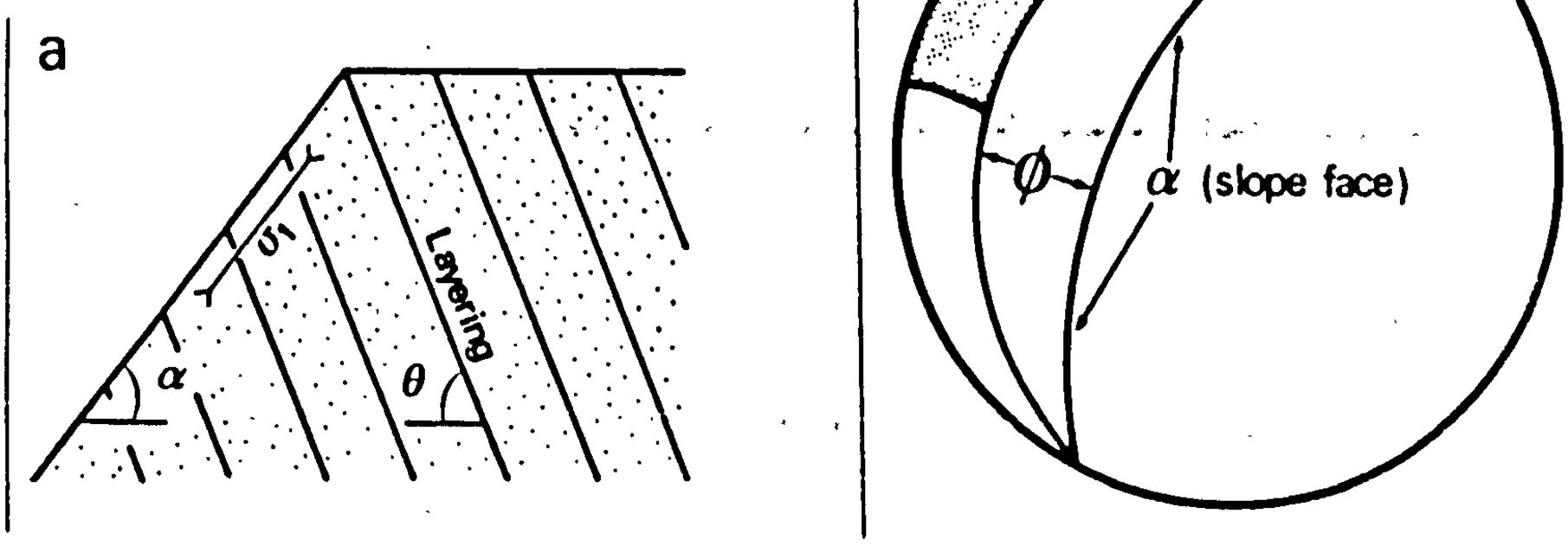

The kinematic test is shown on the stereonet in Figure 2.10b.

The Goodman and Bray criterion for toppling requires that the slope angle is greater than the friction angle of the layers. However, it takes no care of the weight of upslope blocks resting upon the layers, possible cleft-water pressures or cohesive forces. It is

important to note that the value for the slope angle input to the criterion must be the steepest angle encountered upon the slope.

2.7 Discussion

There are a number of problems associated with limit-equilibrium analyses that result from the assumed simplicity of the mechanical models against the relative complexity of the geological-geomorphological environment (Chowdury 1978, Tavenas et al. 1980, Selby 1982). For instance, the damage sustained by shearing along rough joint surfaces indicates that joint-wall contact area may be between 0.1 and 0.001 of the total area (Barton and Choubey 1977). The importance of this finding is that normal stress may be concentrated at asperities whereas conventional analyses assume that normal stress is evenly-distributed across the length of a failure-plane.

A further problem relates to the assumptions made concerning the distribution of stress. Soil mechanics investigations have shown that if the peak strength of a clay is exceeded at any point along a potential failure-surface, failure will occur at that point. Stress will then be transmitted to other points, which may result in failure at these remaining points. Shear strength will consequently be reduced to the residual value (Skempton 1964): a process termed progressive-failure.

A similar process occurs in jointed rocks (Terzaghi 1962, Bjerrum and Jørstad 1968, Barton 1971b). Terzaghi (1962) stated that bridges of intact rock between joints may be sheared through due to the high

levels of stress concentrated at these points. The shear strength intercept for a given level of normal stress will therefore be reduced. The degree of progressive-failure may therefore be expressed as the ratio between intact rock bridges and sheared ones along a potential failure-plane.

A further difficulty is that of evaluating $\emptyset$ and the shear strength intercept. This problem would be compounded by inadequate knowledge of the cleft water-pressure distribution (or other disturbing force) acting at the time of failure. Post-failure solution of Equation 2.7 can be made with varying assumptions (sensitivity analyses) providing a range of strength values. This technique recognises that selection of a single strength value would be subjective.

The assumption of a failure 'surface' (i.e. the limit that terminates a solid) made by limit-equilibrium analyses and kinematic tests has been questioned (Chowdhury 1978). A massive RSF would be unlikely to possess a continuous failure-surface because of the limited persistence of joint surfaces: rather shear displacements may occur along a 'zone' of failure. Eisbacher (1979a) hypothesised that RSFs occurs along zones of failure up to several tens of metres thick in the Mackenzie Mountains, Canada.

Geomorphological research into rock-slope failure has tended to emphasise the slope conditions immediately prior to failure and the post-failure transport of the failed-debris. Rock-slope stability before failure is to a large extent determined by the shear displacement history of the slope. From earlier discussion of rock-

mass characteristics and progressive-failure it is clear that a slope could, theoretically, have undergone numerous phases of limited shear displacement prior to failure. Terzaghi (1950) was of the opinion that all landslides are preceeded by ground movements and Hutchinson (1968) termed these movements 'progressive-creep'.

Progressive-creep of rock-slopes is well documented (Muller 1968, Radbruch-Hall 1978, Voight and Kennedy 1978). Pre-failure displacements of the catastrophic Vajont rockslide, Italy, for instance, reached velocities of 30cm/day in the final days before failure (Muller 1968). Voight and Kennedy described the pre-failure displacements of a 125 m high slope at the Chuquicamata Mine, Chile. The displacements began in 1966 when tension cracks formed at the slope crest and gradually increased the rate at which they opened. An estimated 11-14 x 10^6 tonnes of rock was displaced downslope of the cracks. The maximum vertical displacement of the slope just prior to failure was c. 3 m with horizontal displacements of up to 5 m (Voight and Kennedy 1978).

If shear displacements even of an order of 0.01-0.05 of the total length of a failure plane are possible prior to the mobilisation of peak strength, then large slopes with failure-plane lengths of hundreds of metres could undergo significant pre-failure movements. Barton (1971a) considered that toppling failures with rough joint surfaces may be self-inhibiting because of the shear-stiffness encountered during shear.

Whilst shear-displacement is irreversible and may accelerate failure due to the opening of tension-cracks, a second mechanism

could, at least temporarily, inhibit failure (Fig. 2.11). If effective stresses were sufficiently low to permit overriding of asperities rather than shear through them, the resulting dilation would increase void space between joint walls thereby increasing rock-mass permeability and reducing cleft-water pressures (Barton 1971a). Permeability would be increased and a greater volume of water than that responsible for initiating movement, may then be required to cause further displacement. The voids between joints may be so large as to make build-up of dangerous cleft-water pressures less probable. Paradoxically, the stability of the slope could be increased after limited displacement.

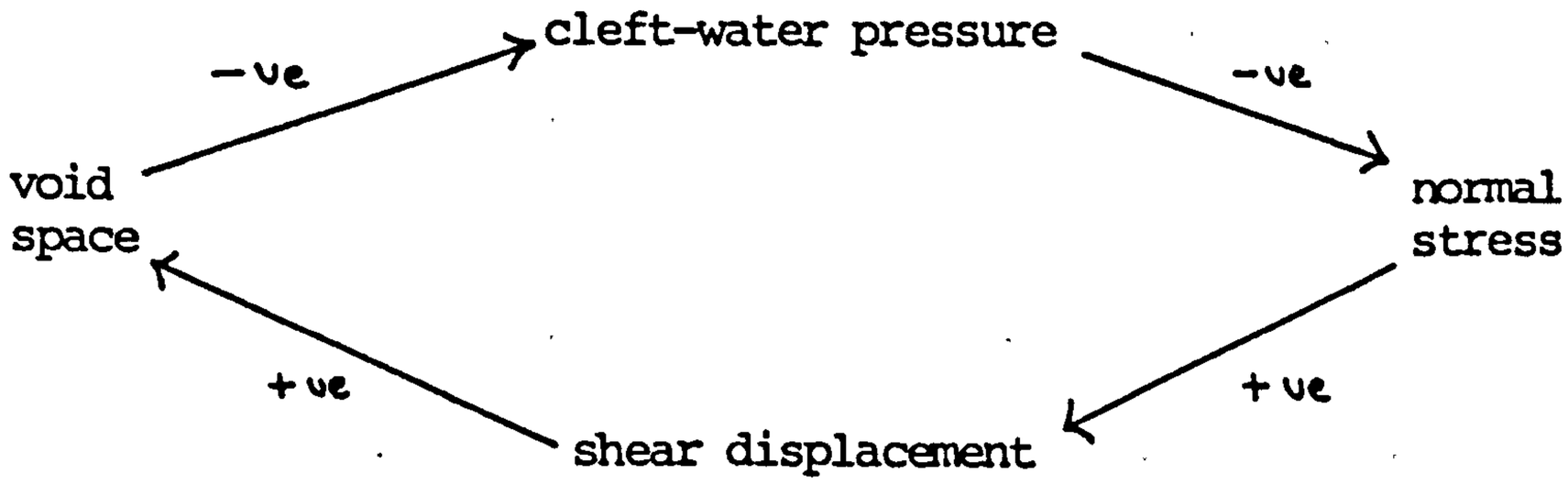

Fig. 2.11: Hypothetical self-inhibiting mechanism for RSF's.

However, stability may not be assured by the negative feedback mechanism since shear stresses could be concentrated towards the 'peaks' of asperities possibly leading to overstressing and their progressive-failure. After 'complete' failure of the slope any evidence for pre-failure displacements would be removed. Only those slope failures that are still 'intact', having suffered only minor displacement, enable testing of the self-inhibiting hypothesis.

2.8 Conclusion

The internal properties of rock-masses have been neglected in many geomorphic studies in the past. Even where rock mechanics techniques have been used, fundamental concepts such as joint shear-stiffness and dilation have received little attention (e.g. Whalley 1974, Wyrwoll 1977). It has been hypothesised that rock-slope displacements prior to mobilisation of peak shear strength may be numerous and self-inhibiting, because of a negative feedback mechanism involving cleft-water pressure, shear stiffness and dilation.

Following from these considerations of rock mechanics a number of joint characteristics require quantification in the field to assist explanation of RSF. The most important are joint attitudes, roughness and shear strengths. These data will provide inputs to models of slope stability of which two forms have been described: kinematic testing and limit-equilibrium models. Kinematic tests are favoured in this study for analyses of large-scale slopes and limit-equilibrium models for more detailed small-scale studies.

Three modes of RSF are generally identified in the engineering-geology literature: plane-sliding, wedge-sliding and toppling failure. Higher-order modes of failure that are intermediate between the three cardinal failure modes may be possible (cf. Goodman 1981), though little work has been undertaken in this research field. The classification of rock-slope failures according to their geometry provides a useful framework for the discussion of form and process and will be used to organise discussion of the case studies.

This Chapter has emphasised the internal properties of rock-slopes. In contrast the next chapter, discussing previous research into RSF in the Highlands, largely concentrates upon the extrinsic factors which affect rock-slope stability.

3: PREVIOUS RESEARCH

3.1 Introduction

A large volume of research has been undertaken on RSFs outside Scotland and will be cited where apposite in later chapters. The purpose of this chapter is to discuss the literature concerned with rock-slope failure in the Scottish Highlands, indicating research areas where further work is required.

Published research on RSFs in the Scottish Highlands occurs within two main periods. In the first of these, 70-110 years ago, officers of the Geological Survey mapped RSFs and collected other basic evidence. This research period will be discussed in Section 3.2. There followed a hia-tus during which no research on RSFs in the Highlands was published until interest in the Quaternary geomorphology of Scotland was renewed some 20 years ago. Since then, studies undertaken by Dr. J.B. Sissons and his students in particular, have yielded much data on the age and evolution of Quaternary landforms, including RSFs.

In order to place the literature on RSFs within a chronological and environmental framework, it is considered pertinent to discuss the Scottish Lateglacial period (c. 15,000-10,000 years B.P.) in Section 3.3, prior to discussion of the more recent phase of research into RSF.

The contribution towards explanation of RSFs given by the engineering-geology approach of R.J. Watters' work will be examined in Section 3.5. For brevity, only those aspects of previous RSF

investigations which have bearing upon the five main research themes of this thesis will be pursued.

3.2 Early literature on rock-slope failure

In the late 19th and early 20th centuries the officers of the Geological Survey located certain RSFs in the Scottish Highlands during the programme of geological mapping. C.T. Clough also contributed sections on "landslips" in some of the memoirs that he co-authored (e.g. Gunn et al. 1897, Peach et al. 1910, 1912). Although they are descriptive rather than interpretive, his references are eloquent testimony to the keen awareness of landscape of many of the early Geological Survey officers. He provided, for instance, a graphic description of a failed slope as being:

> "formed by great hummocks and irregular ridges of slipped material covered by scattered blocks, [having]... a very wild appearance in the landscape... At the top there is usually a somewhat coombe-shaped hollow in the crag, often itself in a somewhat shaken condition, and with deep narrow cracks at the back which the pedestrian has to be on his guard against" (Gunn et al. 1897; 275).

From similar descriptions and cross-checking on aerial photographs it is clear that the majority of 'landslips' mapped on the official Geological Surveys maps are based in rock. Clough (1913) however referred to a recent 'landslip' which was developed in drift material.

Some observations were exceptional to the descriptive style. E.B. Bailey for instance, speculated upon the cause of rock-slope failure when discussing the role of RSFs in sculpturing high mountain relief in the Ben Nevis and Glen Coe areas. He stated that;

> "many of the landslips referred to above have probably resulted from the instability of valley sides oversteepened by glacial erosion" (Bailey and Maufe 1916; 10).

Clough also inferred a connection between RSFs and glaciation making the interesting observation that RSF scars existed in the Cowal district of the SW Highlands with no failed debris below them. These he considered to be:

> "glacial or preglacial, the rubbish of which has now all been cleared away by glacial erosion" (Gunn et al. 1897; 276).

Clough later hypothesised that large scars left by major RSFs could, if subsequently occupied by glacier ice, be the first stage in corrie development (reported by Bailey, in Bailey and Maufe 1916).

The possible influence of joint dip angles, dip directions and foliation planes on slope failure was noted by Clough. For instance, he commented on one example:

> "its formation must have been facilitated by the direction of the local dip of the foliation... which is down the hill" (Peach et al. 1910; 166).

Clough also stated that slope failures occur with foliation directions discordant to the slope but the connection between mode of failure and discontinuity orientations was not explicitly stated.

Some important inferences were made in the early literature concerning the ages of RSFs. Most RSFs were considered to be ancient although Clough referred to a RSF in Glen Kinglas [NN 190 096] which was thought, on the basis of local history, to have occurred c. 1697 A.D. (Gunn et al. 1897). Clough was able to date relatively a RSF at the head of Loch Fyne, SW Highlands, because it disturbed the '20 foot beach' (Gunn et al. 1897). The so-called '20 foot beach' in this area is now known to be the Main Postglacial Shoreline (Sutherland 1981),

indicating that the RSF occurred during the mid-Flandrian. Bailey and Maufe referred to an example on the S-facing slope of Stob Ban [NN 148 654] as being a 'comparatively recent landslip'. Whereas they noted that a larger RSF immediately E of the above example is considerably older[1]. No reason was given for this inference.

The theoretical and methodological problems involved in determining the triggers and chronology of RSFs were insurmountable when the early literature was written. Despite this, the Geological Survey officers provided valuable information on RSFs. Data are now available on the chronology of the glacial sequence in Scotland providing stratigraphic constraints upon RSFs located within former glacial limits. The following discussion is critical to later examination of RSFs within the Highlands and provides an introduction to later sections of this Chapter.

3.3 The Scottish Lateglacial sequence

The Scottish Lateglacial may be subdivided into 3 phases: (i) the retreat of the last ice-sheet, which was punctuated by an unknown number of readvances, (ii) a period of renewed warmth termed the "Lateglacial Interstadial" (between c. 13,000-11,000 years B.P.) which was terminated by, (iii) a short climatic deterioration (the Loch Lomond Stadial) when glacial and periglacial conditions returned to Britain. The Stadial may have lasted approximately 750 years in the Highlands giving way to the present interglacial c. 10,000 years ago. These Lateglacial phases are pertinent to later discussion but only

1. Information given on the reverse of a photograph held at the Geological Museum, South Kensington, London.

brief descriptions of each are given below as good summaries of the literature are available in Sissons (1976a) and Gray and Lowe (1977).

(i) Ice-sheet retreat

The Late-Devensian ice sheet is generally believed to have reached its maximal extent c. 18,000 years ago (Penny et al. 1969), though its timing of retreat is unknown. Erratic boulders and striae have been reported near the summits of Scottish Mountains (at up to 1,100 m O.D. in the Ben Nevis area) but, as Sissons (1981) observed, there is no conclusive evidence that the erratic boulders and striae relate to the last ice-sheet. Boulton et al. (1977) attempted to model the late-Devensian ice-sheet and reconstructed its surface as up to 1,800 m O.D. in the Scottish Highlands. However, they admitted that their model was erroneous as it necessitated very high rates of calving at the supposed ice-sheet margin.

Numerous radiocarbon dates indicate deglaciation of the Highland glens by c. 13,000 years B.P. (e.g. Kirk and Godwin 1963, Sissons and Walker 1974, Lowe and Walker 1977). Coleopteran assemblages from deposits in SW Scotland however indicate a cold climate prior to c. 13,000 years B.P. when mean July sea level temperatures in SW Scotland were around 15° C (Bishop and Coope 1977).

The dichotomy between the dates for deglaciation of the Highland glens and that of climatic amelioration may be explained in two possible ways. First, Sissons (1981) proposed that down-wastage of the last ice sheet, and presumably others before it, may have been caused initially by starvation from precipitation as depressions

tracked along lower lines of latitude in alliance with the polar oceanic front, which was displaced S by polar oceanic water encroaching from the N. An alternate explanation is that the dates from newly deglaciated terrain are erroneous and cannot be used with confidence to correlate between such events. Sutherland (1980) for instance, expressed concern over the accuracy of radiocarbon dates from basal deposits which may provide misleadingly old dates because of the effects of ancient carbon derived from the newly-deglaciated terrain.

Several readvances of the last ice sheet have been hypothesised in the past, including the Aberdeen-Lammermuir Readvance and the Perth Readvance, which have now been refuted (cf. Sissons 1976a, Gray and Lowe 1977). In Wester Ross however extensive end moraines occur outside the limits of the Loch Lomond Advance (Robinson and Ballantyne 1979) and are considered to have been formed by a readvance of the last ice sheet (Sissons and Dawson 1981). The last authors have shown that raised shorelines outside the limits of the Wester Ross Readvance possess a similar gradient to the Main Perth Shoreline in the Forth valley, where there is an abrupt drop in the marine limit suggesting a possible glacial readvance. The raised shorelines in Wester Ross show no such marked fall, indicating instead a gradually falling relative sea level and frustrating correlation between the E and W coast evidence (Sissons and Dawson 1981).

Sissons (1982) discussed evidence for a former ice-dammed lake, impounded by readvancing glaciers which pre-dated the Loch Lomond Advance near Achnasheen, central Ross-shire. The Achnasheen Readvance may correlate with the Wester Ross Readvance though this has not been

established (Sissons 1982).

At Loch Fyne in the SW Highlands the rapid northward retreat of glaciers from their maximum was interrupted at c. 13,000 years B.P. by a halt stage or readvance termed the Otter Ferry Stage (Sutherland 1981). If the cold climate Coleopteran assemblages from SW Scotland (Bishop and Coope 1977) that date to c. 13,000 years ago are symptomatic of the climate prior to the Otter Ferry Stage, then this indicates that deglaciation occurred initially under a cold climate and that a halt or readvance occurred while temperatures were close to those experienced today (Sutherland 1981). Caution must be expressed over the accuracy of the dating of these events. However, Sissons (1981) has proposed that as climate ameliorated towards the end of the cold period, precipitation-bearing depressions may have tracked once more across Scotland nourishing retreating glaciers and causing a readvance.

(ii) The Lateglacial Interstadial

If the radiocarbon dates from basal deposits are correct, then the location of early basal dates from Scottish glens is suggestive, according to Sissons (1976a), of complete deglaciation of Scotland before 12,500 years B.P., though this is disputed by a few workers (e.g. Peacock 1970, Sugden 1970, Sutherland 1981). However, it is not known when high-level glacial refuges were deglaciated as these areas often lie within the limits of the Loch Lomond Advance and any stratigraphical evidence of complete deglaciation would probably have been destroyed during the later Advance.

Figure 3.1: The Loch Lomond Advance in the Scottish Highlands.

Soil development began again in Scotland during the Lateglacial Interstadial, as evidenced by the humus accumulations in lake floor sediments (e.g. Pennington et al. 1972). Pollen analyses of interstadial sediments indicate that open-habitat plants (e.g. grasses, sedges and mosses) predominated and that the low ground of much of Scotland was characterised by park tundra which was replaced to the N, and at higher altitudes, by a treeless tundra (Gray and Lowe 1977). Bishop and Coope's (1977) palaeotemperature curve through the Lateglacial features a decline from the maximum of 15° C at c. 13,000 years B.P. to 12° at c. 12,000 years B.P. after which a further gradual deterioration heralded the onset of the Loch Lomond Stadial.

(iii) The Loch Lomond Stadial

At c. 11,000 years B.P. polar water in the Atlantic began to surround the British Isles (Ruddiman et al. 1977). Foraminifera assemblages from the Firth of Clyde were dominated at this time by polar species (Peacock et al. 1978). In fresh-water lakes, organic deposits that accumulated during the Lateglacial Interstadial are succeeded (often sharply) by a minerogenic layer, indicative of soil erosion. Tundra vegetation dominates the pollen profiles of sediments from the Stadial with high frequencies of Artemisia in drier

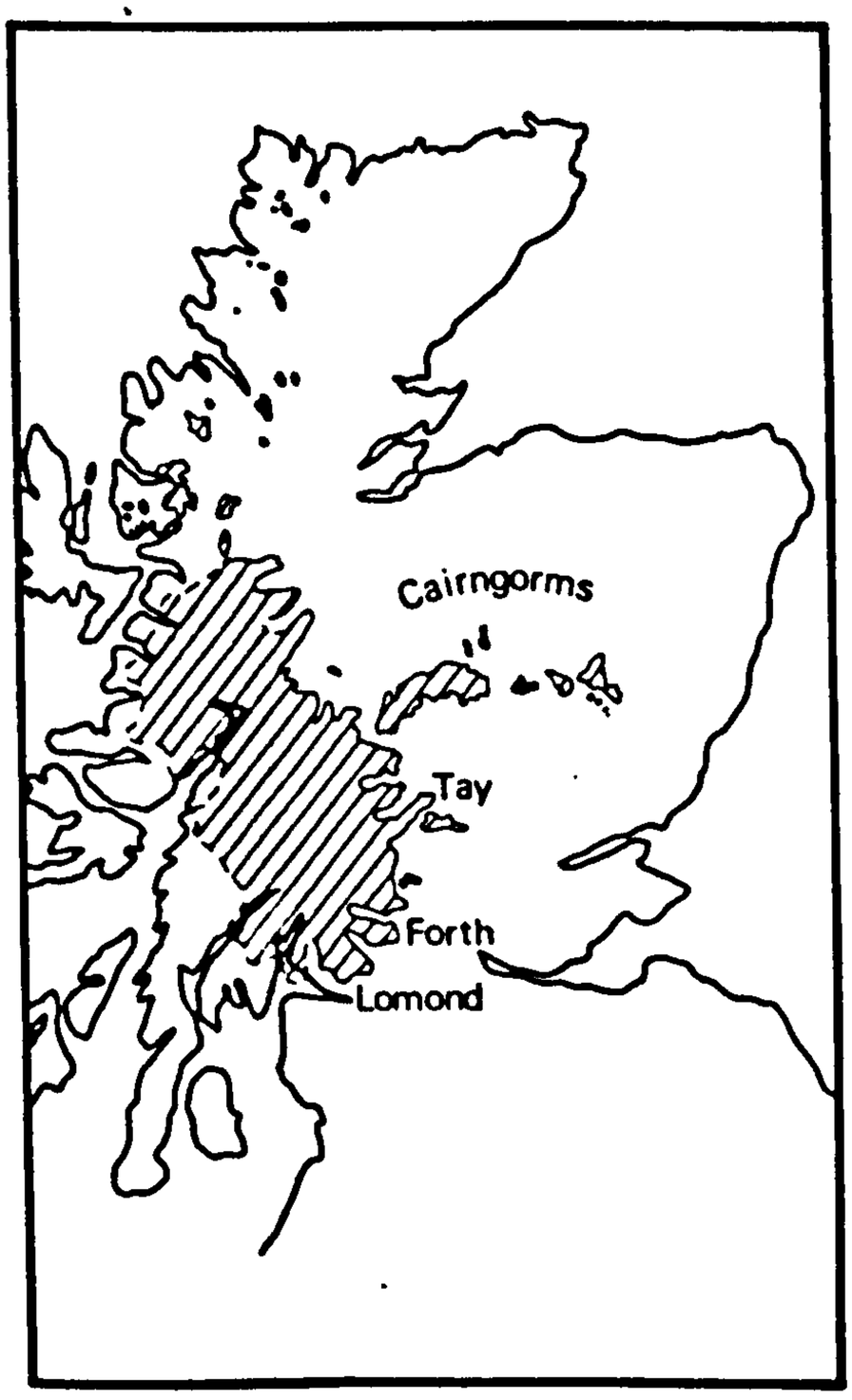

areas.

The climatic deterioration resulted in glacier accumulation in many upland areas of Britain (Sissons 1976a, 1979c, Gray 1982). Large ice masses occupied the W Highlands and plateau ice-caps formed (e.g. the Gaick plateau, central Grampians). Large piedmont glaciers flowed S of the Highland boundary edge in the W and other large glaciers spread out E from the W Highland glacier complex (Fig. 3.1). Pronounced variations in the precipitation of the time (Sissons and Sutherland 1976, Sissons 1979c) produced only small glaciers in the Cairngorms in contrast to the large glaciers in the W Grampians.

Intense periglaciation occurred in upland areas (Ballantyne 1981) and frost-wedges have been found inside Loch Lomond Advance limits that lie close to sea-level (Sissons 1977a), indicating that mean annual temperatures must have been below -1° C. Mean July temperatures at sea-level of 6° and 7° C have been inferred from the glaciers of the SE and SW Grampians respectively (Sissons and Sutherland 1976, Sissons 1979c). At 1,000 m O.D. winter temperatures would have been considerably lower with at least discontinuous permafrost being established (Ballantyne 1981).

The climatic amelioration at the close of the Loch Lomond Stadial occurred, according to Bishop and Coope (1977), with great rapidity. The reconstructions of the enviromental changes at the end of the Stadial are of particular concern in this thesis and will be discussed in greater detail in later chapters.

3.4 Recent research

Additional data on RSF locations have recently been acquired by the Geological Survey in previously unmapped areas (e.g. Sheet 62) and according to Peacock (1975a) over 250 RSFs have been mapped by the Geological Survey in the western Highlands. RSFs have also been mapped in the Highlands by other Quaternary scientists (e.g. Thompson 1972, Sissons unpubl., Sutherland 1981, unpubl., Thorp 1978).

A number of RSF triggers have been suggested in the literature. Godard (1965) discussed several RSFs on Mull, Eigg and Skye. These rotational rock-slope failures are atypical when compared with those found in the Highlands (cf. Sissons 1976a) as slope failure in the Inner Hebrides usually occurs where basalt overlies shale or other incompetent rock. Godard's inferences concerning process are still of interest. Of four possible factors controlling slope failure noted by him, three geologic ones: lithology, the dip of lithological units and rock structure (i.e. jointing/foliation), were stressed. The fourth factor combined glacial oversteepening of valley slopes, increased tensional(?) forces within slopes on deglaciation: "le depart de la glace creait parfois une decompression" (Godard 1965; 630) and high groundwater levels. He did not discuss the mechanism by which groundwater was thought to have led to slope instability.

Sissons (1967) also invoked glacial oversteepening of rockwalls, assisted by the release of water from the melting of permafrost, as a trigger for RSFs. He further hypothesised that 'ice-wedging' may have caused rock-slope failure in Lateglacial times (Sissons 1976a) but the scale of rock-masses which may have been displaced by such a process

was not suggested. Notes accompanying the Drift Edition of the Geological Survey Sheet 62W (Johnston et al. 1975) state that rock-slope failure may have been triggered by 'periglacial processes' though Johnston et al. (1975) did not elaborate on this suggested cause.

Sissons and Cornish (1982) presented detailed data on the altitudes of the fossil Glen Roy ice-dammed lake shorelines (the famous "Parallel Roads"). Instrumental levelling of the shorelines has established their vertical dislocation in at least three areas, at one point by c. 3 m (Sissons and Cornish 1982; Fig. 9). The three areas are associated with landslides (two are RSFs) and Sissons and Cornish speculated that the slope failures were triggered by earthquakes accompanying the stress-release between crustal blocks.

Ballantyne and Eckford (1984) hypothesised that triggering of slope failure near West Lomond Hill, Fife, could have occurred by earthquakes but noted that no faults were shown close to the field site, on Geological Survey maps of the area. They suggested two other possible triggers: (i) withdrawal of supporting ice from oversteepened slopes and (ii) "progressive development of joints through dilation (unloading)" (Ballantyne and Eckford 1984; 28).

Perhaps the most speculative and interesting aspect of rock-slope failure is the relative amount of geomorphic work achieved by high-magnitude events. Some inferences concerning the chronology and magnitude-frequency relationships of RSFs have been made in the literature. Godard (1965) hypothesised that during deglaciation conditions would have been most suitable for the initiation of RSFs.

The main phases of slope instability according to Sissons (1967) would have been during glacial and late-glacial times, with the greatest frequency occurring during deglaciation. He also stated that:

> "Doubtless some masses tumbled down onto the glaciers themselves and contributed to the morainic debris" (Sissons 1967; 227).

Sissons (1976a) suggested that slope failure may have occurred at a reduced rate during the Flandrian and Sissons and Cornish (1982) commented that no major RSFs have occurred in the last 250 years in the Highlands, though the evidence for this inference was not detailed. Ballantyne and Eckford (1984) thought that one slope failure near West Lomond Hill was "ancient". They considered the occurrence of a drystone wall built in 1840 across the failed debris and the 'rounded' appearance of rock exposed in the slide scar to be suggestive of the RSFs old age.

Two case studies in the Highlands have been cited as evidence of an interaction of RSFs with former glaciers. A massive accumulation of Torridonian Sandstone boulders on the floor of the corrie SE of Beinn Alligin in Wester Ross [NG 87/60] was investigated by Sissons (1975). The mass of boulders has a maximum height of 12-15 m, a width decreasing almost linearly from 400 m at the corrie backwall to 200 m near the terminus and is 1.2-km-long. Sissons stated that to his knowledge the feature is unique in the Scottish Highlands. A RSF was evidently the source of the debris on the corrie floor as at the crest of the steep corrie backwall 300-m-above the debris accumulation, a large scar has been formed by two intersecting fault/joint planes.

The excessive travel distance of the boulder debris is the

interesting characteristic of this landform and two hypotheses have been advanced to explain it. Sissons (1975) suggested that the failed rock may have fallen onto a decaying Loch Lomond Advance glacier remnant, which was reactivated under the added load of the debris to form a rock glacier. Whalley (1976) proposed that the 'run-out' of the boulder debris could have resulted from a rock avalanche. Rock avalanches are masses of broken bedrock (supplied by massive RSFs) which move as exceedingly rapid dry flows (Coates 1977). The excessive travel distances of rock avalanches are well documented (e.g. Heim 1882, 1932, Harrison and Falcon 1937, Mudge 1965, Shreve 1966, 1968, Kent 1966, Hsu 1975, Porter and Orombelli 1981a,b) though the exact mode of transport is the subject of controversy.

Whalley (1976) opined that the Beinn Alligin RSF probably occurred during deglaciation when cleft-water pressures within rock masses would have been high. Explanation of the feature is hindered because the morphology of the boulder accumulation is consistent with either a rock glacier or rock avalanche interpretation. Prominent ridges, linear depressions, hummocky surface topography and a well-defined limit, are characteristic of both types of feature (Bock 1977).

Haynes (1977) detailed some of the landforms found in Gorm Coire by Ben Hee [NC 43/34]. She inferred that the corrie backwall was subjected to RSF during glaciation citing two observations in support of this. First, the failed debris is fronted by "streamlined drift" (Haynes 1977; 338) and secondly, an anomalously-large accumulation of drift is found on the NE side of the corrie. The drift accumulation, larger than any found in other corries near Ben

Hee, contrasts with bare rock on the SW side of Gorm Coire itself. Haynes considered the source of the debris accumulation to have been RSF. Sissons (1977a) also suspected a connection between RSF and glaciation at this site.

3.5 The work of R.S. Watters

The most significant contribution towards an understanding of the mechanics of rock-slope failure in the Scottish Highlands was provided by the reconnaissance engineering-geology survey of Watters (1972). The primary aim of his research was to assess the current stability of metamorphic rock-slopes in the Highlands.

Watters classified RSFs according to their failure mode(s), distinguishing between plane-sliding, wedge-sliding, toppling and toppling/sliding modes of slope failure. A major finding of his work was the first field evidence for large-scale toppling of slopes, in particular his detailed examination of the slope at Glen Pean [NN 910 905] (de Freitas and Watters 1973). He visited seventy localities where slope instability had occurred, all of the sites were gleaned from the published and unpublished work of the Geological Survey. No attempt was made by him to establish an independent inventory of RSFs.

Watters thought that the geographic distribution of slope failures is controlled by rock type, discontinuity attitudes and topography. The inherent weakness of phyllites, mica-schists and schistose grits in the Cowal district of the SW Highlands, for instance, were cited as the cause of the high incidence of slope instability in this area.

Watters considered it possible to identify dominant slope failure modes in different parts of (the) Cowal. In the W Cowal steeper foliation dips were considered to have caused mainly translational-shear modes (cf. plane-slides and wedge-slides). Nearer to the axis of the Cowal peninsula however, lower foliation dip angles were supposed to have given rise to toppling and toppling/sliding failures. He also stated that low-angle joints may account for the high incidence of rock-slope failure in the Knoydart area.

Limit-equilibrium techniques were employed by Watters to model a number of possible cleft-water pressure distributions and rock strength characteristics for his detailed studies. Laboratory testing of the main metamorphic rock types provided shear strength data for use in the limit-equilibrium models. Watters discovered significant differences in the strengths of these rocks, particularly lower shear strengths along lines of foliation. He constructed height/angle diagrams for slopes composed of phyllite, mica-schist and psammite, but did not analyse gneiss.

The majority of the case studies, he considered, required high cleft-water pressures to trigger failure and were most likely to have occurred during deglaciation. At such times, he stated, glacially oversteepened slopes and the thawing of frozen-ground would have provided optimum conditions for slope instability. He hypothesised that ground-water levels during deglaciation would have been at or near the surface.

All of the 70 slope failures discussed by him were considered to be post-glacial (i.e. post Loch Lomond Advance) though he was

cognizant of the possibility that RSF debris may have been removed between and/or during glacial advances/readvances. He also proposed that certain failures could have occurred well after deglaciation: triggered by progressive-failure. He commented of a RSF on the E face of Fraoch Bheinn [NM 98/94];

> "the overall impression is that the slide has occurred recently.. .. the slide debris does not support any substantial amounts of vegetation, the main growths only being of fungus" (Watters 1972; 146).

He also suggested that progressive-failure of a number of small-scale RSFs was still occurring. He made no attempt to date the RSFs.

3.6 Discussion

Little is known about the controls on the distribution of RSFs in the Scottish Highlands at the large-scale. Watters (1972) inferred a connection between RSFs and rock structure/type and topography, but obtained insufficient data to enable testing of his hypotheses for the whole of the Highlands. He emphasised the importance of slope failure in phyllites, schists and schistose grits. If his inferences concerning the inherent weakness of these rock types are correct, then their outcrops in the Highlands should be important areas for slope instability.

Data on RSF locations however are themselves incomplete. There are published geological maps, such as Sheet 65 (Balmoral), where RSFs are not mapped and yet are known to have occurred (Sissons unpubl.). A consistent approach to RSF mapping is required prior to analyses of their spatial distribution.

Several possible causes of RSFs in the Highlands have been

referred to above. The different hypotheses are summarised in Table 3.1 which illustrates that the inferred triggers of rock-slope failure have tended to move away from early emphasis of the possible direct effect of glaciers on rock-slope stability (glacial oversteepening of slopes) towards other indirect affects (e.g. hydrological changes and seismic events). The rock mechanics techniques discussed in Chapter 2 provide a means of assessing the role of each possible trigger. As processes may have exerted a combined effect upon individual slopes, however, the relative importance of each may be indeterminable.

Authors	Glacier erosion	Hydrologic changes	Periglacial processes	Seismic events	Progressive-failure
Bailey (1916)	X				
Godard (1965)	X	X			
Sissons (1967)	X	X			
Watters (1972)	X	X			X
Whalley (1976)		X			
Johnston et al. (1975)		X			
Sissons (1976a)		X			
Sissons and Cornish (1982)				X	
Ballantyne and Eckford (1984)	X			X	

Table 3.1: Suggested causes of RSFs in the Scottish Highlands

A connection, whether direct or indirect, between glaciation and rock-slope failure has been implicitely recognised in the literature (cf. Sissons 1975, 1976a, Peacock 1975a, Haynes 1977) and yet little work has been undertaken to assess whether the limits of former glaciers correlate with the occurrence of slope failures. The Loch Lomond Advance has now been mapped across much of the Highlands (Fig.

3.1) enabling testing of this hypothesis.

Most geomorphological work on RSFs in the Scottish Highlands has been qualitative though Watters' thesis was a valuable advance on this work. His back-analyses of failed slopes however may be criticised because he often failed to employ sensitivity-analyses that would indicate the relative importance of each of the assumptions which he made. He recognised the importance of progressive-failure in causing rock-slope failure after deglaciation but mainly utilised peak shear strengths in back-analyses. Consequently, more pessimistic cleft-water pressure distributions would be necessary to model failure at peak strength than when mobilised resistance to shear is assumed to be below its peak.

The possibility that earthquakes could have triggered slope failure is an exciting development which requires testing on a larger scale than that permitted by Sissons and Cornish's (1982) work. A major difficulty however is that the magnitudes, distribution and frequency of the hypothesised earthquakes are unknown. Although Sissons and Cornish have suggested rapid localised uplift at Glen Roy, it is not known whether the inferred fault displacement occurred by a series of minor displacements or by one displacement. It is possible that the fault-scarp described by Sissons and Cornish is a glacio-isostatically induced "pop-up". Pop-ups are features caused by localised and rapid relief of stress often encountered during quarrying operations (cf. Coates 1977, Nicholls 1980). According to Eyles and Paul (1983), such features should be frequent in formerly glaciated terrain though drift-cover above the rockhead may hinder their identification.

Certain of the suggested causes of RSFs necessitate assumptions as to when failure occurred. The operation of ice-wedging as a cause of RSFs (if at all) for instance, would have been restricted to cold periods in the Lateglacial. In addition, if glacial oversteepening of slopes was the dominant process leading to slope instability, then RSFs would have been largely confined to the period during and immediately following deglaciation. Progressive-failure may have led to sporadic slope failure throughout the Flandrian and many authors have hypothesised a phase of high RSF frequency during deglaciation with decreasing activity during the Flandrian (e.g. Watters 1972, Sissons 1967, 1976a). Since no study of RSF chronology has been made in Scotland this hypothesis is so far untested.

The relative contribution of high-magnitude RSFs to the denudation of the Scottish mountains is unknown. Some measure of their efficacy can be gained by comparison between RSF and, for instance, protalus rampart volumes. The Beinn Alligin slope failure involved roughly 8.0×10^5 m^3 rock and this may be compared with the 6.0×10^5 m^3 of rock debris composing the protalus rampart at the base of the Creag an Fhithich slope in Wester Ross [NG 85/67] (Sissons 1976b). Sissons considered that the protalus rampart was formed by ice-wedging of blocks along joints over a period of c. 750 years, during the Loch Lomond Stadial. The amount of erosion achieved by the Beinn Alligin RSF (in perhaps a matter of minutes) attests to the possible importance of RSF in the denudation of mountain environments.

3.7 Conclusion

Research concerning rock-slope failure in the Scottish Highlands began with the work of Clough in the late 19th Century and since then little research has been undertaken specifically on RSFs in the Highlands. Mapping of RSFs is incomplete and little is known about the environmental controls on their spatial distribution. Watters (1972) suggested however that phyllites, mica-schists and schistose grits are particularly susceptible to slope instability but was only able to test this hypothesis using the Geological Survey information, which is known to be incomplete.

Much geomorphic research has emphasised glacial oversteepening of rock-slopes as the dominant trigger of slope failure, though no attempts have been made to test this mechanically. Other indirect affects, in particular high cleft-water pressures which could have prevailed during deglaciation and progressive-failure, have been suggested by Watters (1972). Sissons and Cornish (1982) hypothesised that earthquakes accompanying the stress-release between isostatically uplifted blocks may have triggered slope failures. The distribution, magnitude and frequency of possible earthquakes during deglaciation is unknown.

Most authors have hypothesised a phase of high RSF incidence during deglaciation with continued activity but decreasing frequency, throughout the Flandrian (cf. Watters 1972, Sissons 1976a). Sissons and Cornish stated that no major slope failure is known to have occurred in the Highlands in the last 250 years yet few attempts have been made to assess the age of slope failures in Scotland.

A number of different and as yet unsatisfactorily answered research themes, have been identified in Section 3.5. Within the framework of this thesis, these themes require answers to the questions of: where? when? how? how much/when? and why? As all these questions are inter-related and the previous literature on each limited, this thesis attempts explanation of RSFs using a multidisciplinary approach (cf. Whalley 1974, Selby 1982). The first theme (where?) will be pursued in the next chapter.

4: ROCK-SLOPE FAILURE DISTRIBUTION IN THE SCOTTISH HIGHLANDS

4.1 Introduction

Because of the variation in the quality of previous mapping of RSFs highlighted in Chapter 3, it was decided that the first task of the research project should be to compile an inventory of RSFs in the main mountain areas of the Scottish Highlands. The inventory would serve two main purposes: first, as a reconnaissance survey to isolate areas that warranted detailed study and secondly, to permit statistical investigation of possible environmental controls upon the distribution of RSFs.

The stability-threshold of a rock-slope is determined by its internal properties, in particular its geometry and joint shear strengths. As stability-threshold magnitudes vary in space, because of variations in rock type and slope angle, for instance, statistical analyses of the spatial distribution of RSFs may permit inferences as to why slope failure occurred. Extrinsic influences on slope stability, such as the degree of glaciation, may also vary in their distribution.

A number of RSF distribution studies have been made within various mountain areas of the world (e.g. Carrara and Merenda 1976, Eisbacher 1979b, Whalley et al. 1983) but to the author's knowledge, no previous study has attempted to test in detail the hypothesis that glaciers, either directly or indirectly, reduce rock-slope stability. The significance of this chapter is that it tests this hypothesis by analyses of the spatial distribution of RSFs and the limits of former

glaciers in the Scottish Highlands.

4.2 Previous RSF distribution studies

Most of the previous RSF distribution studies have been undertaken for engineering purposes. Emphasis has therefore been placed upon: determining the regional environmental-controls upon slope failure, assessing regional slope failure risk and identifying areas which are particularly prone to slope failure.

A plethora of variables have been suggested as controls on the distribution of RSFs. However, lithology is often cited as the most important determinant of RSF distribution (e.g. Rybar and Nemcok 1968, Radbruch-Hall and Varnes 1976, Eisbacher 1979b, Whalley et al. 1983). A major survey of landslides in Czechoslovakia revealed 9,000 examples of which relatively few were located on granites, limestones, dolomites and the metamorphic rocks (Rybar and Nemcok 1968). Most of the Czechoslovakian landslides occur where resistant rocks, such as volcanics, overlie poorly consolidated sedimentary rocks.

Eisbacher (1979b) considered that the Canadian Cordillera can be divided into eight zones that are characterised by different forms of landsliding on different lithologies. He attempted to identify the dominant landslide type for different areas, an approach that assumes that variations in geology control slope failure type. Rockfalls were found to be most frequent in granitic and metamorphic rocks while rock avalanches were common in the southwest-dipping limestone, quartzite and dolomite strata (Eisbacher 1979b).

Whalley et al. (1983) observed that Icelandic RSFs occur

dominantly on the Tertiary basalt, only eight RSFs being reported on other rock types. Landslides in Japan are most commonly found in phyllites, schists, Tertiary tuffaceous rocks and where Neogene sedimentary rocks are overlain by basalt (reported in: Radbruch-Hall and Varnes 1976). Radbruch-Hall (1976) has shown that the physical state (i.e. the amount of fracturing and shearing) of rock and its lithology, can be used to predict slope stability in part of the northern Coast Ranges, California. She speculated that these two factors may be used to prepare maps of RSF susceptibility elsewhere.

A number of additional factors have been cited as influencing the intensity of landsliding in areas of homogenous lithology. Eisbacher (1979b) for example, attempted to account for landslide-type distribution by reference to precipitation, seismic risk and relief. These factors have been identified as important causes of RSF by a number of workers (e.g. Sharpe 1939, Zaruba and Mencl 1969, Radbruch-Hall and Varnes 1976, Coates 1977). Eisbacher classified the above factors into groups of high, intermediate and low magnitude. He superimposed the groups onto a map to indicate areas of potential high landslide risk; these areas correlated with the regions of high landslide incidence.

Whalley et al. (1983) noted a spatial correlation between the locations of RSFs and glaciated valleys in Iceland though they cautioned that any connection between glaciers and RSFs may be complex. They did not present detailed data on the limits of the former glaciers nor did they investigate the supposed correlation at a smaller scale.

4.3 Data collection

The RSF data in this study were collated from analyses of mostly c. 1:27,000-scale stereoscopic black and white aerial photographs. This scale was recommended by Svatos (1974) for RSF investigations though Patton and Hendron (1974) suggested the use of small-scale photographs for reconnaissance surveys with large-scale aerial photographs for later detailed investigations. Certain areas were surveyed with 1:10,000-scale photographs during this study, a scale which was found to be less suited to RSF identification as large examples require several prints to cover them. Large-scale photographs were however found to be useful in detailed mapping of the case study RSFs. Each of the aerial photograph runs was analysed twice or more and all the main mountain areas in the Highlands were covered by the survey (Fig. B.1).

A number of morphological features indicative of slope failure (Watters 1972, Patton and Hendron 1974) were utilised during the survey to identify RSFs. These characteristic features include: deranged surface drainage, irregular (hummocky) terrain, arcuate scarps, major cracks/furrows, ridges, boulder debris-tongues, "bulging" of a slope and anomalous concentrations of springs. All these features were readily identified on the 1:27,000-scale photographs. The only topographic evidence of limited slope failure in some instances is the occurrence of ridges and furrows.

Care was taken when surveying N-facing slopes as RSFs could have been obscured by shadow. The possibility of RSFs having been omitted from the inventory due to shadowing is reduced by two factors. First,

most aerial photographs were taken during the summer months when shadows were comparatively shallow and secondly, the size of many RSFs often precludes the possibility of whole features being cast in shadow. Cross-checking of areas where official geological maps are available established that N-facing RSFs were not under-represented: rather RSFs were identified during the survey on N-facing slopes which were not observed by the Geological Survey officers.

Using aerial photographs, the areas affected by RSFs were plotted by eye onto 1:50,000-scale base maps. Later aerial photograph and field mapping of RSFs within the field areas established that the RSF boundaries defined on the base maps were sufficiently accurate for the analyses made in this chapter. Rockfalls much smaller than the lower size limit (c. 2,000 m^3) were visible on the aerial photographs.

Four-hundred and thirty-two RSFs have been mapped within the limits of the survey: their locations are shown in Figure 4.1 (in map folder). Appendix B lists the grid reference, aspect and area of each slope failure. Grid references are given for the centroid of the area affected by slope instability and the sites are grouped under the 10,000 km^2 grid square letters. Area was estimated using a transluscent grid overlay with 100 x 100 m squares. The total area affected by slope failure, including the scar, is given for each example; following the convention of the Geological Survey. Although area is a poor estimate of the "size" of a RSF, as it is affected by the degree of displacement, it is considered the most consistent statistic as RSF volumes would be difficult to estimate due to the lack of subsurface data. The RSFs affect a total area of > 76 km^2.

Figure 4.2: Morphological classification of RSF positions. 1 = valley side, 2 = slope crest, 3 = spur, 4 = mountain top and 5 = corrie headwall.

A simple morphological classification (Fig. 4.2) describes slope failure position. The classes are similar to those used by Whalley et al. (1983). Some of the RSFs have scars with no failed-debris below them. These are termed "debris-less RSFs" here. Those rock-slope failures which have failed debris below their scars (cf. Fig. 1.1) are termed "in situ RSFs".

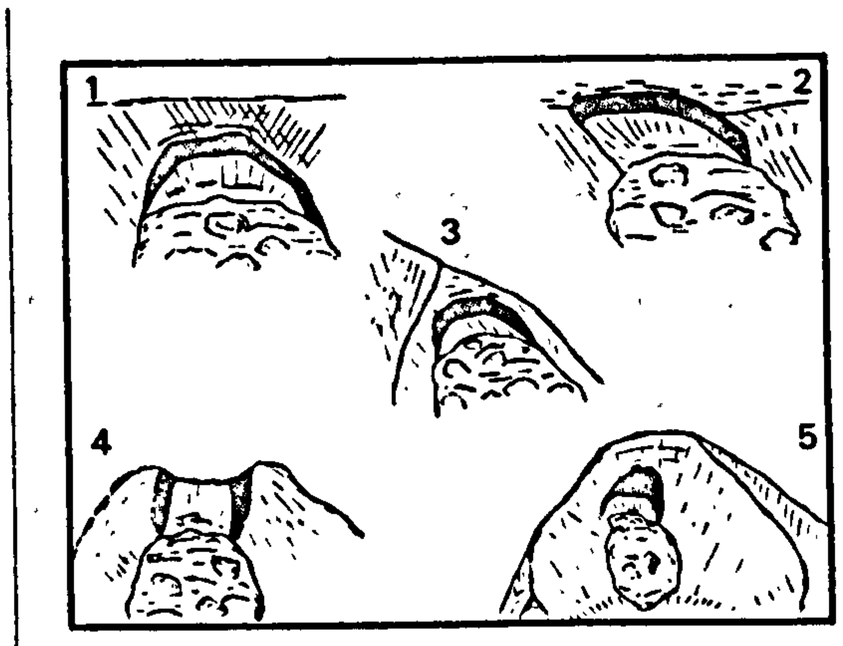

The simplest explanation for the removal of failed debris after slope failure is by glacial transportation (cf. Clough: in Gunn et al. 1897). Similar landforms were observed in Norway by Bjerrum and Jørstad (1963) who commented that:

> 'Huge rock slide scars were seen without the corresponding debris below, these evidently having been moved away by the glacier, or they occurred before the last glaciation. Some rock slides across a valley seem to have been moved a bit by a glacier' (Bjerrum and Jørstad (1963; 172)

Addison (1981) described a debris-less RSF in Cwm Graianog, Snowdonia, which was thought to have involved c. 60,000 m^3 of material. Large-scale bedding-plane ripples characterise the failure-surface of the RSF and the only blocks that are so marked are located in "corrie moraines" several hundred metres distant from the RSF scar. He hypothesised glacial transportation of the debris though it was not possible to infer whether the failed material pre-dated the advance of the glacier or if it fell onto the former glacier surface. Slope failures are known to have fallen onto currently active glaciers, leaving behind debris-less RSFs (e.g. Marangunic and Bull 1968, Gordon et al. 1978).

During the aerial photograph survey of RSFs, other criteria that may indicate disturbance of failed debris by glaciers were considered. Downvalley displacement (cf. Bjerrum and Jørstad 1963) or truncation of failed-debris would be evidence of interaction between RSFs and glaciers. Four examples in addition to the debris-less RSFs are thought to have been disturbed by former glaciers. These are at: Maol Chean-dearg [NG 932 497] (Robinson 1977), Meall nan Fuarnan [NH 398 899], Carn Ghluasaid [NH 139 118] and at Mullach Coire Mhic Fhearchair [NH 047 738]. Only two RSFs are thought to be possible "rock avalanches": the Beinn Alligin feature [NG 866 610] described earlier (p 39) and an example at Carn Alladale [NH 392 898].

4.4 Controls on RSF distribution in the Scottish Highlands

Analysis of the spatial distribution of RSFs, using the inventory data, is possible at the population and individual levels. At the population level, there is a marked contrast in RSF densities between W and E (Fig. 4.3a). Although the main mountain areas are found in the W and local relief is often cited as an important factor in the distribution of rock-slope failures (e.g. Eisbacher 1979b), variation in relief provides a poor descriptor of the RSF distribution in the Highlands. The Cairngorms for instance have only one RSF despite their extensive area, steep slopes and high relief.

Rock type provides a better explanation of the distribution of the RSF population. Some 93% of RSFs where geologic information is available occur in the metamorphic rocks listed in Table 4.1. The

Figure 4.3: (a) Distribution of RSFs in the Scottish Highlands.

(b) Outcrop of schistose rocks.
1 = Lower Dalradian
2 = Upper Dalradian and Moinian schists.

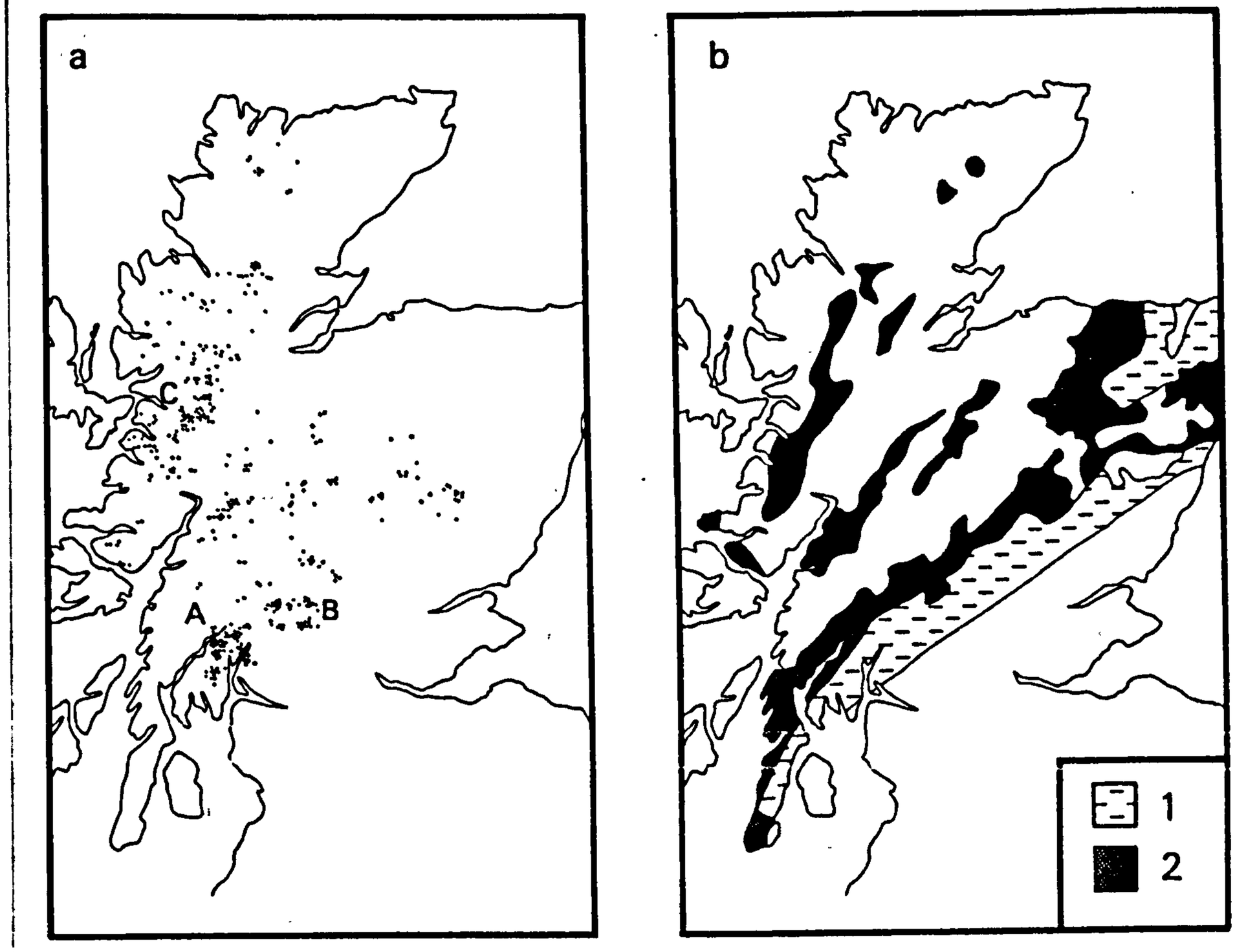

Rock type	Number	Percentage
schist	201	52
psammite	67	17
pelite	42	11
gneiss	26	7
quartzite	23	6
granite	10	3
sandstone	3	1
others	16	4

Table 4.1: Distribution of RSFs on different rock types.
n = 388 (90% sample).

'schist' class in Table 4.1 includes schists which were undifferentiated by the Geological Survey officers. Where schists are

differentiated on geology maps the pelitic-schists, or mica-schists, (representing the more clayey horizons of the parent rock) and the psammites, or granulites, (which are derived from metamorphism of the more sandy layers) are classified separately. Eighty percent of the sample are located on schists of all types.

Of particular interest is the strong spatial correlation between the Dalradian and Moinian Series outcrops and RSFs (Fig. 4.3b). Metamorphic rocks have peak friction angles some 5-10° lower than the hard igneous rocks such as granite (Hoek and Bray 1977). This characteristic combined with the strong mechanical anistropy caused by foliation, significantly reduces the stability thresholds of the metamorphic rock types. Slopes composed of rocks with high shear strengths therefore require a greater environmental change to trigger failure than slopes of the same slope angle and discontinuity patterns but with lower stability thresholds.

The data for the whole Highlands concur with Watters' (1972) statement that slope instability is most frequent in the schists. Schists are renowned as being highly susceptible to slope failure in other countries (cf. Huder 1976, Radbruch-Hall and Varnes 1976).

Within the outcrop of the Moinian and Dalradian Series, areas of high RSF densities occur, the principle ones being: the Cowal district, The Trossachs and the Knoydart/Kintail area (A, B and C respectively: Fig. 4.3a). Schists dominate the geology of all three areas.

The level of annual precipitation has been cited as an important influence upon RSF distribution (Radbruch-Hall and Varnes 1976,

Figure 4.4: Relationship between RSF frequency/ 100 km^2 and annual precipitation (w/e).

Eisbacher 1979b) and a visual comparison between annual precipitation and RSF distributions in the Highlands is also suggestive of a correlation.

To establish more satisfactorily whether the Scottish RSF distribution is sensitive to variations in annual precipitation, the number of RSFs occurring within 100 km^2 National Grid squares was

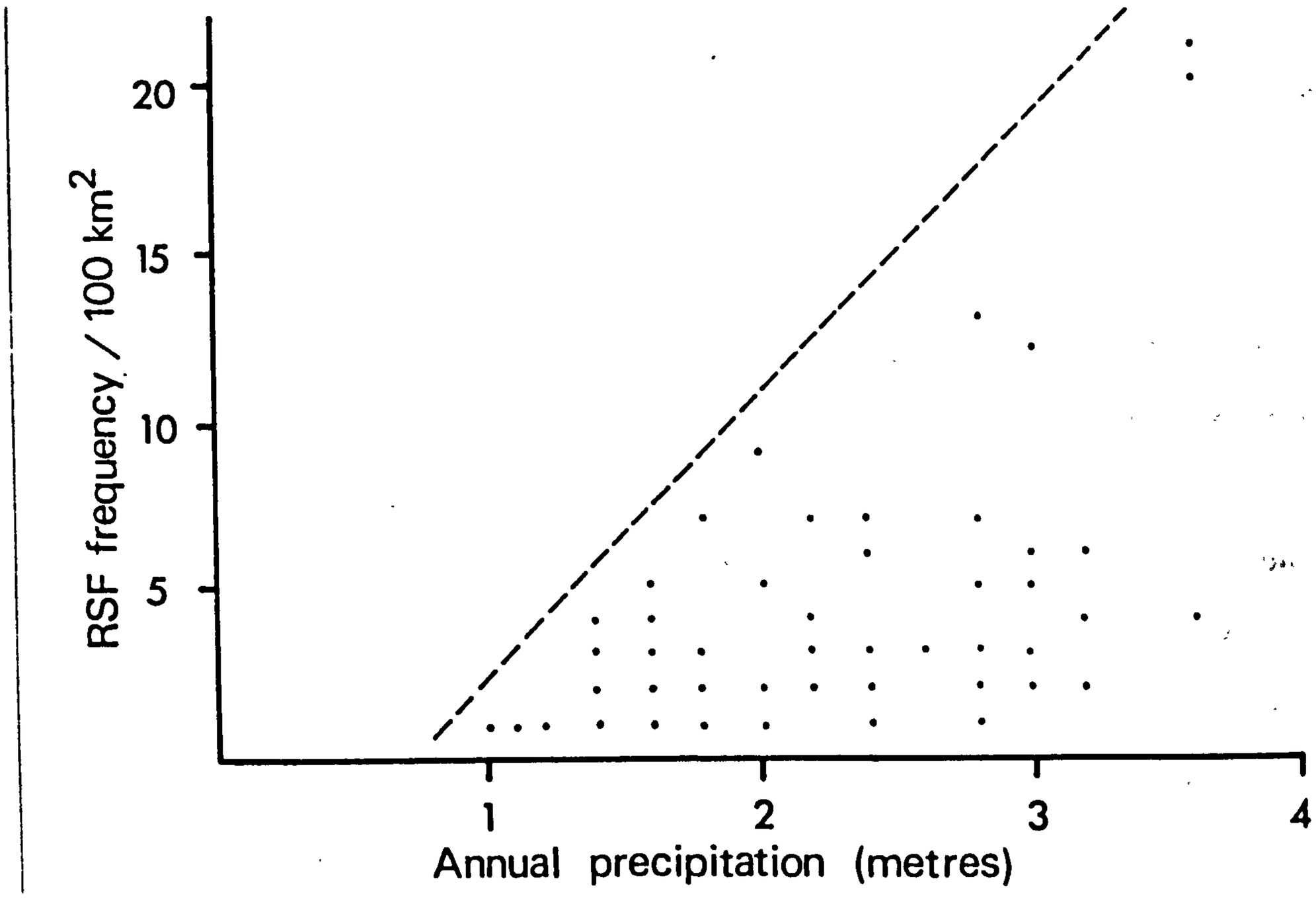

recorded with the annual precipitation value for the centre of each grid square. The results of this analysis are given in Figure 4.4. The frequency (density) of RSFs increases with increasing precipitation. The dashed-line on the graph indicating the minimum likely RSF frequency/100 km^2 for given precipitation values.

Although a statistical connection exists between annual precipitation and RSF densities, causality has not been proven. Other factors, such as the degree of glaciation (cf. Fig. 4.1), have similar

distributions to that of precipitation, which is also controlled to some extent by the distribution of mountainous areas. It could be argued that if increased rockfall frequency was related to excessive accumulation of water in the past (e.g. Grove 1972) then the spatial variation in rainfall should influence RSF occurrence. However, any relationship is likely to be complex.

It was stressed in Chapter 2 that the orientations of discontinuities such as joints and foliation control the failure modes of rock. A relationship between rock structure and the occurrence of RSFs in the Highlands should be expected.

As the RSF location data were collated, dip angle and azimuth data (if known) of joints and foliation near to each RSF were recorded from geological maps. It soon became obvious that the foliation, bedding and joint measurements recorded on the Geological Survey maps were insufficiently detailed to permit testing of the hypothesis at the inventory level. Detailed joint surveys (described later) established that even where several joint sets occur on a slope only 1 or 2 are recorded on the official Geological Survey maps. Moreover, the joint sets shown on the geological maps may not be those critical in understanding why a RSF occurred at a particular location. The structural controls upon the mode of failure are investigated in greater detail in Chapters 6, 7 and 8.

Some explanation of individual RSF locations may be made with reference to the orientations of the debris-less RSFs and <u>in situ</u> RSFs. Figure 4.5a gives the orientations of <u>in situ</u> RSFs. All

Figure 4.5: (a) Orientations (in 10° intervals) of <u>in situ</u> RSFs

(b) Orientations of debris-less RSFs

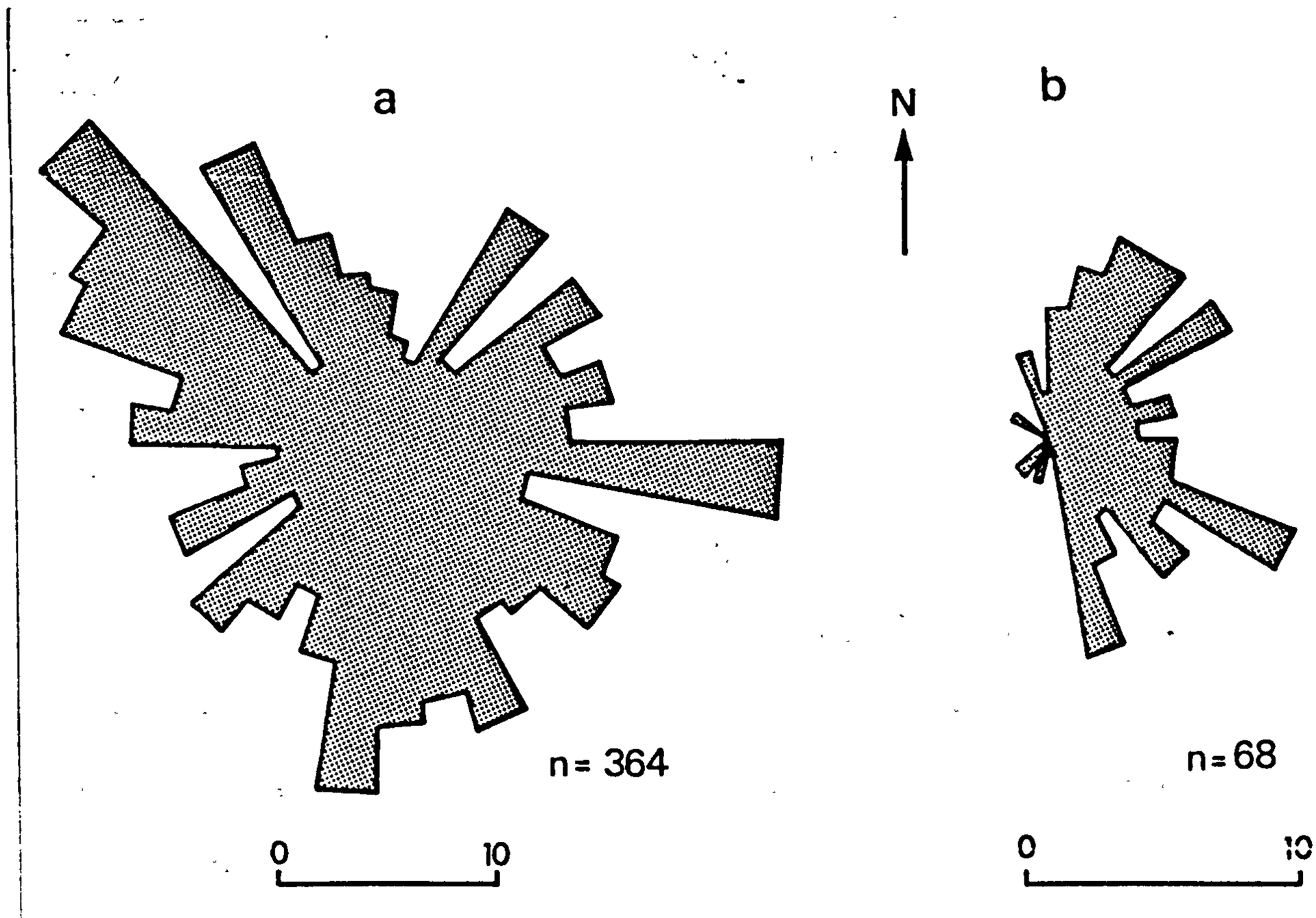

orientations are represented but there is a slight NW-SE preference in the data. The latter probably reflecting the main valley-axis directions in the W Highlands (E-W and NW-SE) where the majority of RSFs are located. Debris-less RSFs (Fig. 4.5b) show a strong easterly preference with 60 examples (88%) having orientations between 0 and 170°.

In situ RSF and debris-less RSF positions are given in Table 4.2. Significant differences occur in the two data sets. Valley side positions account for 68% of the in situ RSFs, compared to the 35% of debris-less RSFs that occur on valley sides. Relatively higher percentages of debris-less RSFs occur in spur and corrie-backwall positions, compared to in situ RSFs.

Position	In situ RSFs	Debris-less RSFs
valley side	248 (68%)	24 (35%)
valley crest	56 (16%)	15 (22%)
spur	37 (10%)	15 (22%)
mountain top	12 (3%)	3 (5%)
corrie headwall	11 (3%)	11 (16%)

Table 4.2: RSF Frequencies within the position classes, n= 432.

There may be a rock mechanics explanation for the preferred position of debris-less RSFs. Spurs are geometric weakpoints of mountains (Gerber and Scheidegger 1969, Whalley 1974) which may be oversteepened by selective glacial erosion because of their relative exposure. It may be argued that slopes in spur and corrie backwall positions, having suffered relatively greater erosion, may fail first (and have a greater chance of being transported along a glacier surface) than slopes occupying other positions.

The strong easterly orientation of debris-less RSFs suggests that a combined climatic-rock mechanic effect may have operated. The orientation data may be biased however by the preferred attitudes of corries and spurs. Corrie aspects are dominantly NE facing and as corrie-headwalls are arcuate in plan, RSFs with corrie headwall positions should be expected with NE, E and SE aspects. The aspect and positional data for all RSFs (Table 4.3) provide some evidence for this.

Numerous RSFs are sited midway up a slope and do not extend to the valley floors. This observation contradicts Muller's (1964) statement that the preferred position of a failure-plane outcrop will

be at the slope foot where shear stresses are greatest. A possible explanation for the preferred mid-slope positions of the Scottish RSFs is given in Section 4.5.

Position	Aspect			
	0-89°	90-179°	180-269°	270-359°
valley side	61 (23%)	74 (27%)	61 (23%)	75 (28%)
slope crest	24 (34%)	24 (34%)	10 (14%)	13 (18%)
spur	12 (25%)	21 (44%)	5 (10%)	10 (21%)
mountain top	4 (29%)	3 (21%)	3 (21%)	4 (29%)
corrie headwall	5 (20%)	15 (60%)	2 (8%)	3 (12%)

Table 4.3: Frequency (row% in brackets) of RSF positions/aspects

Explanation of the spatial distribution of both RSF individuals and population is further enhanced when RSF locations are compared with the known limits of the Loch Lomond Advance glaciers. The correlation is best observed on 1:50,000 or larger scale maps, examples of which will be given later (see also Fig. 4.1). A summary statistic however has been used to simplify the locational data. The horizontal distances of RSF centroids from the upper limits of Loch Lomond Advance glaciers (if present) in contiguous valleys/corries have been measured. Distances of RSFs from glacier limits are classified in 200-m-intervals in Appendix B. All RSFs are included in areas where the glacial limits are known.

A 30% sample of RSFs (133 cases occur in areas where the extent of the Loch Lomond Advance is known in detail) has been analysed and the distances of their centroids from the former glacier limits are summarised in Figure 4.6. Although the accuracy of the distance

measure may be criticised, it provides an initial indication of the nature of the spatial correlation between RSF locations and former

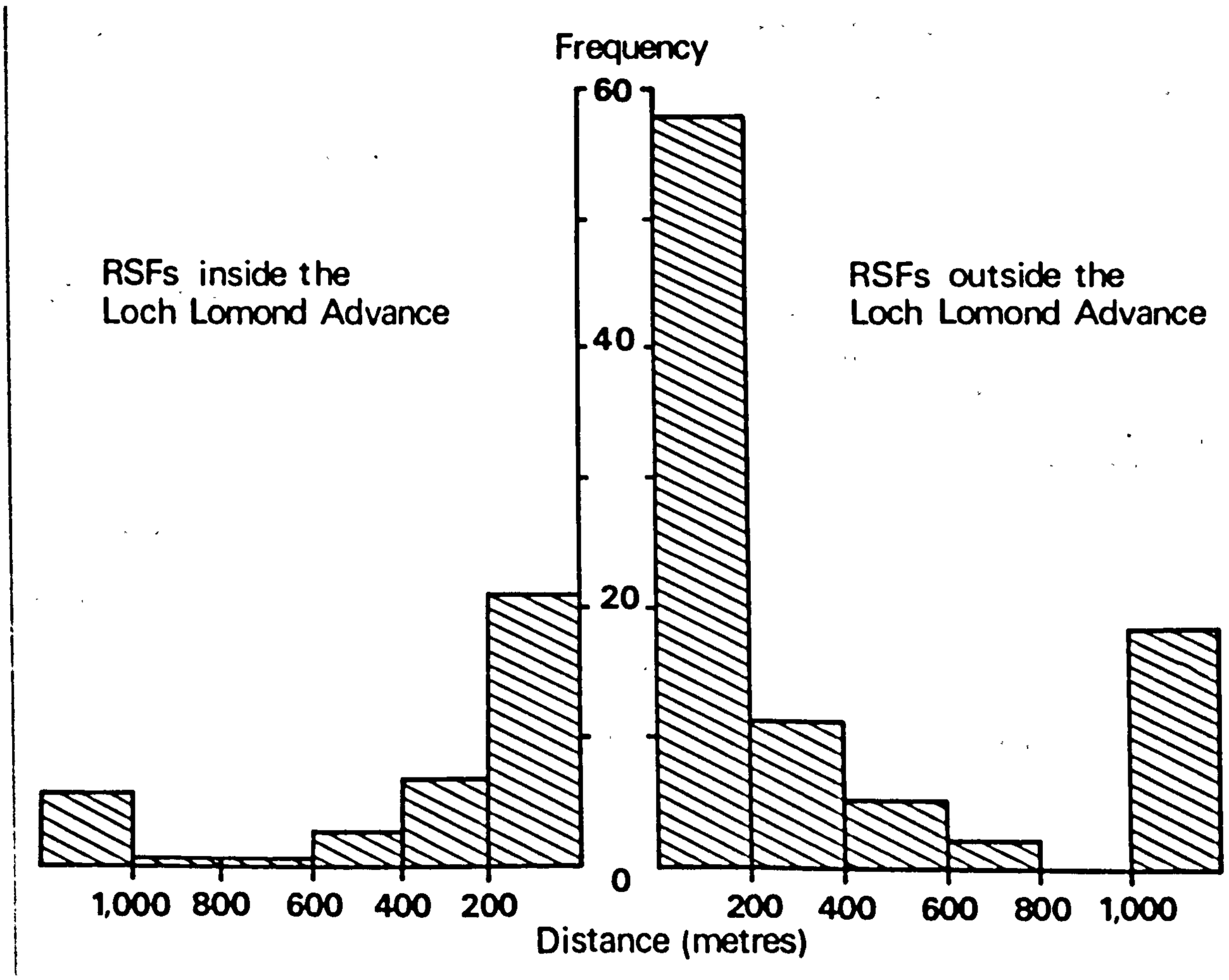

glacial limits and is an advance on previous work which purported to demonstrate a spatial correlation between RSFs and glaciers (e.g. Whalley et al. 1983).

Accepting the limitations of the descriptive measure of distance, a remarkable correlation has been found to exist between RSF centroids and the upper limits of the former glaciers. Some 59% of the sample RSFs occur within +/- 200 m of the upper limits of former glaciers and a total of 79% occur within +/- 600 m. Of greatest interest however is that 44% of the sample RSF centroids occur within 200-m-outside the upper limits of the former glaciers.

The Loch Lomond Advance glaciers must therefore have led either directly or indirectly, to rock-slope instability and the cause(s) of instability must also have had their greatest affect when the former glaciers were at, or close to, their limits. Possible causal mechanisms are discussed in the following section.

4.5 Glaciers and rock-slope stability

The proximity of RSF centroids to glacier limits might be cited as evidence of glacial oversteepening. There are difficulties however with the oversteepening mechanism. Relatively few RSFs (29% of the sample) are sited inside the former glacial limits, where the slopes could have been oversteepened by the Loch Lomond Advance glaciers. A second problem is that if glacial oversteepening was the only triggering mechanism, then a greater proportion of the RSFs should have interacted with glacier ice, as slopes would have failed comparatively soon after the lateral support provided by glaciers was removed. The preferred positions of debris-less RSFs indicate that glacial oversteepening may have been important at spurs and at corrie backwalls but less so on valley sides (further discussion of this point is made in Chapter 10).

Whalley (1974) has suggested a model for the increased frequency of RSFs in formerly glaciated areas which may explain the correlation of RSFs with former glacial limits without recourse to the oversteepening mechanism. He considered the most important RSF trigger was high cleft-water pressure build up in rock-slopes. Adapting the ideas of Terzaghi (1962), Muller (1964) and Bjerrum and Jørstad (1968), Whalley hypothesised that glaciers raise water-tables

within adjoining mountain slopes (Fig. 4.7a,b). This would increase the shear-stresses acting upon discontinuities lying immediately above the margins of glaciers and may have caused failed debris to fall onto glacier surfaces. It would also increase the slope areas affected by cleft-water pressures. Whalley asked:

> 'is it possible ..... that the presence of glaciers merely provides a supply of water for rock failure?' (Whalley 1974; 29).

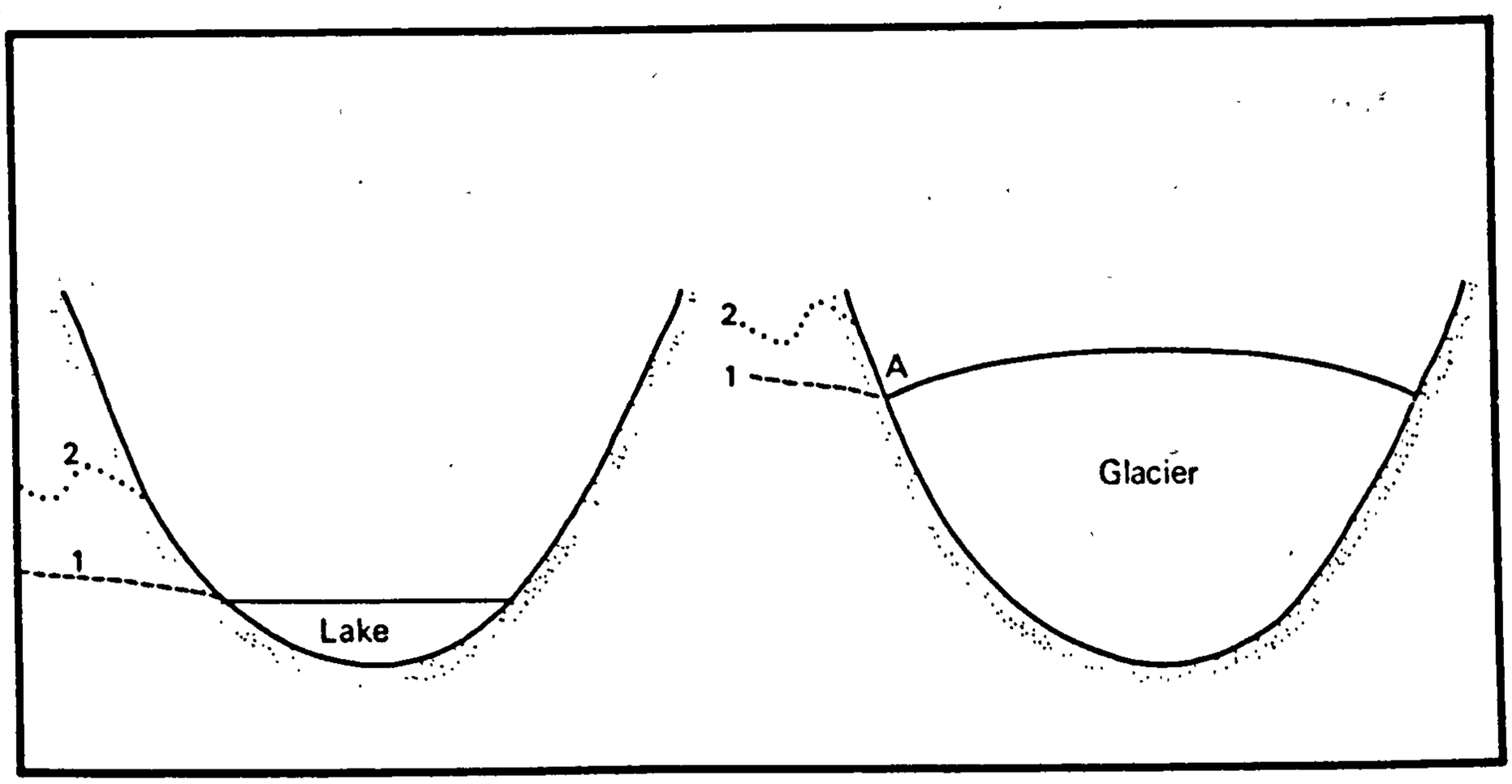

He also suggested that high cleft-water pressures would be most important in deglacial times.

During glacier advances/readvances, discontinuities lying inside the glacier limits would be subjected to cleft-water pressures but would be successively covered whilst new potential failure lines were exposed to increased shear stresses as mountain water-tables rose in response to rising glacier surfaces. Whalley (1974) hypothesised that rapid deglaciation could cause a "drawdown affect" where a perched water-table was produced: a similar destabilising process is thought to occur when a reservoir is rapidly drained

(Terzaghi 1950). Whalley noted that considerable variations in the altitudes of glacier surfaces may occur over decades and that such rapid changes would be conducive to slope failure.

If deglaciation occurred under a cold regime however, a possibility that Whalley did not discuss, then freezing of the outer layers of rock-slopes could have produced perched water-tables (Fig. 4.7b). It was observed earlier (p 17) that one of the most significant destabilising forces that may act upon an undrained slope is a static or rectangular cleft-water pressure distribution. A rectangular distribution, it was suggested, could occur if joint exits were frozen. Whalley (1974) proposed that freezing of the outer layers of a rock-slope could raise mountain water-tables above the levels associated with glaciers though he did not refer explicitly to the increased shear stresses that would be produced by the rectangular pressure distribution of water confined to joints by freezing.

If a perched water-table within a rock-slope was left above the glacier surface then the region of maximum stress where the rock-slope was unconfined (Addison 1981), would be located theoretically at the junction between the glacier margin and the rock-slope (A in Fig. 4.7b). It is not clear whether Whalley (1974) considered that mountain water-tables could have been affected by freezing in extra-glacial areas. He stated that the melting of snow patches outside the immediate vicinity of glaciers could have provided sufficient groundwater for slope failure.

The large numbers of meltwater channels and extensive fluvioglacial deposits which lie outside the Loch Lomond Advance

limits (Sissons 1967, 1976a, Young 1974, Sugden and Clapperton 1977) indicate that copious amounts of meltwater were released during the melting of the last ice sheet. If high cleft-water pressures are accepted as an important cause of rock-slope failure then it may be hypothesised that many of the RSFs that lie outside the Advance could date from the deglaciation of the last ice-sheet.

However, assuming that the sample data can be extrapolated to the population only 19% of the population of RSF centroids occur greater than 400 m horizontal distance outside the limits of the Loch Lomond Advance (cf. Fig. 4.1). In addition, some 2% of the debris-less RSFs occur inside the limits and may therefore pre-date the Loch Lomond Advance. Even accepting the maximum number of c. 21% of the population, which may have occurred during the deglaciation of the last ice sheet, the greater majority of RSFs are clearly associated with the limits of the Loch Lomond Advance. A possible explanation is offered for these data.

Rock slopes above glacier surfaces may be subjected to a gradual weakening process due, possibly, to fluctuating high water-tables (Bjerrum and Jørstad 1968) and the build-up of static cleft-water pressures if joints were frozen. If the last ice sheet was sufficiently thick to leave only the highest Scottish mountains above its surface as nunataks, then few rock-slopes would have been exposed to freezing of their outer layers and the consequent affects on cleft-water pressures. Although rock-slopes within the limits of the last ice sheet may well have been exposed during deglaciation to high cleft-water pressures, none of these would have already suffered

significant and, more importantly, localised weakening, and therefore would not have been as prone to failure. Because of the nature of glacier advances/retreats discontinuities immediately below, at and immediately above the former glacier limits would theoretically have suffered the weakening process for the longest period of time.

It is possible to relate some of the RSFs that occur greater than 400-m-outside the Loch Lomond Advance to readvances of the last ice sheet (specific examples are discussed in Chapter 5) and it will be interesting to compare the remainder with other glacial limits when/if they become available. The weakening process is therefore not considered to have been confined to the Loch Lomond Advance but may have occurred during previous glaciations where rock-slopes were only partially covered by ice at readvance limits.

Taking the number of debris-less RSFs in addition to those that show morphological evidence indicative of minor disturbance by glaciers, some 17% of the RSF population are known to have interacted with glacier ice. The proportion that occurred during the Loch Lomond Advance is unknown.

The in situ RSFs that are located inside the Loch Lomond Advance limits (27% of the sample) must postdate the deglaciation of their areas. For these examples and those in situ RSFs that are sited at the former glacial limits a delayed-response between deglaciation and slope failure must have occurred. Possible reasons for the delayed-response and evidence on its relative duration are suggested in Chapters 9 and 10. Whalley et al. (1983) stated that progressive-failure of slopes (p 23) caused the delayed-response of RSF to

deglaciation in Iceland. Progressive-failure of rock-slopes has also been invoked for RSFs in Scandinavia (Bjerrum and Jørstad 1963, 1968) and in Canada (Wyrwoll 1977). According to Bjerrum and Jørstad (1963; 173):

> 'A considerable part of the delay of rock slides in Norway is caused by the fatigue effect produced by the intermittent increase and decrease of the cleft-water pressure'.

These affects, as noted earlier, would be compounded at former glacier margins, where melting and re-freezing at the begining and end of each ablation season would have caused rapid peizometric-level fluctuations.

4.6 Conclusion

Four-hundred and thirty-two RSFs, affecting a total area in excess of 76 km^2, have been mapped in the Highlands. Two subclasses of RSF have been identified, debris-less RSFs and <u>in situ</u> RSFs. The first type do not have debris beneath their scars and are thought to have interacted with former glaciers which have swept or carried away their failed debris. The failed-debris belonging to the second type of RSF have not been removed. Sixty-eight debris-less RSFs and 364 <u>in situ</u> RSFs have been mapped.

The spatial distributions of both forms of RSF have been analysed at the population and individual scales and it is inferred that different factors influence their locations at each scale. At the population level rock type was found to be important, particularly the different forms of schist which account for 80% of a sample. The distribution of RSFs follows closely the outcrop of the Moinian and

Dalradian Series, where schists predominate. Few RSFs occur in granite and the comparatively high shear strength of this rock type has been invoked to account for the dearth of RSFs in the Cairngorms Mountains. Discontinuity orientations are thought to determine whether a slope failure takes place at a particular site. Areas of high RSF density occur within the Highlands and have been correlated with high annual precipitation values, though causality has not been demonstrated.

The position of an individual RSF on a slope is considered to be partly a function of the limits of the Loch Lomond Advance glaciers. Some 56% of a sample of RSF centroids occur less than 600-m-outside the Loch Lomond Advance limits and a further 23% are sited 600 m, or less, within the limits. Most importantly 44% of the sample occur within 200-m-outside the Loch Lomond Advance limits.

It is hypothesised that fluctuating mountain water-tables, raised by the proximity of glaciers and the possible build-up of static cleft-water pressure distributions due to freezing of the outer layers of slopes, weakened discontinuities in the vicinity of the upper limits of glaciers. This mechanism would be most effective when a valley glaciation leaves portions of slopes uncovered by ice. Detailed examination of case study rock-slope failures are required to test this hypothesis. Such data will be examined in Chapters 6, 7 and 8 after brief discussion of the field areas and the field techniques in the following chapter.

5: FIELD-AREA DESCRIPTIONS AND FIELD TECHNIQUES

5.1 Introduction

This chapter provides an introduction to later discussions of the case studies within the field areas. Section 5.2 provides brief descriptions of the topography, solid geology and Lateglacial history of each field area. Section 5.3 discusses the field techniques used in this study.

5.2 The field areas

The selection of field areas was enhanced by the aerial-photographic reconnaisance survey which was used to compile the inventory of rock-slope failures. Data and experience accrued during the survey enabled a number of criteria to be used in field area selection, these favouring areas where:

(i) former glacier limits were known or were in the process of being mapped, including areas where pre-Loch Lomond Advance limits were known:

(ii) interesting examples of rock-slope failure were located. These included sites where possible fault-scarps and complex modes of failure occurred or where morphological relationships between RSFs and periglacial features were observed;

(iii) previously unstudied examples of RSFs are located. Most of the case studies were not listed by Watters (1972) and some are not mapped on official Geological Survey maps.

Figure 5.1: Locations of the field areas:

1 = Fannich Mountains

2 = Glen Clova

3 = Affric/Kintail

4 = N Cowal.

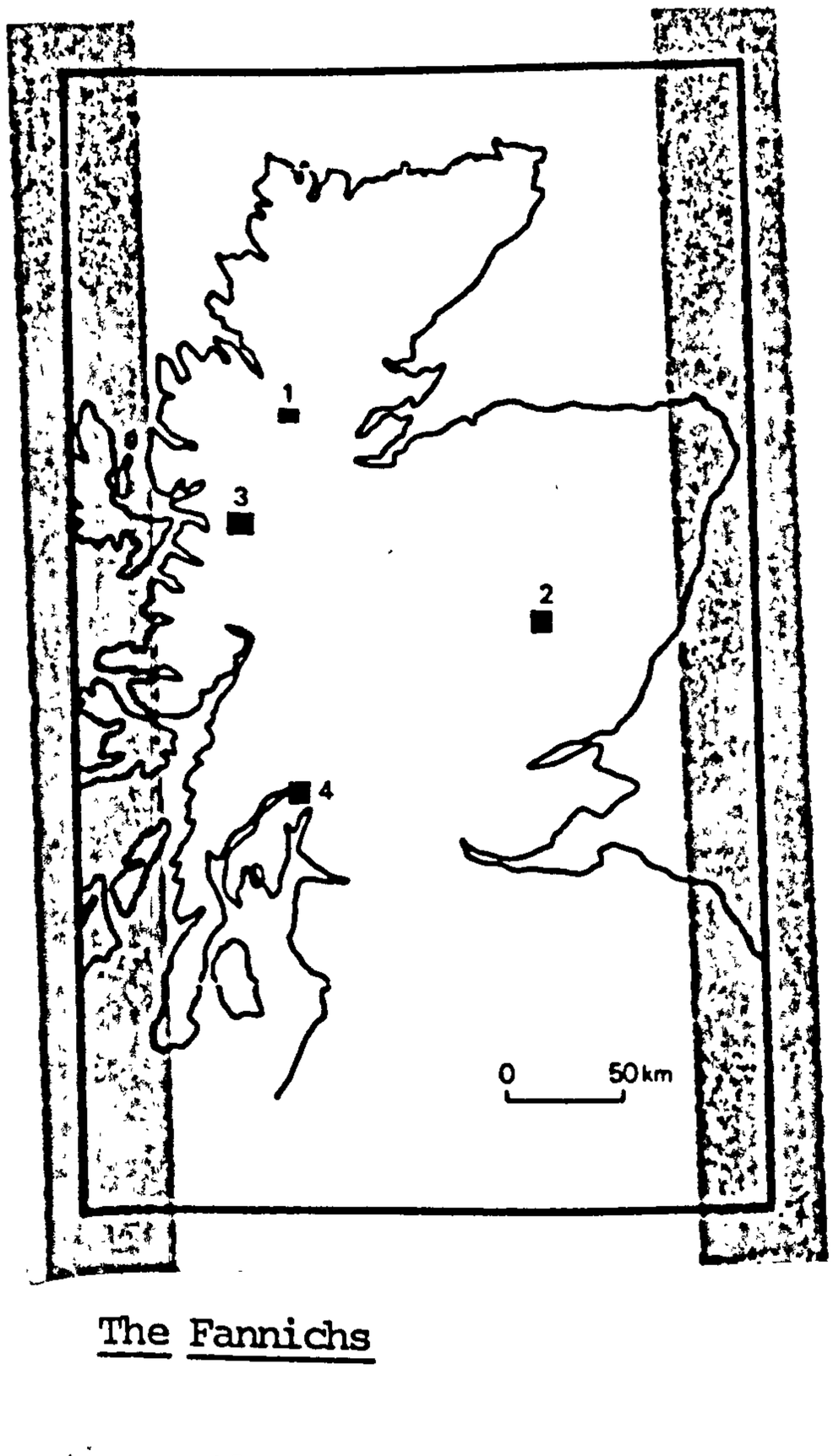

The Fannichs

Field area choice was a function of all these considerations, though each criterion varied in its importance for selection of the individual area. Four field areas were chosen: the Fannich mountains [5°, 57° 40'N], Glen Clova area [3° 15'W, 56° 51'N], Kintail-Affric area [5° 10'W, 57° 15'N] and N Cowal [5° 53'W, 56° 12'N] (Fig. 5.1). The last two field areas were identified in Chapter 4 as being areas of high RSF density.

The Fannichs are a mountain group located N of Loch Fannich, central Ross-shire, which culminate in Sgurr Mór (1,110 m O.D.). Gneisses and schists of the Moine Series dominate the geology of the area, though Lewisian gneisses crop out along the N shore of Loch Fannich and on the floor and S side of the Nest of Fannich, a large compound corrie. The mean annual rainfall of the area is 2,600 mm. Three RSFs were studied in this field area, the two largest are located in the Nest of Fannich (1a and 1b in Fig. 5.2), the third (1c) being in Garbh Choire Mór.

The Fannichs lie within the much larger area of the northern Highlands in which Sissons (1977b) mapped the limits to the Loch Lomond Advance. The Nest of Fannich was unglaciated during the

Figure 5.2: The Fannich Mountains field area:

1 = former glacial limits (after Sissons 1982b)

2 = RSF and its reference number

3 = Contours (200 m intervals).

Figure 5.3: The Glen Clova field area:

1 = Limits of the Loch Lomond Advance (after Sissons 1972)

2 = RSF and its reference number

3 = Contours (200 m intervals).

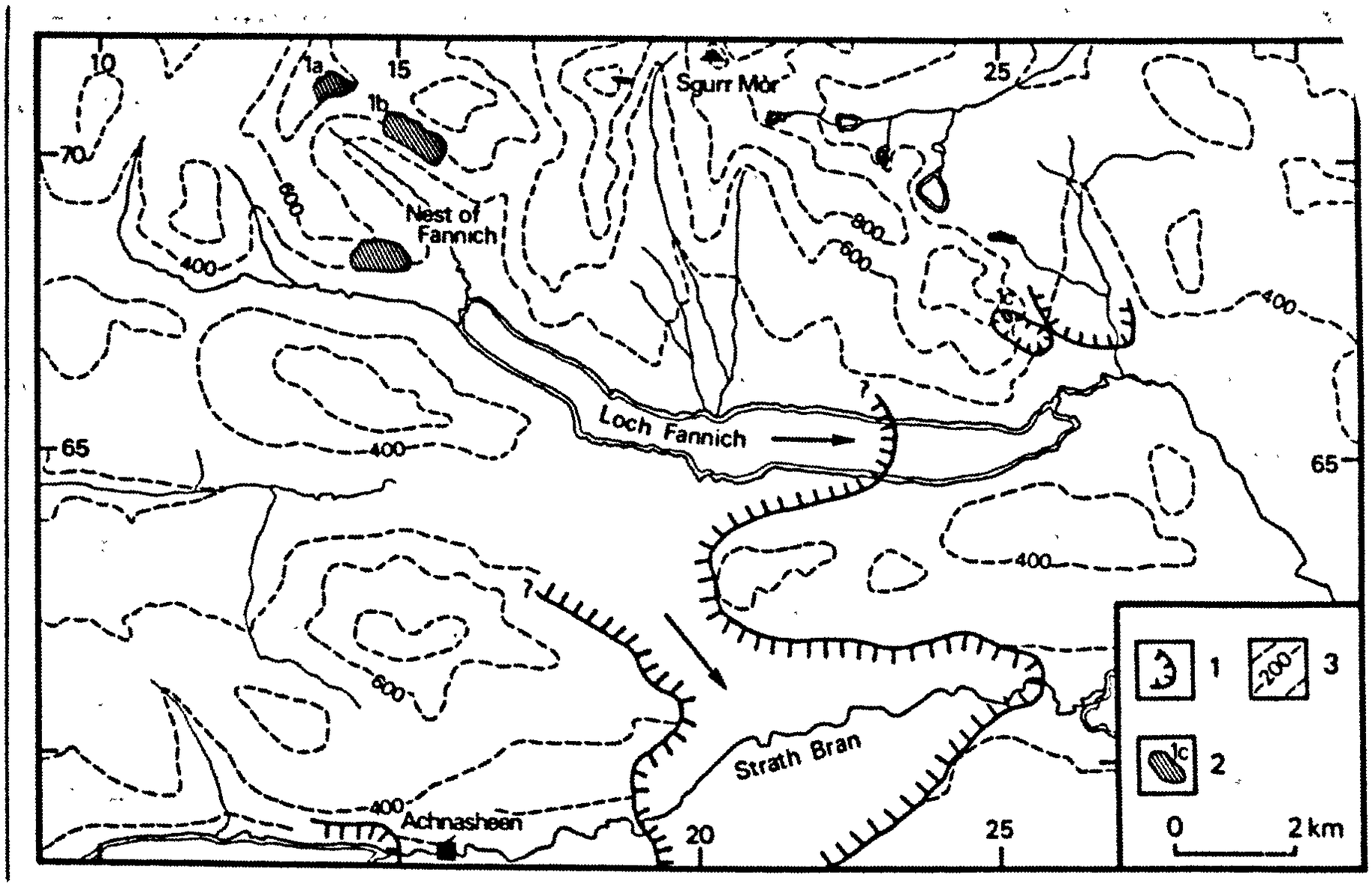
10
15
25
1a
1b
Sgurr Mòr
70
600
Nest of Fannich
400
800
600
400
Loch Fannich
65
65
400
400
600
Strath Bran
400
Achnasheen
20
25
1
3
200
2
1c
0
2 km

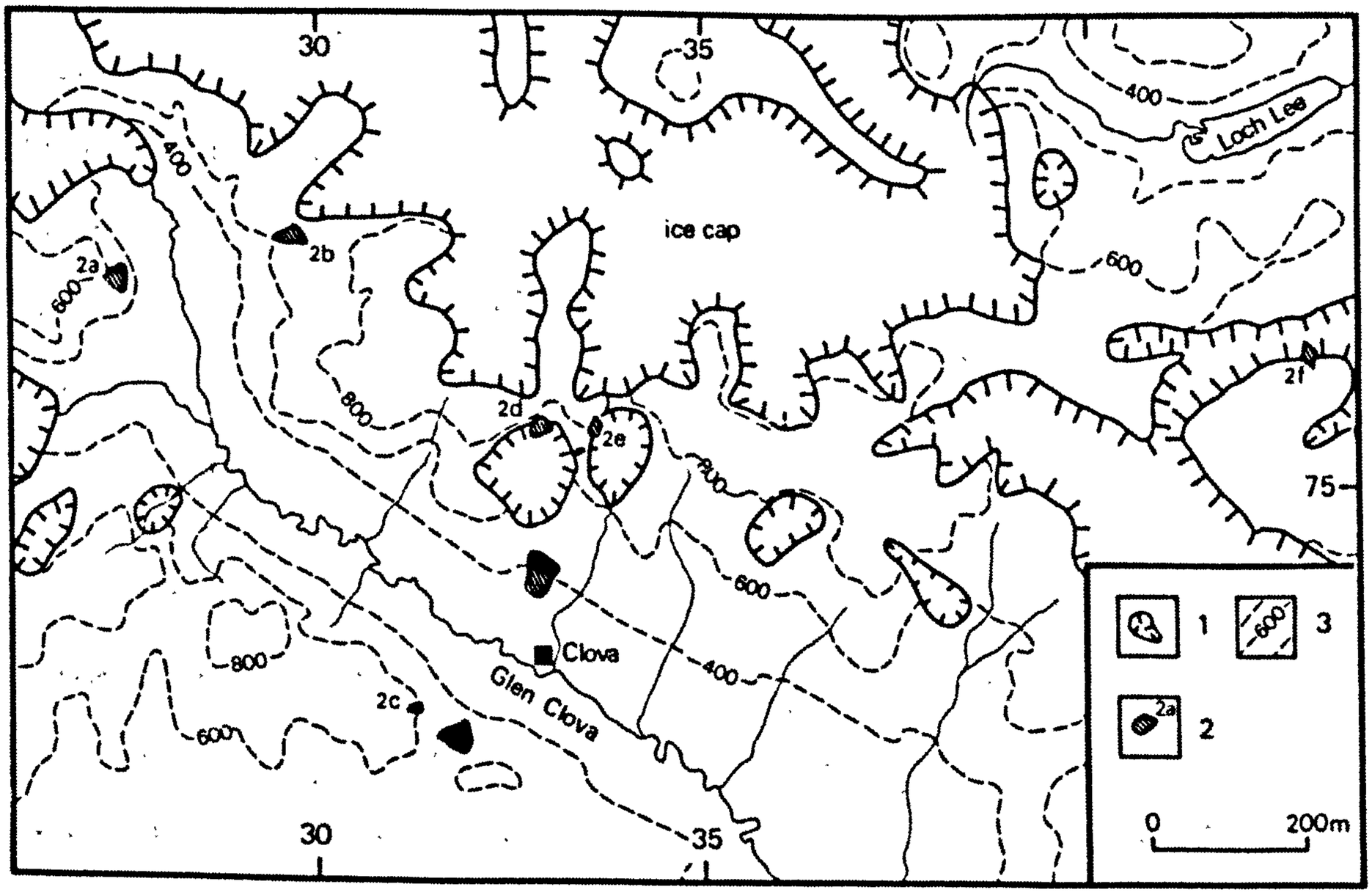
30
35
400
Loch Lee
ice cap
2a
2b
600
800
2d
2e
600
800
2f
75
600
400
Clova
800
2c
600
Glen Clova
30
35
1
600
3
2a
2
0
200m

Advance according to Sissons (1977b), but Garbh Choire Mór was thought to have contained a small glacier, as evidenced by an impressive end moraine the distal slope of which is up to 14-m-high.

The reconstructed equilibrium firn line (the location where total accumulation equals total ablation at the end of the ablation season) for the Garbh Choire Mór glacier at its maximum extent lies 190 m below that of the trend surface computed for equilibrium firn lines of other Loch Lomond Advance glaciers throughout the northern Highlands (Sissons 1977a). The glacial limits in this area have recently been re-interpreted however and the Garbh Choire Mór glacier is now considered to have pre-dated the Loch Lomond Advance (Sissons pers. comm.): which would assist explanation of its anomalously low firn line altitude.

During the Achnasheen Readvance (p 34), a glacier readvanced to the S and crossed the watershed between Loch Fannich and Strath Bran (Sissons 1982). Sissons postulated that another glacier extended c. 5 km east of this watershed and down the valley presently occupied by Loch Fannich to where its readvance limit, thought to have been achieved approximately contemporaneously with the Strath Bran glacier, is indicated by the termination of abundant drift mounds on the S shore of Loch Fannich.

Sissons traced the limit of the Strath Bran glacier around the NE side of Fionn Bheinn until at the W limit to Sissons' mapping, it attained a height of 500 m O.D. (Fig. 5.2). It is therefore probable that the Nest of Fannich was glaciated during the Achnasheen Readvance, being the nearest source for renewed glacier accumulation. Correlation between the Achnasheen Readvance glaciers and the Garbh

Choire Mor glacier, from the morphological evidence, is not possible.

Glen Clova

The geology of this field area is characterised by Dalradian felspathic gneisses with diorite intrusions at the head of Glen Clova. The main topographic feature is the 500-m-deep glacial trough of Glen Clova, which trends NW-SE and separates a remarkably uniform high-plateau (700-850 m O.D.) to the NE from more undulating topography to the SW. Seven RSFs were studied in this area (Fig. 5.4) all being composed of coarse felspathic gneiss. Mean annual rainfall equals 1,400 mm.

The Glen Clova area was partly glaciated during the Loch Lomond Stadial when a 66 km^2 ice-cap developed upon the plateau NE of Clova (Sissons 1972, Sissons and Sutherland 1976) from which distributary glaciers flowed into the valleys that radiate from the plateau. At the head of Glen Clova larger valley glaciers emanated from the high ground to the N. The S-facing corries above Clova village, despite their unfavourable southerly aspect, contained glaciers at this time One of these, the Corrie Brandy glacier, deposited an end moraine up to 14-m-high.

Affric-Kintail

This area contains some of the most impressive evidence of glacial erosion in the Scottish Highlands, featuring truncated spurs, hanging-valleys, arêtes and corries (Gordon 1977). The two highest mountains NW of the Great Glen, Carn Eige (1,183 m O.D.) and Mam Sodhail (1,181 m O.D.), are also found here. The field area is

bounded to the N and S by the E-W trending Loch Mullardoch and Glen Shiel glacial troughs respectively (Fig. 5.). Moinian psammites and pelites of variable metamorphic grade dominate the geology of the area. Pegmatites are often found trending parallel with the foliation. The annual rainfall of the area is high (3,600 mm).

The glacial sequence of this field area is poorly understood. However, an impressive end moraine near Tomich is known to mark part of the E limit of the Loch Lomond Advance Glen Affric glacier (Peacock 1975b, Sissons unpubl.). Its margin is also evidenced by a lateral moraine in Gleann nam Fiadh (Sissons unpubl.), indicating that the Glen Affric glacier reached a local maximal height of 650 m O.D. Peacock did not refer to this evidence and based his interpretation of the regional ice flow of the Affric-Kintail area upon 18 striations, limited erratic boulder evidence in Strath Clunie and the supposed over-riding of high altitude cols.

The lateral moraines at Gleann nam Fiadh and near Tomich indicate that the Glen Affric glacier was of similar dimensions to the Loch Lomond Advance Moriston glacier (Sissons 1977b) S of Glen Affric (Fig. 5.3). Correlation between the two glaciers has not been established but they are likely to have been confluent with one another through the An Caorann Mór valley.

Peacock (1975b) stated that the Loch Lomond Advance ice-shed in Glen Affric lay close to Altbeithe, though no reasons were given for the postulated ice-shed position. He further suggested that the Glen Affric glacier crossed the 600-m-high col at [NH 157 180] and the col at [NH 130 177] which rises to a height of 610 m. These data provide,

Figure 5.4: The Affric/Kintail field area:

1 = RSF and its reference number

2 = Limits to the Loch Lomond Advance (after Sissons 1982, unpubl.).

3 = Contours (200 m intervals).

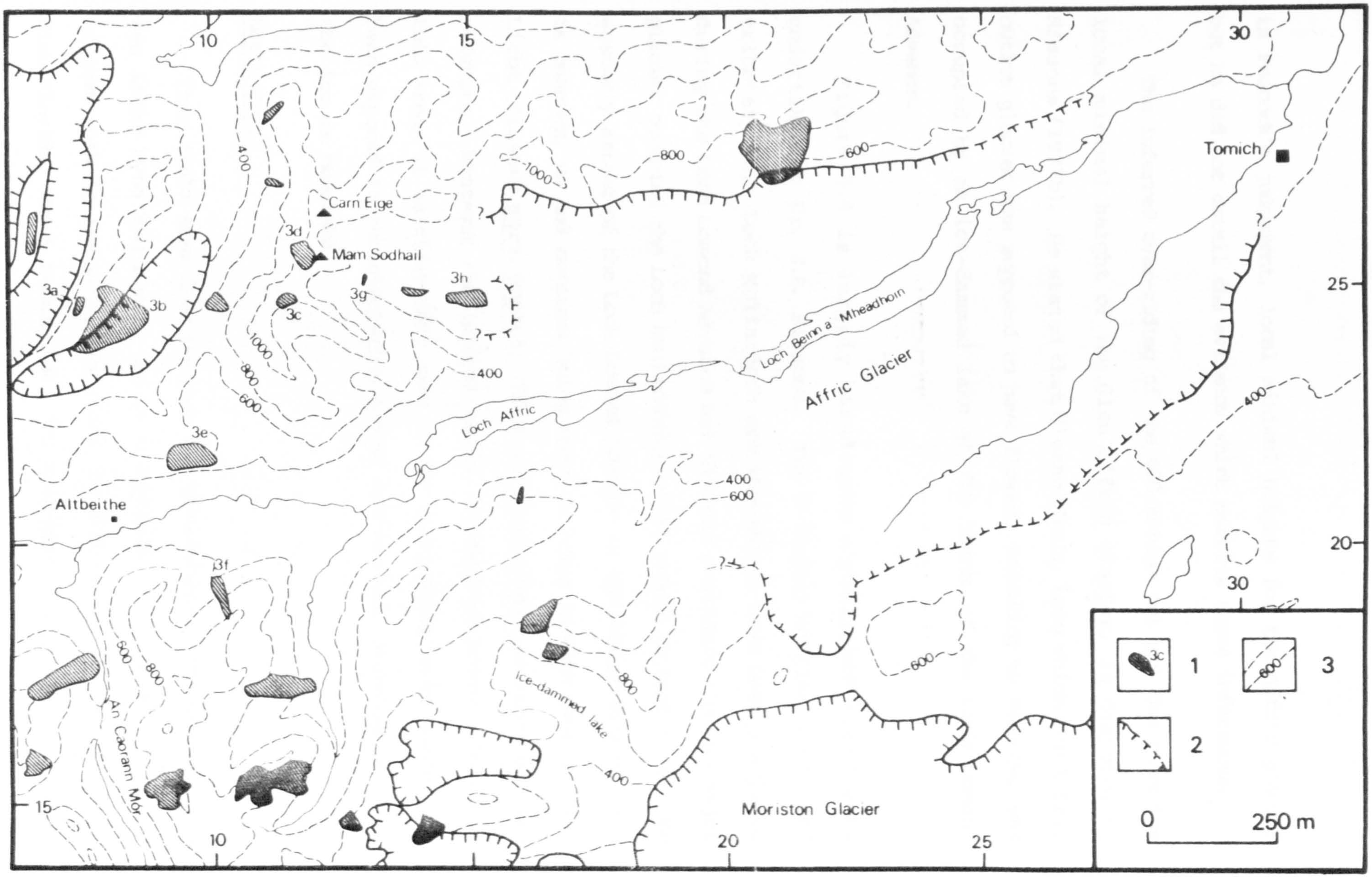
10
15
30
25
20
Carn Eige
3d
Mam Sodhail
3a
3b
3c
3g
3h
3e
3f
400
600
800
1000
Loch Beinn a' Mheadhoin
Affric Glacier
Loch Affric
Tomich
Altbeithe
An Caorann Mór
Ice-dammed lake
Moriston Glacier
1
2
3
0
250 m

in Peacock's judgement, local minimal heights for the Affric glacier but he did not detail the evidence which permits these inferences.

The inferred over-riding of the 600-m-high col and therefore the local minimal height of the Glen Affric glacier, is disputed by Sissons (1977b). He stated that Gleann Fhada, into which the Affric outlet glacier was supposed to have flowed, according to Peacock, was occupied by an ice-dammed lake at the limit of the Loch Lomond Advance.

Figure 5.4 is largely based upon unpublished field work undertaken by Dr. J.B. Sissons. The N-facing corries S of, and tributary to, Loch Mullardoch are thought to have been glaciated during the Loch Lomond Advance but Sissons considers that no major glacier occupied the Loch Mullardoch glacial trough at that time. The westerly extent of the Loch Lomond Advance in the Affric-Kintail area is unknown, no end moraines being known to occur in Glen Shiel or Glen Licht (Sissons pers. comm.). The Loch Lomond Advance limit may lie offshore. Whatever the lateral extent of the Loch Lomond Advance in this area, it is clear that many of the surrounding peaks would have been exposed to periglaciation during the Stadial, standing proud of the ice as nunataks.

North Cowal

This field area lies between the northernmost extensions of the sea lochs Fyne and Long. Beinn an Lochain (901 m O.D.) being the highest peak in the area, overlooks the 800-m-deep glacial trough of Glen Kinglas, which trends E-W. The geology of the area is dominated

Figure 5.5a: The N Cowal field area.

1 = Nunatak above the Loch Lomond Advance glaciers

2 = RSF with reference number.

Figure 5.5b: Geology of the N Cowal field area

1 = Phyllite

2 = Mica-schist

3 = Schistose grits

4 = 'Green Beds' - schistose grits with some mica-shist

5 = Main faults

6 = Foliation dip angle and direction

7 = General dip of foliation

8 = Contorted foliation

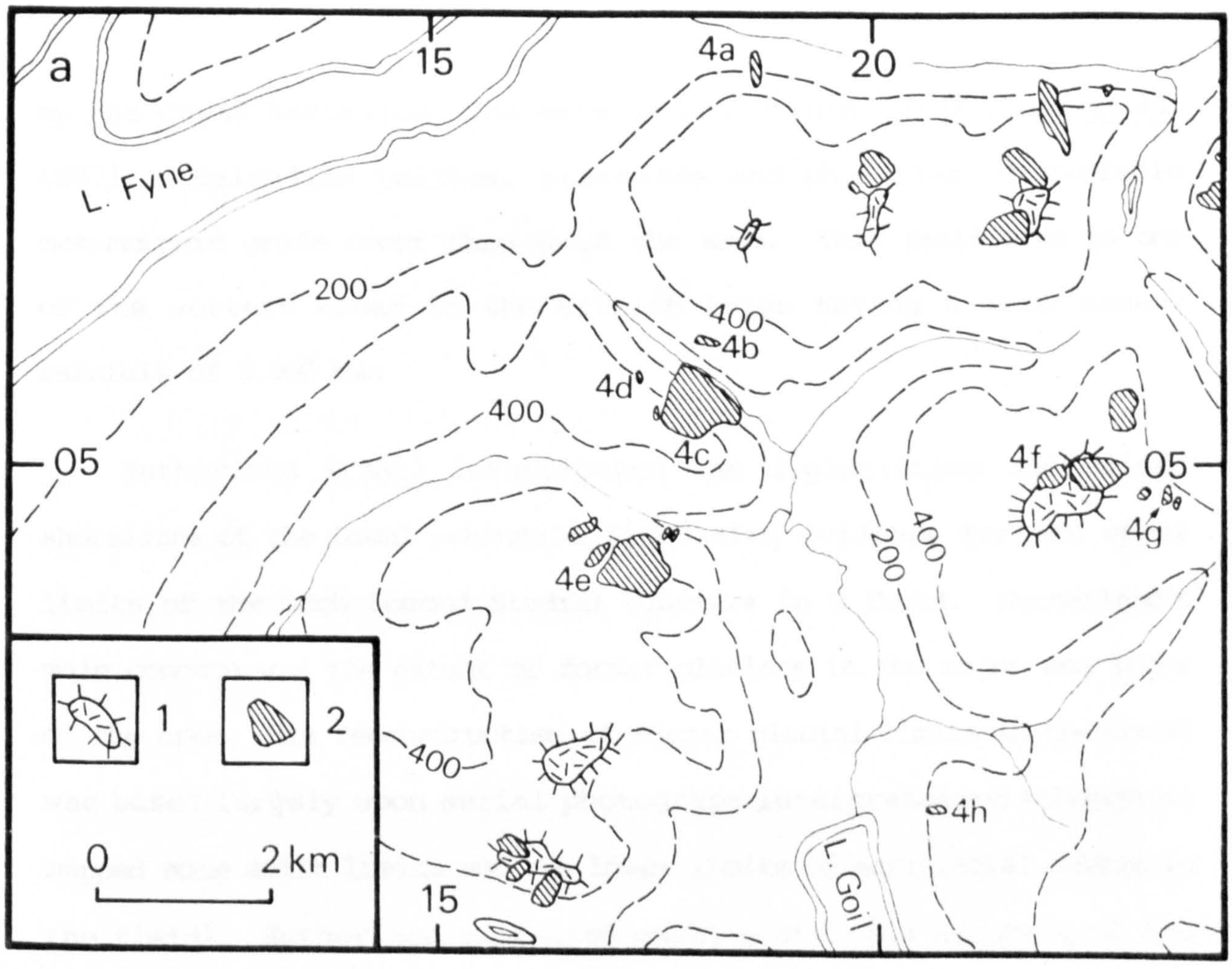
a
15
20
L. Fyne
4a
200
400
4b
4d
400
4c
05
4f
05
4g
4e
200
400
1
2
400
0
2 km
15
L. Goil
4h

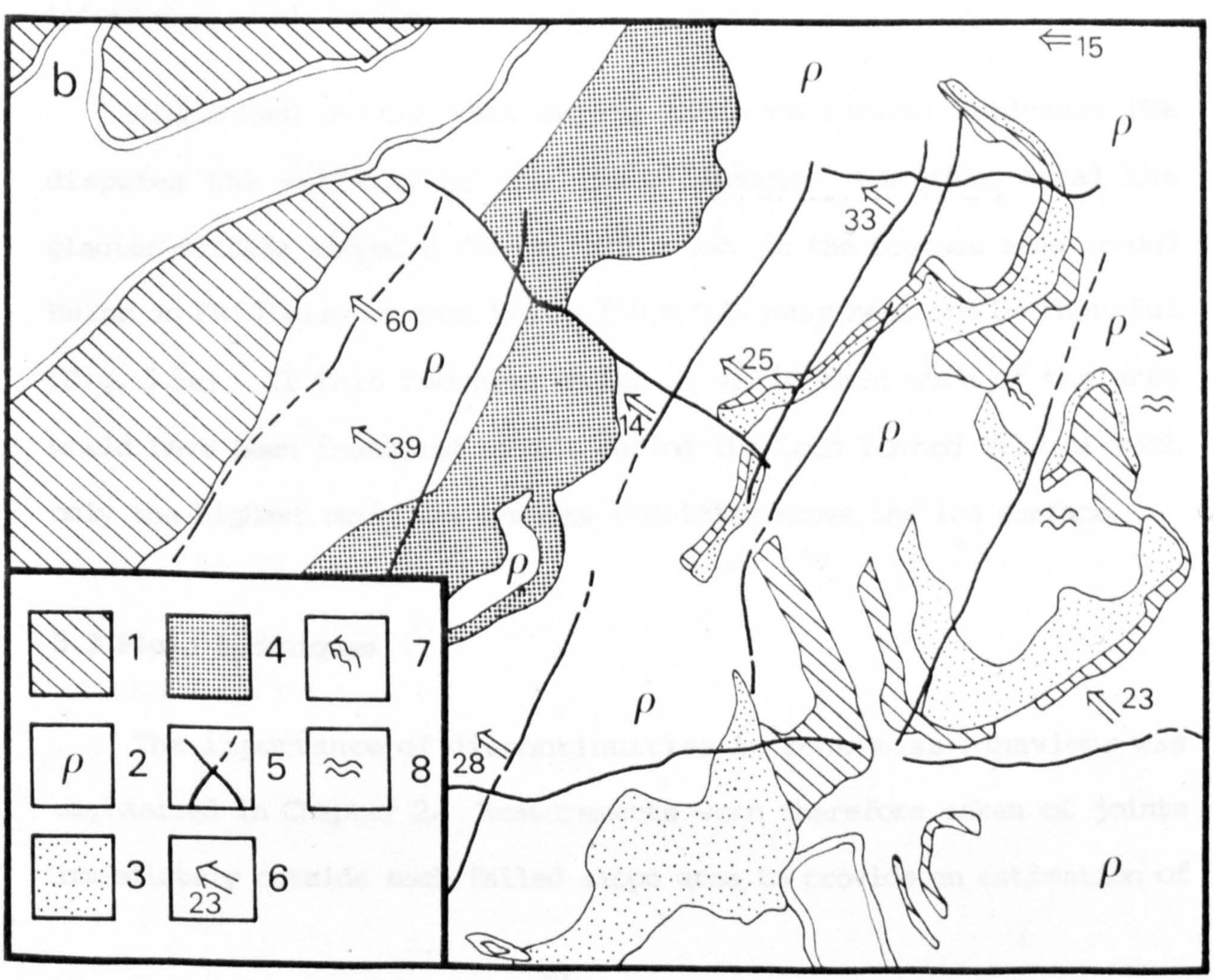
b
⇐15
ρ
ρ
33
60
ρ
39
25
14
ρ
ρ
ρ
1
4
7
ρ
2
5
8
3
6
23
28
23
ρ

by the Cowal Anticline, the axis of which runs SW-NE (Gunn et al. 1897). Dalradian pelites, psammites and phyllites of variable metamorphic grade occur throughout the area. This field area is one of the wettest areas in the British Isles having a mean annual rainfall of 3,200 mm.

Sutherland (1981) investigated the deglaciation and raised shorelines of the Cowal peninsula discussing evidence for the upper limits of the Loch Lomond Stadial glaciers in N Cowal. Sutherland's main concern was the extent of former glaciers in the major sea lochs of the area. His reconstruction of former glacial limits in the Cowal was based largely upon aerial photograph interpretation (though he mapped some drift limits and the lower limits of periglacial debris in the field). Sutherland expressed caution over the accuracy of the inferred glacial limits.

Sutherland stated that during the Loch Lomond Readvance (He disputes the validity of the term 'Advance' for this area) the glacier surface sloped S from c. 800 m O.D. in the plateau area around Beinn an Fhidleir, to just below 750 m O.D. near Rest and be Thankful (Fig. 5.5a). If this reconstruction is valid then much of the area would have been inundated by ice during the Loch Lomond Stadial with only the highest mountain summits remaining above the ice surface.

5.3 Field techniques

The importance of discontinuities in rock-mass behaviour was emphasised in Chapter 2. Measurements were therefore taken of joints immediately outside each failed slope area to provide an estimation of

the attitudes and mechanical properties of discontinuities that may have controlled failure.

Four joint characteristics were recorded: the dip angle (sometimes termed the 'altazimuth' e.g. Jaeger 1979), the azimuth, the surface roughness in the direction of shear and the sliding friction angle. Joint persistence, width and spacing were only estimated as detailed data on these joint parameters were considered to be of limited value in the post failure analyses of RSFs. The techniques used to measure dip angle, azimuth and surface roughness follow the recommendations of Brown (1981) and were found to be suited to the researcher working alone in mountainous terrain. The field techniques have not been accepted uncritically but it is considered more appropriate to discuss their accuracy in the following chapters.

Joint attitudes

A Sunto-type geological compass was used to record the dip angle and azimuth of exposed joint surfaces. In order to reduce the variability in these parameters caused by small-scale roughness (cf. Fecker and Rengers 1971) a 10-cm-radius aluminium plate was placed onto each surface prior to measurement, the true-dip angle and its azimuth were then recorded from the plate. Dip angles were measured to the nearest 2°, azimuth in 1° intervals. One joint pole value (dip angle/azimuth) was recorded for each discontinuity, care being required not to re-measure the same joint due to its repeated exposure along a sample section. At most sites 200 joint poles were measured, occasionally over areas of several hundred m^2.

Plate 5.1: Typical sample rock outcrop.

Figure 5.6: L.H. stereonet for the outcrop (arrow indicates direction of view of Plate 5.1).

All L.H. stereonets are contoured at the following intervals: 2% - 3.9%, 4% - 5.9%, 6% - 7.9%, 8% and over.

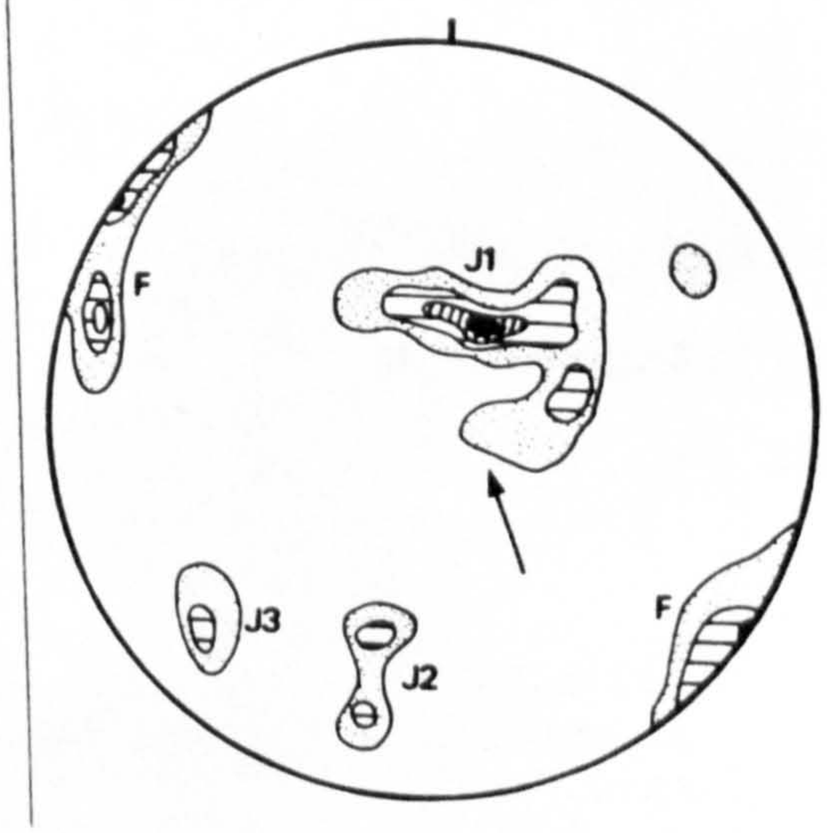

Major sampling along the face of a planar outcrop was avoided because joints striking parallel to the face may not be observed (Terzaghi 1965). Most joint measurements were made from compound surfaces. A typical sample area is shown in Plate 5.1 with the lower-hemisphere stereonet for the outcrop in Figure 5.6. The two figures demonstrate that there are no major 'blind' zones when compound surfaces are used.

Joint data were plotted onto lower-hemisphere stereonets in the field, enabling critical joint sets (areas on a stereonet with high joint densities) to be identified on site. Contouring of areas of equal pole density was undertaken in the field by hand using a 1% counting-circle, following the method described in Hoek and Bray (1977), rather than by computer mapping.

As certain joint data were collected over large areas around the margins of RSFs, the spread of joint poles about each set pole can be large. This characteristic is advantageous however as it provides an indication of the variability of joints over a large RSF site whilst still giving the statistical evaluation of the most likely attitude of joints belonging to a set. The failure-surfaces of intact RSFs (p 26)

Figure 5.7: Simplified section along a natural joint showing the method for determining i.

were estimated using the joint poles. Such interpretation must be made with care however as 'rogue' joints located at depth may go unrecorded but may still have controlled failure. As Patton and Deere (1971) observed, the orientation of a discontinuity set is a very important rock-mass characteristic and yet is one of the most difficult to quantify.

Joint roughness

An approximation of joint roughness is given on the stereonet by the distribution of poles belonging to a single discontinuity set (Goodman 1981). The joint survey data however cannot alone indicate whether variability in dip angles is due to first-order asperities or, for instance, a large-scale structural fold. Joint roughness was therefore estimated by measuring the values of i (p 12) as shown in Figure 5.7 along 10-m-long sample sections. A mean value for i was computed for joints lying outside the failed slope area using measurements of asperities with wavelengths greater than 30 cm. This arbitrary limit was selected because compared with the scale of the failure-surface smaller asperities were considered to contribute little to the failure-plane roughness. If minor asperities were measured along a sample section the computed mean i would be biased because of their larger number and high i values.

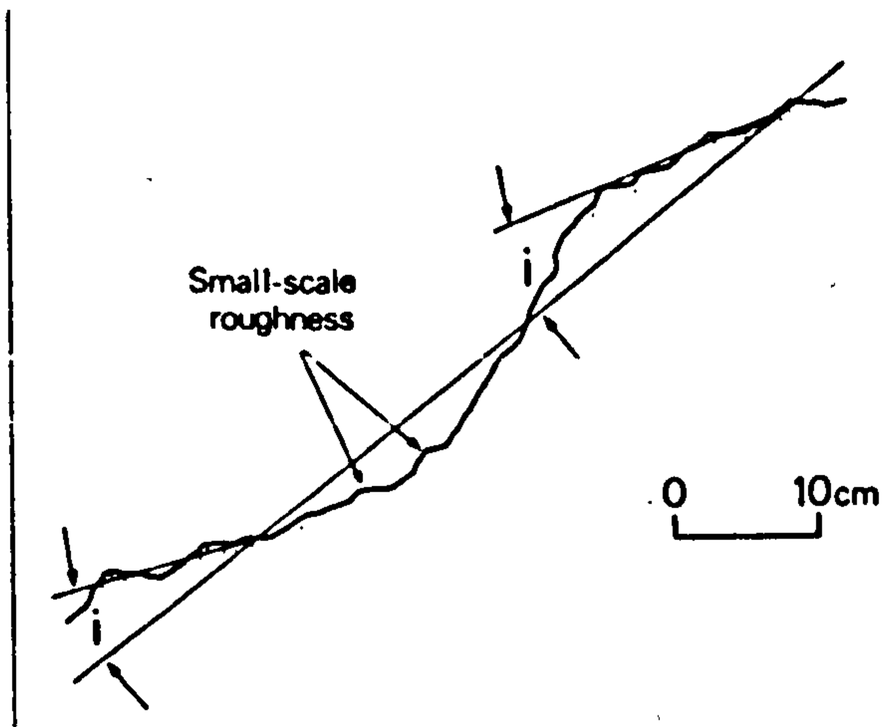

Sliding friction angle

Tri-axial shear testing of rock joints was not justified for this

study, particularly as most Highland metamorphics (excluding gneiss) had been tested by Watters (1972). A cheap alternative was therefore required to derive ϕ values for gneiss and to check the data from the triaxial tests given in Watters (1972). Schmidt hammers, devices which impact a known mass against a test surface recording the distance of rebound, have been used by engineering-geologists to evaluate the shear strength of rocks (e.g. Barton and Chaubey 1977). The hammer measures the 'hardness' of a rock surface but is sensitive to the presence of discontinuities below test surfaces. The rebound numbers (R) may be lowered by a hair line fracture below the surface by over 20%. The hammer cannot be used with confidence on metamorphic rocks as at least 6 cm of intact rock must lie below the surface which is tested (Selby 1982). The presence of foliation planes with mean spacings of less than 1 cm prevented its use in this study.

A simple estimate of the effective ϕ however may be provided by tilt-tests on rock joints (Cawsey and Farrar 1976). Two mating halves of a rock joint are required. The blocks are matched together and tilted slowly until the uppermost begins to slide, the angle of the lower block from the horizontal is then recorded. Despite the simplicity of the technique, correlations between the sliding friction angle and ϕ values derived from shear tests were noted by Cawsey and Farrar (1976). Henscher (1976) also observed a correlation between values for ϕ obtained from various shear apparatus and the sliding friction angle. The results of the sliding friction tests for a number of rock types are given in Appendix C. These tilt test data are plotted as histograms, the modal values of which are used in subsequent analyses.

It should be noted that a major drawback of the sliding friction angle test is that it is difficult to evaluate ϕ_r. Additionally, the test is particularly sensitive to small-scale roughness, as the normal stresses on the test surfaces are low (Henscher 1976). Although, therefore, the tilt tests are made along planar surfaces which, according to Goodman (1981), should have friction angles close to the residual, the sliding friction angle is likely to be higher than ϕ_r.

Definition of RSF geometries

The geometry of RSFs must be defined accurately for limit-equilibrium models. Slope angle data, in particular, are also required by the kinematic tests. The average slope angles of large slopes may be computed with reasonable accuracy from topographic maps (the field maps used in the geomorphological mapping were all enlarged to 1:5,000-scale plans). More detailed data are usually required because a failure-plane may crop out in a minor but steeper than average portion of the slope.

The only one-man survey technique available was that described by Sissons (1976b) which uses: an Abney level, measuring tape and ranging-poles. A prismatic compass was also used to prepare large-scale plans of RSFs. Straight-line traverses, recording slope angles and the length of the slope, were controlled by positioning ranging-poles along a compass bearing. The Abney level was sighted onto each ranging-pole (station) whilst rested on top of a ranging-pole. Variations in heights between sections were computed using simple trigonometry. Sissons considered this technique to be accurate to 1 metre.

6: TRANSLATIONAL MODES OF ROCK-SLOPE FAILURE: FIELD EXAMPLES

6.1 Introduction

This chapter deals with field examples of translational (cf. plane- and wedge-sliding) modes of failure and, like Chapters 7 and 8, addresses itself to the mode of failure and the processes that caused failure. Five examples of plane-sliding are discussed in Section 6.3 and five wedge-slides in 6.4.

Translational modes of rock-slope failure have been recognised by a number of geomorphologists (e.g. Rapp 1960, Wyrwoll 1977, Eisbacher 1979a, Addison 1981). Most of the data on translational modes of failure however have been accrued by engineering-geologists. Hoek and Bray (1977), Voight (1978) and Goodman (1976) provided useful descriptions of engineering case-studies.

Examples of translational failure are analysed using engineering-geology techniques to attempt to establish if slope instability was triggered by glacial oversteepening or whether other disturbing forces such as high cleft-water pressures or progressive-failure were responsible. This geomorphological approach differs from the usual engineering application of kinematic and limit-equilibrium models that attempts to construct shear strength curves for a rock type over a wide range of normal stresses (cf. Goodman 1981, e.g. Barton 1971b, Watters 1972). However, as Eisbacher (1979a) noted, it is often difficult to quantify the effects of possible high cleft-water pressures or earthquakes in back-analyses of ancient RSFs. Consequently, sensitivity-analyses are employed here to determine the possible

effects of different cleft-water pressures.

The approach taken here is dominantly descriptive but is justified because the modes of failure need to be demonstrated before detailed analyses of failure mechanisms are attempted. Figures and Plates are used whenever possible to minimise descriptive text.

6.2 Plane-sliding modes of failure

Corrie Brandy [NO 336 758] (2e).

A mass of schist with an estimated volume of 2.8×10^5 m^3 has been displaced vertically by up to 2.5 m and horizontally by 3 m on the 61° slope of the E-facing headwall of Corrie Brandy (Plate 6.1). A 1-m-wide tension-crack, located 10-m-E of the summit cairn, forms a cave which may be traced southwards into the hillside for at least 7 m. To the N of this point the tension-crack is exposed and widens to 3 m at its northernmost extremity. The total height of the displaced block is estimated to be 85 m which, taken with the vertical displacement, indicates a shear displacement of c. 2% of the slope height.

Although a number of joint sets have been recorded on the slope, kinematic testing of the slope geometry and joint patterns indicates that plane-sliding along joint set J1 is the only feasible failure mode (Fig. 6.1). The pole of joint set J1 is inclined towards the SE at 40°. The tension-crack is

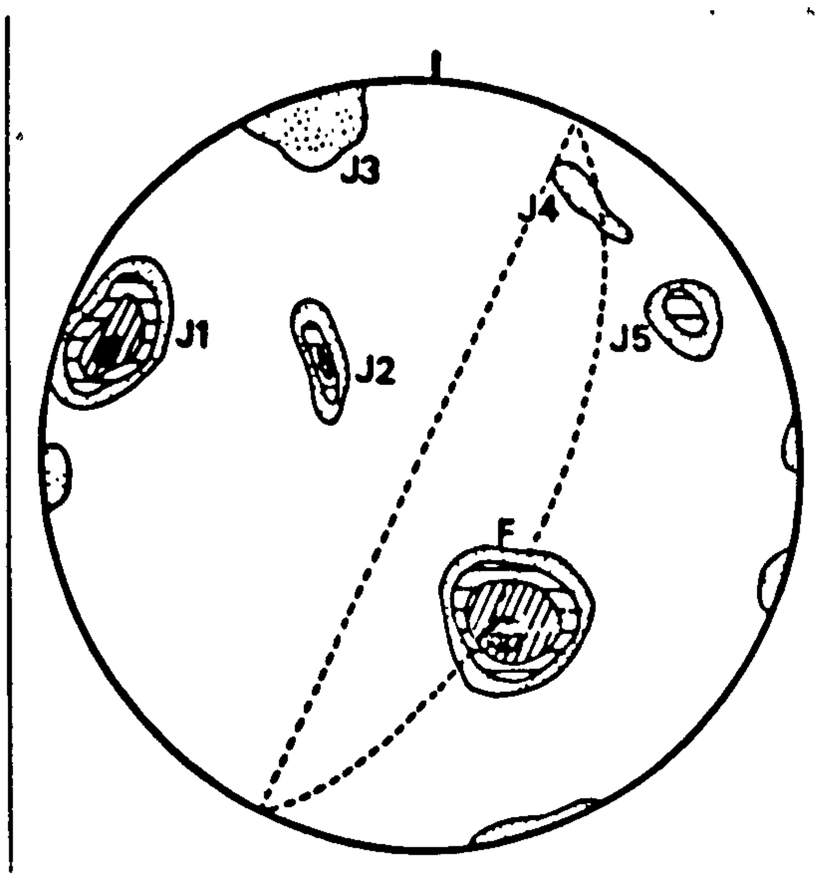

Plate 6.2: The Corrie Brandy RSF viewed from the N. Note the open tension-crack and areas of fresh bedrock on the slope face.

Plate 6.2: The Garbh Choire Mor RSF. The failed-debris is located at the bottom-centre and the scar is sited to centre-right. The large 'ramp' in the centre of the Plate is a debris-less RSF scar.

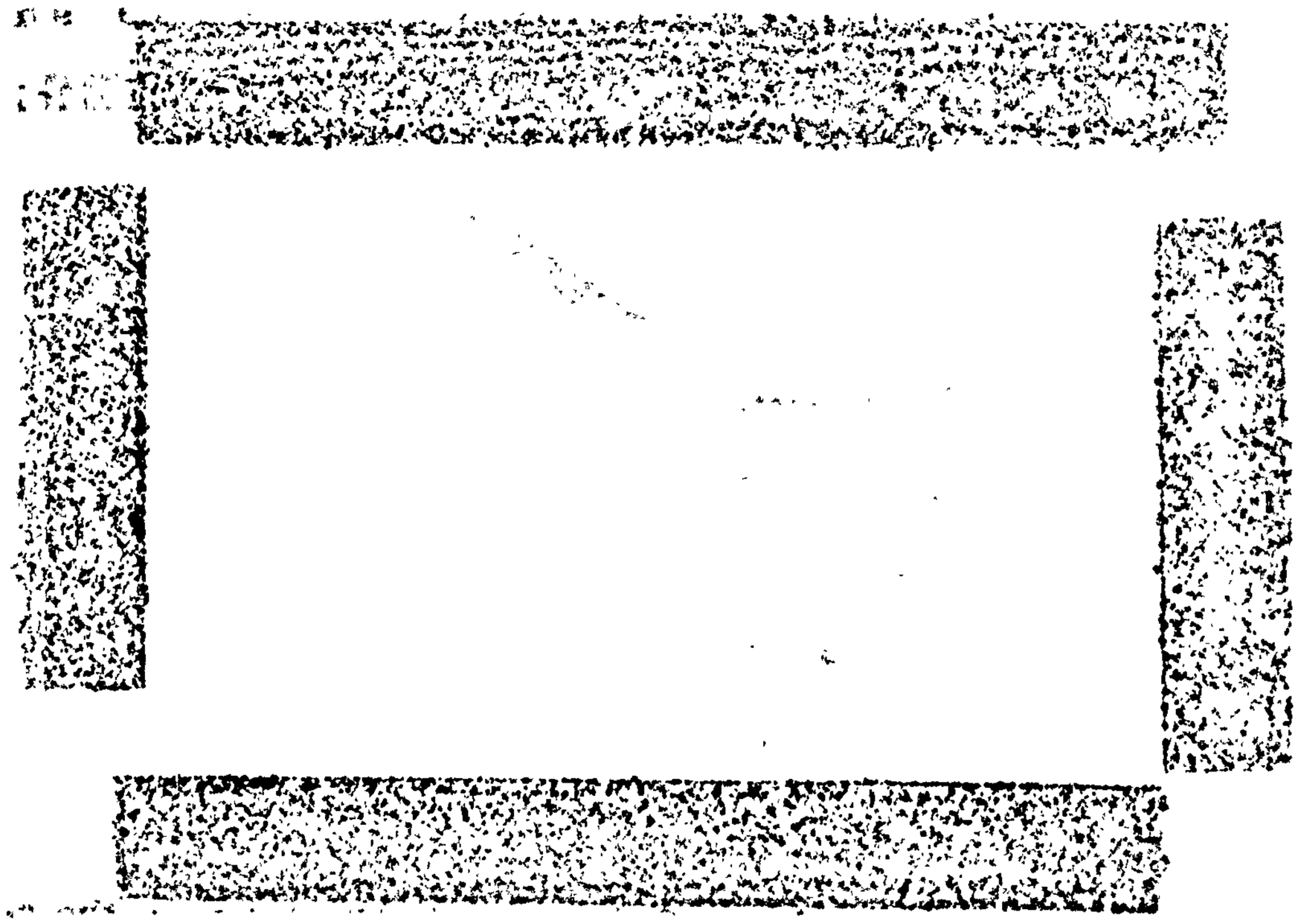

Figure 6.2: Surveyed section along the Corrie Brandy RSF. The inferred potential failure-surface is indicated by a dashed-line.

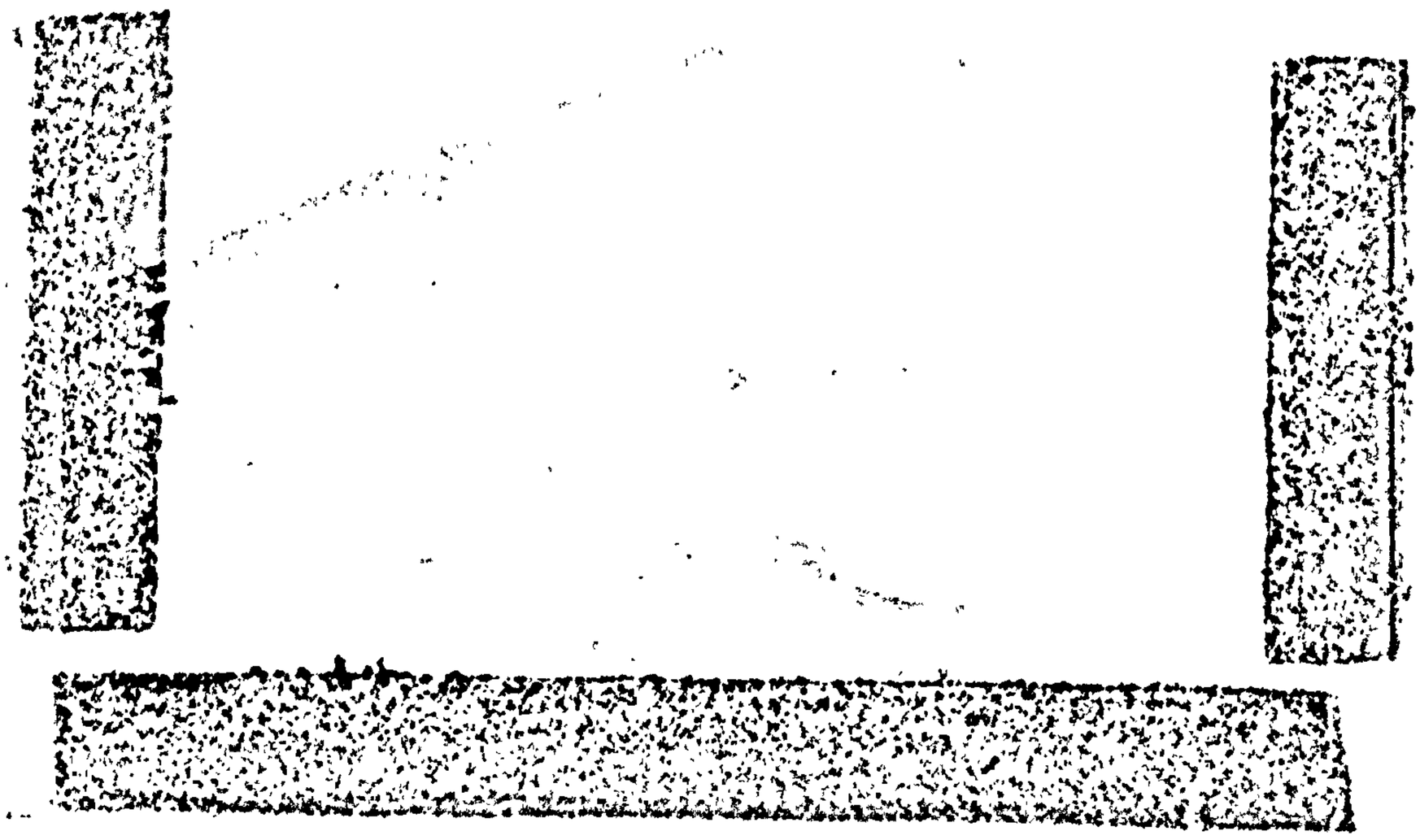

a compound feature which is mostly composed of J2 and J3 surfaces which dip steeply E and SE respectively. Joints running parallel with the foliation dip shallowly NW, into the slope.

The present day stability of the rock-slope can be computed using the analysis for plane-sliding given in Appendix A. Tilt tests on fresh, planar joint surfaces at the site gave an average sliding friction angle value of 42°. The average measured roughness of J1 surfaces in the direction of failure was 4°, suggesting a peak friction angle between 42 and 46°. The simplified geometry of the displaced block is given in Figure 6.2. It is assumed that the potential failure-surface is oriented parallel with the pole of J1 and that displacement has only been sufficient to mobilise the peak shear strength along the surface. The limited shear displacement indicates that shearing through of large-scale asperities has not occurred.

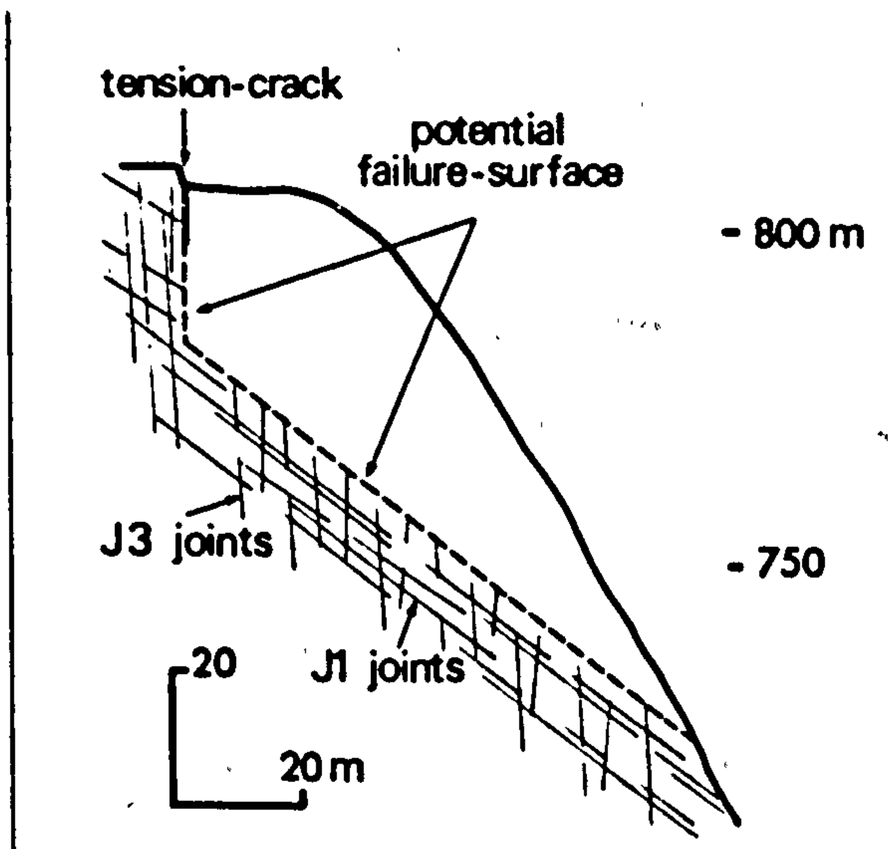

The dry-rock density of the mica-schist was taken to be 26.2 kN (Watters 1972), though this only affects the computation of the factors-of-safety when cohesive forces are assumed in the model. The F values for different shear strengths are given in Table 6.1 assuming that the slope is freely-drained.

Cohesion along the potential failure-surface may be imparted by the interlocking of asperities and possibly intact rock bridges. As

the mean normal stress along the potential failure-surface is computed to be 495 kPa cohesion may be quite high. The cohesion along the

	ø			
	44°	46°	48°	50°
(zero cohesion)	1.24	1.33	1.42	1.52
(cohesion = 100 kPa)	1.49	1.58	1.68	1.79
(cohesion = 200 kPa)	1.74	1.83	1.93	2.04

Table 6.1: Factors-of-safety for the Corrie Brandy slope assuming free-drainage.

assumed failure-surface is unknown but values of 100 and 200 kPa are used in the sensitivity analyses to illustrate the effect on the factors-of-safety. The F values all exceed unity, indicating that the slope would remain stable if the effective ø exceeds 40° and the slope was freely-drained (Table 6.1).

Table 6.2 gives the F values for the block assuming that the slope is fully-saturated. The tension-crack is assumed to be filled with water which is allowed to seep along the potential failure-surface to exit at atmospheric pressure. If the slope was subjected to this cleft-water pressure distribution then its factor-of-safety would be dramatically reduced but would still exceed unity, unless ø equalled 42° and the cohesion was zero. The mean effective normal stress acting on the surface were the slope to be fully-saturated, would equal 333 kPa: illustrating the effect of force U.

	ø				
	42°	44°	46°	48°	50°
(zero cohesion)	0.96	1.03	1.10	1.18	1.26
(cohesion = 100 kPa)	1.36	1.43	1.50	1.58	1.66
(cohesion = 200 kPa)	1.76	1.83	1.90	1.98	2.06

Table 6.2: Factors-of-safety for the Corrie Brandy slope, assuming a fully-saturated slope.

It may be hypothesised that the rock-mass has dilated sufficiently to enable free-drainage of the slope even during intense rainfall (cf. Section 2.5), thus reducing the possibility of dangerous cleft-water pressures acting upon it. Aerial photographs (c. 1:10,000-scale) taken in 1964 show that the RSF has not displaced significantly in the last 20 years. Progressive-failure may be occurring very slowly. It is possible that the RSF moved once, or more often, over a short period of time and then ceased, perhaps because of interlocking of asperities during shear displacement and dilation enhancing slope permeability.

Garbh Choire Mór [NH 254 673] (1c).

A large mass of Moinian gneiss boulders, covering c. 17,000 m^2 of the floor of Garbh Choire Mór, has evidently originated from a planar scar located on the S-facing corrie headwall (Plate 6.2). The debris mass is estimated to be up to 35-m-thick and contains several massive boulders the largest of which exceeds 3,000 m^3.

The failure-surface faces SE and dips at 35°. It is oriented

Figure 6.3: L.H. stereonet for the Garbh Choire Mór RSF (n = 200 poles).

subparallel with the pole of joint set J1 which is inclined at 30° → 130° (Fig. 6.3). Joint set F runs parallel with the foliation, which trends 25° → 082°. J2 joints strike E-W and were recorded as dipping both steeply north and south. Joint set J3 dips steeply W controlling the orientation of prominant rock ribs which strike N-S.

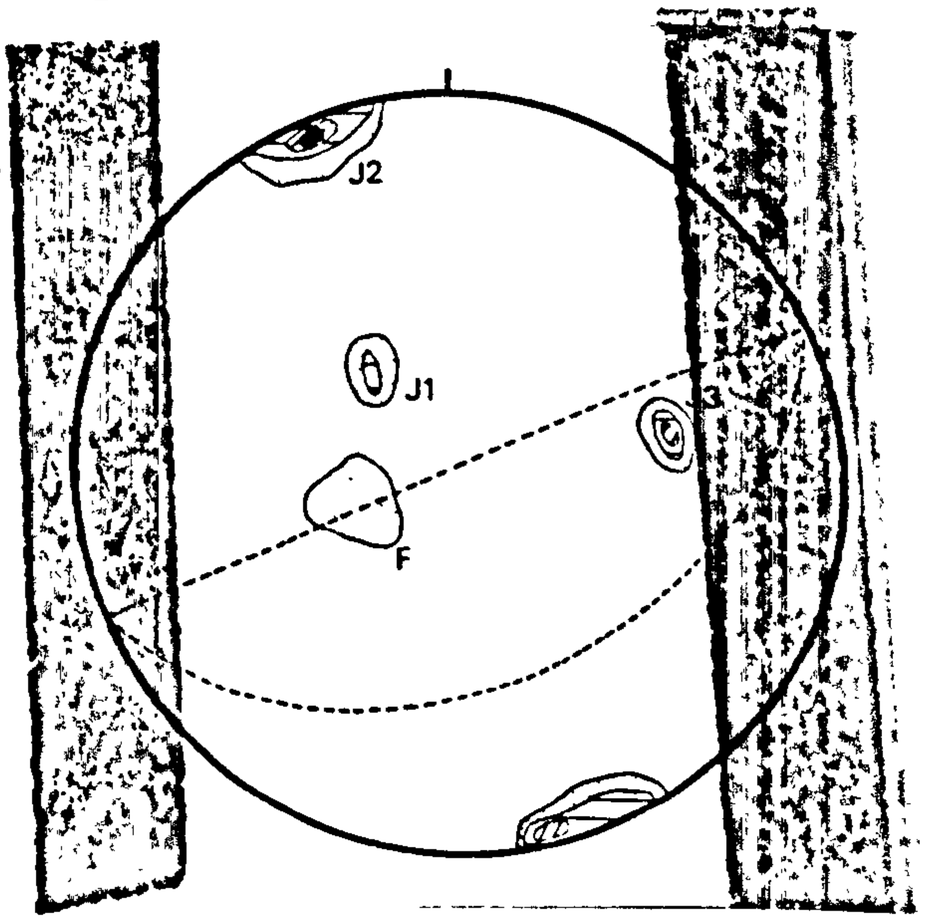

The rock structure, given the orientation of the slope face, is ideal for plane-sliding with J1 joints forming the main failure-surface. J2 joints may have permitted tension-cracks to have opened prior to failure and J3 joints would have enabled lateral release of the sliding block.

It is not possible to reconstruct the former block shape at this site and therefore not possible to attempt limit-equilibrium analysis of it. However, the kinematic test indicates that self-weight plane-sliding along the failure-surface could not have occurred unless the effective friction angle mobilised along it was less than 36°. The effective friction angle is a function of the cohesion mobilised along a failure-surface, its friction angle and any cleft-water pressures that may have existed.

As the inclination of the failure-surface is 6° below that of the sliding friction angle of the pelitic gneiss (41°), it is likely that failure was triggered by either cleft-water pressures acting on the plane or by some other force augmenting gravity.

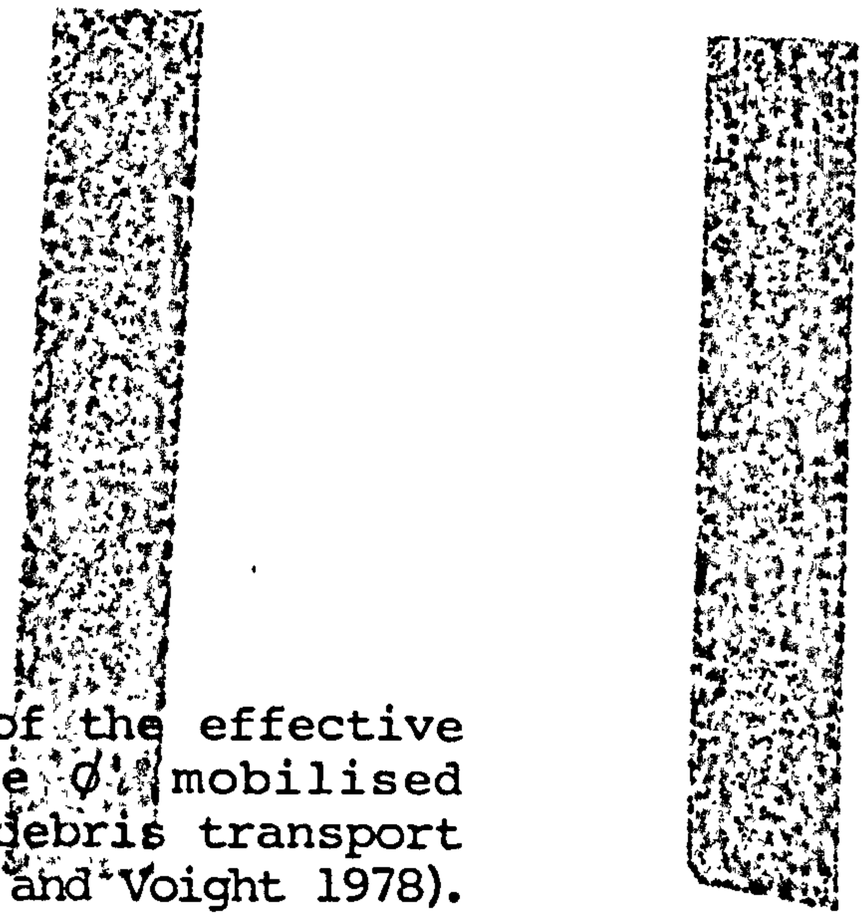

Figure 6.4: Determination of the effective friction angle ϕ' mobilised during failed-debris transport (after Pariseau and Voight 1978).

The centre of the debris mass lies 220 m distant from the mid-point of the scar. It may be asked, what caused the debris to move so far away from the scar over a comparatively gentle gradient. Some explanation may be possible by analysis of the mechanics of debris transport after failure. Pariseau and Voight (1978) have shown that if dynamic analysis of a RSF is undertaken from the initiation of slide movement to its cessation, then $h = d \tan\phi'$ (Fig. 6.4), or the inclination of a line drawn between the mass centres of a block prior to movement and after movement, equals the effective friction angle (ϕ') mobilised during debris transport. This is true regardless of the trajectory of the block during transport. The value for ϕ' may be compared with the residual friction angle for the consituent rock material (e.g. Cruden 1976, 1980) to indicate if pore-water pressures were necessary during debris transport. If ϕ' is less than ϕr then pore-water pressures, or some other force, must have acted upon the failed-material during transport away from the scar.

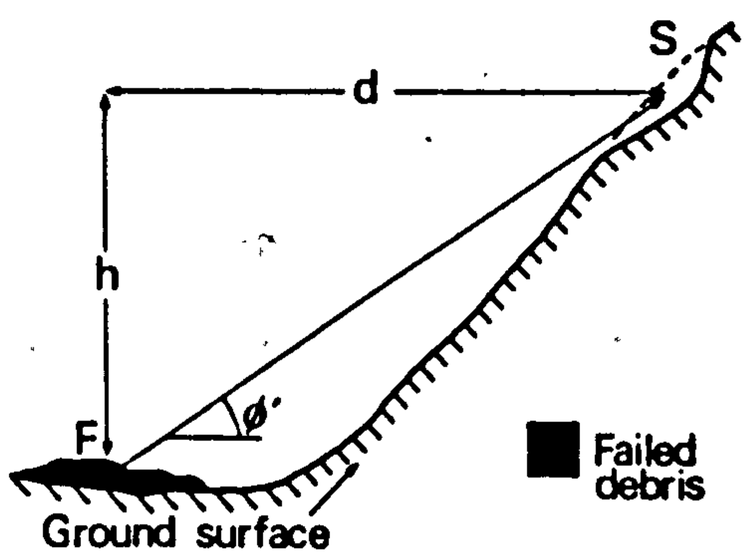

It is possible that excess pore-water pressures, acting with a friction angle greater than the residual, could have combined to produce an ϕ' less than the peak friction angle for the material, or even less than the residual friction angle. It may be countered that if the line connecting the mass centres is inclined between the residual and the peak friction angle, then the <u>simplest</u> mechanical

Figure 6.5: L.H. stereonet for the Sgurr na Lapaich ridge RSF (n = 200 poles).

explanation is that no pore-water pressures acted.

The effective friction angle of the Garbh Choire Mór debris mass during transport was found, using the above analysis, to equal 26°. This value is thought to be close to the residual friction angle for gneiss (cf. Hoek and Bray 1977, Goodman 1981) and so excess pore-water pressures need not have assisted in the transportation of the rock debris once failure had occurred.

Sgurr na Lapaich ridge [NH 130 250] (3g)

A complete slope failure has occurred on the steep S-facing slope of Corrie Leachavie. Psammite and pelite boulders extend up to 120 m from the ridge crest to where a scar is sited. The morphology of the scar indicates that a 2.0×10^3 m^3 block of rock translated to the S along a failure-surface inclined at c. 26°.

Three important joint sets were recorded on the slope (Fig. 6.5). The pole of set J1 dips 24° towards the S. A foliation set (F) strikes approximately normal to J1, its pole trending 80° → 074° The foliation set provided the lateral release surfaces for the block. The only kinematically feasible mode of failure is by plane-sliding along J1 surfaces, indeed the failure-surface trends subparallel to the J1 pole.

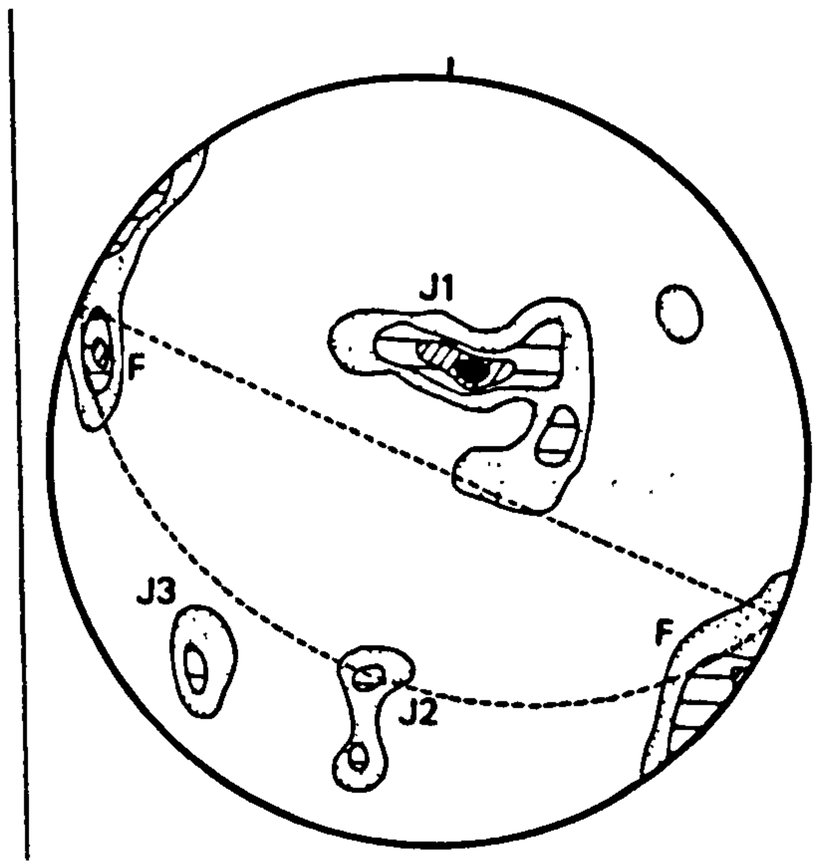

The failure-surface is inclined at less than the residual

friction angle for psammite and, therefore, the RSF could not have occurred by progressive-failure alone. Cleft-water pressures must have acted on the rock-mass and it is possible to model the minimal disturbing force required to cause failure.

As the failure-surface crops out in the N side of the ridge, a tension-crack would probably not have been formed. It is assumed that force U is given by ($0.25 \cdot \gamma w \cdot H_w^2 \cdot \text{Cosec } \theta$). This cleft-water pressure distribution (the same as that given in Appendix A, for wedge-failure) would have been sufficient to reduce the factor-of-safety of the block to 1.07: assuming ϕ equals 38° and the shear strength intercept was zero.

The shear strength intercept was unlikely to have been zero as asperities along the failure-plane would have contributed to the shear strength. A more unfavourable cleft-water pressure distribution could have acted on the block to yield failure at higher mobilised shear-strength values. The effective friction angle must have been reduced to less than 26° for failure to have occurred.

The line connecting the mass centres prior to and after failure is inclined at 37°, a value between the peak (42°) and residual (32°) friction angles for psammite (Watters 1972). This indicates that debris transport could have occurred without pore-water pressures acting upon the failed debris mass.

Ben Donich SE slope [NN 233 046] (4g).

The structure of this slope is relatively simple (Fig. 6.6). A joint set was recorded running parallel with the foliation which dips

Figure 6.6: Lower hemisphere stereonet for the Ben Donich SE slope (n = 200 poles).

Figure 6.7: Section through the Ben Donich SE slope: note the modelled phreatic surface.

shallowly NW at 4°. Two other joint sets were recorded on the slope.

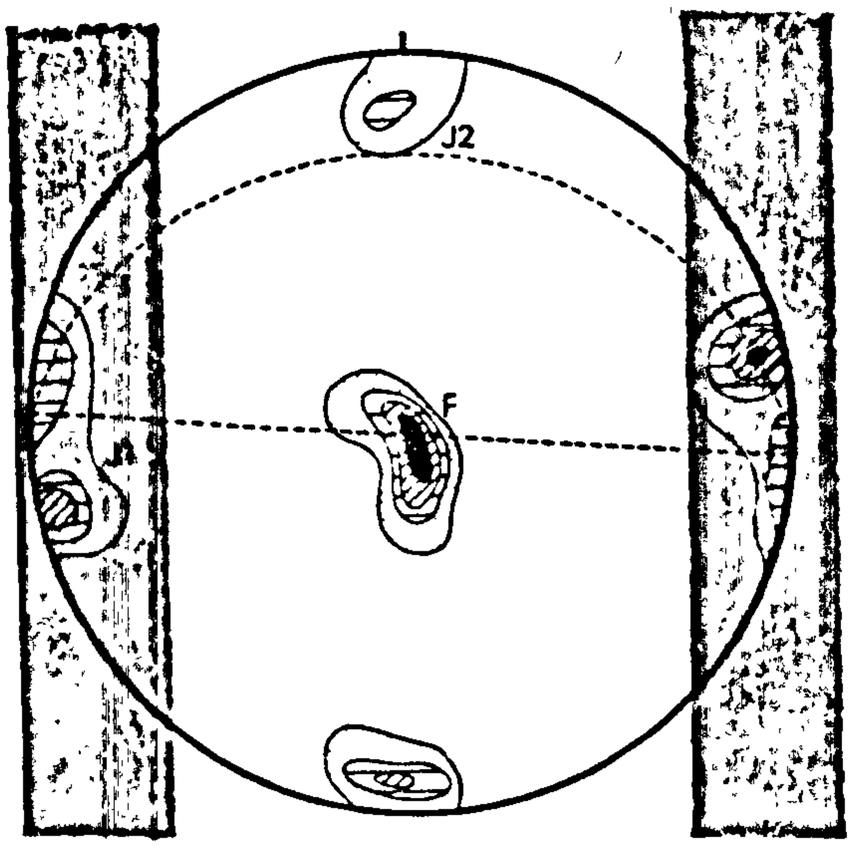

The first (J1) strikes N-S, its pole oriented 82° → 258°. Set J2 strikes at right-angles to J1, its poles trending 80° → 002° and 73° → 176°. The foliation shows considerable large-scale roughness in the direction of failure and i was estimated to be 15°.

Three joints sets separate the rock-mass into cubes and several large blocks have translated to the N forming deep tension-cracks between them. The largest tension-crack was found to be 18-m-deep, even though it is partly infilled with rubble, and is up to 3.5-m-wide. Plane-sliding along F surfaces is kinematically feasible (Fig.

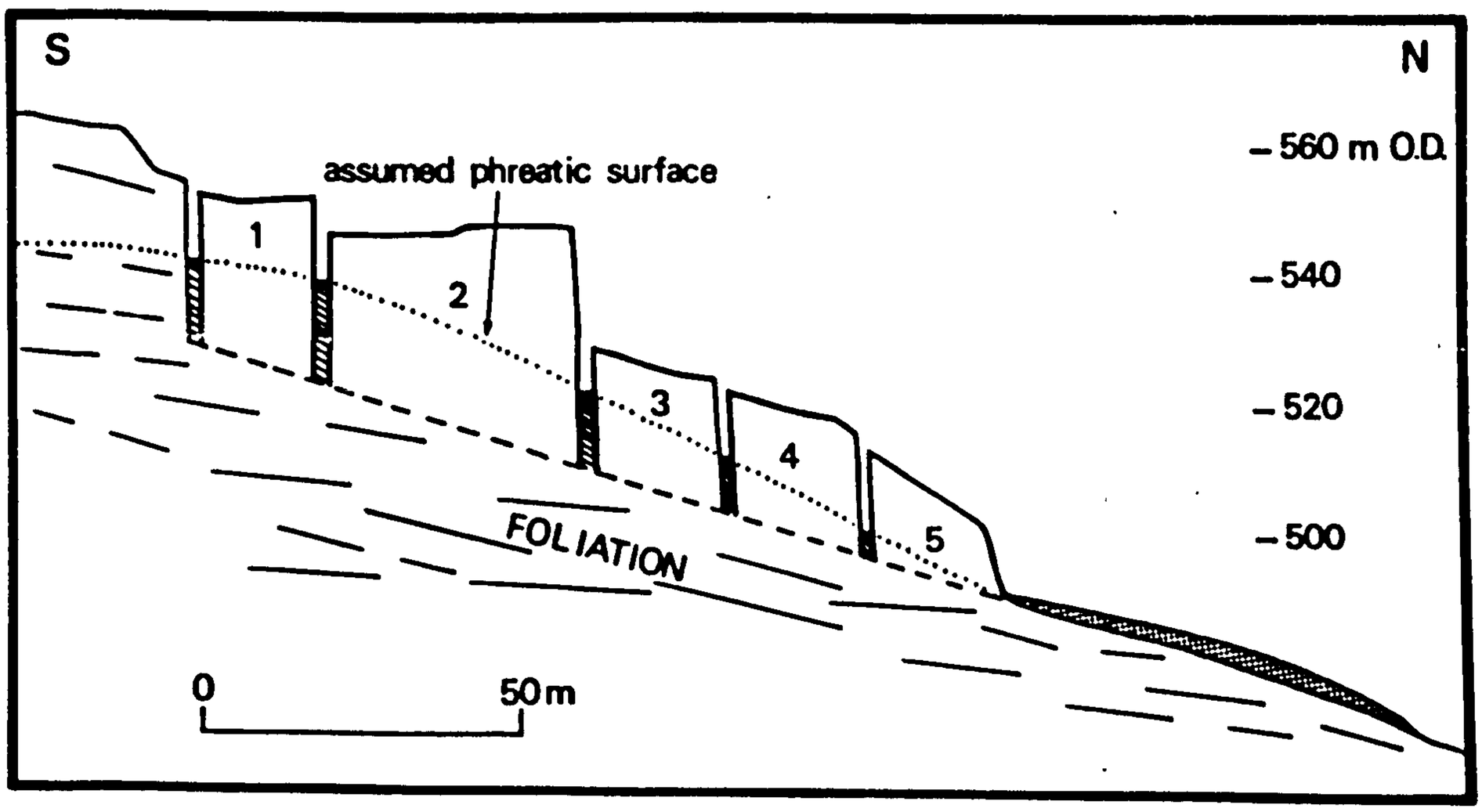

6.7). Although the nature of the surface along which sliding has

occurred can only be speculated upon, the depths of the tension-cracks have been used to estimate the minimal height of each block and the inclination of the failure-surface. The largest block, assuming that the failure-surface is inclined at 17° and is sited 25-m-below the surface, weighs c. 1.4×10^5 tonnes.

Cleft-water pressures probably acted on the blocks as the inferred failure-surface almost certainly lies below the residual friction angle for schistose grit. Table 6.3 gives the depth to which the tension-cracks upslope of the blocks would need to be filled with water to satisfy limit-equilibrium, assuming that ϕ_r equals 24°. The nature of the piezometric surface is illustrated in Figure 6.7. As a shear displacement of around 12% of the base length of each block has occurred, it is likely that asperities have been sheared away decreasing the failure-surface strength to the residual.

	A	B
Block 1	zw = 15 m	35°
Block 2	zw = 13 m	31°
Block 3	zw = 12 m	31°
Block 4	zw = 9 m	34°
Block 5	zw = 4 m	38°

Table 6.3: Depths of water in tension-cracks at F = 1.0, assuming ϕ = 24° (column A) and the minimum friction angle required to sustain stability if the tension-cracks were full of water (column B).

The ϕ' values required to sustain limit-equilibrium assuming the

Figure 6.8: L.H. stereonet for the Sgurr na Lapaich RSF (n = 200 poles).

tension-cracks were full of water are given in column B. The sliding friction angle of schistose grit equals 41° and the peak friction angle may be as high as 50°. A fully-saturated slope would not, therefore, have caused failure assuming peak strength. Consequently, it may be inferred that either the strength of the failure-surface was reduced to below its peak, by progressive-failure, or that a more unfavourable cleft-water pressure distribution developed within the slope than that modelled.

Sgurr na Lapaich [NH 152 246] (3h)

A very large mass of psammite (6.8-7.5 x 10^6 m^3) has slumped up to 3.5-m-vertically on the 205-m-high N slope of Sgurr na Lapaich. This represents a displacement of c. 1.7% of the slope height. The rear-scarp of this RSF appears arcuate in plan view but is formed by a series of linear joint surfaces (Plates 6.3 and 6.4).

The structure of the slope is complex (Fig. 6.8) yet individual joints exhibit remarkably little variance from their joint poles even though sampling was made over a wide area. J2 is a stress-relief joint set which trends at 38° → 351°, though individual joints dip between 30 and 48°. The foliation on the slope dips at 70° NW and the pole of J3 dips 73° westwards. Wedge-sliding along F and J3 surfaces is not feasible as their lines of intersection would dip at 10° to the N. Plane-sliding along J2

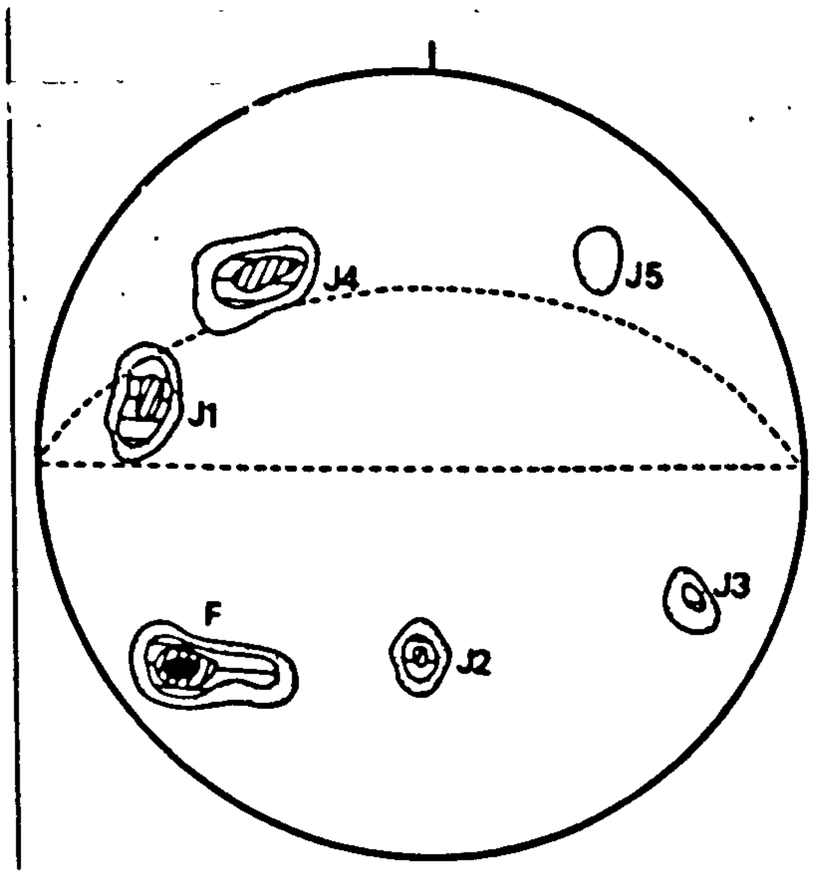

Plate 6.3: Vertical aerial photograph of the Sgurr na Lapaich RSF (c. 1:12,000-scale). The top of the photograph is N. Note the step-like feature that trends SE-NW (arrowed).

Plate 6.4: The Sgurr na Lapaich RSF as viewed from the W. The step-like feature (arrowed) may be traced onto the gently-sloping ground below and outside the RSF.

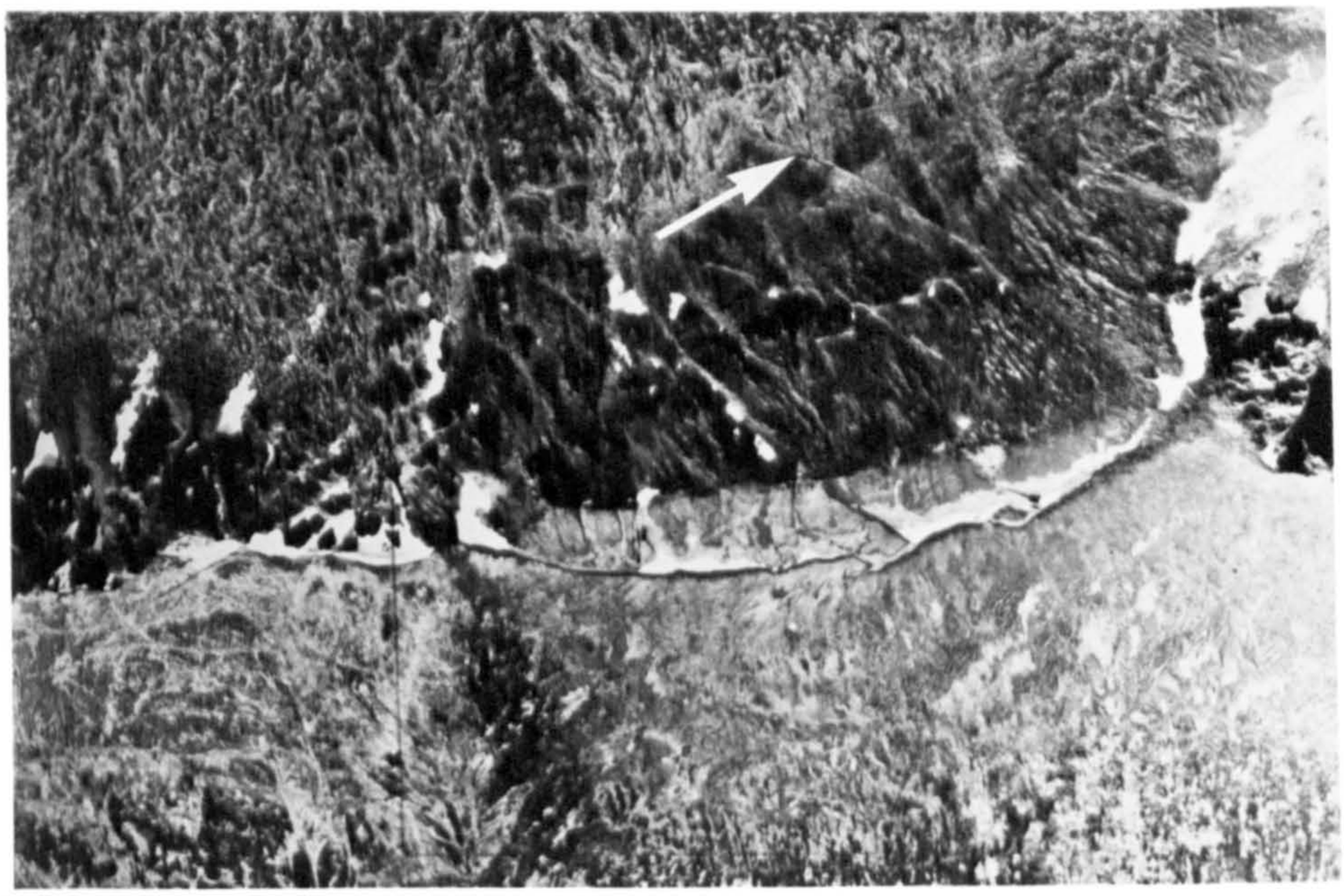

surfaces is possible.

This RSF is not amenable to conventional limit-equilibrium analysis because of its size. However, an infinite-equilibrium model (after Skempton and Delory 1968) may be used to estimate the factor of safety of the slope (when freely-drained), using:

$$F = \frac{(\gamma z \,.\, \mathrm{Cos}^2\theta - u)\ \mathrm{Tan}\phi'}{z \,.\, \mathrm{Sin}\theta \,.\, \mathrm{Cos}\theta} \qquad 6.1$$

Where: F = the factor of safety against sliding;
γ = the unit weight of the potential slip mass;
z = the constant vertical thickness of the potential slip mass;
θ = the constant slope (to the horizontal) of the potential failure-surface.

Assuming that a potential failure-plane has developed parallel to J2 the factor of safety is computed to be 1.32. The contribution of asperities and intact rock bridges is unknown and so the F value given above is likely to be a minimum.

As the slope is calculated to have a factor-of-safety greater than unity, even ignoring possible cohesion, it is inferred to be relatively safe. It may be questioned what caused displacement of this RSF. It may be hypothesised that cleft-water pressures formerly acted upon the block, causing it to displace temporarily before equilibrium was regained. Minor shear displacement could have led to dilation of the rock mass enabling free-drainage and an instantaneous reduction in cleft-water pressure. Alternately, progressive-failure could be occurring very slowly though the old age of the feature (p 208) disfavours this argument.

The upper surface of this RSF is interrupted by a series of transverse steps (scarps) that trend NW-SE (Plate 6.3). The highest of these is 2.5-m-high and runs sub-parallel with the poles of F and J5. The scarps also crop out in the N slope of the RSF. One example extends outside the limits of the RSF onto gently-sloping ground immediately in front of it and cannot, therefore, have formed solely by RSF. The feature is up to 1-m-high and terminates upslope at the rear-scarp immediately N of the summit cairn (Plate 6.3). The feature decreases in height to the N until it is covered by drift.

An attempt was made to excavate into this step-like feature but was frustrated by large boulders which have been disrupted by movement along the scarp. Sections in the river banks of Abheinn Gleann nam Fiadh (due N of the slope) were checked but no disruption of the rockhead was evident.

It is possible that this step-like feature is a so-called 'pop-up' (cf. Eyles and Paul 1983) that was caused by localised rebound, separate from the regional glacio-isosatic uplift. However, it is not possible to infer that an earthquake resulted from the displacement which occurred along it, nor is it possible to estimate the relative duration of the displacements.

6.3 Wedge-sliding modes of failure

Mullach Fraoch-choire [NH 101 189] (3f)

An impressive tongue of psammite rock debris, up to 20-m-thick, dominates the W-facing headwall of Fraoch-choire (Plate 6.5). The

Plate 6.5: The Mullach Fraoch-choire RSF viewed from the SE (note levées and ridges on the feature).

Figure 6.9: Surveyed section along the Mullach Fraoch-choire RSF.

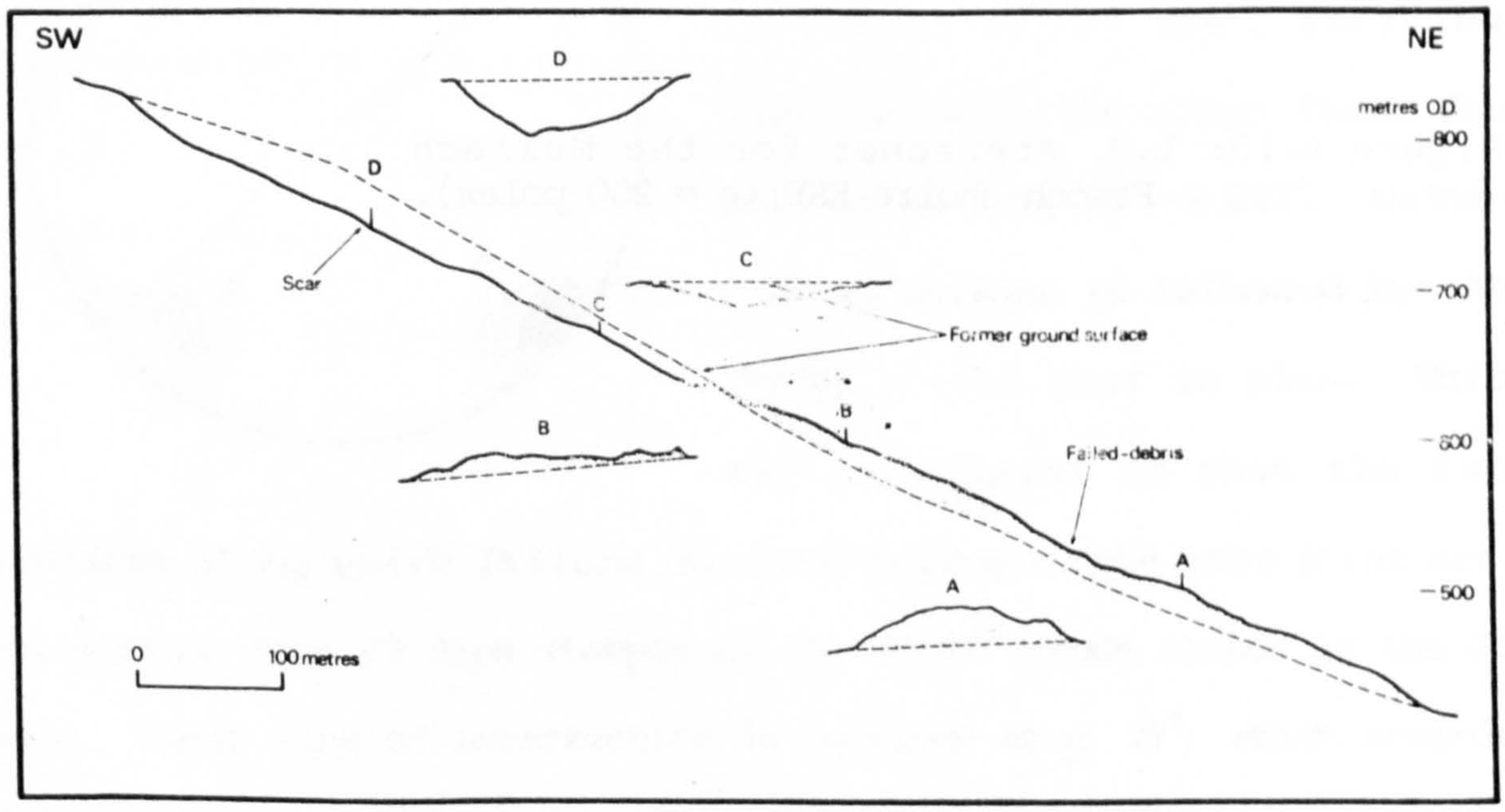
SW
NE
D
D
Scar
C
C
Former ground surface
B
B
Failed-debris
A
A
0
100 metres
metres O.D.
−800
−700
−600
−500

Figure 6.10: L.H. stereonet for the Mullach Fraoch-choire RSF (n = 200 poles).

total length of the RSF is 830 m and its debris mass is 420-m-long (Fig. 6.9). It reaches from the corrie floor to the top of the headwall, a height of 380 m. The volume of displaced rock is estimated to be between 6.8 x 10^5 m^3 (based upon the approximate volume of the scar) and 7.5 x 10^5 m^3 (based on debris mass volume, assuming 35% porosity). Levées occur on the debris-tongue sides and reach up to 4-m-high while towards the toe of the failed-debris a small debris tongue has bifurcated from the main body of debris. Transverse ridges occur across the main debris mass whose frontal slope is inclined at 37°.

The structure of the rock-slope is comparatively simple (Fig. 6.10). Two major discontinuities dip steeply and strike at right-angles to one another. The pole of J1 trends 80° → 316°, striking parallel with the slope face. The pole of J2 runs 62° → 042°. Wedge-sliding failure is indicated by the shape of the scar in plan. This RSF is unusual in that the two surfaces along which failure occurred belong to the same joint set. One surface from J2 dips steeply SW the other trends closer to the J2 pole. Their line of intersection is inclined at c. 29°, which accords exactly with the topographic data (Figs. 6.9 and 6.10).

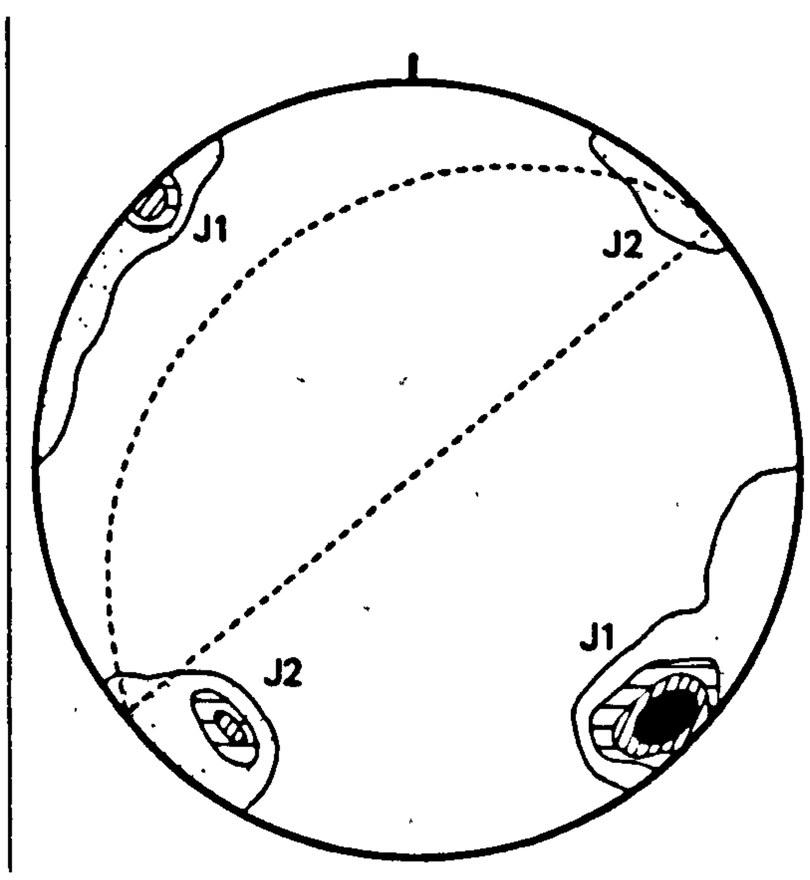

The kinematic test for wedge-sliding shows that in order for self-weight sliding to have occurred, the mobilised friction angle

must have been less than 29°, that is, below the residual friction angle for psammite. It is probable therefore that high cleft-water pressures led to failure, permitting wedge-sliding at a friction angle greater than, or equal to, the residual. The size of the RSF prohibits limit-equilibrium analysis but an approximation of the disturbing forces may be gained (after Skempton and DeLory 1968) using:

$$Ruf = \frac{uf}{Yz} = \cos^2\theta \left(1 - \frac{\tan\theta'}{\tan\phi}\right) \qquad 6.2$$

where: Ruf = the pore-water pressure ratio acting at the time of failure;
ϕ' = the effective friction angle;
θ = the slope of the failure plane;
Yz = the unit weight of the mass.

Even assuming ϕ' equalled 45°, the pore-water pressure acting at the time of failure is computed to have been 0.34 (broadly equal to a fully-saturated slope). The analysis is not strictly valid however because it assumes sliding along a single plane and not, as observed here, along the line of intersection of two surfaces. The analysis may therefore predict a higher pore-water pressure than otherwise necessary to attain limit-equilibrium, because of the wedging action of the failure-surfaces. Opposing this, the effective friction angle may have been higher than 45° because of a mobilised shear strength intercept.

The line connecting the mass centre of the study RSF prior to failure with that after failure is inclined at 26°, which is less than

Figure 6.12: L.H. stereonet for the Glen Kinglas RSF (n = 200 poles).

the residual friction angle for psammite. This indicates that pore-water pressures probably acted upon the debris mass during its transport.

Glen Kinglas [NN 190 096] (4a).

This RSF has formed in mica-schist with massive bands of schistose grits. The RSF has produced a mass of debris up to 12-m-thick and 260-m-long which rests upon a 28° slope (Plate 6.6). Some very large blocks are found within the debris, the largest observed on the surface having an estimated volume of c. 1300 m^3. The RSF is calculated to involve c. 7.0 x 10^4 m^3 of intact rock. The length of the debris mass is twice that of the scar. This RSF is unusual in that it has two failure-surfaces (Fig. 6.11) the uppermost of which terminates at a vertical scarp up to 5-m-high.

A low-angle joint set runs parallel with the foliation on the slope, dipping between 20 and 50° NW, the pole being oriented 32° → 329° (Fig. 6.12). Four joint sets dip steeply eastwards. Of these, J2 forms the W margin of the RSF. Measurements of the W failure-surface produced an average orientation of 80° → 082°. The E failure-surface trends 32° → 324°, subparallel with the pole of F. The line of intersection of the two failure-surfaces is directed almost due N and is reconstructed as being inclined at 25°, which accords exactly with the inclination of

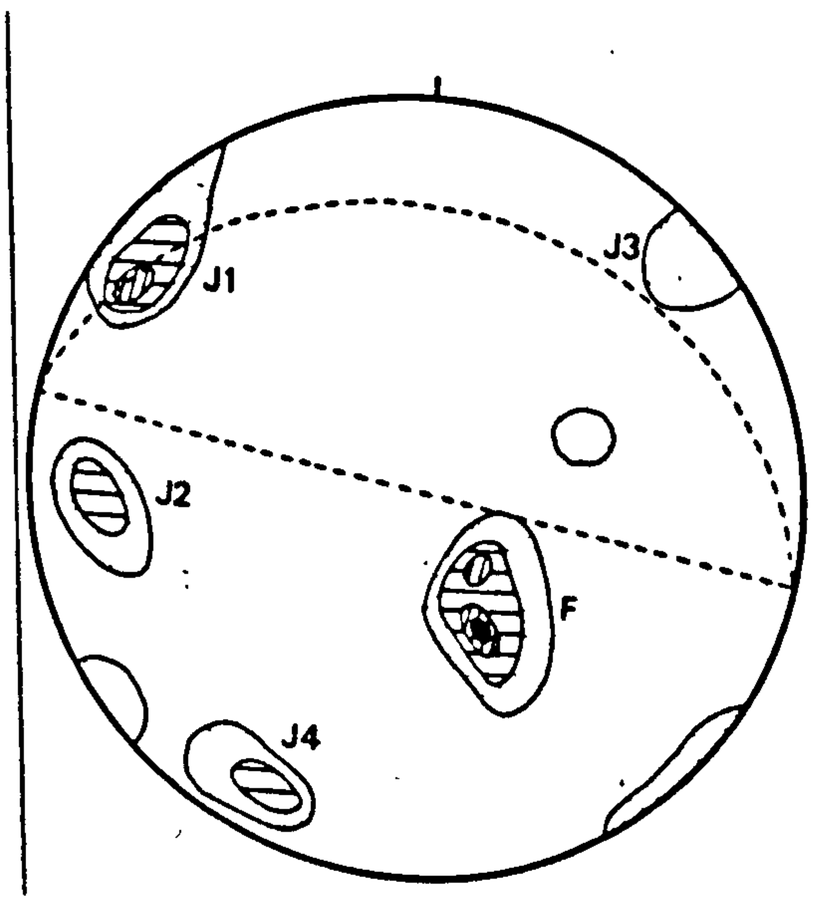

Plate 6.6: The Glen Kinglas RSF viewed from the NE.

Figure 6.11: Surveyed section along the Glen Kinglas RSF.

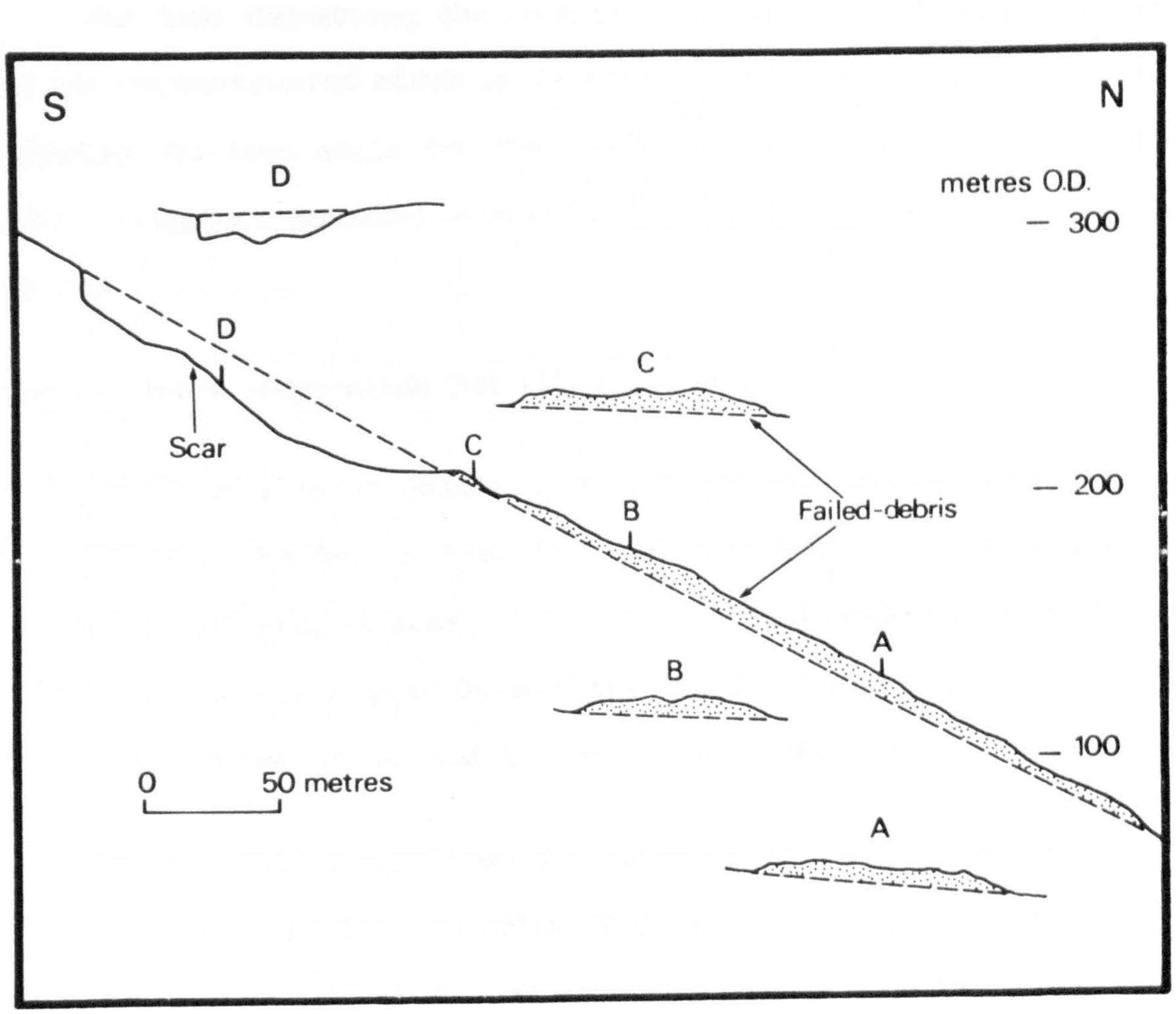
S
N
metres O.D.
— 300
— 200
— 100
D
D
Scar
C
C
B
B
A
A
Failed-debris
0
50 metres

Plate 6.6: The Glen Kinglas RSF viewed from the NE.

Figure 6.11: Surveyed section along the Glen Kinglas RSF.

the upper failure-surface in cross-section. The lower failure-surface is inclined at 21°, below the residual friction angle for mica-schist (cf. Watters 1972).

It is not possible to analyse this example using limit-equilibrium analysis because of the complexity of the failure surfaces. In particular the upper 'wedge' is terminated upslope by a vertical joint (Fig. 6.11). However, kinematic analysis for wedge-sliding indicates that the wedge could not have failed unless some force augmented gravity. It is suggested that cleft-water pressures acted along the failure surfaces reducing their effective friction angle below 21°, the inclination of the lower failure-surface.

The line connecting the centroid of the failed-debris with that of the reconstructed block prior to failure equals 26°: close to the residual friction angle for the rock. It is therefore possible that debris transport occurred without pore-water pressures acting upon the debris.

Hell's Glen S wedge-slide [NN 173 059] (4d).

On the S side of Hell's Glen a slope failure has occurred in mica-schist. The debris from this failure extends up to 90 m from the apex of the V-shaped scar. The W side of the scar is formed by a cliff which reaches up to 24-m-high. The debris terminates at a 3-m-high toe inclined at 34° and is completely vegetated.

The two failure-surfaces are oriented 34° → 312° and 61° → 076°, that is, parallel with the poles of J1 and F respectively (Fig. 6.13). The intersection of these failure-surfaces is oriented almost due N

Figure 6.13: L.H. stereonet for the Hell's Glen S wedge-slide (n = 200 poles).

and is inclined at 26°. The wedge height is taken to be 34 m, determined by extrapolation of the line of intersection of planes A and B from the known apex of the wedge to the former slope face.

The geometry of the wedge-slide is known in detail and limit-equilibrium analysis is considered feasible for this RSF. The factors-of-safety computed for a freely-drained slope are in excess of 1.5 even taking the residual friction angle for mica-schist of 24°. Cleft-water pressures must therefore be considered in the back-analysis. Using the wedge-sliding model given in Appendix A and assuming a fully-saturated slope, the factors of safety were computed for a number of strength values (Table 6.4).

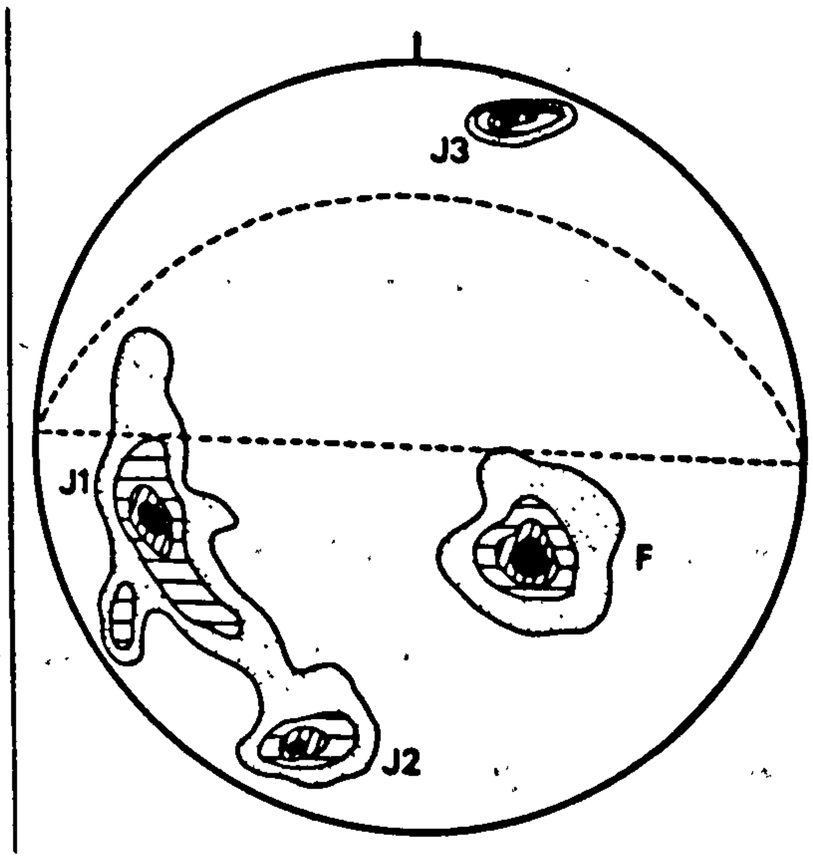

		Plane ∅A				
		35°	40°	45°	50°	55°
Plane ∅B	35°	0.68 {49}	0.75 {39}	0.84 {24}	0.94 {9}	1.06 {-ve}
	40°	0.74 {39}	0.82 {27}	0.90 {15}	1.00 {0}	1.13 {-ve}
	45°	0.82 {27}	0.89 {17}	0.97 {5}	1.06 {-ve}	1.20 {-ve}
	50°	0.90 {15}	0.97 {5}	1.06 {-ve}	1.16 {-ve}	1.28 {-ve}
	55°	1.01 {-ve}	1.07 {-ve}	1.16 {-ve}	1.26 {-ve}	1.39 {-ve}

Table 6.4: Factors-of-safety and shear strength intercept {kPa} assuming different friction angles for the Hell's Glen wedge-failure (fully-saturated slope).

Figure 6.14: L.H. stereonet for the Glen Effock RSF (n = 200 poles).

The values for the shear strength intercept (S_i) given in Table 6.4 are those required to maintain limit-equilibrium or alternately the maximum S_i values mobilised in association with the ϕ along the failure-surfaces at the instant of failure. Assuming peak values for the friction angles of the surfaces (40° for plane A, the foliation surface, and 45° for plane B), the cleft-water pressure distribution would have been sufficient to have caused failure, with a mobilised S_i of 17 kPa along both planes.

The RSF debris rests upon a 20° slope and the angle of the line joining the block centroid prior to failure with that of the debris mass after failure is inclined at 27°. This value is taken to be the effective friction angle and since it is greater than the residual friction angle for the mica-schist rock, pore-water pressures need not have acted during debris transport.

Glen Effock [NO 429 767] (2f).

This RSF is the best example of a wedge-sliding failure observed by the author in the Scottish Highlands. It is based in schist and has suffered only minor displacement of c. 3-m-vertically, representing a shear displacement of c. 3% of the wedge height.

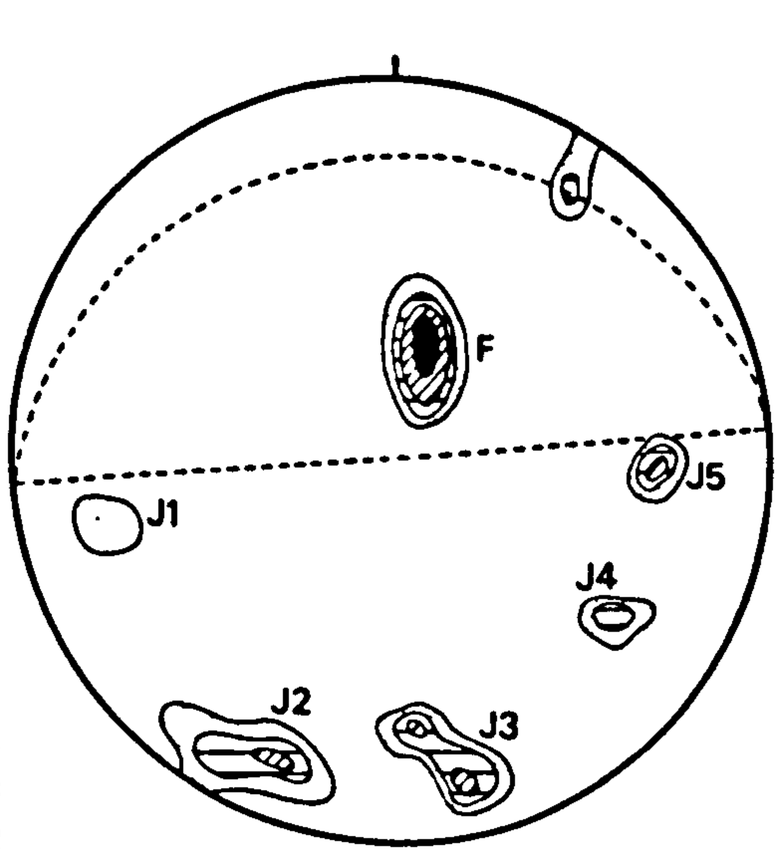

A low-angle foliation joint set was found to dip negatively (Fig. 6.14). Wedge-sliding is permitted along sets J1 and J4 and is also kinematically feasible along J1 and J5. The intersection of the last two surfaces however would be

inclined at less than 20° towards the N. The orientation of the E failure-surface indicates that wedge-sliding has utilised J4 surfaces in combination with J1, which would intersect to form lines trending almost due N and inclined at 32°.

Despite the size of the RSF (approximately three times as large as the Hell's Glen wedge example) the topographic and joint attitude data are known in sufficient detail to permit computation of the factor-of-safety of the wedge, using the limit-equilibrium model in Appendix A.

If the slope remains freely-drained and assuming that ϕ equals 50° and cohesion is zero along each plane, then F is calculated to be 3.84. Even using the residual friction angle of 24° for each failure-surface the factor-of-safety of the wedge equals 2.10 (c = 0). If cleft-water pressures built up along the potential failure-surfaces stability would be drastically reduced. Taking the cleft-water pressure distribution assumed by the model and assuming peak friction angles the factor-of-safety would be less than unity. It is likely, however, that intact rock bridges provide very high cohesion and that the slope is probably very stable. A temporary build up of high cleft-water pressures may have caused displacement of the wedge that ceased in response to shear-stiffness effects.

Hell's Glen N wedge-slide [NN 181 062] (4b).

On the N side of Hell's Glen several tension-cracks have opened below a 3-m-high rear-scarp (Plate 6.7). The tension-cracks are up to

Figure 6.15: L.H. stereonet for the Hell's Glen N wedge-slide (n = 200 poles).

Plate 6.7: Open tension-cracks on the surface of the Hell's Glen N wedge-slide.

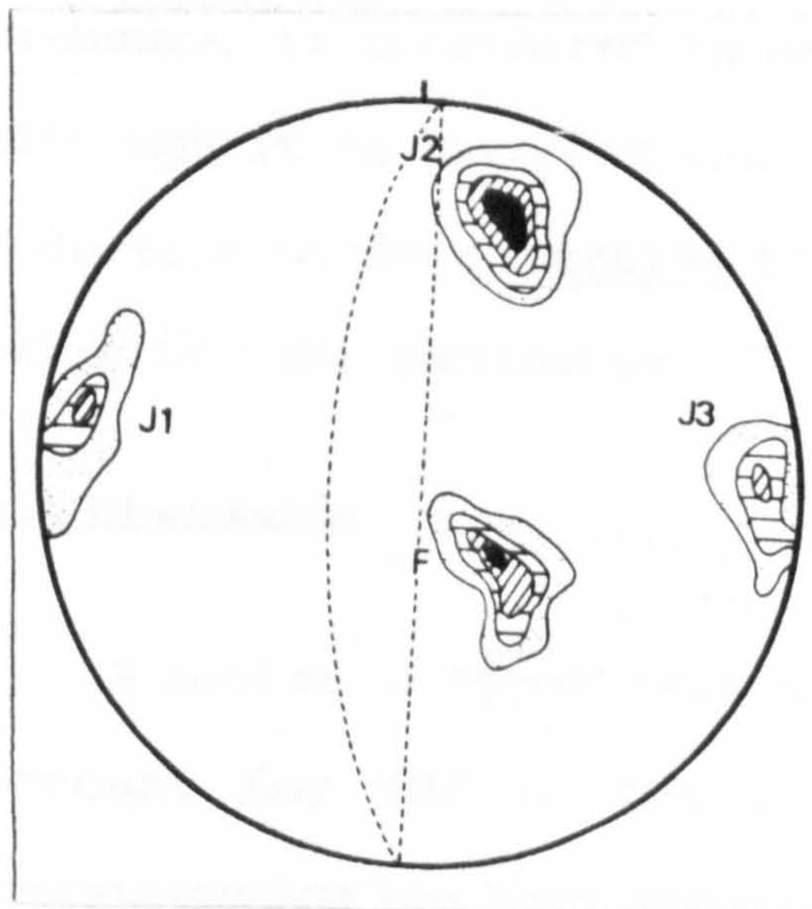

15-m-deep and 1.75-m-wide and strike parallel with J1, J2 and J3 poles (Fig. 6.15). The N-S trending cracks are formed by J3 joints which dip steeply W indicating that translation has occurred normal to the strike of these joints. The crack widths indicate shear displacement of approximately c. 5% of the block width.

The rear-scarp is oriented sub-parallel with the J2 pole. Plane-

sliding along surfaces formed by F joints would not be possible as this set dips gently NW, into the slope. The only possible failure mode is wedge-sliding to the W along J2 and F surfaces. Lines of intersection formed by these two sets crop out (dipping at 18°) in the E wall of a gorge. Since this RSF is unlikely to have occurred under

self-weight sliding, some other force, such as high cleft-water pressure, is considered to have augmented the effects of gravity. Although it is not possible to model such forces for this RSF the reduction in the effective friction angle must have been dramatic: below 18°, the inclination of the inferred failure-surface.

6.4 Discussion

A number of hypotheses have been advanced in the literature to account for RSF in the Highlands (cf. Table 3.1). Glacial oversteepening has been emphasised most frequently, but other possible processes include high cleft-water pressures, progressive-failure and seismic activity. The effects of some of these possible failure triggers have been modelled in back-analyses of certain of the examples discussed above and it is possible to make a number of inferences from these analyses.

It has been shown that all of the translational RSFs were unable to slide under gravity alone assuming that peak strength was mobilised. Glacial oversteepening has therefore been found to be relatively unimportant as a direct cause of slope failure.

Progressive-failure may have played a significant role in the failure of the Glen Kinglas, Mullach Fraoch-choire and Ben Donich SE examples, where the failure-surfaces lie close to or below the residual friction angles of the rocks in which they are formed. It is possible that progressive-failure of rock bridges could have led to minor displacements within the slope at depth, the surface expression of these small shear displacements being magnified into larger

movements on the slope surface (Barton 1971b, Hoek and Bray 1977). The opening of tension-cracks is the first sign of progressive-failure and in some instances their development may have permitted cleft-water pressures to act upon the upslope faces of blocks resulting in slope failure. In other cases it appears that tension-crack development has not been fatal to the slope and any forces (V) mobilised have been insufficient to cause complete failure and the rock-slopes remain intact.

At the majority of sites, some other force is required to augment gravity (even assuming ϕ_r) in order to cause failure. It has been reasoned that the most likely triggering mechanism was cleft-water pressure build up, perhaps in association with other factors. The cleft-water pressures which have been modelled are those used by slope engineers for design purposes and are thought to be representative of the conditions which may ensue during/after a heavy rainstorm (Hoek and Bray 1977).

Five of the case studies have failed completely, with debris transport occurring up to twice the length of their scars. It has been shown that most of the lines connecting the mass centres prior to failure with those after failure are inclined close to the residual friction angle for the material. Although, pore-water pressures, cohesive forces and friction angles could theoretically produce a plethora of different ϕ' values, their correspondence to the residual friction angles is suggestive that failed-debris transport can be accounted for by the residual strength properties of the rock-mass. It is therefore inferred that pore-water pressures did not act during transport of the majority of failed-debris masses.

The angle of the slope onto which RSF-debris falls is of major importance in determining the distance over which the debris is transported. If the angle of slope is well in excess of the effective friction angle of the debris then deposition is unlikely to occur on that slope. Equally, if a major free-face intervenes between a RSF scar and a slope inclined at less than the residual friction angle for the material, then the debris will be transported over a distance approximately equal to $d = h/\mathrm{Tan}\phi'$. The results of these mechanical analyses indicate that the residual friction angle can be substituted for ϕ' to yield a predicted distance of transport. At all of the study sites a slope inclined at close to the residual friction angle lay immediately downslope of the scar and therefore, unless excess pore-water pressures acted upon the RSF debris, excessive travel distances were improbable.

The cessation of movement of the intact failures can be explained by the shear-stiffness and dilation accompanying the displacement along a potential failure-surface (cf. Section 3.5). It is considered significant that the amount of displacement, generally up to 3% of the length of the failure-surface, is only slightly greater than that encountered in small-scale shear tests before peak shear strength is mobilised (e.g. Barton 1971a).

6.5 Conclusion

Five examples of plane-sliding failure and five wedge-failures have been described and analysed using rock mechanics techniques. Five of the examples are intact RSFs which have undergone comparatively minor displacements along their potential failure-

surfaces. Pre-failure displacements impeded by shear-stiffness effects are thought to have caused cessation of block displacement at these sites.

Many of the RSFs have translated along failure-surfaces inclined well below the angle of sliding friction and occassionally below the residual friction angle. The most satisfactory explanation for the triggering of translation is considered to be high cleft-water pressures which are inferred to have been created when the slopes were fully-saturated. Cleft-water pressures would have reduced the effective friction angles of the failure-surfaces enabling translation in some cases along failure-surfaces inclined below the residual friction angle.

Five RSFs have failed catastrophically, their debris being transported up to 420 m from their sources. The mechanics of debris transport have been analysed to attempt to ascertain whether pore-water pressures acted on the debris during transport. The inclination of lines connecting the mass centres of the failed-debris with the centres of blocks prior to failure (assumed to be inclined at ϕ') were found in four cases to approximate the residual friction angles of the rock material involved. In all but one instance pore-water pressures need not have acted upon the debris during transport.

7: ROCK-SLOPE TOPPLING AND COMPLEX FAILURE MODES: SMALL-SCALE FIELD EXAMPLES

7.1 Introduction

Until the early 1970's, recognition of rock-slope failure by toppling was restricted in the geomorphological literature to observations on the collapse of single rock slabs/columns. The fall of 'threatening rock' (Schumm and Chorley 1964) being a classic example of a massive toppled block. It is now recognised that toppling modes of failure may involve more than one block (Goodman and Bray 1976). Watters (1972) was one of the first authors to describe field examples of large-scale toppling of numerous interacting blocks. At the time at which he wrote however, mathematical models of toppling were restricted to Ashby's (1971) criterion for toppling of a slab on an inclined base (p 21). The Goodman and Bray (1976) kinematic test (cf. Section 2.4) has since provided an analysis for toppling failure of multiple non-rectangular shaped blocks permitting significant advances on the analyses of toppling made by Watters (1972).

The aims of this chapter are two-fold. First, to describe the failure modes of complex rock-slope failures and topples, using morphological and joint data, and secondly, to examine and discuss possible failure triggers. Four small-scale topples (less than 0.25 km^2) from the field areas are discussed in Section 7.3.

The potential for higher-order failure modes in the Scottish Highlands, given the complex structure of the Highland metamorphic rocks, was suggested in Chapter 2. Six examples showing complex failure modes, toppling combined with an element of translation, are

Figure 7.1: Modes of toppling failure (after Goodman and Bray 1976).

(a) Flexural-toppling

(b) Block-toppling

(c) Block-flexural-toppling

discussed and analysed in Section 7.4.

7.2 Previous research

Goodman and Bray (1976) have provided a useful tri-partite

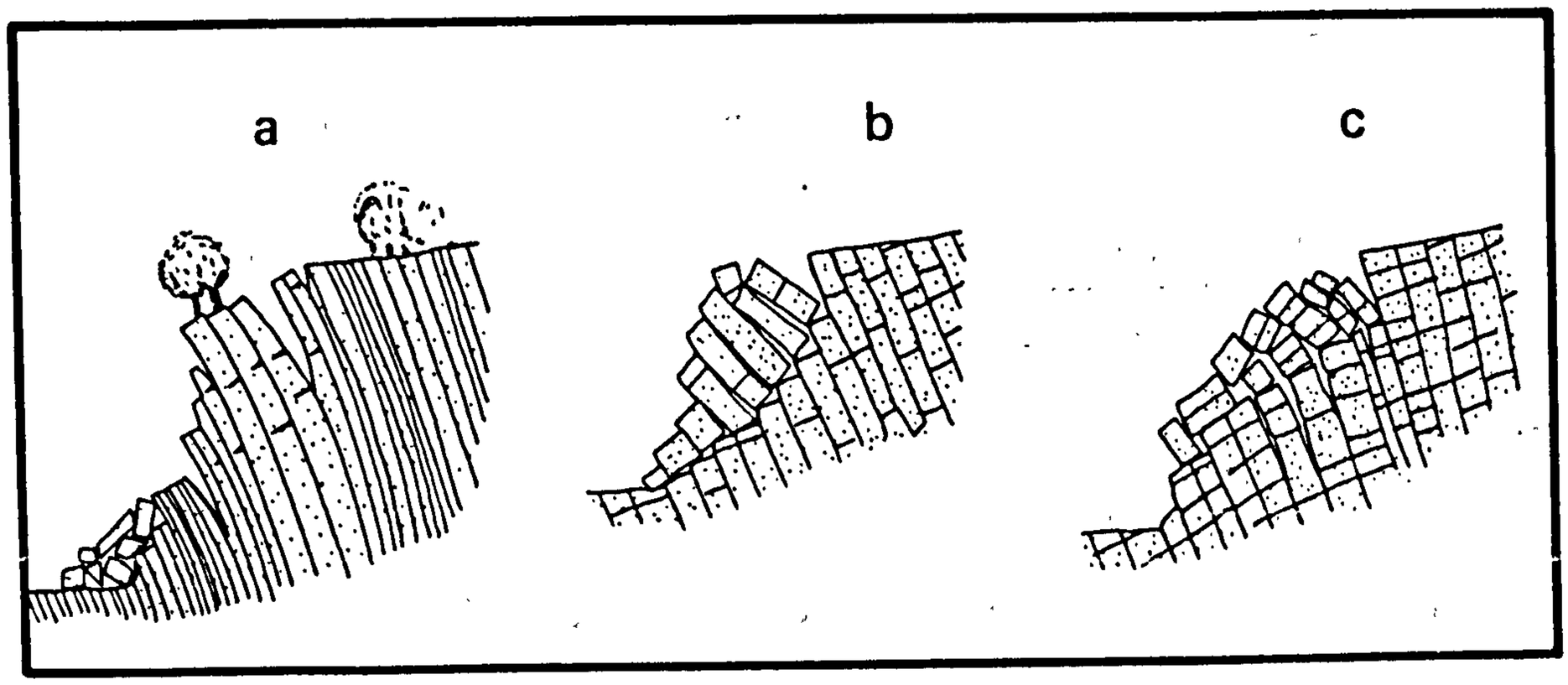

classification of types of toppling failure. Their scheme (Fig. 7.1 a-c) includes:

(a) Flexural-toppling. This occurs when continuous rock columns break in flexure as they bend forward. This type of topple is most likely to occur in schists, slates and phyllites (Goodman and Bray 1976);

(b) Block-toppling. This may occur when the rock-mass is divided into columns by widely-spaced cross joints. Little intact-rock breakage occurs with this form of toppling, distinguishing it from flexural toppling;

(c) Block-flexural-toppling. This form of toppling may occur in rock-masses with closely-spaced cross-joints. Instead of intact-rock fracture however accumulated movements along numerous cross-joints causing steepening of the highest cross-joints in columns: leading to

toppling and sliding. There are fewer edge-to-face and more face-to-face contacts in this form of toppling than block toppling.

Goodman and Bray also note that 'secondary' toppling can occur on slopes where independent toppling was unlikely to occur providing that other factors operate to excite failure. Complex failure modes may involve secondary toppling, where forward rotation of blocks is initiated by translational movements.

Distinctive geomorphic features result from toppling (Goodman and Bray 1976). These include: deep tension-cracks, obsequent- (or uphill-facing) scarps, flexural cracking and normal fault-type flexural slip (Goodman and Bray 1976). Toppling is also characterised by the greatest displacement of blocks occurring at the slope crest, as forward rotation of blocks increases upslope.

Few examples of toppling failure have been discussed in the literature, most of these having occurred in open pit mines, though many unpublished examples from various countries are known to Goodman and Bray (1976). Large flexural-topples are common in the slate quarries of N Wales. Goodman and Bray cited examples from the Dinorwic and Penn Rynn quarries where toppling failure utilises the steeply-inclined slatey cleavage.

Wyllie (1980) described an example of a topple in an open pit mine in the eastern foothills of the Rocky Mountains. The slope was composed of shales, sandstones and coal and, from his description, probably failed by flexural-toppling. Toppling at the foot of a large slope had evidently removed support from the slope above this leading to the collapse of 6.0×10^5 m^3 of material into the pit. The slope

was monitored prior to failure and Wyllie ascribed the measured decreases in the velocity of movement of the slope to reductions in the groundwater-pressure and to the transference from edge-to-face contacts between blocks to face-to-face contacts. Face-to-face contact during toppling will mobilise more resistance to deformation (Goodman and Bray 1976).

Brown (1982) discussed an analysis for toppling based upon the principles of energy-minimisation. The analysis subjects the entire slope system to a small rotational displacement, enabling evaluation of the net work. The blocks composing the topple are assumed to be rectangular, their sides being normal to the surface upon which they rest. This assumption necessitates considerable simplification of the slope geometry and prevents the use of the model in many geomorphological circumstances.

Brown's work is of particular interest as it illustrated the effects of cleft-water pressures upon rock-slope toppling. He showed that blocks resting on a surface inclined positively at 30°, their faces normal to the surface, would require a friction angle of 30° to maintain stability when the slope is freely-drained. In a fully-saturated slope, the friction angle required to maintain stability would be 60°. Clearly, high cleft-water pressures may have a detrimental affect in toppling failure as well as other modes of rock-slope failure.

Natural slope topples are particularly common along the N Devon coast (de Freitas and Watters 1973, Goodman and Bray 1976). Goodman and Bray showed that their kinematic criterion for toppling

successfully discriminates between failed and stable slopes in N Devon. de Freitas and Watters (1973) discussed a natural slope topple from SE Wales which occurred in sandstones and shales overlying a coal seam. The topple involved a block which rotated forwards through 20° and eventually translated down the slope. These authors also commented upon a massive topple in Glen Pean, Scotland (described in Section 8.2).

Sijing (1981) described an example of a complex rock-slope failure at the Jinchuan open pit mine in China. Toppling (which formed obsequent-scarps) was found to have occurred in combination with translational modes of failure. These failures took place within a larger rock-mass which was itself progressively-failing. No other small-scale published examples of toppling-combined with translation are known to the author, though numerous larger-scale examples been described in the literature (cf. Section 8.2).

7.3 Toppling modes of failure: field examples

Hell's Glen [NN 182 055] (4c).

A major block-topple developed in mica-schist has occurred on the N-facing slope of Hell's Glen. The major characteristic of the failed slope is a large block which has rotated by up to 30° to the N (Fig. 7.2a Plate 7.1). A rear-scarp rises to 28 m and has approximately 4° of overhang. Downslope of the large block a chaotic assemblage of boulders, resting on average at 30°, reaches to the valley floor.

The slope angle prior to failure was estimated, by averaging the

Figure 7.2: (a) Plan view of the Hell's Glen topple.

(b) Hypothetical section through the Hell's Glen topple.

Plate 7.1: The Hell's Glen topple (see Fig. 7.2a for direction of view).

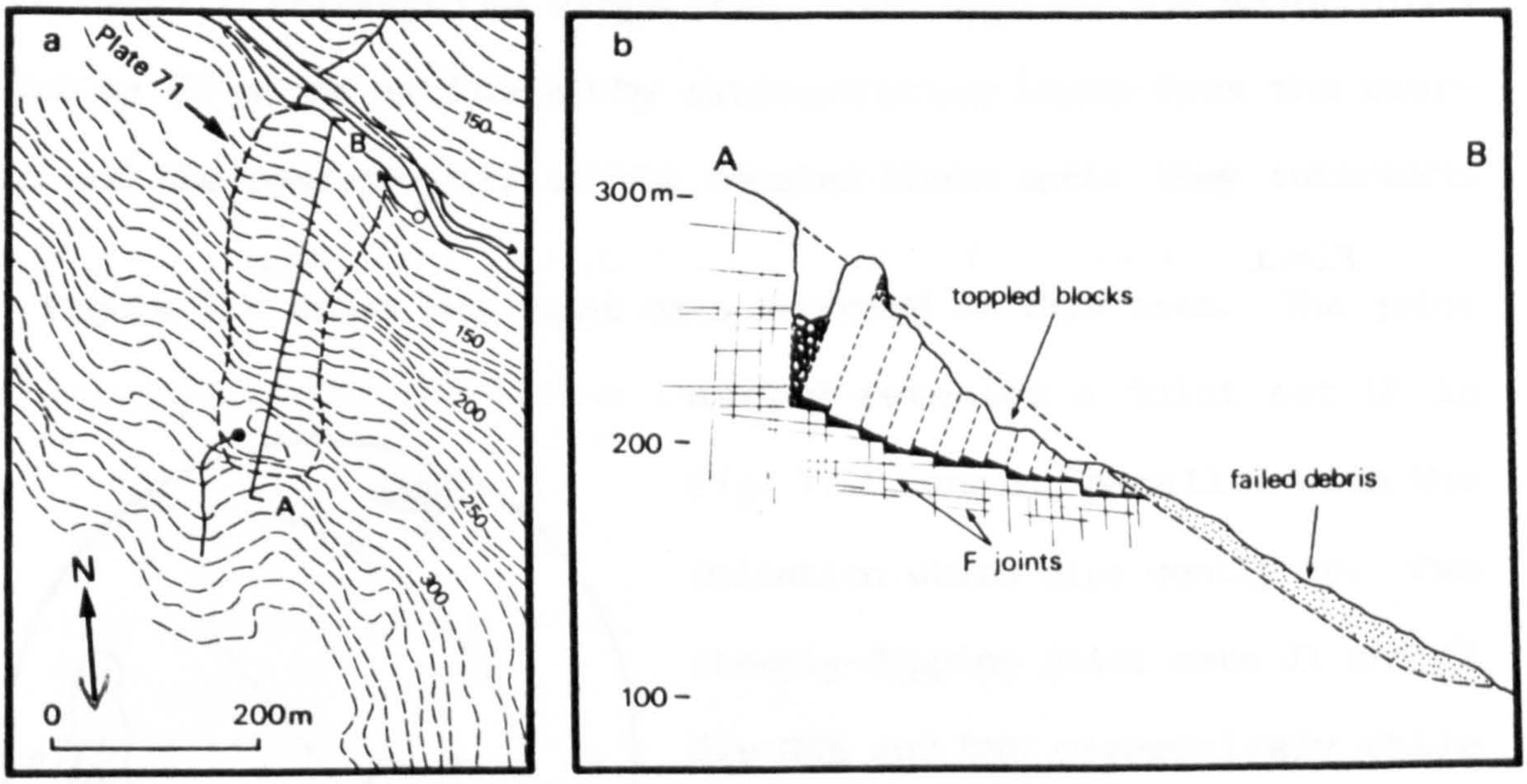
a
Plate 7.1
B
A
150
150
200
250
300
N
0
200m
b
A
B
300m
200
100
toppled blocks
failed debris
F joints

slope angles immediately outside the failed slope area, to be 34°. A cross-section through the slope (Fig. 7.2b) depicts the major block height as 60 m, as estimated by extrapolating lines from the rear-scarp and the upslope-wall of the toppled block until they intersect.

Figure 7.3 shows the joint data recorded at this site. The joint survey revealed a joint set (F in Fig. 7.3) running parallel with the foliation which dips gently NW. Two steeply-dipping joint sets J1 and J2 dip NNE and ENE respectively while the pole of J3 dips at 85° to the SE. The roughness of J3 surfaces was estimated to be 4° in the direction of interlayer-slip.

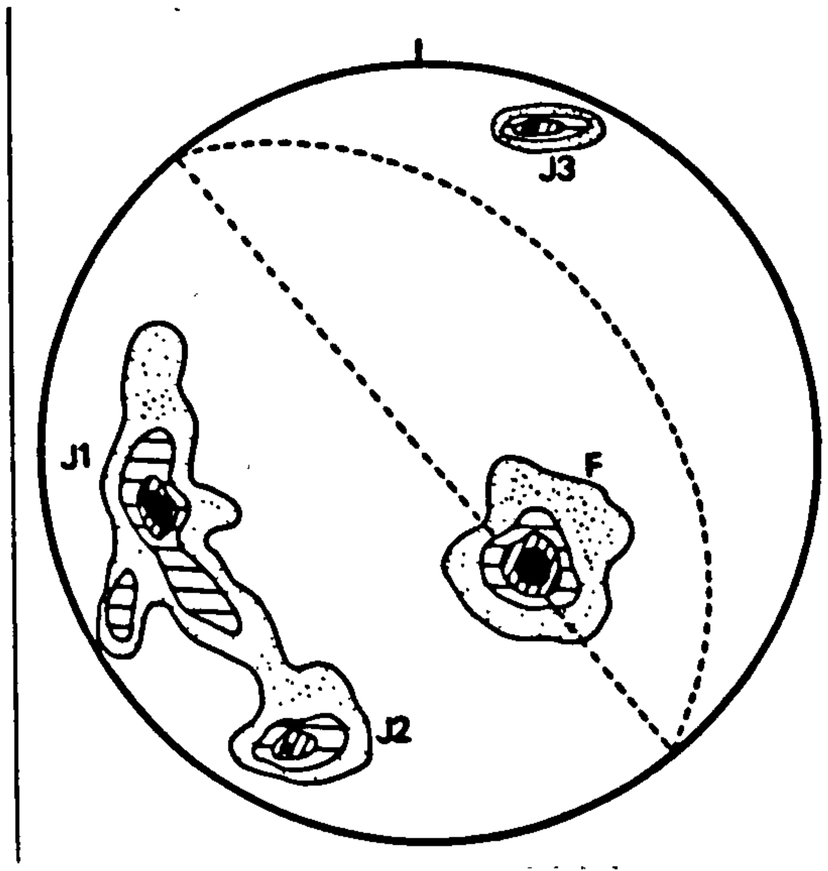

The pole of set J3 strikes within 2° of the strike of the reconstructed slope face and falls within the region on the stereographic projection which satisfies the kinematic toppling criterion. Toppling under self-weight stresses however could not have occurred along joints dipping at 86° (the dip angle of the rear-scarp) if ϕ was greater than 34°. This value is much less than the sliding friction angle of mica-schist and less than the peak friction angle (given i equals 4°). The residual friction angle of mica-schist is c. 24° (Watters 1972).

The peak shear strengths of the failure-surfaces will have been exceeded during slope failure. As noted in Section 2.4, the kinematic test assumes that the slope is freely-drained and that no shear

Figure 7.4: L.H. stereonet for The Steeple RSF (n = 200 poles).

strength intercept was mobilised. It is possible that cohesive force was mobilised against failure. The effective friction angle of the block faces must have been less than 34° ($\emptyset' < \alpha$ cf. Fig. 2.10) at the instant of failure and high cleft-water pressures may have acted upon the steeply inclined J3 joints.

The Steeple [NN 206 009] (4h).

Immediately W of The Steeple summit a 25-m-high rear-scarp, formed by a major joint, overhangs towards its base. The rear-scarp surface is planar, in the direction of shear, possessing an estimated i value of less than 3°. The major joint belongs to joint set J1 the pole of which trends 84° → 102° (Fig. 7.4). A further joint set F forms gently dipping cross-joints within the mica-schist. Joint set J2 provided lateral release surfaces which strike parallel to the direction of the slope.

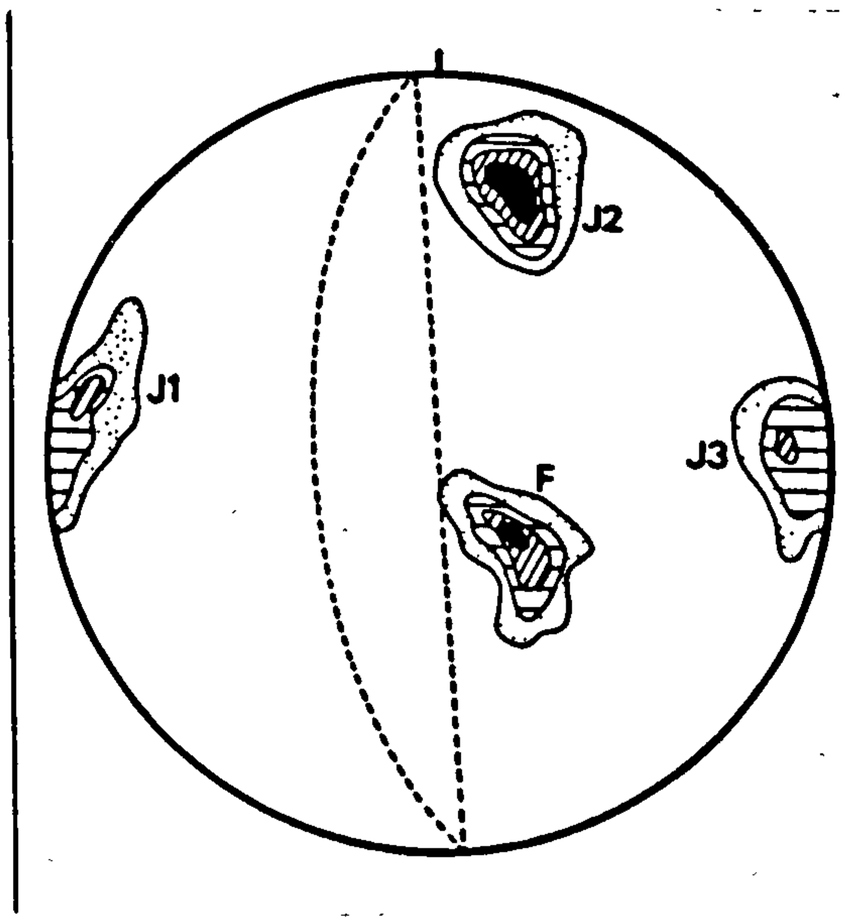

Downslope of the rear-scarp a major block has toppled, the toppling motion being evidenced by F joints on the block which are inclined towards the W at angles in excess of 45°. Extrapolation of the rear-scarp and the upslope face of the uppermost toppled block indicates tension-crack development at least 35 m below the original slope face. The uppermost block in the topple disintegrated during failure producing, with material from blocks formerly standing downslope of it, a debris mass that extends 150 m from the rear-scarp.

Slope angles outside the failed slope area average 43° and this value has been used for the pre-failure slope angle in the kinematic test. Self-weight toppling would have been possible along J1 discontinuities which dip at 86° into the slope, if the friction angle was below 43°. It is likely however, given the low normal stresses that would have acted upon J1 surfaces, that the full i value of 3° would be appropriate in the kinematic analysis. The peak friction angle may therefore be as high as 45°. In order to overcome the peak friction angle and any cohesive force, so producing an effective friction angle less than the slope angle, cleft-water pressures probably acted upon the slope.

Ben Donich N [NN 220 048] (4f).

A cliff composed of mica-schist and rising to a height of 40 m occurs upslope of a mass of coarse debris on the N-side of Ben Donich. Boulders up to 1000 m^3 in size occur within the debris mass with clefts between them up to 5-m-deep. Smaller boulders occur near the margin of the failed debris. The debris mass has an estimated thickness of up to 15 m and terminates abruptly 350-m-downslope of the rear-scarp, its frontal slope inclined at 34°.

A joint set (F) is directed parallel with the foliation which trends approximately horizontal. Joint set J1 trends 60-70° → 062° and a further set J2 is directed 85° → 135°. J3 runs 76-86° → 170° and strikes parallel with the rear-scarp. J3 surfaces possess an average roughness in the direction of failure of 5°.

To the W-margin of the rear-scarp, an area of relatively

Figure 7.5: L.H. stereonet for the Ben Donich N RSF (n = 200 poles).

unweathered rock is taken to define the former slope profile, which is reconstructed as sloping at 62° in the direction of failure. A pole concentration of greater than 4% of the joint sample occurs within the area satisfying the toppling criterion (Fig. 7.5). Toppling along J3 surfaces would have been kinematically feasible even assuming mobilisation of the peak friction angle (c. 45-50°). There is no need to infer that toppling was triggered by high cleft-water pressures.

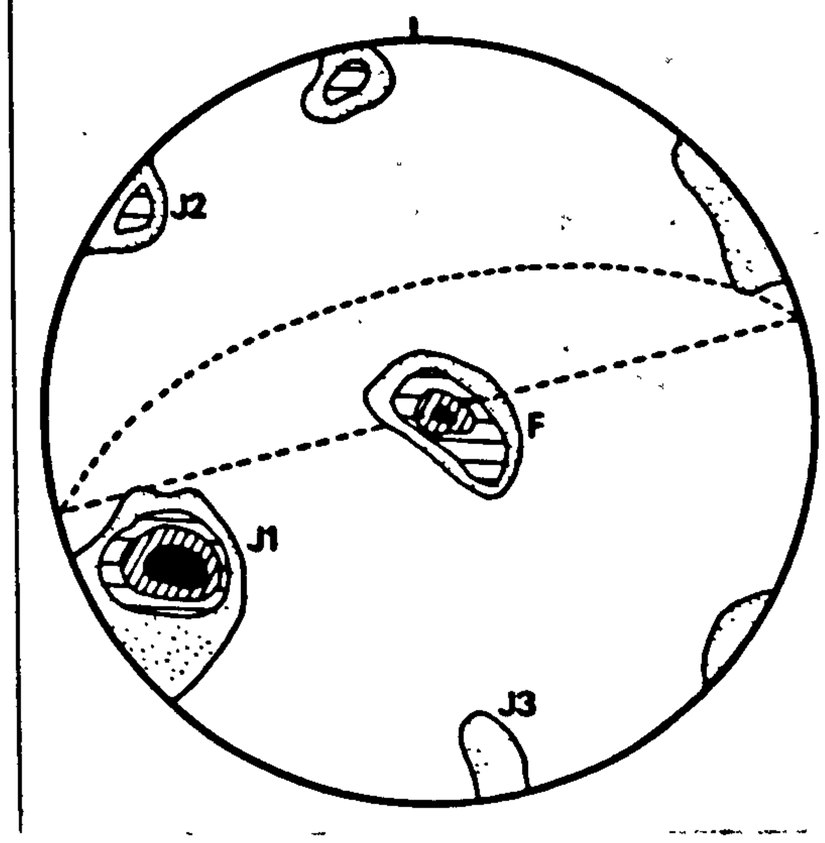

Using the mechanical analysis explained in Section 6.2, the mechanics of debris transport can be investigated by measuring the inclination of a line drawn between the centre of a mass before movement and its centre after cessation. At Ben Donich this line (ϕ') is inclined at 38° which lies between the residual friction angle for mica-schist (c. 24°) and the sliding friction angle (c. 41°). There is, therefore, no need to infer that excess pore-water pressures acted during debris transport.

Carn na Con Dhu summit [NH 073 242] (3a)

Immediately W of the summit of Carn na Con Dhu, a block-flexural topple has occurred on a psammitic rock-slope which is inclined at up to 48°. Several obsequent-scarps extend behind the crest of the slope onto the almost flat summit of the ridge. The obsequent-scarps trend E-W, are up to 2-m-high and are closely-spaced, some being just 5-m-

Figure 7.5: L.H. stereonet for the Ben Donich N RSF (n = 200 poles).

apart. The deformation of the slope appears to continue for c. 150 m below the ridge crest to where the slope angle decreases.

The structure of the slope is dominated by joint set J1, the pole of which dips negatively at 87° (Fig. 7.6). A foliation set (F) strikes E-W, dipping steeply northwards. The Goodman and Bray kinematic test illustrates that self-weight toppling would occur along J1 joints, providing that the mobilised friction angle was less than 39°. J1 joints were found to have an average i value of 8° in the direction of dip (i.e. parallel to the direction of interlayer slip). The roughness values when combined with the sliding friction angle for psammite, indicate a peak friction angle perhaps up to 52°. This angle is marginally greater than that required for self-weight toppling, according to the Goodman and Bray test and may have been sufficient to have prevented complete failure.

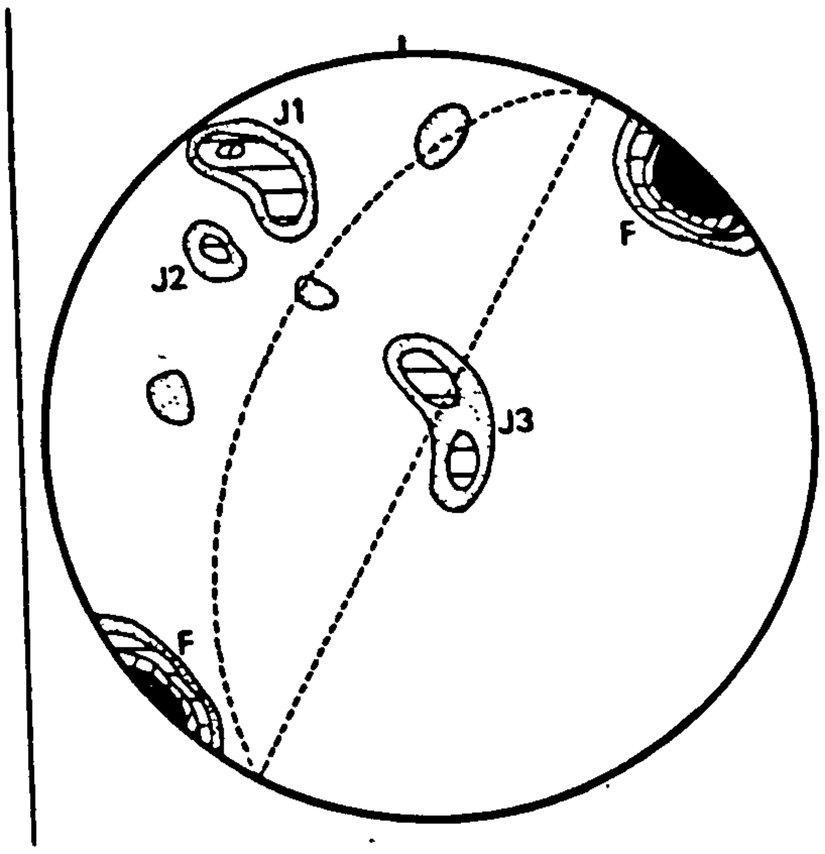

It was noted in Section 2.4 that minor shear displacements, of the order of 1-2% of the length of tested rough-joint surfaces, occur before peak shear strengths are mobilised. The shear displacement at Carn na Con Dhu is c. 1.3%, as indicated by the height of the obsequent-scarps and taking a slope height of 150 m. The correspondence between the relative amount of displacement at Carn na Con Dhu and that experienced during small-scale shear tests is suggestive that peak shear strength has been mobilised, causing

cessation of displacement. A section through part of the slope failure revealed open joints which may be the product of block-flexural-toppling or dilation accompanying shear displacement. Either way the permeability of the rock-slope has clearly been increased and this may prevent the build up of high cleft-water pressures within the slope. Further pertinent discussion concerning the cessation of toppling failures will be made in Chapter 8.

7.4 Complex modes of rock-slope failure

Mullach Coire a' Chuir [NN 172 037] (4e)

This example is a highly complex toppling-sliding failure developed on the comparatively gentle N-facing slope of Mullach Coire a' Chuir. Blocks have toppled at the crest of the slope forming V-shaped clefts up to 5-m-deep between the rear-scarp and their upslope faces (Plates 7.2 and 7.3). The angles between the rear-scarp and toppled blocks indicates forward rotation of blocks through angles of up to 30°. Downslope of the uppermost toppled blocks others have survived the degradation of the slope standing proud of the surrounding coarse debris (cf. Plate 7.2). The upslope and downslope walls of some blocks trend subparallel with one another, though the gaps between them may be up to 3-m-wide (Plate 7.4). This indicates translational movement of certain blocks within the RSF.

Three major joint sets were recorded on the slope, one of which (F) trends parallel with the foliation, which dips gently NW (Fig. 7.7). J2 strikes subparallel with the slope face and dips steeply

Plate 7.2: The Mullach Fraoch-choire RSF. Plate 7.3 is taken viewing from the NW along the trench between the rear-scarp and the uppermost toppled block.

Plate 7.3: The slope trench located between the uppermost toppled block and the rear-scarp at Mullach Choire a' Chuir. The rear-scarp is c. 8-m-high.

Plate 7.4: Translated blocks in the centre of the Mullach Choire a' Chuir RSF. The tension-crack is c. 3-m-wide and the blocks are up to 9-m-high.

Plate 7.5: View N along the deepest obsequent-scarp at Cairn Broadlands (p 131). The trench is up to 2.5-m-deep.

Figure 7.7: L.H. stereonet for the Mullach Choire a' Chuir RSF (n = 200 poles).

into it, its pole being directed 70° → 230°. Translation of blocks may have occurred along F joint surfaces.

Goodman and Bray (1976) observed that complex sliding and overturning (both uphill and downhill) of blocks is possible when toppling occurs on horizontal surfaces. It is thought likely that a stepped surface has been produced by F and J2 surfaces at Mullach Choire a' Chuir. It seems likely that toppling occurred first allowing upslope blocks to translate and topple (Plate 7.2).

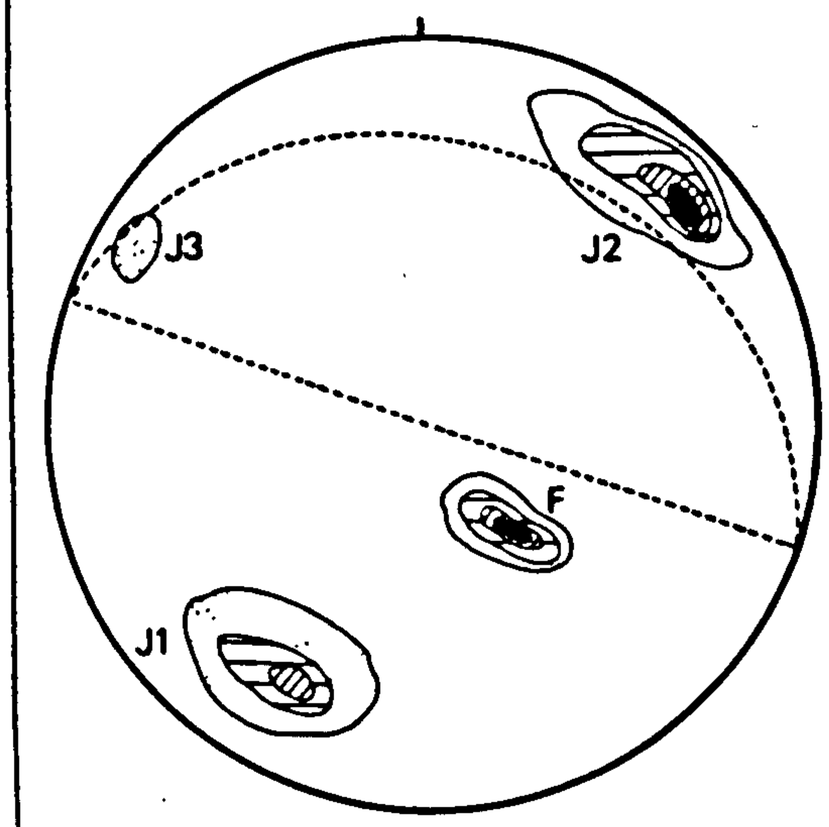

This example possesses a similar morphology to the "roller bearing" type of rock-slope failure described by Eisbacher (1979a) for certain large cliff collapses in the Mackenzie Mts, northwestern Canada. These forms of failure occur on slopes on slopes inclined below 25° and may be triggered, according to Eisbacher, by earthquake-loading of rock-slopes. They are typically characterised by complete break-up of the rock-slope with components of toppling and sliding occurring within the failing mass (cf. Eisbacher 1979a; Fig. 8).

Cairn Broadlands [NO 273 776] (2a).

Four major joint sets were recorded on the slope (Fig. 7.8). J1 is a well-developed set which dips both steeply positively and negatively, having an average trend of 86° → 236°. Joint set J2 dips steeply NW while J3 is oriented 60° → 146°.

Plate 7.6: Vertical aerial photograph (c. 1:10,000-scale) of the Cairn Broadlands RSF. Top of the photograph is N.

Figure 7.9: Surveyed section along the Cairn Broadlands RSF.

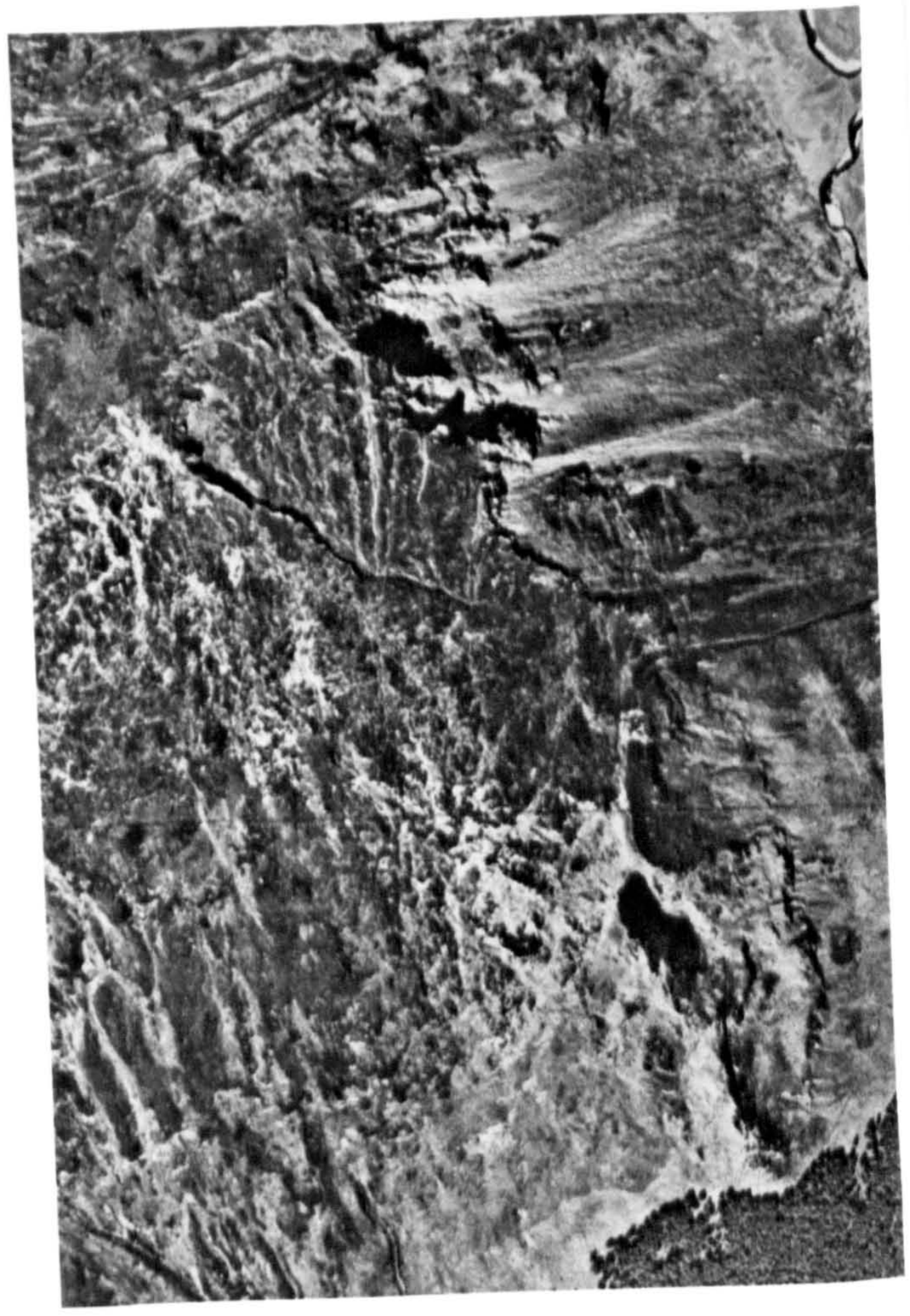

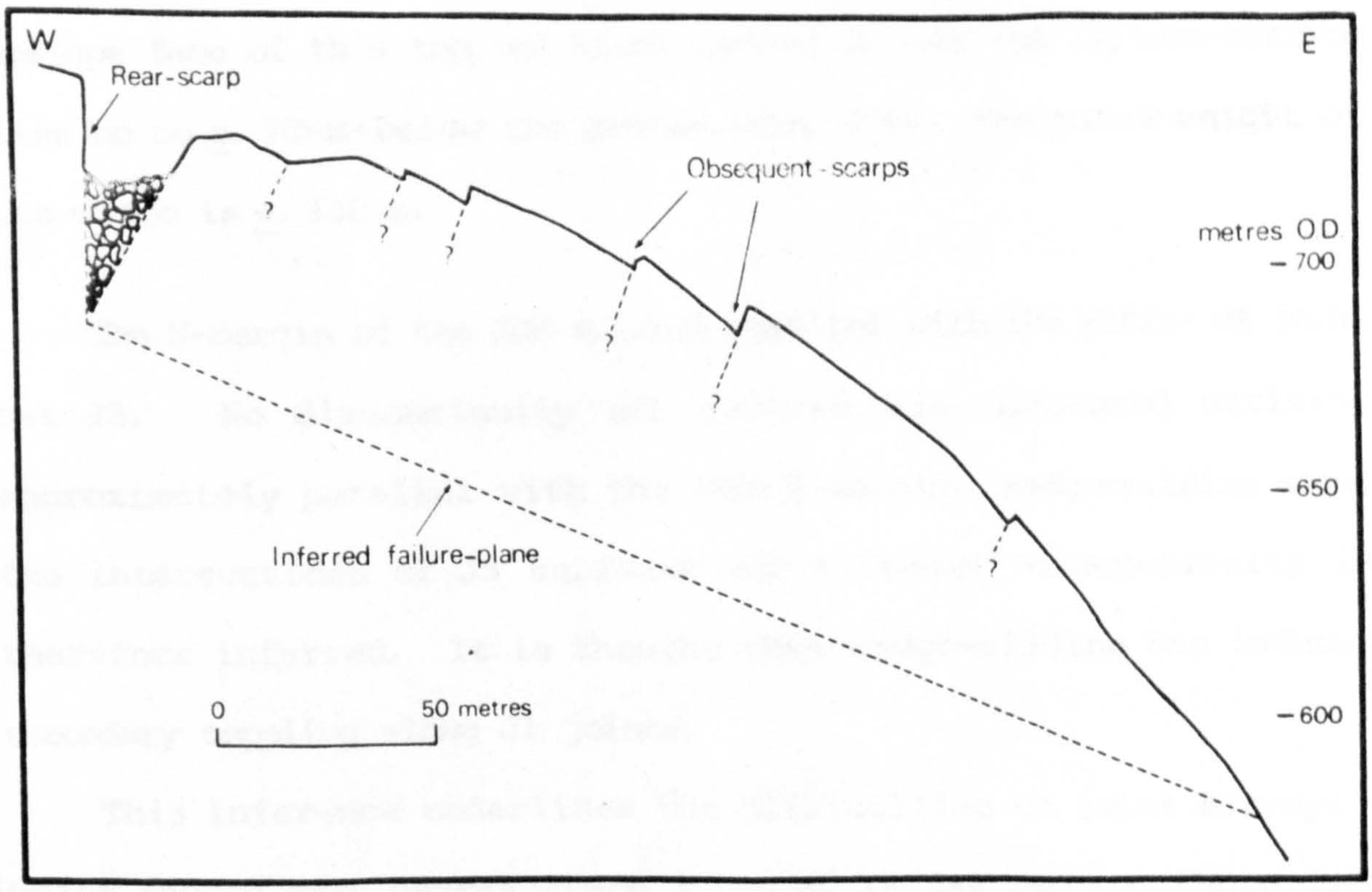
W
E
Rear-scarp
Obsequent - scarps
metres OD
– 700
– 650
– 600
Inferred failure-plane
0
50 metres

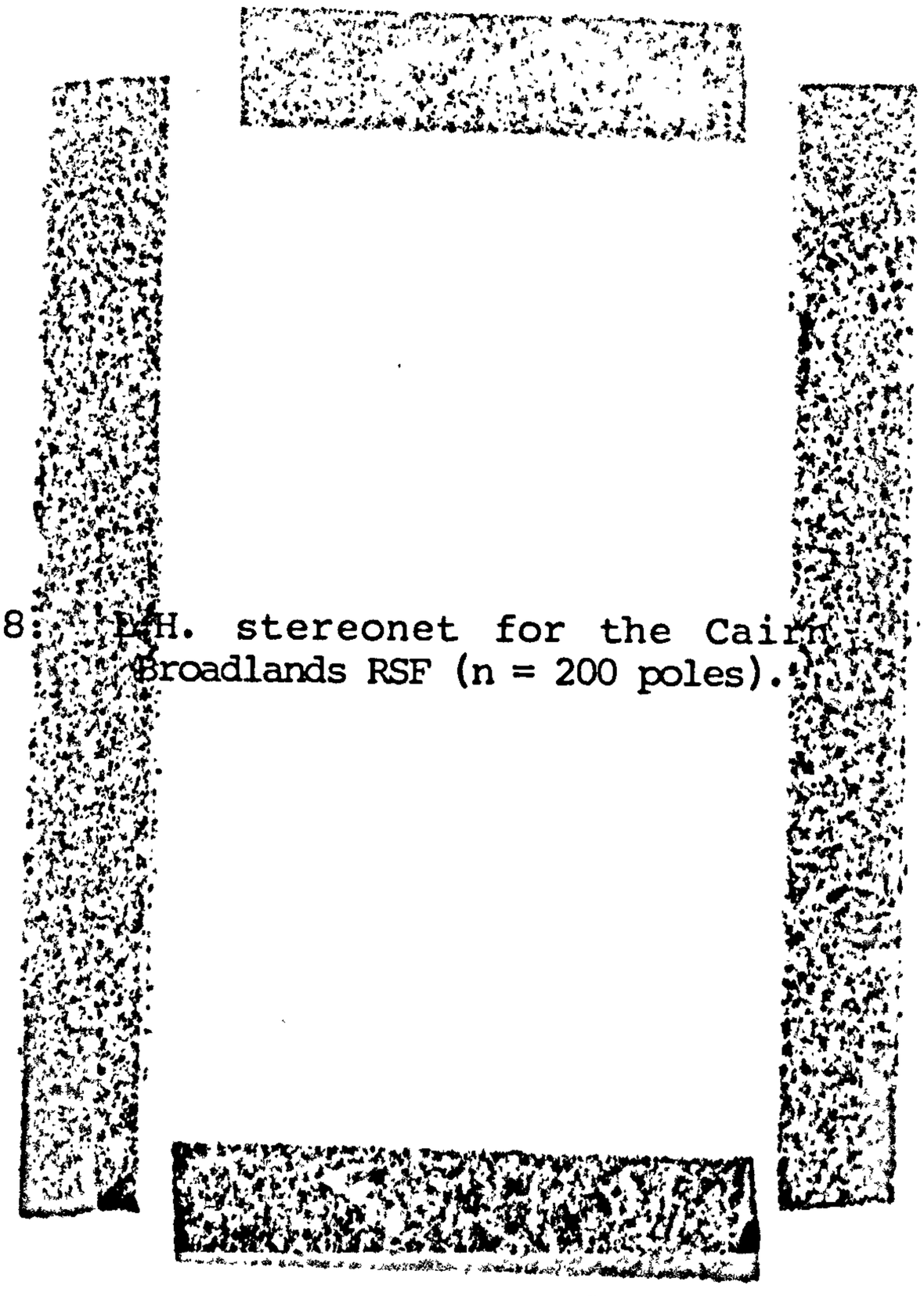

Figure 7.8: P-H. stereonet for the Cairn Broadlands RSF (n = 200 poles).

Several obsequent-scarps, the largest of which is 200-m-long and 6-m-deep (Plate 7.5), occur within a trapezoidal-shaped (in plan) intact-RSF at Cairn Broadlands. The limits to the displaced mass are delimited by a 1-4-m-deep cleft to the S and by cliffs (up to 8-m-high) to the N. The shape of the mass is indicative of a wedge-slide (Plate 7.6). It is thought that toppling has occurred within the scale of a wedge-slide. The obsequent-scarps on the slope strike parallel with the pole of J1. Downslope of the scarps localised oversteepening has led to rockfalls at the toe of the wedge-slide.

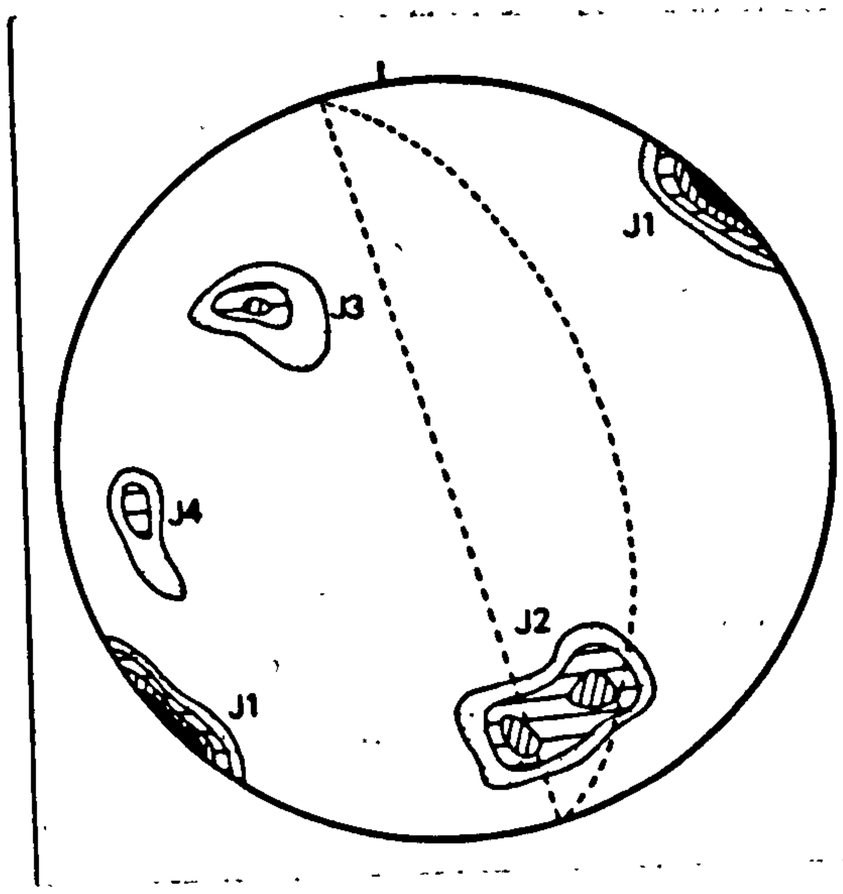

At c. 730 m O.D. a 21-m-high rear-scarp has been exposed by forward rotation of blocks. Extrapolation of the rear-scarp and the upslope face of this toppled block indicates that the failure-surface lies up to c. 70-m-below the ground (Fig. 7.9). The total height of the wedge is c. 150 m.

The N-margin of the RSF strikes parallel with the strike of joint set J3. No discontinuity set however was measured striking approximately parallel with the RSFs S-margin. Wedge-sliding along the intersections of J3 surfaces and a "rogue" discontinuity is therefore inferred. It is thought that wedge-sliding has induced secondary toppling along J1 joints.

This inference underlines the difficulties of joint surveys - which record only near-surface joint attitudes and not those deep

Figure 7.10: L.H. stereonet for the Cairn Inks RSF (n = 100 poles).

within a rock-slope - and warns of the possibility that potential failure-surfaces may go unrecognised until shear displacement occurs.

Cairn Inks [NO 312 722] (2c)

Four joint sets were recorded on this slope (Fig 7.10). The pole of J1 the most important set trends 82° → 222°, though individual joint poles from this set were recorded as dipping both steeply negatively and positively. J2 is orientated 62° → 150° and strikes subparallel with the strike of the NW surface of the RSFs V-shaped scar. The steep SW wall strikes 115/295°, subparallel with the strike of the J3 pole and the NW wall strikes approximately 042/222°, subparallel with the average strike of set J1.

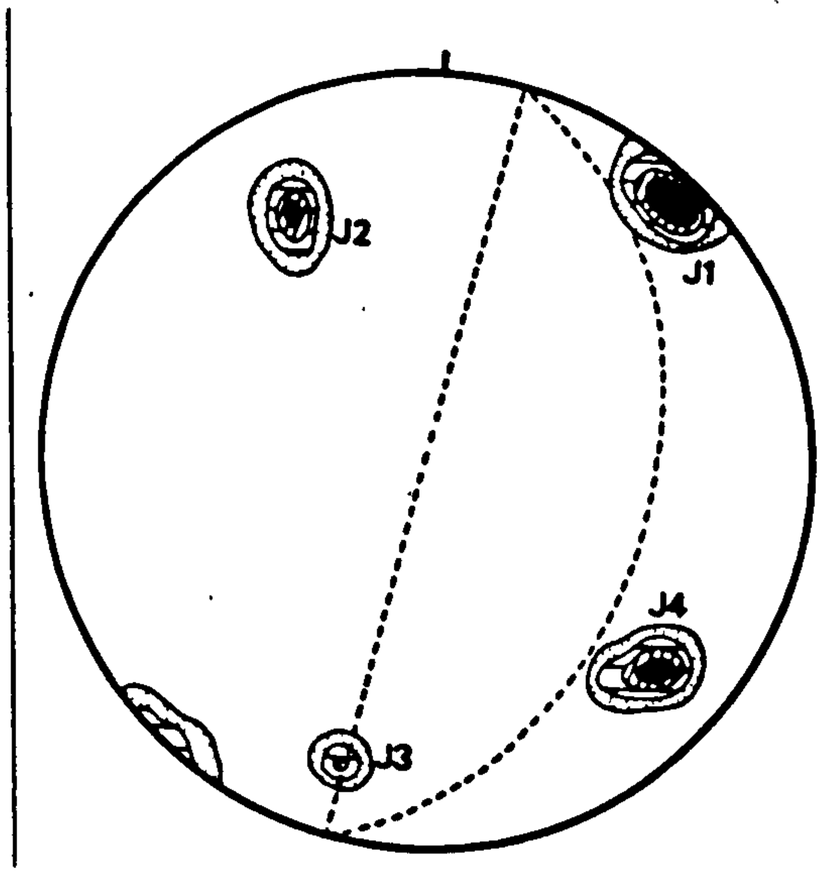

The shape of the rear-scarp is indicative of a wedge-slide and the kinematic test for wedge-sliding indicates that potential failure-surfaces could have been formed by J2 and J3 joints. The average intersection of these two joint sets is inclined at 2°, below the peak friction angle for mica-schist. It is therefore suggested that cleft-water pressures acted to cause failure.

Like the Cairn Broadlands example, obsequent-scarps produced on the displaced rock indicate limited toppling. The scarps trend parallel with the J1 pole and are thought to have been produced by

Figure 7.11: L.H. stereonet for the Capel Burn RSF (n = 200 poles).

secondary toppling along J1 joints as the wedge translated downslope.

Capel Burn [NO 297 781] (2b).

Obsequent-scarps on this RSF indicate limited toppling during shear displacement. The scarps are up to 3.5-m-high and trend sub-parallel with the strike of the slope face and approximately parallel with the strike of J1 (Fig. 7.11).

In cross-section the slope steepens markedly towards its base. Oversteepening of this lower slope unit may have been achieved by the action of glacial meltwaters from the ice-cap outlet glacier (Section 5.3) forming an 8-m-deep gorge. Immediately above the gorge, slope angles average 44°. This value has been used in the kinematic test for toppling because, as noted earlier, toppling could occur on the steepest portion of the slope then spread upslope onto more gently sloping ground. The slope upon which the obsequent-scarps have developed is inclined at 25°.

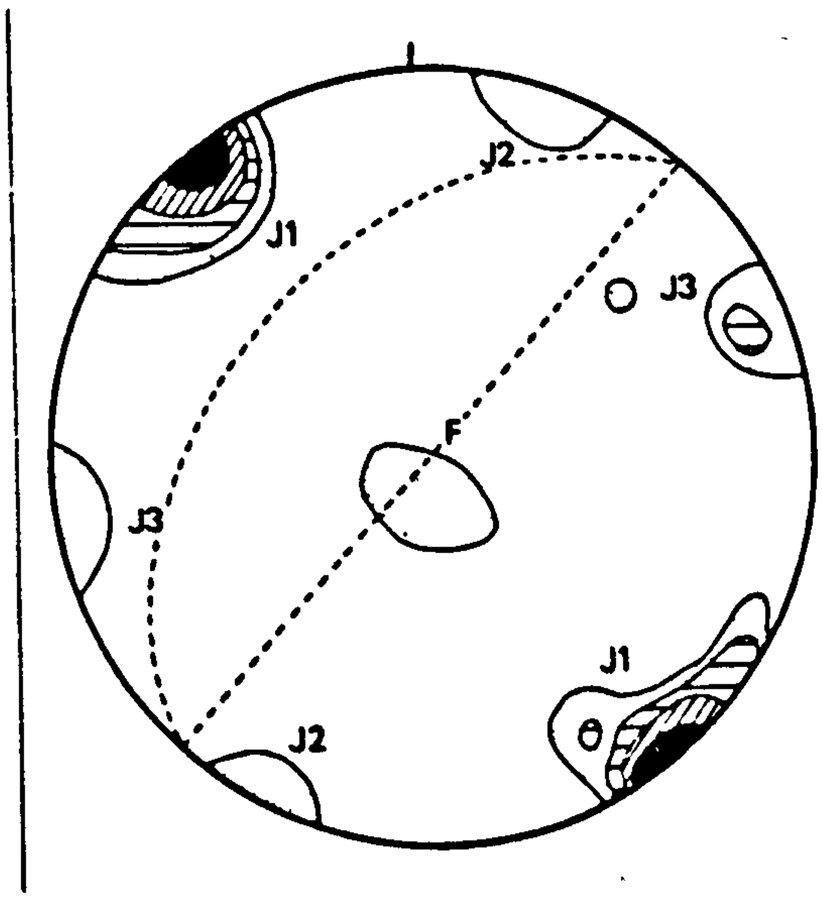

Simple toppling of the RSF is not indicated by the morphology of the slope as a 10-m-high rear-scarp is located upslope of the toppled blocks. A low angle plane-slide appears to have occurred along F joint surfaces, some of which dip positively at up to 32°. It is likely that toppling occurred at the base of the slope first, proceeding upslope until sliding took place behind the uppermost toppled block.

Figure 7.12: L.H. stereonet for the Mam Sodhail ridge RSF (n = 200 poles).

Mam Sodhail Ridge [NH 114 246] (3c).

Downslope displacement of a 400-m-wide block is evidenced at this site by a 10-m-high rear-scarp. One large (up to 5-m-high) obsequent-scarp occurs within the displaced block and strikes approximately parallel with the slope face, which dips at up to 52°.

The structure of the slope is very complex, six major joint sets were recorded (Fig. 7.12). Set J1 is composed of joints with dip directions between 102 and 164°. The dip angles of joints belonging to this set range from 56 to 90°. Vertical joints from set J1 were found to strike parallel with the strike of the slope face. J2, a stress-relief joint set, is positively inclined between 10 and 45°. J3 and J4 are steeply dipping while J5 joints dip at 34-44° into the slope.

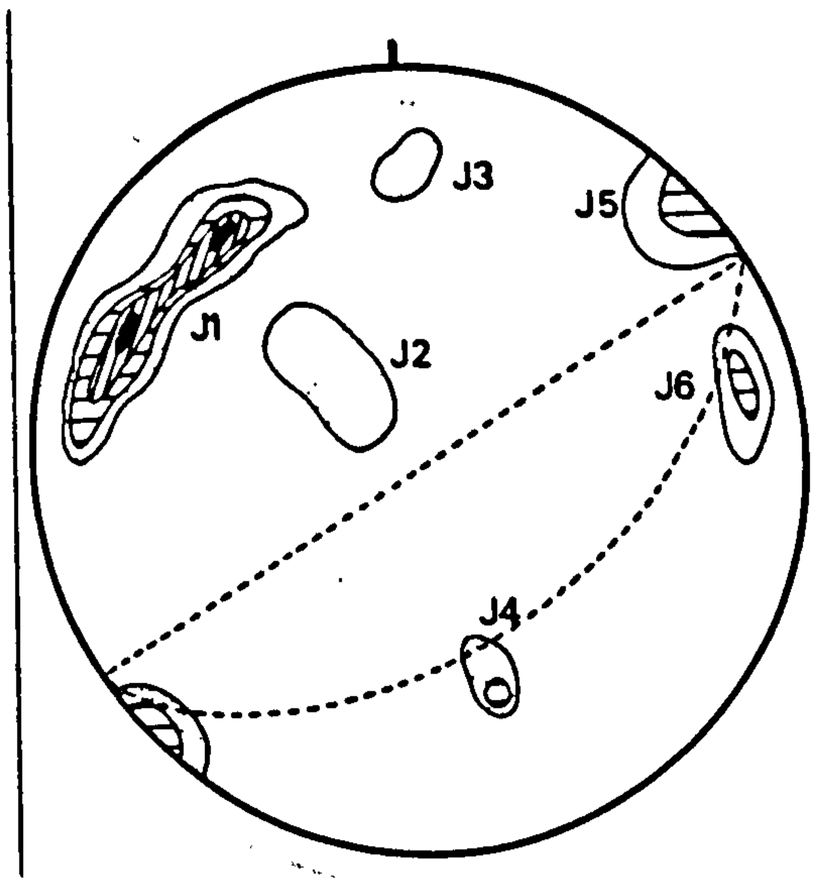

Plane-sliding is kinematically feasible along joint set J2 but J5 surfaces are insufficiently steeply-dipping to occur within the region on the stereonet satisfying the toppling criterion. The only possible surfaces along which toppling could have occurred are the vertical J1 joints. It is therefore inferred that translation of the rock-mass along J2 surfaces caused rotation of J1 joints, exciting secondary toppling failure. It is likely that the initial plane-sliding movement occurred in response to high cleft-water pressures as the J2 joints which may form the sliding surface are inclined, on

Figure 7.13: L.H. stereonet for the Corrie of Clova RSF.

average, below the sliding friction angle.

Corrie of Clova [NO 329 758] (2d)

The geologic structure of this corrie is comparatively complex (Fig. 7.13) enabling a number of possible failure modes around its headwalls. At the corrie backwall a mass of coarse felspathic gneiss has displaced to the S, forming several obsequent-scarps. The scarps run sub-parallel with joint sets J1 and J3 and are up to 1.5-m-high.

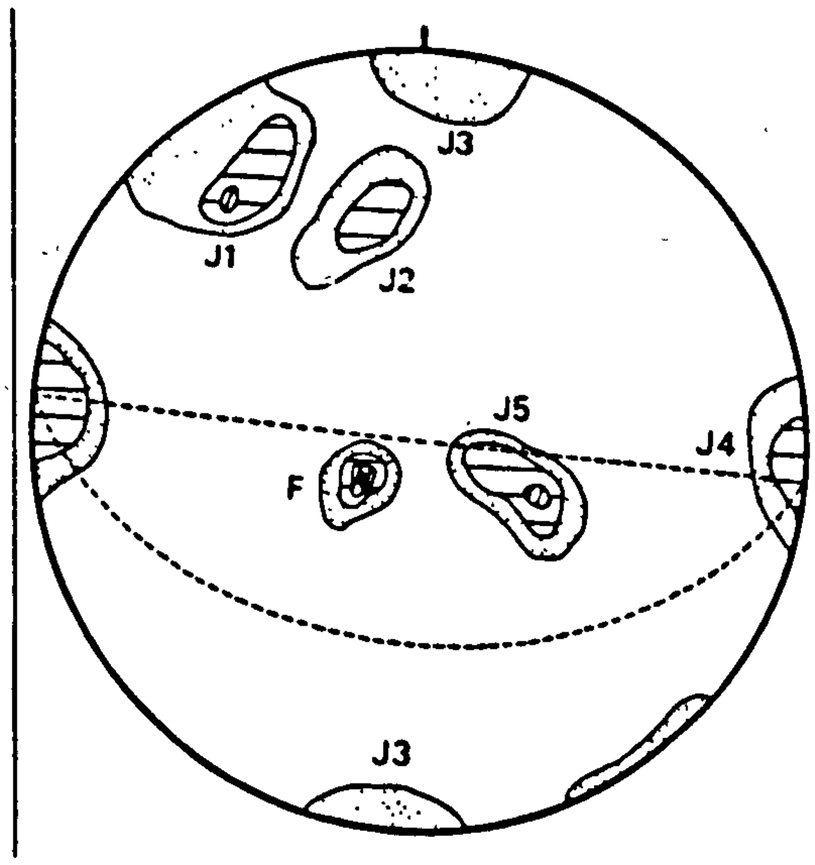

Both J1 and J3 sets possess joints that dip steeply into the slope. Joint set F parallels the foliation on the slope and dips at 12° towards the NE. The pole of a second low-angle joint set dips 16° NW. Upslope of the obsequent-scarps a 50-m-high rear-scarp crops out. Kinematic testing shows that plane-sliding along J2 surfaces would be possible if the slope exceeded 40°: thus permitting J2 joints to crop out into the corrie backwall. The backwall dips on average at 41° in the vicinity of the RSF. No RSF toe was found below the lowermost obsequent-scarp.

Toppling along J1 and J3 joints dipping at 89° into the slope could also occur if the friction angle was less than 48°. It is suggested that toppling has occurred within a mass that translated along J2 surfaces causing secondary toppling. Unfortunately, due to the lack of sub-surface information, it is not possible to provide a more penetrating analysis of the mechanics of this RSF. Its

complexity however is illustrative of the difficulties inherent in analysing slopes with numerous joint sets.

7.5 Discussion

Goodman and Bray (1976) stated that toppling failure of a rock-slope may be violent but does not usually produce high velocites. According to them the rock material in a toppling failure will invariably break up during gradual rotation of blocks, forming a talus deposit at the base of the slope.

Inferences concerning the velocity of failure of the field examples are difficult to make. However, the downslope margin of the Ben Donich topple is sharp. It would seem unlikely that such a clear margin could have been formed by sporadic release of blocks from the faces of larger toppling blocks. The explanation proposed here is that the debris mass was produced by catastrophic toppling failure of the slope. In contrast, the toppling failure at the summit of Carn na Con Dhu probably occurred relatively slowly by progressive-failure which was terminated by the mobilisation of peak shear strength along negatively-dipping joints.

It is considered significant that the two toppling failures which have failed completely possess similar joint patterns, which define blocks which are approximately rectangular, their front faces striking parallel/subparallel with the slope face and their sides trending approximately normal to the slope. The block bases are delimited by cross-joints, which are usually joints trending parallel with the foliation for the case studies.

Figure 7.14: Idealised joint set patterns for toppling failure.

The forementioned joint patterns approximate to the ideal combination of cross-joints shown in Figure 7.14. In this hypothetical slope the lateral release joints (L) are nearly vertical and so the normal stresses along these surfaces will approach zero. If joints strike normal to the slope face but are inclined, they will contribute more lateral resistance to toppling because of the increased shear strengths activated by higher normal stresses. The potential for high velocity failure of slopes by toppling would be increased if the joint patterns followed the ideal.

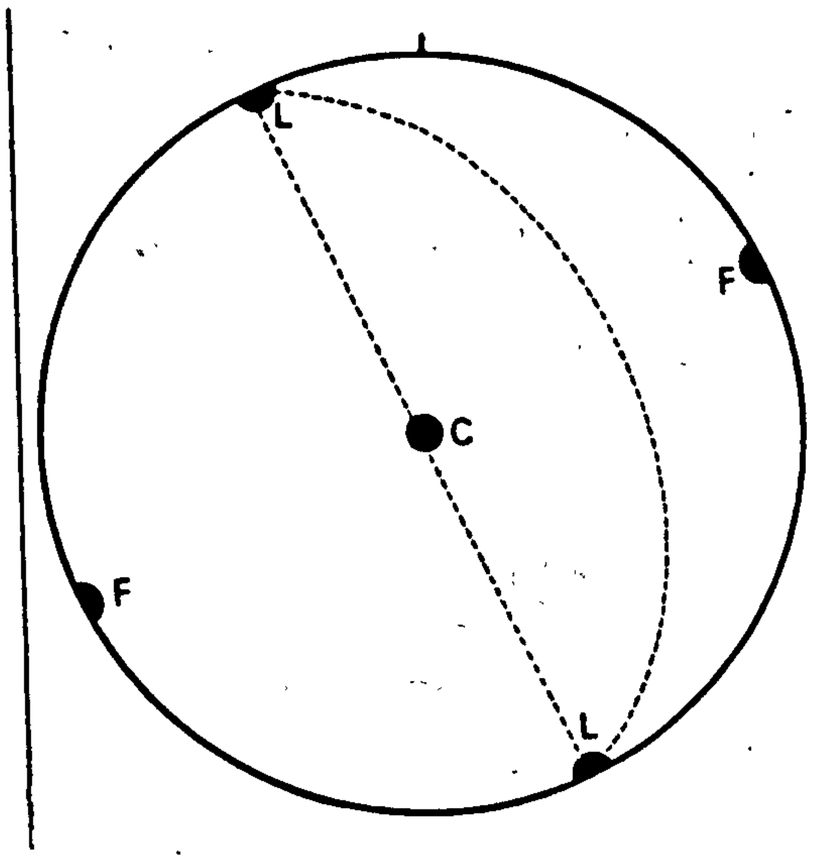

Toppling under self-weight stresses it has been inferred could not have occurred at Hell's Glen and The Steeple unless ϕ values below the peak were mobilised. Toppling failure due solely to oversteepening of the slopes is therefore rejected at these two sites. At Capel Burn meltwater erosion may have led to localised slope oversteepening and at Ben Donich, the failed slope being the headwall of a large compound corrie, glacial oversteepening may have occurred.

As noted in Section 2.4 the kinematic test for toppling takes no account of possible cleft-water pressures acting upon the upslope faces of the blocks. Neither does the test cater for the force imparted upon a toppling block by the weight of blocks upslope of it.

Toppling at Hell's Glen, Ben Donich and The Steeple has left free-faces which are inclined at +/- 10° from the vertical. Further

toppling under self-weight stresses is kinematically feasible at these sites, even assuming peak friction angles, yet the slopes appear to be stable as no major tension-cracks crop out upslope of the rear-scarps. The potential for further toppling it may be hypothesised is dependent upon the continuity and spacing of joints, particularly L-surfaces, behind the rear-scarp. If L-joints terminate at the rear-scarp, or extend beyond it for a distance less than the spacing of F-joints, then toppling will be inhibited (Fig. 7.13). This situation has arisen at The Steeple where J1 joints terminate at the rear-scarp. No lateral release surfaces occur behind the scarp and toppling is consequently prohibited. It is not known whether a similar situation occurs at Ben Donich or Hell's Glen as vegetation cover prevents the tracing of joint outcrops.

If cross-joints cut across a toppling block, it is more likely to break-up by small-scale plane-sliding or by block-flexural toppling (cf. Goodman and Bray 1976) particularly if forward rotation of blocks inclines the cross-joints above their sliding friction angle. Degradation of blocks will take place from the lowest working upslope. Much depends upon the spacing of L and F-joints as some large toppled blocks (e.g. Hell's Glen) have rotated without breaking-up. Caine (1982) suggested that preservation of toppled blocks may be due to a "cushioning-effect" provided by thick talus deposits. The debris deposited as a coarse scree in front of toppled blocks may also provide support to the slope thus preventing further block rotation.

Toppling failure has been demonstrated to occur in association with translational forms of failure. As resistance to sliding has

clearly been mobilised within the displaced mass by secondary toppling, conventional limit-equilibrium techniques of plane and wedge-sliding are not applicable to these cases. Limit-equilibrium models assume that the displaced block behaves rigidly.

Relatively little attention has been given to complex failure modes in the engineering-geology literature compared to the plane, wedge-sliding and toppling modes. The recognition of such RSFs is of practical importance, especially where back-analyses of natural slope failures are used in design proc-edure.

Steeply-dipping discontinuities, which strike approximately normal to the direction of displacement, occur at all the sites of complex failure where obsequent-scarps have formed. This indicates that secondary toppling may occur whenever this condition is satisfied and that these RSFs may fail catastrophically. Care must therefore be taken in using obsequent-scarps alone as indicators of toppling (cf. Goodman and Bray 1976) and by implication slow RSF velocities.

7.6 Conclusions

Four examples of small-scale toppling failure have been discussed from the field areas. The diagnosis of toppling failure has been based upon geomorphological evidence, particularly the occurrence of obsequent-scarps, the attitudes of displaced blocks and from the availability of kinematically suitable joints. Analyses of toppling have been made using the Goodman and Bray (1976) kinematic criterion. The potential for toppling has been shown to be dependent upon the spacing and continuity of joint surfaces, factors which are difficult

to account for in kinematic or mathematical modelling.

In order for interlayer slip to have occurred at Hell's Glen, The Steeple and at the Carn na Con Dhu summit topples, the effective friction angles must have been less than the peak friction angles for the rock. Glacial oversteepening of slopes can be rejected as the sole triggering mechanism in these instances since for self-weight toppling the slope angle would need to be steeper than the peak friction angle. High cleft-water pressures have been suggested as a possible cause of failure where the self-weight toppling criterion is unsatisfied. It is not possible to model the nature of cleft-water pressure distributions in the kinematic test for toppling but their effects can be assessed using the effective friction angle concept.

Complex failure modes have been proven to occur on natural slopes where discontinuity patterns are themselves complex. Secondary toppling is associated with both wedge-sliding and plane-sliding failures. It is suggested that wherever discontinuities strike approximately normal to the direction of failure and dip steeply into the slope then secondary toppling may be excited by translational movement. Joints dipping vertically and striking subparallel with the slope face may also be overturned causing toppling failure.

The control of joint patterns on the failure modes of the examples discussed in both this and the preceeding chapter has been established. When exposed by complete failure of the RSF, the scars have been found to possess linear surfaces which are generally sub-parallel with pre-existing joints. As size increases however the possibility arises that shear displacement may not occur along linear

surfaces but thick zones of rock (cf. Eisbacher 1979a). The following chapter discusses RSFs which are an order of magnitude or more larger than those dealt with so far and considerably more complex.

8: OBSEQUENT-SCARP DEVELOPMENT AND LARGE-SCALE SLOPE DEFORMATION IN THE SCOTTISH HIGHLANDS

8.1 Introduction

Numerous authors have commented upon the formation of obsequent-scarps (sometimes termed counter-scarps or antislope-scarps) in high-mountain areas. These landforms have been described as occurring in Japan (Kobayashi 1956, Yagi 1981), the Carpathian Mts. (Jahn 1964, Nemčok 1972), North America (Tabor 1971, Patton and Hendron 1974, Radbruch-Hall et al. 1976, Eisbacher 1979b, Bovis 1982), New Zealand (Beck 1968), the French Alps (J.J. Jarvis pers. comm.), the Pyrenees (Rengers and Soeters 1982), the Peruvian Andes (J.N. Hutchinson pers. comm.) and in Britain (de Freitas and Watters 1973).

The obsequent-scarps reported by these workers are up to 10-m-high. Some are located downslope of elongate ridge-top furrows (Tabor 1971) and may be associated with slope 'bulging' (Radbruch-Hall et al. 1976). These topographic features are considered by some researchers (e.g. Radbruch-Hall 1978) to have formed in response to 'deep-reaching gravitational deformation', which Radbruch-Hall et al. (1976) defined as a flow-type displacement of rock, where motion takes place by relative movement of particles within a moving mass without formation of a continuous shear surface. This mode of deformation is similar to the 'sackung' (or sagging) movement of slopes reported by Zischinsky (1966, 1969). There is no evidence that the mode of deformation inferred by Radbruch-Hall et al. (1976) occurs.

Radbruch-Hall et al. (1976) termed obsequent-scarps, ridge-top furrows and slope bulging 'sackung features': thereby implying a

specific mode of deformation as the cause of these features. Radbruch-Hall et als. genetic classification is unjustified however since it is not known if factors other than gravity (e.g. earthquakes) can cause their formation. Sackung-like deformation of slopes is known to have occurred without formation of obsequent-scarps (e.g. Zischinsky 1966).

Watters (1972) investigated a number of slopes with obsequent-scarps in Scotland and proposed that these slope features are generally caused by toppling failure. He made no reference however to the papers by Jahn (1964), Zischinsky (1966, 1969), Beck (1968) and Tabor (1971). Conversely, many eastern European and North American researchers have omitted mention of toppling as a possible cause of obsequent-scarp formation. For example, in a paper reviewing large-scale slope deformations, including those which have formed obsequent-scarps, Radbruch-Hall (1978) failed to refer to toppling failure.

The study of large-scale slope deformation is of interest to both geomorphologists and engineering-geologists (Rengers and Soeters 1982) and an engineering-geology approach to obsequent-scarp development at sites in the United Arab Emirates, the Pyrenees and Scotland is being undertaken by J.J. Jarvis, Imperial College.

This Chapter draws upon evidence collected during the RSF survey and attempts to reconcile the different views on the development of obsequent-scarps and large-scale slope deformations by referring to seven examples studied in the field areas.

8.2 Previous research

Table 8.1 summarises the hypotheses proposed within the recent literature to account for the formation of obsequent-scarps in various mountain areas. All the authors invoke an opposing (also termed 'antithetic') movement along discontinuities to explain obsequent-scarps though the possible cause(s) of the movement are disputed (Table 8.1). The various explanations of obsequent-scarp formation

1964	Jahn	suggested toppling of blocks combined with preferential erosion upslope of fissures for examples in the Carpathian Mts.
1966	Zischinsky	recorded valleyward bending of foliation planes and proposed 'sackung' (lit=sagging) form of deformation.
1968	Beck	hypothesised summit-ridge foundering to explain scarps in New Zealand.
1971	Tabor	observed ridge-top depressions in the U.S.A., and inferred a valleyward bending of sandstone beds to account for obsequent-scarps.
1972	Watters	utilised re-orientation of foliation planes to infer block toppling at Glen Pean, Scotland.
1972	Nemčok	discussed obsequent-scarps on the Chabenec ridge, Czeckoslovakia and considered that deep-seated gravitational-creep was responsible for the features.
1974	Patton and Hendron	proposed that obsequent-scarps were formed by faulting in response to isostatic uplift.
1976	Radbruch-Hall et al.	discussed 'sackungen' in U.S.A. and thought that dilation, caused by the expansion of ridges, may have caused 'bulging' of slopes.
1977	Mollard	speculated that faulting, due to isostatic uplift, was the cause of Nagle Mt.'linears' in Canada.
1977	Mahr	invoked contraction of rock at depth and dilation at the surface to account for the obsequent-scarps on the Chabenec Ridge.
1982	Bovis	inferred that toppling and preferential erosion upslope of tension cracks was responsible for uphill-facing scarp formation.

Table 8.1: A summary of the literature concerning obsequent-scarp development and large-scale slope deformation.

Figure 8.1: Suggested modes of large-scale rock-slope deformation (see text for explanation of various models).

made in the literature can be grouped into 5 slope deformation models (Fig. 8.1 a-e).

Model (a) requires the gradual valleyward-bending of rock layers and has been recorded by Zischinsky (1966, 1969) and Tabor (1971) at sites in the Austrian Alps and the U.S.A. respectively. Zischinsky invoked 'plastic deformation' of the lower part of the Matrei-Glunzerberg slope in the Austrian Tyrol, with 'solid' behaviour at the top part of the slope. In this way he sought to explain the occurr-

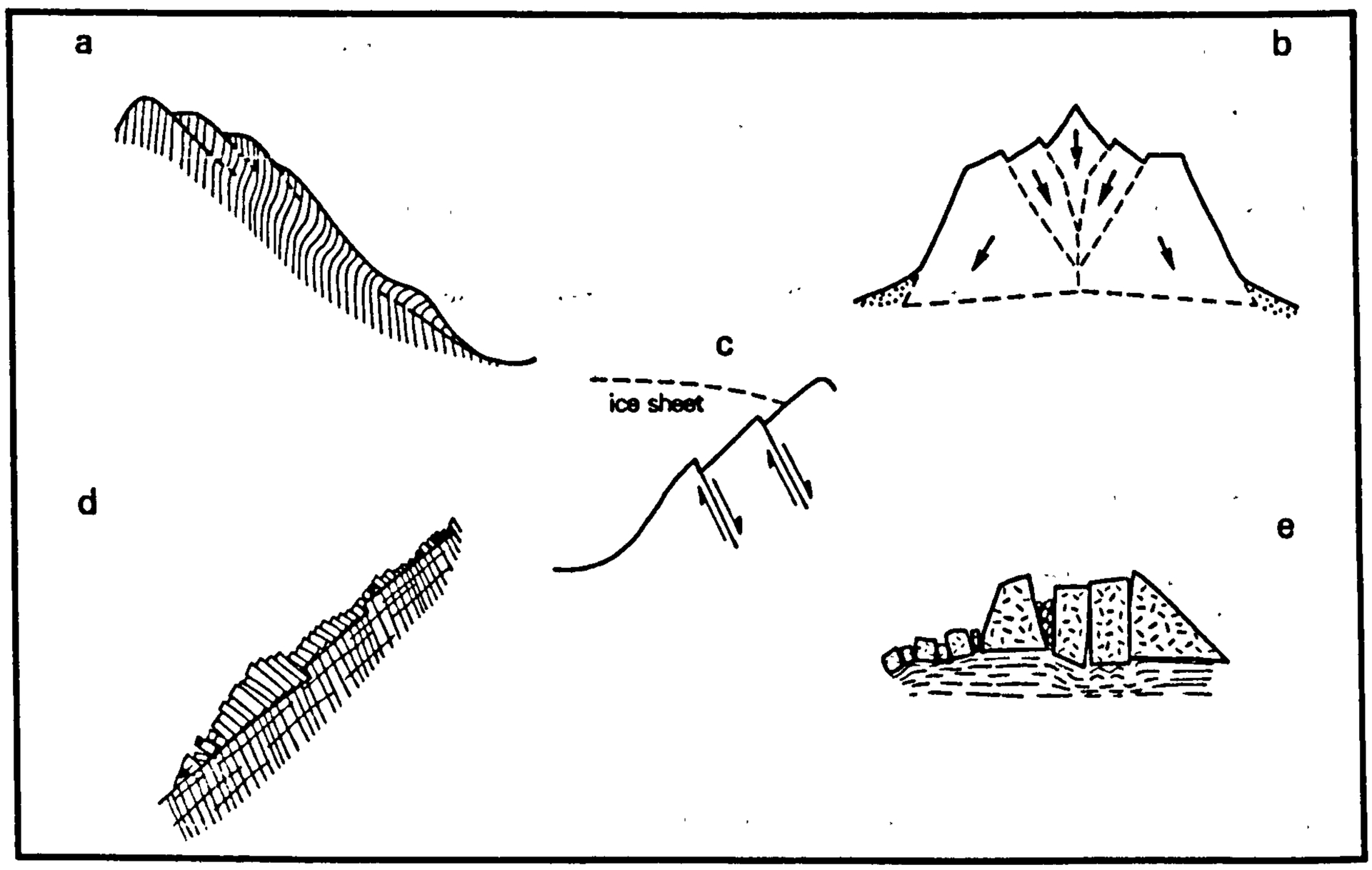

ence of shear planes towards the slope crest and overturning of strata at its base. The existence of these two domains was thought by him to be a function of the distribution of stress beneath a slope and the mechanical properties of the rock mass. Model (b) involves the foundering of a ridge core which may be the cause of obsequent-scarp formation (e.g. Beck 1968) or the effect of lateral spreading of a ridge which also produces obsequent-scarps (e.g. Radbruch-Hall et al.

1976).

Model (c) was proposed by Patton and Hendron (1974) and hypothesises that obsequent-scarps result from fault movement triggered by uneven isostatic adjustment. Patton and Hendron suggested that the uneven rebound could reflect former variations in ice-sheet thicknesses above rock-slopes. Their hypothesis was utilised by Mollard (1977) to attempt explanation of obsequent-scarps or 'linears' on Nagle Mt., Canada. Model (d) invokes toppling of blocks on a slope (e.g. Watters 1972, de Freitas and Watters 1973) which may be combined with preferential erosion upslope of the tension-cracks between blocks according to Jahn (1964) and Bovis (1982). Finally, model (e) involves the lateral spreading of competent rock blocks which overlie incompetent rocks such as shale (Radbruch-Hall et al. 1976, Mahr and Nemčok 1977).

A major difficulty in the investigation of large-scale slope deformations, and consequently the testing of the above hypotheses, is the lack of subsurface data. Unless tunnels are available beneath deformed slopes (e.g. Zischinsky 1966, 1969, Radbruch-Hall et al. 1976, Rengers and Soeters 1982) the depth to which deformations reach can only be speculated upon. Nemčok (1972) for instance, estimated that slope deformations in the Carpathian Mountains extend 200 to 300-m-below the surface while Tabor (1971) inferred a zone of bending up to 200-m-beneath the surface at sites in the Olympic Mts., Washington. Nemčok et al. (1972) classified such deformations as 'deep-seated creep' and other authors have similarly inferred deep-seated movements (Terzaghi 1962, Ter-Stepanian 1966, 1974). Estimations of the depths

to which deformations extend have been made from limited surface evidence by Beck (1968) and Rengers and Soeters (1982), but their reconstructions must be treated with great caution as they are based entirely upon inference.

Most of the authors listed in Table 8.1 have emphasised a connection between obsequent-scarp development and pre-existing discontinuities which dip steeply into the slope. If a strongly-developed discontinuity set with a favourable orientation is present on a rock-slope, the variations in discontinuity attitudes across the slope may be used to reconstruct the form of block movement. This analytical technique was used by Zischinsky (1966, 1969) to demonstrate valleyward bending of strata and by de Freitas and Watters (1973), who showed that toppling of blocks had formed obsequent-scarps up to 7-m-high at Glen Pean.

Radbruch-Hall (1978) stated that the majority of slopes described as possessing obsequent-scarps occur within or near areas of convergent or transform tectonic plate boundaries. She omitted mention however of de Freitas and Watters' (1973) paper, which discussed excellent examples of obsequent-scarps in Britain. Radbruch-Hall cited four important factors that may favour large-scale rock-slope deformation at or near tectonic plate boundaries, these are: high seismic activity, tectonic uplift, high erosion rates and oversteepened slopes; caused by the rapid downcutting of streams. Bovis (1982) commented that the majority of slopes with obsequent-scarps in North America occur in presently or formerly glaciated terrain. He hypothesised that deglaciation of oversteepened slopes may provide the potential for deformation though structure will

control the response (if any) of rock-slopes to the deglacial 'trigger'.

Slopes with either ridge-top furrows, prominent bulging or very extensive obsequent-scarps have been recognised by the writer in the Scottish Highlands. The majority have been identified from aerial photographs, though seven have been investigated in the field. Data on slopes featuring obsequent-scarps were collated during the RSF inventory and will be analysed in Section 8.3. Sections 8.4 to 8.6 provide detailed descriptions and discussion of seven study-sites.

8.3 Obsequent-scarps in the Scottish Highlands

Appendix A includes 56 slope failures (13% of the RSF population) with areas greater than 0.25 km^2 that feature obsequent-scarps; all feature comparatively little displacement in relation to their height. The 56 slopes account for a total area of 34 km^2 and the largest example is at Ben Attow [NH 010 184] which affects a slope area of 2.21 km^2.

Obsequent-scarps occur mostly in the metamorphic rocks showing

Rock type	Number
schist	25 (51%)
psammite	11 (23%)
pelite	5 (10%)
gneiss	4 (8%)
quartzite	3 (6%)
others	1 (2%)

Table 8.2: Obsequent-scarp distribution by rock type (88% sample).

a similar relationship to rock type as the RSF population (compare Tables 4.1 and 8.2). No obsequent-scarps are known to the author to have developed in granite or sandstone. The different types of schist, in contrast, account for 84% of the sample. Beck (1967) observed that obsequent-scarps are usually developed on slopes composed of schists and greywackes and that comparatively few examples are found in granite. Zischinsky (1966) commented that schists have a high componental mobility and that creep (or flow) occurred in high rock-slopes composed of phyllite, mica-schist and amphibolite in the Austrian Alps. Obsequent-scarps in the Canadian Cordillerra are generally developed in the metamorphic rocks of Eisbacher's (1979b) "Cassiar-Columbia" zone.

The locations of 28 slopes with obsequent-scarps are known in relation to the Loch Lomond Advance limits. Obsequent-scarps are delicate morphological features which would be unlikely to survive overriding by glaciers and the eight examples (29% of the sample) which lie inside the limits probably postdate the Loch Lomond Advance. Eleven of the sample centroids (39% of the sample) occur less than 200-m-outside the Advance limits. These statistics must be treated with caution because many of the RSFs which feature obsequent-scarps affect large slope areas. The correlation between 68% of such slopes and former glaciers is however suggestive of a glacial influence.

8.4 Site descriptions

A: Carn na Con Dhu [NH 080 240]

A large RSF extends from near the foot of the east slope of Coire na Con Dhu to the slope crest, a height of 500 m (Fig. 8.2a). It has

Figure 8.3: L.H. stereonet for the Carn na Con Dhu RSF (n = 200 poles).

an average slope angle of 22° and is composed of Moinian psammite with E-W striking bands of pelite. Joint data collected outside the failed slope area are summarised in Figure 8.3. The foliation set (F) is directed 86° → 230° though individual foliation planes trend 75° → 050° to 70° → 230°. Joint sets J1 and J2 dip steeply valleyward (78° → 148° and 62° → 136° respectively) and are intersected by cross-joints belonging to set J3.

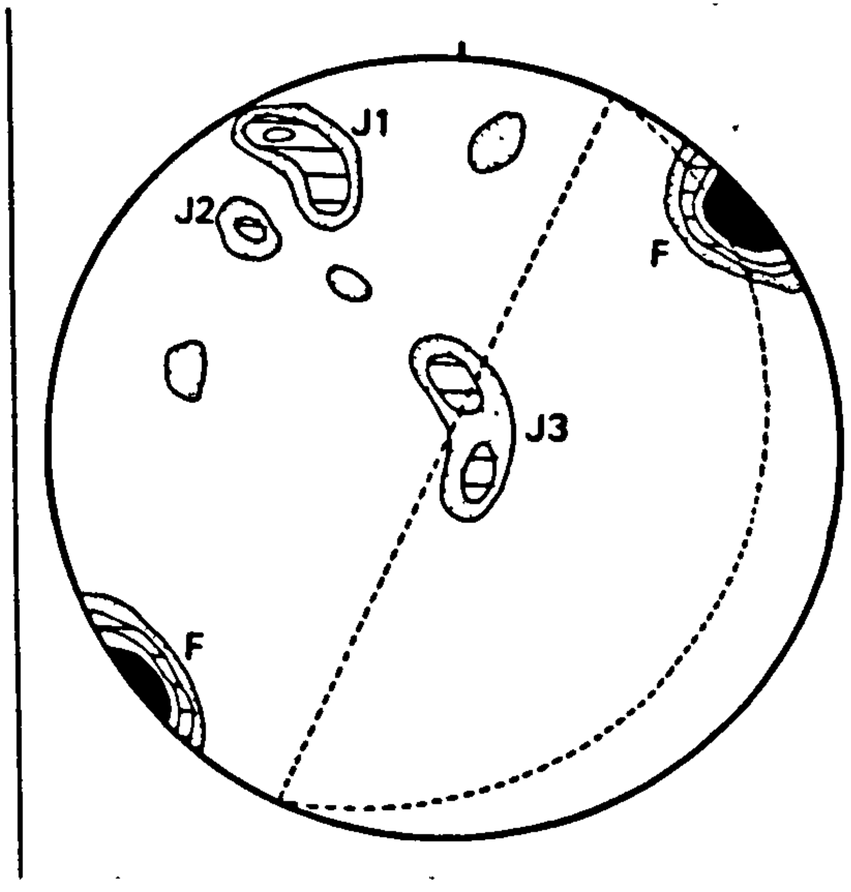

In cross-section the whole slope appears to have sagged (Fig. 8.2b) and yet the slope failure has not formed a slide toe despite the amount of deformation indicated by its rear-scarp which crops out at c. 920 m O.D. (Fig. 2a,b). Horizontal displacement appears to have been compensated for by bulging of the slope at c. 650 m O.D. which is most obvious on the ground when the slope is viewed from the S (particularly at 1 in Fig. 8.2a). The rear-scarp is formed by discontinuities belonging to sets J1 and J2.

Numerous slope trenches and obsequent-scarps occur across the slope (Plate 8.1). The obsequent-scarps are up to 200-m-long and 2.5-m-high: many of the trenches upslope of the scarps are partly infilled by colluvium and peat. A 2.25-m-deep section excavated at the intersection of one obsequent-scarp and its trench, failed to locate bedrock (Plate 8.2) but exposed coarse periglacial debris

Plate 8.1: The Carn na Con Dhu RSF. The direction of view is indicated in Figure 8.2.

Plate 8.2: A 2.5-m-deep section dug into the upslope face of one obsequent-scarp. Location given in Figure 8.2a. The section revealed peat overlying coarse slope debris.

Figure 8.2: a) The Carn na Con Dhu RSF

1 = obsequent-scarp

2 = rear-scarps

3 = small-scale failure

4 = contours (50 m intervals).

b) Section through the Carn na Con Dhu RSF

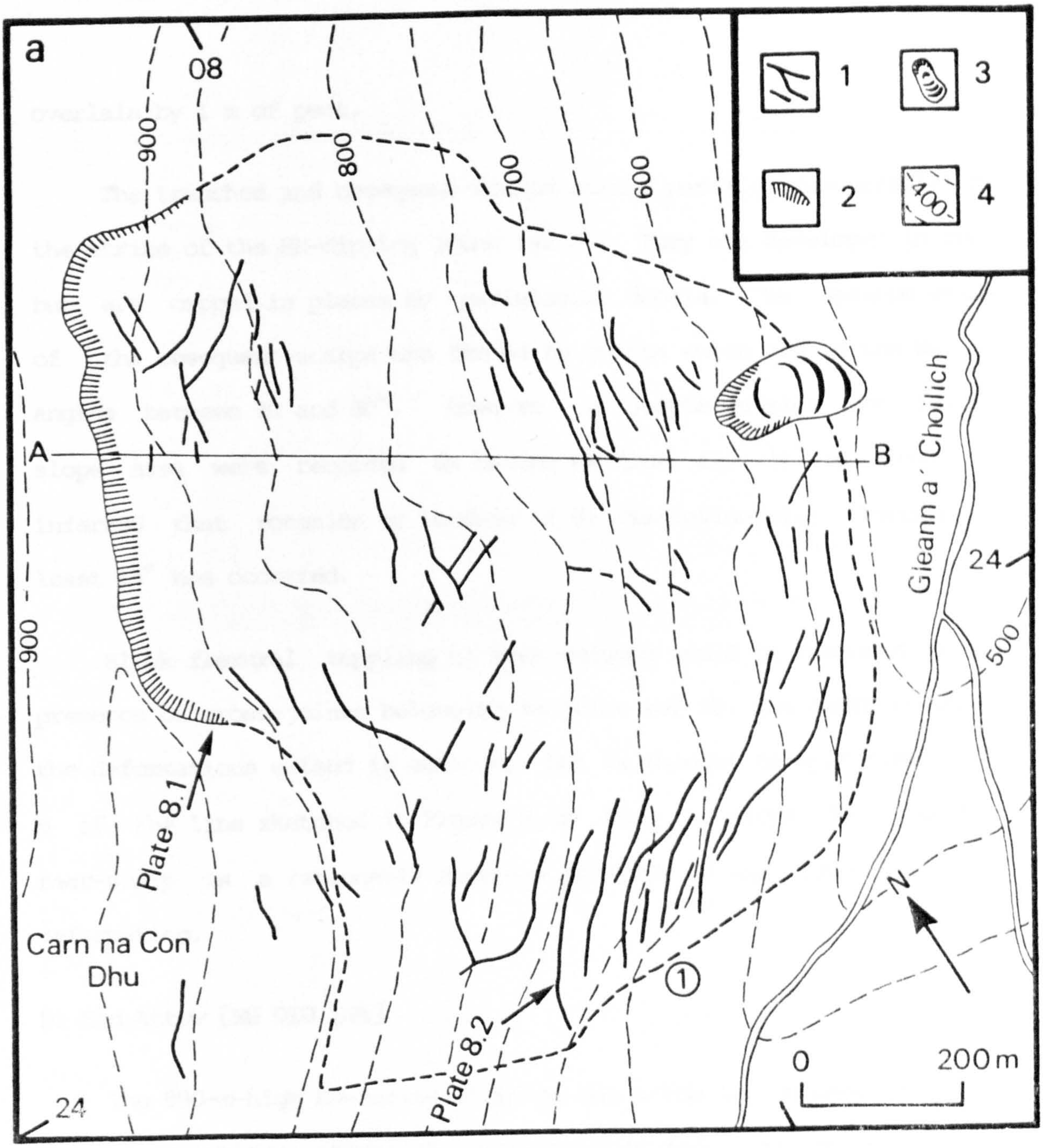
a
08
900
800
700
600
1
2
3
4
A
B
Gleann a' Choilich
24
500
Plate 8.1
Carn na Con Dhu
Plate 8.2
N
0
200 m
24

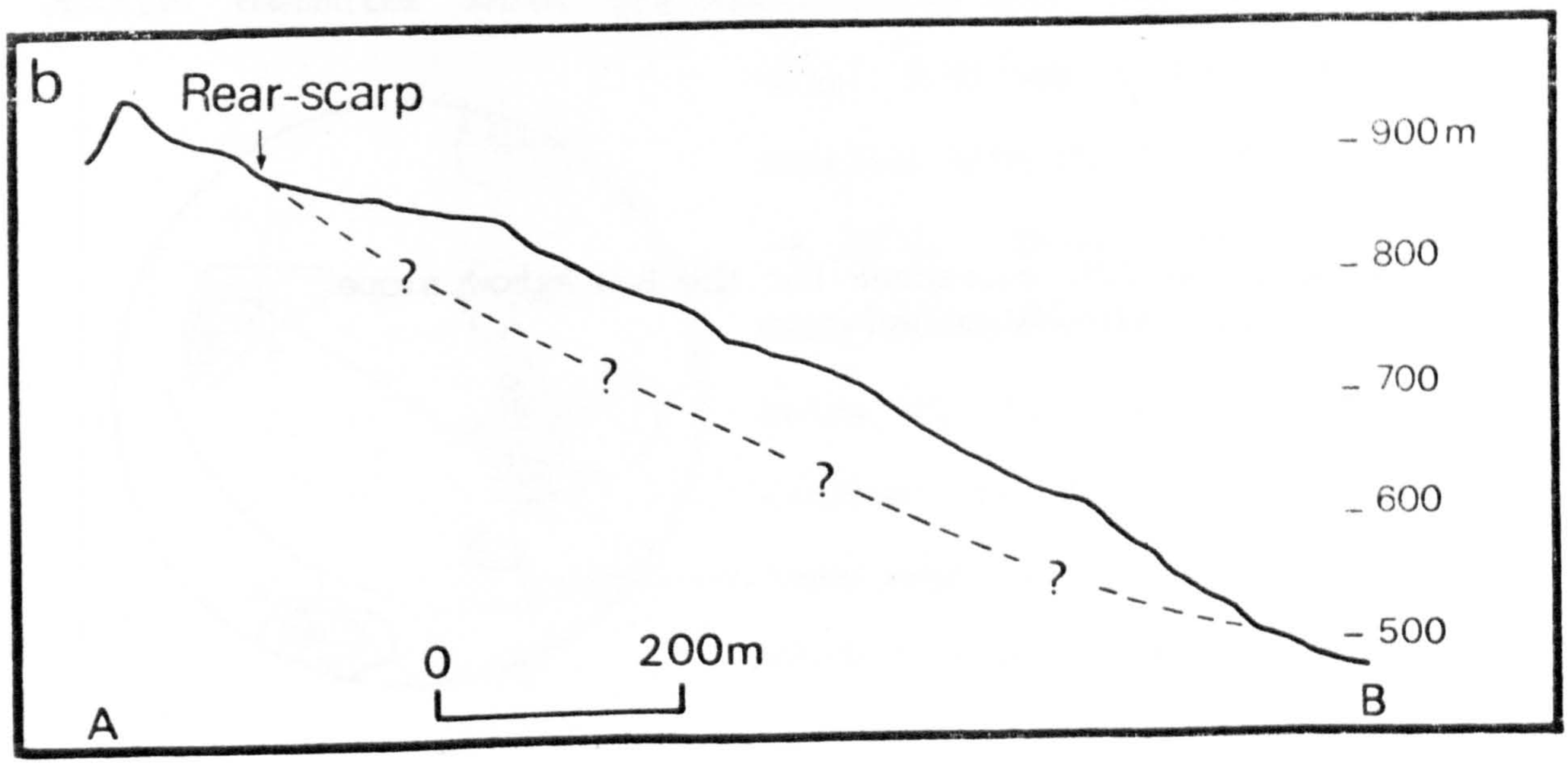
b
Rear-scarp
900 m
800
700
600
500
?
?
?
0
200m
A
B

Figure 8.4: L.H. stereonet for the Ben Attow slope (n=200 poles).

overlain by 1 m of peat.

The trenches and obsequent-scarps strike parallel/sub-parallel to the strike of the SE-dipping joint set J1. They are developed in rock but are capped in places by periglacial debris. The upslope walls of the obsequent-scarps are formed by joints which dip to the NW at angles between 70 and 80°. However, no joints outside the failed slope area were recorded as having NW dips and it is therefore inferred that rotation or bending of J1 discontinuities through at least 14° has occurred.

Block-flexural toppling of rock columns would be favoured by the presence of cross-joints belonging to joint set J3. The depth to which the deformations extend is unknown, but is thought to approximate 120 m if the line sketched in Figure 8.2b from the slope foot to the rear-scarp is a reasonably accurate estimate of the lower limit of deformation.

B: Ben Attow [NH 010 184]

The 990-m-high SW-facing slope of Ben Attow is composed of coarse Moinian psammites which are segregated by four discontinuity sets (Fig. 8.4) one of which, (F) trends parallel with the foliation (c. 60° → 125°). Three other joint sets were measured, the most important being J1, the pole of which is directed c. 80° → 024°. J2 is a lower angle stress-relief joint set which dips gently valleywards and J3

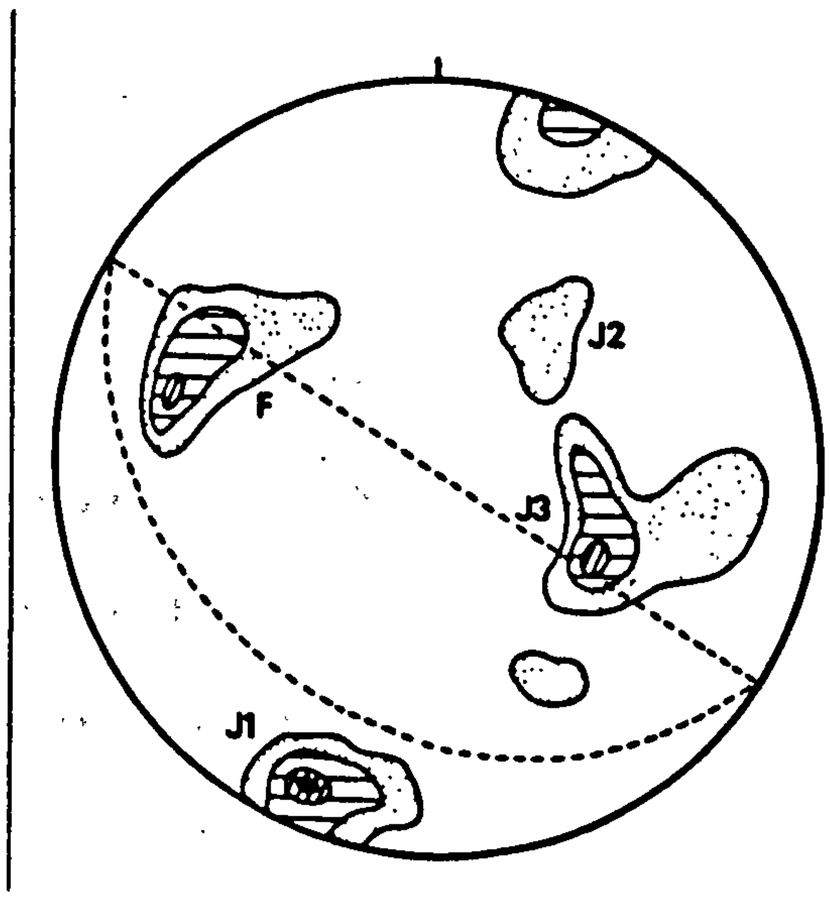

joints are directed NW.

The morphology of the Ben Attow slope is very similar to that of Contact Mountain, Montana, U.S.A., where a 1220-m-high slope, composed of Precambian basic layered intrusives, features prominent obsequent-scarps (Radbruch-Hall et al. 1976). Obsequent-scarps par excellence are also developed on the Ben Attow slope (Plates 8.3, 8.4, 8.5 and 8.6). The most striking examples of these features are 400 to 800-m-long and between 4 and 10-m-high (Fig. 8.5, Plates 8.5 and 8.6). The scarps are orientated parallel/subparallel with both the slope crest and the strike of J1.

Watters (1972) studied only the W portion of this slope failure and concluded that the obsequent-scarps were formed by successive upslope separation and translation of blocks. He also hypothesised that tension-cracks produced by this movement are now partially infilled by debris. Watters rejected the possibility of toppling failure at Ben Attow because the foliation within the failed area showed little variation in attitude from the foliation pattern outside. However, as Holmes and Jarvis (in press) have observed, the foliation strikes parallel/subparallel with the direction of slope and therefore little change in the foliation attitude would be expected even if significant rotation had occurred.

At c. 850 m O.D. a rear-scarp is inclined at up to 53° and has a maximum height of 90 m. This feature indicates considerable deformation of the rock-mass below it and yet no slide-toe has developed at the base of the slope. Holmes and Jarvis inferred that a sackung-like deformation (based upon the appearance of sagging in

Plate 8.3: Obsequent-scarps on the Ben Attow slope. The examples shown here are up to 5-m-high. The location and direction of view is shown in Figure 8.5.

Plate 8.4: Closely-spaced obsequent-scarps on Ben Attow (at 1 in Figure 8.5). These examples range in height between 4 and 5 m.

Plate 8.5: Obsequent-scarps on the Ben Attow slope. Note the accumulation of scree (the light areas) behind the obsequent-scarps.

Plate 8.6: The largest obsequent-scarp on the Ben Attow slope. This example is up to 10-m-high. The blocks in the foreground have fallen from the uphill face of the scarp.

Figure 8.5: The Ben Attow RSF:

1 = Obsequent-scarps

2 = linear slope trenches

3 = Contours (100 m intervals)

4 = Spring

5 = Swallow-hole

6 = Rear-scarp.

Plate 8.7: The An Sornach RSF viewed from the SW. Note the major obsequent-scarp (arrowed) referred to in the text.

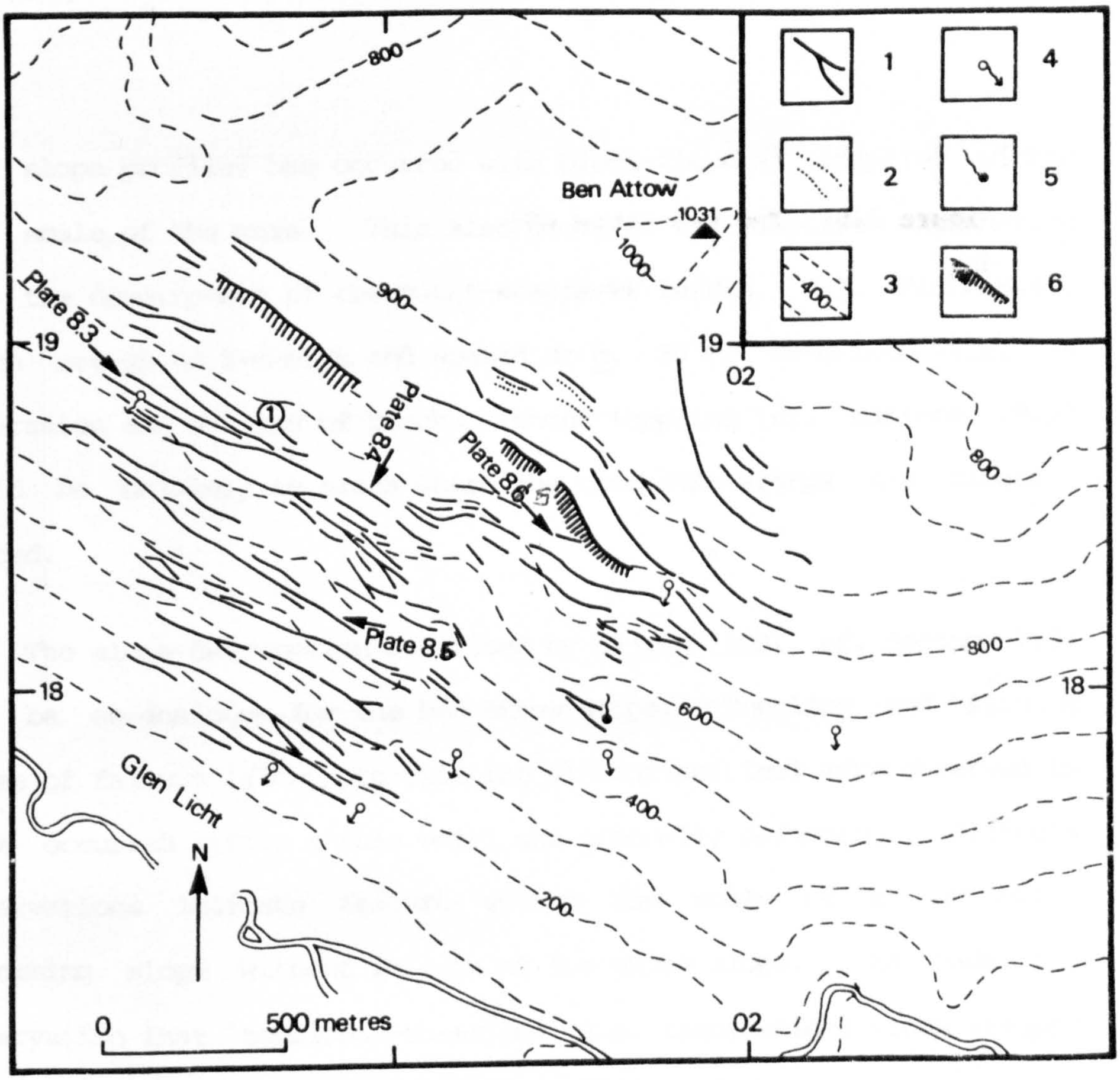
800
Ben Attow
1031
1000
900
Plate 8.3
19
1
Plate 8.4
Plate 8.6
5
Plate 8.5
18
600
400
200
Glen Licht
N
0
500 metres
02
1
2
3
4
5
6
400

the slope profile) has occurred with block-flexural toppling within the scale of the mass. This also provides the simplest explanation for the development of obsequent-scarps (1 in Fig. 8.5, Plate 8.4), which are up to 5-m-high and spaced at c. 30 to 40-m-intervals, as separation and sliding of blocks without toppling (cf. Watters 1972) would be unlikely in areas where the obsequent-scarps are closely-spaced.

The slope deformation described by Sijing (1981, cf. Section 7.2) may be an analogue for the Ben Attow slope. Toppling and sliding modes of failure (along pre-existing discontinuities) were observed to have occurred within a mass which was gradually deforming. Sijing's observations indicate failure within the scale of a gradually deforming slope without failure of the whole slope. He made the observation that 'tensional-shearing' (i.e. translation) along steeply inclined positive joints combined with limited forward rotation can lead to the formation of obsequent-scarps directly below small consequent-scarps. This observation concurs with that made at Ben Attow by Holmes and Jarvis (unpublished). The Ben Attow slope failure however is an order of magnitude larger than that observed by Sijing.

Structural-creep (cf. Sijing 1981) or rheologically-controlled deformation along pre-existing discontinuities, has probably occurred at Ben Attow with toppling and translational shear failure within the scale of the deformed mass. An estimation of the depth to which the deformations extend may be given by a line connecting the rear-scarp to the lowermost obsequent-scarp; yielding a possible maximal depth of

Figure 8.7: L.H. stereonet for the An Sornach RSF
(n = 200 poles).

deformation of 120 m. However, it is not known if a continuous failure-surface exists at Ben Attow.

C: An Sornach [NH 095 214]

This slope is composed of Moinian psammite and has an impressive series of obsequent-scarps which differ from those previously described in that they strike up to 37° from the orientation of the slope crest (Fig. 8.6). They are generally less than 1.5-m-high and disrupt periglacial slope deposits. The largest obsequent-scarp on the slope extends for 400 m, strikes 34° from the slope crest and is up to 4-m-high.

Three discontinuity sets have been measured at An Sornach (Fig. 8.7). A strongly-developed foliation set (F) dips steeply into the slope its pole trending 78° → 160°. The pole of set J1 is vertical and strikes almost at right angles to F. A stress-relief set J2 trends c. 24-36° → 104° or roughly parallel with the slope face. The slope face is inclined at 34°. The obsequent-scarps have two strike directions, being developed along F and J1 surfaces. A 40-m-high rear-scarp at c. 700 m O.D. appears (in plan view) to indicate circular failure, but is a compound feature its shape being controlled by F, J1 and J2 discontinuities. Again, no slide toe has developed at the base of the slope despite its large

Plate 8.8: View along the major obsequent-scarp that runs diagonally across the face of the An Sornach RSF. The scarp is up to 4-m-high at this point.

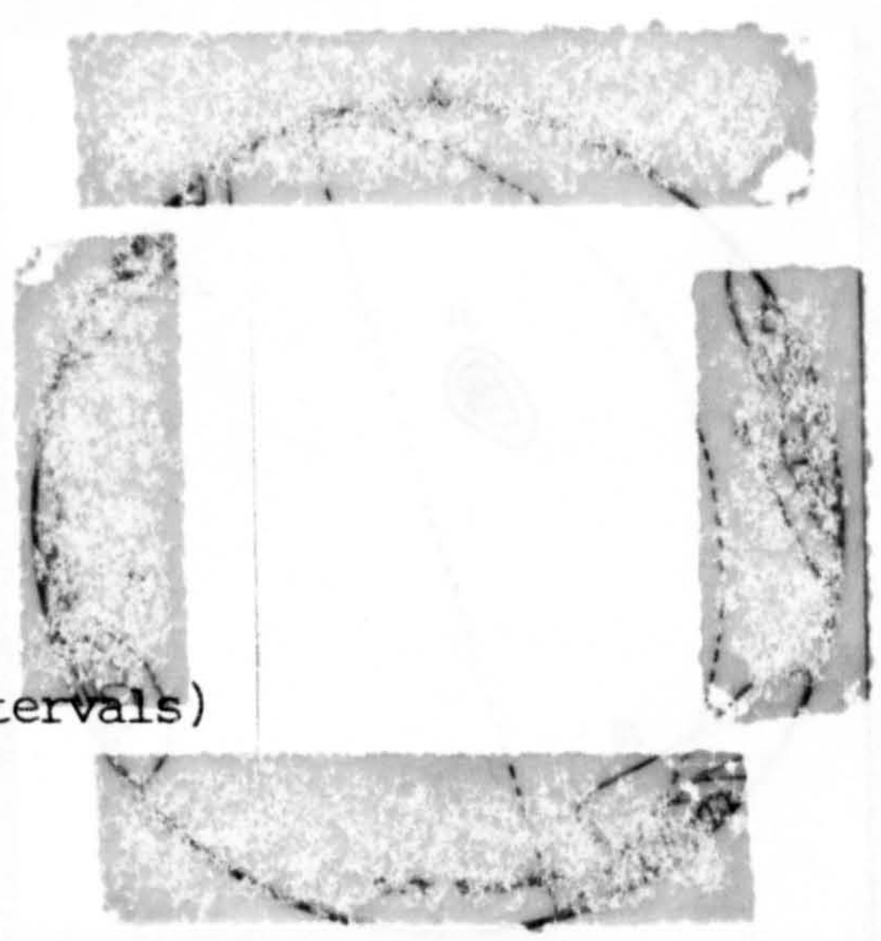

Figure 8.6: The An Sornach RSF

1 = Rear-scarp

2 = Obsequent-scarps

3 = Contours (50 m intervals)

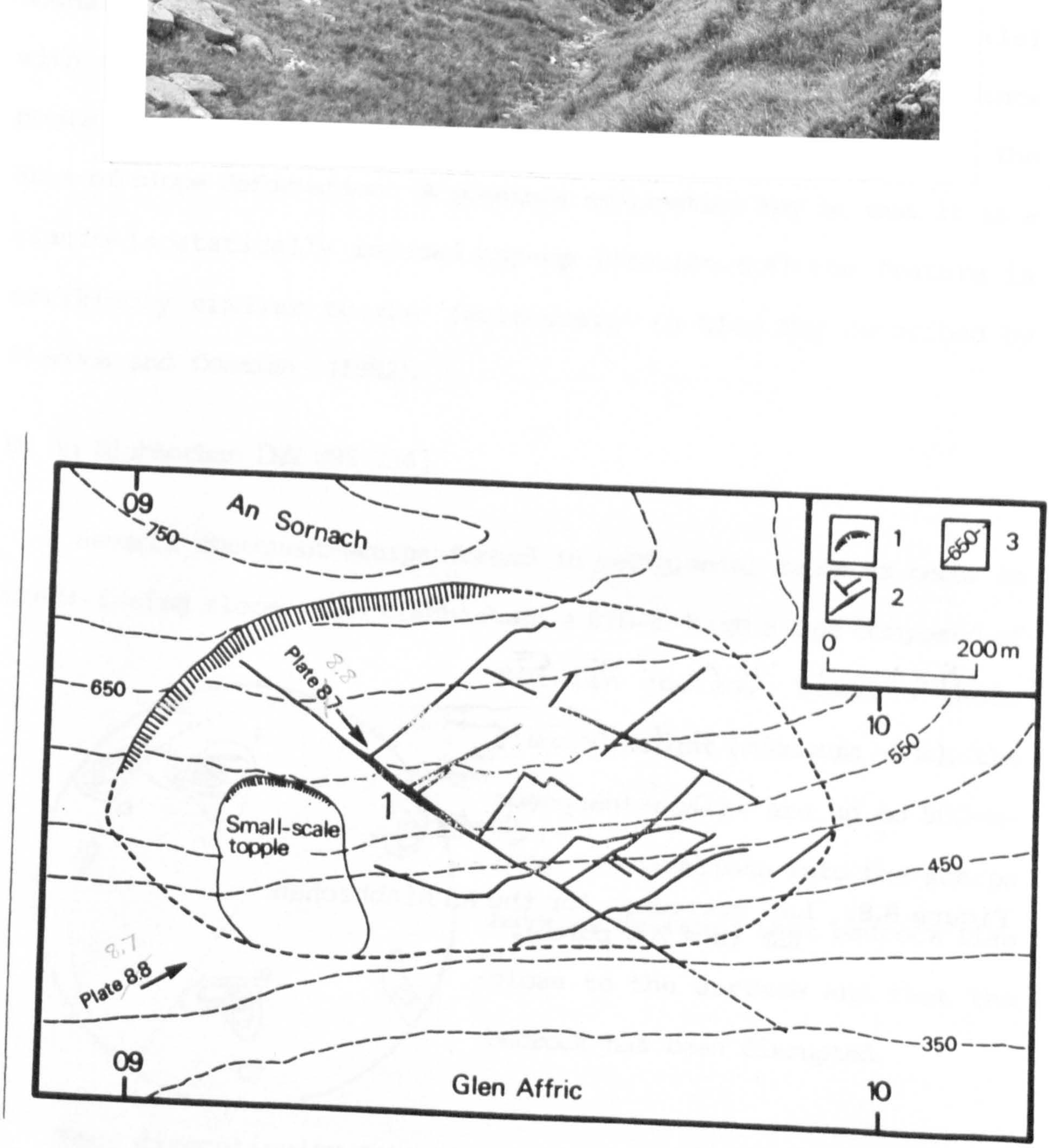
09
An Sornach
750
650
Plate 8.7
8.8
1
Small-scale topple
8.7
Plate 8.8
450
350
09
Glen Affric
10
1
2
3
650
0
200 m
10
550

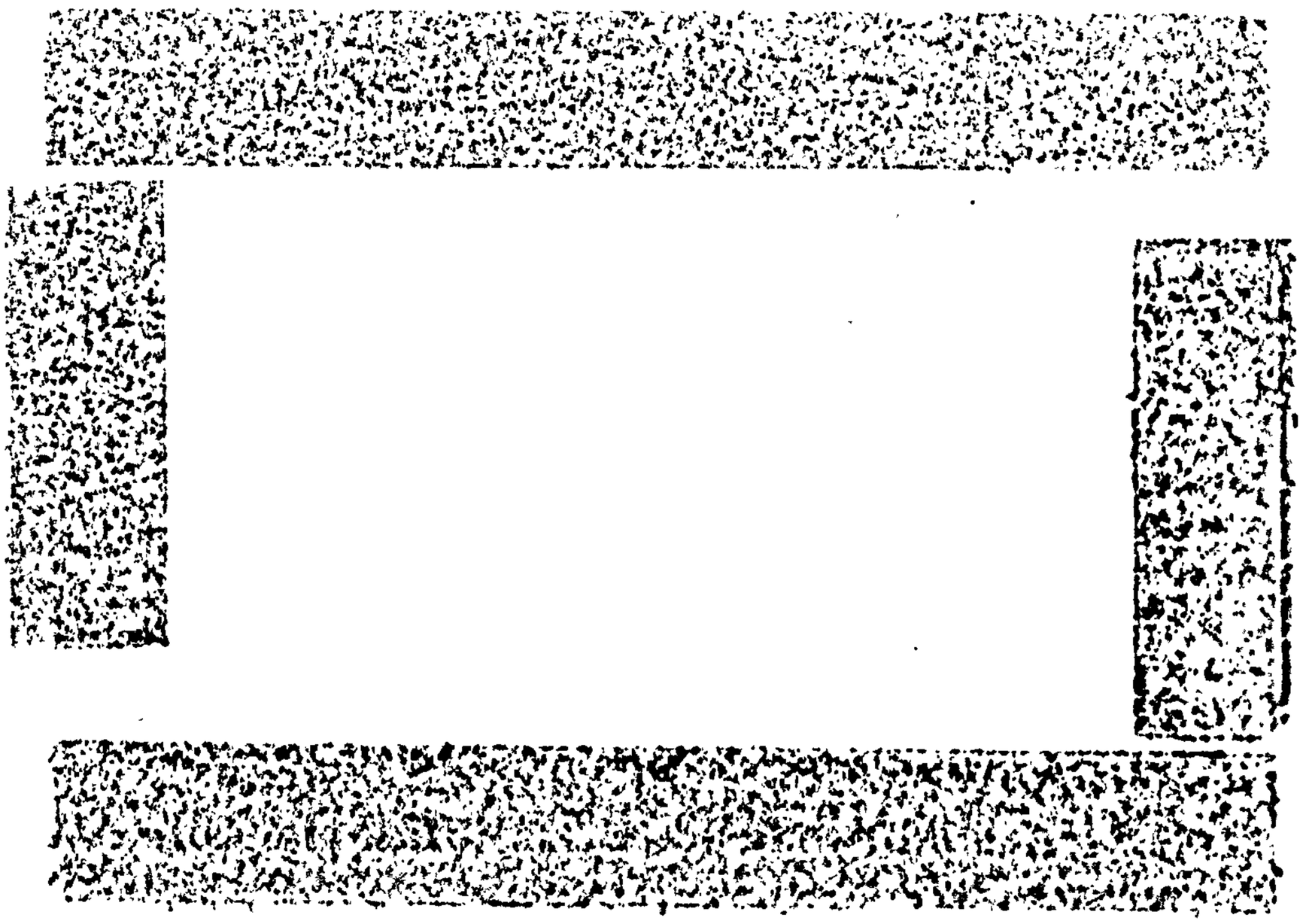

Figure 8.8: L.H. stereonet for the An Riabhachan RSF (n = 200 poles).

rear-scarp.

The large obsequent-scarp (1 in Fig. 8.6, Plate 8.7) is the most interesting feature of this slope as it may be traced outside the margin of the RSF until it is covered by hummocky drift. The scarp shows no sign of disruption by the movement of the RSF (Plate 8.8) and is therefore inferred to have been formed after the main phase of downslope displacement was complete. The feature strikes parallel with the pole of J1. It is difficult to envisage toppling movements producing this obsequent-scarp particularly as it extends outside the area of slope deformation. A possible explanation may be that it is a glacio-isostatically induced pop-up (Section 6.4): the feature is strikingly similar to the 'fault-scarp' in Glen Roy described by Sissons and Cornish (1982).

D: An Riabhachan [NH 095 334]

Several obsequent-scarps formed in periglacial deposits occur on theNW-facing slope of An Riabhachan, a 670-m-high slope composed of Moinian gneiss. Despite their limited height (maximum 1 m), the obsequent-scarps are up to 500-m-long. Excavations into the scarps have established that bedrock lies close to the surface and that the bedrock has been disrupted.

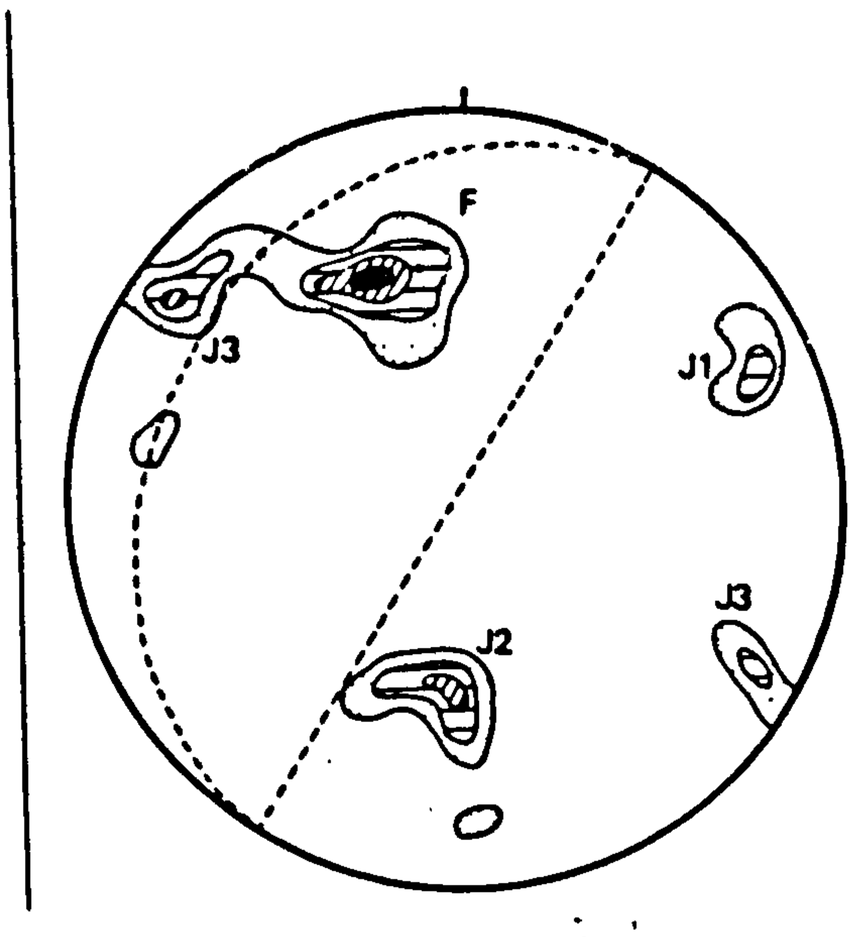

Four discontinuity sets were measured on the slope (Fig. 8.8). The foliation set trends c. 50 → 156°. Obsequent-scarps on the

Figure 8.9: L.H. stereonet for the Mam Sodhail RSF (n = 200 poles).

slope are orientated parallel with the strike of J3. This joint set is bi-polar with joints dipping steeply NW and SE.

The margin of the RSF is difficult to determine but has been inferred from the lateral extension of obsequent-scarps. No rear-scarp delimits the upper margin of the deformed rock but disrupted blocks may be found to the E of the summit, indicating that the deformations extend under the summit ridge. A failure-surface was not found to crop into the headwall of the corrie SE of the summit.

E: Mam Sodhail [NH 118 253]

Two obsequent-scarps have developed on the W-facing 30° slope of Mam Sodhail which is formed of Moinian psammite. The obsequent-scarps run parallel with the pole of the foliation set (F), which is vertical and trends c. 90° → 288/108°. Two other joint sets were recorded (Fig. 8.9). J2 strikes at right-angles to F, its pole also directed vertically, and a second set dips between 15 and 25° towards the SE.

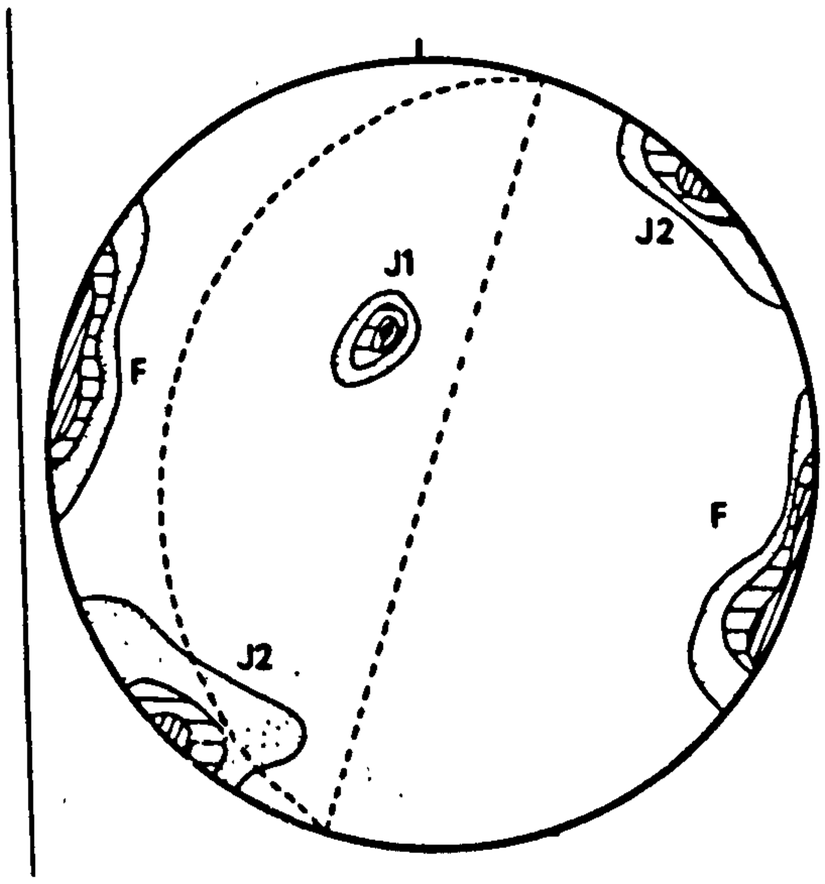

The obsequent-scarps are up to 100-m-long and occur below a small ridge top depression (located 20-m-E of the summit cairn), which is up to 3-m-wide, 2.5-m-deep and is partly infilled with periglacial debris. The scarps are badly degraded, with disrupted blocks up to 1 m^3 separated from one another by widened joints. The trenches

Figure 8.11: L.H. stereonet for the Sgurr Breac RSF (n = 200 poles)

upslope of the obsequent-scarps have been partly infilled by periglacial deposits. Portions of the scarps are completely buried by periglacial debris.

F: Sgurr Breac [NH 150 705]

The SW slope of Sgurr Breac and the SE slope of A' Chailleach (example G) form part of the headwall of a compound corrie in the Fannich Mts. The Sgurr Breac slope is 660-m-high, composed of Moinian gneiss and inclined on average at 28°. A 35-m-high rear-scarp crops out at c. 850 m OD (Fig. 8.10). Downslope of this feature the slope bulges markedly. This bulging may be observed on aerial photographs and is clearly visible in cross-section (Fig. 8.10, Plate 8.10). At the base of the RSF the slope is oversteepened to 34-36° and small block-flexural topples have occurred.

Shallow slope trenches run across the slope, trending subparallel with the poles of J1 and J4 (Fig. 8.11). Joint set J1 dips positively between 36 and 84° and J4 trends c. 50 → 024°. A foliation set, (F) dips shallowly positively and negatively. The rear-scarp is up to 30-m-high and is formed of J1, J2 and J3 joints. The toppling failures at the base of the slope have not occurred along J4 joints as the tension-cracks at the crest of the failures dip greater than 70° towards the NW. Overturning of discontinuities belonging to J1 is therefore inferred.

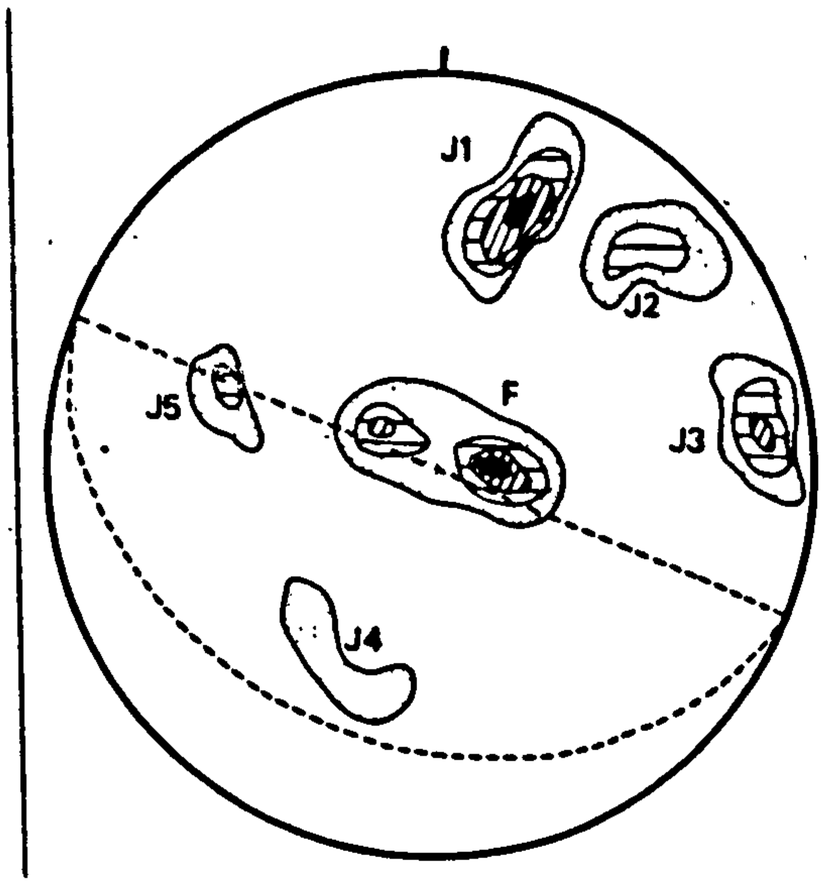

Figure 8.10: Section through the Sgurr Breac RSF with a schematic representation of joint attitudes.

Figure 8.12: Section through the A' Chailleach RSF with a schematic representation of joint attitudes. See text for explanation of (1).

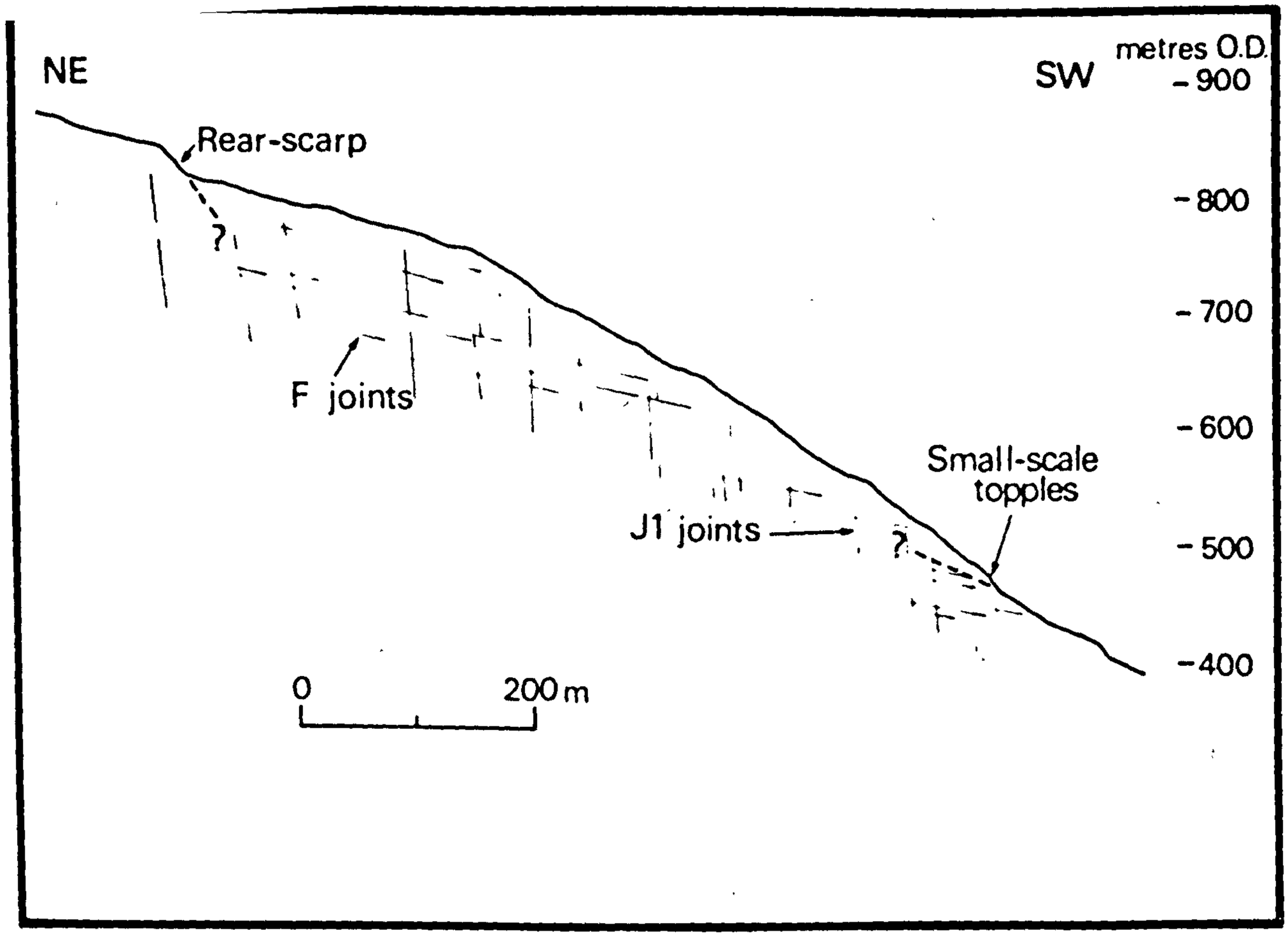
NE
SW
metres O.D.
-900
-800
-700
-600
-500
-400
Rear-scarp
?
F joints
J1 joints
Small-scale topples
0
200 m

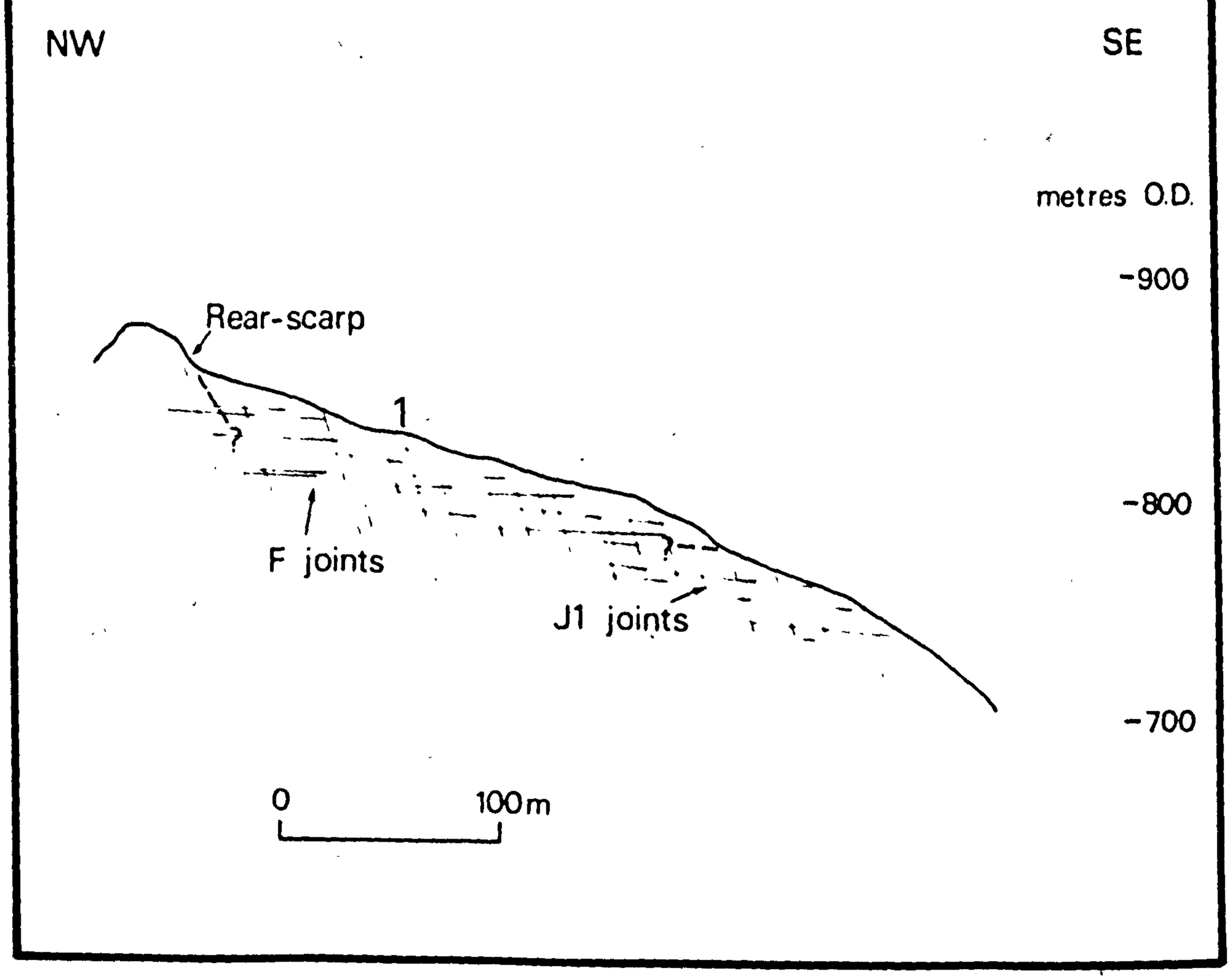
NW
SE
metres O.D.
-900
-800
-700
Rear-scarp
1
?
F joints
J1 joints
0
100 m

Figure 8.11: L.H. stereonet for the A' Chailleach RSF (n = 200 poles).

G: A' Chailleach [NH 137 712]

As at Sgurr Breac, bulging and deformation of this slope has occurred downslope of a prominent rear-scarp (Fig. 8.12, Plate 8.11). The scarp reaches to the summit and is highly complex in shape, following the contact between the Moinian gneiss and mica-schist. The RSF itself is developed in the gneiss. At 1 in Figure 8.12, 1.5-m-wide and 2-m-deep tension-cracks are developed.

The tension-cracks strike subparallel to J1, which trends 70° → 144° (Fig. 8.13). A low-angle foliation set dips both shallowly positively and negatively, its pole is directed 4° → 310°. F joint poles were recorded dipping up to 15° positively. Deformation of the slope may have may have occurred along these gently-dipping surfaces.

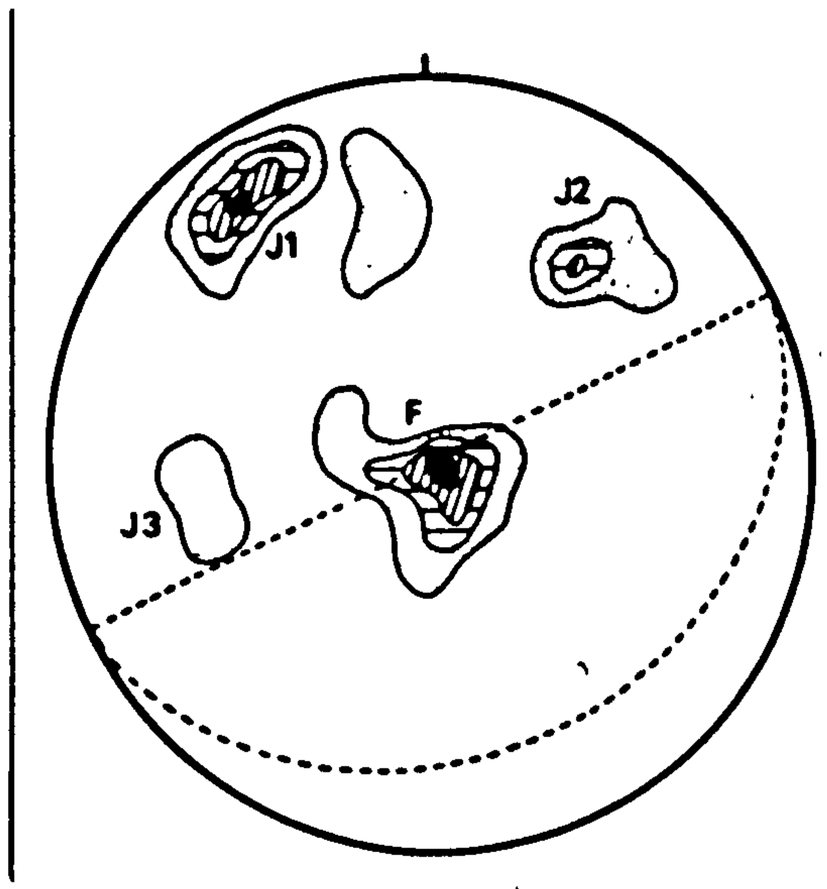

A further joint set J2 trends 52° → 218° or subparallel with the NE margin of the RSF.

At around 750 m O.D., the slope steepens from 24°, on the surface of the RSF, to c. 30°. The failure-surface of the RSF is thought to crop out immediately below this break of slope. No slide toe has developed at the base of the RSF and it is inferred that the horizontal displacement signified by the rear-scarp has been compensated for by bulging of the slope.

Plate 8.10: View of the Sgurr Breac RSF from A' Chailleach. The arcuate rear-scarp may be observed with 'bulging' towards the slope foot.

Plate 8.11: Looking E from the summit of A' Chailleach. The rear-scarp of the RSF may be observed centre-left. Note the extensive coverage of the scarp with periglacial deposits.

8.5 Analysis for toppling failure potential

The obsequent-scarps at study sites A-E have generally been found to strike approximately parallel with steeply-dipping discontinuity set(s). A number of authors have also observed this correlation (e.g. Jahn 1964, Tabor 1971, Goodman and Bray 1976, Radbruch-Hall et al. 1976, Bovis 1982). The obsequent-scarps usually trend parallel with the strike of their slope faces except at An Sornach where they strike up to 37° from it.

It may be hypothesised that the simplest explanation for obsequent-scarp development on a slope with a negatively-dipping discontinuity set is formation by toppling failure. However, a dichotomy exists in that in order for interlayer shear to occur, the slope angle must exceed the friction angle for the layers: as the normal to the layers must be less than or equal to the slope angle minus the friction angle. At An Raibhachan, An Sornach, Ben Attow and Mam Sodhail, the rock-slopes are inclined at angles below the peak friction angles: at Mam Sodhail by up to 15°. According to the Goodman and Bray (1976) kinematic model self-weight toppling could not have occurred at these four sites.

Holmes and Jarvis (in press) used the Goodman and Bray (1976) kinematic test to assess the potential for toppling at Ben Attow. They found that the toppling criterion was not satisfied assuming that the friction angle was greater than 33° (the average slope angle). Moreover, the peak friction angle of psammite may exceed 45°.

High cleft-water pressures could according to them, have lowered

the shear resistence to interlayer slip and enabled toppling failure at a lower slope angle than that predicted by the self-weight toppling criterion. The effective friction angle must have been less than 33° to have enabled toppling of the Ben Attow slope and at An Sornach less than 30°. Holmes and Jarvis have therefore suggested that cleft-water pressures could have acted to reduce the effective friction angle but were either insufficient or too short-lived to cause complete failure of the slope.

Bovis utilised the kinematic test at Affliction Creek but his work may be critised because he used a comparatively low shear strength ($\phi = 30°$) in the kinematic test for toppling whereas peak shear strength may be much higher. He justified the selection of this value on the grounds that the joints were 'smooth' and that silty-sand material may infill joint cavities. Interestingly, if ϕ' was assumed to be 40° then the kinematic test for toppling at Affliction Creek would not have been satisfied. Cleft water-pressures may have contributed to the stresses on that slope too.

8.6 Discussion

No evidence has been found of recent displacement along the obsequent-scarps at any of the study sites. The scarps are generally vegetated with weathered rock surfaces and the trenches which lie upslope of them are usually infilled with lichen-covered scree and/or active periglacial landforms and peat. At Sgurr Breac and A' Chailleach, where obsequent-scarps have not developed, undisturbed periglacial debris overlaps their rear-scarps. It follows from this that deformation has probably ceased at the study sites; more detailed

data concerning the age of these features are discussed in Chapter 9.

The field evidence raises three further problems which require discussion in this chapter: (i) what was the mode(s) of deformation which occurred at the study sites? (ii) what triggered the deformation? and (iii) what caused the deformation to cease? Possible solutions to these problems are given below. Discussion of sites A-E (which feature obsequent-scarps) is undertaken first, followed by sites F and G.

It was noted in the introduction to this chapter that obsequent-scarps, and other morphological features on slopes, have been linked with a form of slope deformation termed 'sackung'. However, this linkage between form and process has resulted from cyclical argument: Zischinsky used the term 'sackung' to describe a slope that had 'sagged' and deformed without the formation of a through-going failure surface, Radbruch-Hall et al. (1976) observed slope 'sagging' in association with obsequent-scarps and ridge-top depressions, Radbruch-Hall et al. then called such landforms 'sackung features'.

It is important to break this cyclical reasoning and encourage the view that obsequent-scarps and ridge-top depressions may be formed by a variety of processes, including models b to e (Fig. 8.1). Other possible processes include graben-like displacement, outcrop of a rear-scarp on the opposite slope of a ridge or sliding over an undulating failure-surface. The lack of sub-surface data is a major hinderance to further explanation, though it is possible to reject certain models for the case studies.

The origin of the small ridge-top depression at Mam Sodhail is

uncertain. It does however resemble the gaps observed between the upslope walls of toppled blocks and stable blocks at Mullach Choire a' Chuir (Section 7.4). The remaining sites have no similar feature, terminating upslope at either a prominent rear-scarp or behind the summit where deformation has occurred through the ridge (e.g. An Riabhachan). The ridge-core-foundering model (Fig. 8.1b) is therefore rejected as a possible cause of obsequent-scarp formation at the sites discussed. A major ridge-top depression was however observed on aerial photographs during the compilation of the RSF inventory. This example occurs at Aonach Sgoilte [NG 837 025] and is estimated to be up to 200-m-long and 5-m-deep. All the case studies are developed in homogenous rock so that sliding of competent blocks over incompetent rock (Fig. 8.1e) is also inapplicable.

No slickensides were identified on any of the obsequent-scarp faces though they may, if exposed, have been removed by weathering. It is considered significant however that slickensides were not observed on the obsequent-scarp walls uncovered by sections dug into slope trenches. The opposing movements along the discontinuities forming obsequent-scarp walls are therefore inferred to have occurred under comparatively low stresses. As normal stress is inversely related to the cosine of layer inclinations, for unit rock thicknesses, the normal stress acting upon the steeply-inclined joint sets would have been low. Bovis (1982) invoked this factor to account for the lack of slickensides on obsequent-scarp walls at Affliction Creek, Canada. Faulting in response to isostatic uplift, the hypothesis proposed by Patton and Hendron (1974) for obsequent-scarp development, was also rejected by Bovis.

Toppling has been suggested as the most probable cause of obsequent-scarp development at study sites A-E but this mode of deformation could only have occurred under self-weight stresses on the steepest slopes. Effective friction angles between 30° and 34° are implied by the kinematic tests, indicating a considerable reduction in shear strength. High cleft-water pressures, or other factors, may have enabled toppling at lower slope angles (Holmes and Jarvis in press).

Slope deformation at Sgurr Breac and A' Chailleach has not formed obsequent-scarps. Both examples occur in gneisses which have strongly-developed low-angle joint sets directed parallel/subparailel with the foliation and inclined positively. Deformation may have occurred along these joints but due to the lack of subsurface data it is not known whether a continuous failure-plane (or through-going failure-zone) has developed.

Significantly, the A' Chailleach and Sgurr Breac foliation surfaces dip close to the residual friction angle of gneiss (24°). Both slopes are also inclined at angles close to ϕ_r. It may be hypothesised that at these two study sites progressive-failure, which was further excited by former high cleft-water pressures, may account for their deformation. If the shear strengths along the failure-surfaces decreased to the residual (which is likely given the amount of deformation signified by their rear-scarps) then increases in water pressures along their failure-surfaces may lead to renewed deformation. Neither of the two slopes feature joints dipping steeply into their slopes and this may account for their lack of obsequent-

scarps.

Jaeger (1979) commented that time-dependent creep of schist may occur under extended periods of loading, citing tests undertaken in France which showed that when shear stress is applied to schist a time-dependent deformation occurs. Some of the deformation may not be recovered once the load is removed. The work undertaken in Switzerland by Huder (1976) into the creep of natural slopes composed of Bundner schist is also instructive. He commented upon a slide at Schuders where horizontal deformationsof up to 10 mm $year^{-1}$ were recorded and a total displacement of 60 m occurred between 1945 and 1965. Bedding layers dipped positively at c. 22-26° and were thought to have controlled the deformation at the site. Huder states that the creep movements can be explained by progressive-failure of the rock.

Sites F and G exhibit similar morphological characteristics to the Matrei-Glunzerburg slope which Zischinsky (1966) described as a sackung. It is proposed that the Sgurr Breac and A' Chailleach slopes have deformed in a manner similar to that illustrated in Figure 8.1a. If so, they are the first examples to be described as sackung in Britain.

The Carn na Con Dhu, Ben Attow and An Sornach slopes appear to be intermediate in type between the toppling failure modes and the sackung-type slope deformations at Sgurr Breac, and A' Chailleach. Overturning of negatively-dipping joints at Carn na Con Dhu and Sgurr Breac is thought to have been caused by the increased load imparted by the weight of rock material above them.

Sissons and Cornish (1982) hypothesised that earthquakes accompanying the stress release between isostatically-uplifted blocks may have triggered rock-slope failure in Glen Roy, Scotland. Jahn (1964) suggested that earthquakes may trigger movements of steep slopes in the Carpathian Mts. and Beck (1968) also stated that ridge-core-foundering in New Zealand may have been caused by earthquakes. A direct link between faulting and obsequent-scarp development was inferred by Patton and Hendron (1974). The possibility that earthquakes may have caused, or contributed to, obsequent-scarp development in the Scottish Highlands cannot be dismissed, particularly as the large obsequent-scarp at An Sornach is considered to be an isostatically-induced pop-up. No evidence of the frequency and magnitude of former earthquake activity is available to the author. The simplest and most probable explanation, that the deformations were likely to have been assisted by high cleft-water pressures, is accepted here, though earthquake loading of slopes could have assisted in slope deformation, particularly on slopes which were already saturated.

All of the case studies are located in formerly glaciated valleys and it may be argued that the most probable time for their initiation would have been during glacier decay. At such times, according to Bovis (1982), oversteepened slopes would have toppled as the lateral support of glaciers was removed. He has shown that obsequent-scarps at Affliction Creek began to form c. 140 years ago (the Neoglacial maximum) and stated that the Affliction Glacier has wasted down about 100 m since that time. Toppling failure during deglaciation would also be favoured because of meltwater production.

Rock mechanics theory may already have possible explanations for the inferred arrested toppling at the study sites. Barton (1971) hypothesised that toppling failures with rough-joint surfaces may be self-inhibiting because of the shear-stiffness encountered during shear. He recorded attenuation of displacement by models which developed toppling forms of failure. Bovis (1982) also suggested that shear-stiffness could have led to cessation of obsequent-scarp formation at Affliction Creek.

Pre-failure displacements of the order of 8% of the joint lengths (assuming toppling columns are c. 120-m-high) would be required to form the 10-m-high obsequent-scarps at Ben Attow. Most of the obsequent-scarps, being smaller, would require only 3% shear displacement. It was noted in Chapter 2 that as joint length in the direction of shear displacement is increased, the area of contact between joints will be transferred from minor and steeply-inclined asperities to major less steeply-inclined ones with higher asperity wavelengths. A greater relative amount of shear displacement along a large-scale joint may therefore be required to bring asperities into contact. Pre-failure shear displacements greater than 1% may then be possible.

A factor neglected in the literature is the dynamic effect of forward rotation on the normal stresses acting upon layers. This effect can be easily demonstrated. If a joint is inclined at 89° for instance, a point 50-m-below the surface (assuming a rock-mass density of 24.5 kN) will have a normal stress acting upon it of 0.37 kPa (cf. Equation 7.2). Forward rotation of the joint by 10° will increase the

Figure 8.14: The calculated increases in normal stress experienced at a point 50-m-below the surface on a forward rotating joint.

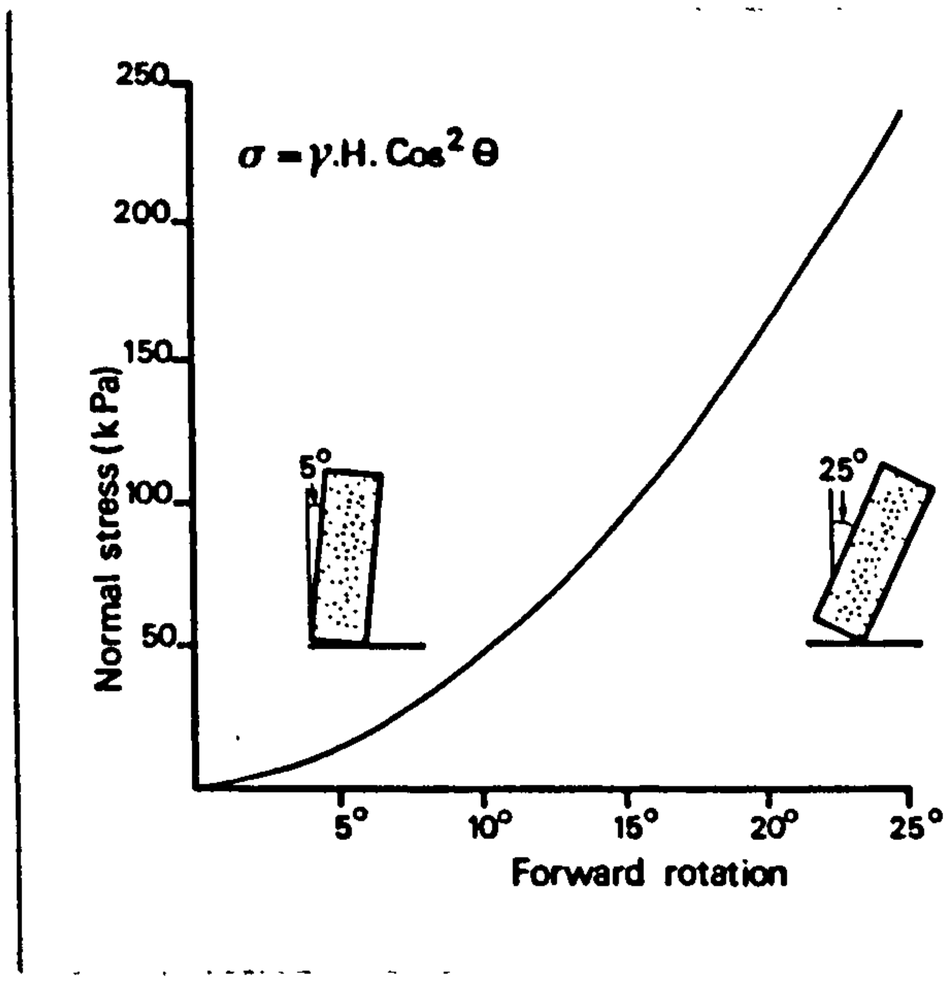

normal stresses acting at point 50-m-below the surface to 44.6 kPa: an increase in normal stress by two orders of magnitude. The increases in normal stress experienced by a theoretical joint are illustrated in Figure 8.14 for forward rotations up to 25°. The rotation will also produce a decrease in the vertical thickness of rock material above the rotating point on the joint, but this change would be of little significance for small rotations.

The importance of an increase in normal stress, activated by rotation, is that shear strength will not only be increased by displacement along the layers because of shear-stiffness effects, but also because of increasing normal stress (cf. Equation 2.1). The increased shear strength caused by these two factors may be sufficient to inhibit further forward rotation after minor tilting has occurred and may alone explain the inferred cessation of toppling at study sites A-E. Over large tilts, say beyond 15°, the shear displacement will be so large so as to reduce the strength of the layers to the residual.

Shearing of rough-joint surfaces prior to mobilisation of peak strength also leads to joint dilation (Section 2.2). Bovis (1982) suggested that dilation has occurred within the Affliction Creek slope. However, a point that he omitted to make is that dilation will enhance free-drainage thus reducing the risk of a build-up of

dangerous cleft-water pressures. If high cleft-water pressures were important, a factor which Bovis did not consider, then their reduction must be important in maintaining stability.

Evidence for dilation at the study sites is indirect being inferred from the drainage patterns on the slopes. Drainage from the Ben Attow slope for instance, is markedly different inside and outside the RSF. Springs and swallow-holes occur across the length of the RSF (Fig. 8.9) whereas no sinkholes were found on stable slopes; the springs emanating at the slope foot. A similar disruption in drainage was noted by Bovis at Affliction Creek.

Data are available which indicate possible cessation of obsequent-scarp development at other sites in the world. Radbruch-Hall (pers. comm., 1983) reported that no movement had been recorded on the survey courses across two RSFs (Crested Butte and Bald Eagle Mt., U.S.A.) which feature obsequent-scarps. The survey courses were emplaced before 1976 (cf. Radbruch-Hall et al. 1976) and the horizontal distances between the target points sited on the slope and the survey origin were thought to be accurate to +/- 15 mm. It is not yet possible to infer if movements have ceased completely or whether they occur in increments of rapid movement but Radbruch-Hall's work has established that continuous gravitational creep does not occur at the surveyed sites.

According to Rengers and Soeters (1982), the operators of a water tunnel which runs through nearly the whole portion of unstable slope at the Muro, Pyrenees, have reported no disruptions to its operations over c. 25 years. This is supportive of the hypothesis that

deformation has now ceased. These authors emphasised possible morphological evidence for continued displacement of the slope (though the depth to which it reaches is unknown) and considered that the obsequent-scarps are still developing.

If the obsequent-scarps at An Sornach were produced by toppling then this form of deformation may occur along discontinities with strike directions within 30° of the slope face. This angle was assumed by Goodman (1981) to be the maximum likely deviation of a discontinuity from the slope face along which toppling could occur and may be insufficient if the interpretation of toppling at An Sornach is valid. Toppling may produce the graben-like features observed by Jahn (1964), Beck (1968), Tabor (1971) and Radbruch-Hall et al. (1976), if blocks topple on either side of a steep-sided ridge.

8.7 Conclusion

Fifty-six large RSFs (greater than 0.25 km^2) with obsequent-scarps are known in the Scottish Highlands. The examples recorded by the author are as spectacular as any previously recorded in the world. Radbruch-Hall (1978) observed a correlation between the global locations of obsequent-scarps and tectonic plate margins. The Scottish data however indicate that obsequent-scarps may form wherever slopes are steep and discontinuities dip favourably. A connection between RSFs featuring obsequent-scarps and former glacial limits in the Highlands has been suggested.

A number of slope deformation models have been proposed in the literature to account for obsequent-scarp development. It is

suggested that toppling modes of failure may account for bulging of slopes, graben-like displacement of a ridge crest and obsequent-scarp formation. These features have been linked, though may not always occur with, large-scale slope deformation. Goodman and Bray (1976) suggested that the bending of strata inferred by Zischinsky (1966) may have been a form of flexural toppling. Despite evidence for overturning (rotation) of joints at Carn na Con Dhu and at Sgurr Breac, valleyward-bending of layers has not been proven. The presence of cross-joints however would have permitted block-flexural toppling at these sites.

The Goodman and Bray (1976) kinematic test for toppling has been used to assess the potential for toppling at the study sites but the criterion for toppling is not satisfied for the overall slopes. High cleft-water pressures have been invoked to account for this dichotomy, as they would add to shearing stresses on the slope. Water pressures are not included in the kinematic test. Increases in shear stresses produced by possible earthquake activity may have triggered obsequent-scarp development. However, no slickensides have been found on the obsequent-scarp walls and the hypothesis that obsequent-scarps are produced directly by faulting at the study sites is therefore rejected.

Two rock-slopes (Sgurr Breac and A' Chailleach) have suffered a mode of deformation which closely resembles the 'sackungen' described by Zischinsky (1966). The Ben Attow and Carn na Con Dhu slopes also feature 'sagging' along their slope profiles but in these cases obsequent-scarps have developed. Failure-scarps are taken to indicate downslope deformation at the four sites, possibly along shallowly

dipping discontinuities, but slide toes have not developed. Holmes and Jarvis (in press) noted that if a slide toe had formed at Ben Attow but was later removed by glacial erosion the obsequent-scarps would have been destroyed as well.

As obsequent-scarps are unlikely to survive overriding by glaciers they are thought to postdate the last glaciation of the slopes on which they are found. The most probable time for the build-up of the postulated high cleft-water pressures would have been during deglaciation. A connection between deglaciation and obsequent-scarp development has also been inferred by Tabor (1971) and Bovis (1982) but both of authors hypothesise glacier oversteepening as the cause of deformation.

It is inferred that the obsequent-scarps are now fossil and are not progressively-failing at present. The proposed attenuation of movement could have been caused by shear-stiffness affects combined with an increase in normal stress as rotation proceeds. This change in normal stress is peculiar to the initial stages of toppling failure. Drainage from the slope may have been enhanced by dilation which would reduce the risk of high cleft-water pressure build up.

No evidence for continuous gravitational-creep (sensu Radbruch-Hall et al. 1976) has yet been collated, despite numerous studies across the world. It is advanced that the large-scale slope deformations (including massive topples) studied here, are best explained by a relative short period of rapid movement which was terminated by either improved drainage, an alteration in the hydrologic regime or by factors intrinsic to the rock-mass system or

some combination of these factors.

9: THE CHRONOLOGY OF ROCK-SLOPE FAILURE IN THE FIELD AREAS.

9.1 Introduction

A major concern of geomorphology is the rate of operation of geomorphic processes (identified in Chapter 1 as one of the themes of this research). This concern demands a historical perspective and consequently the chronology of RSFs is considered in this chapter, prior to discussion of the magnitude/frequency relationships of RSFs in Chapter 10.

Several authors have hypothesised that RSFs occurred with greater frequency in the past than at present. Only seldom have attempts been made to date RSFs and test this hypothesis: such research is summarised in Section 9.2. Investigation of the chronology of RSF is subject to the general difficulties of dating Quaternary landforms, which are often compounded in mountainous areas because of the lack of datable deposits in the correct stratigraphic position.

In view of the problems encountered by the author in attempting to ascertain whether datable deposits exist under RSFs in the field a research strategy was decided upon early in the first field season. This approach utilises relative dating techniques that are commonly used by N American Quaternary scientists (e.g. Birkeland 1973, Carroll 1974, Andrews and Miller 1981, Dowdeswell 1982) but have rarely been used in Britain.

This chapter details the techniques used, their assumptions, the analyses of the field data and the inferences reached. Discussion of the results is organised by field area. The relative dating results

are summarised and interpreted in Section 9.5.

9.2 Related studies

Despite the large volume of literature concerning landslides from various parts of the world, few attempts have been made to date RSFs. Important contributions however have been made in this field of study and foremost amongst these must be that made by Jonsson (1976), who dedicated much of his life to research into the age and formation of Icelandic RSFs.

Jonsson's (1976) book catalogues scores of slope failures ('berglaup') in Iceland which he visited in the field. He attempted to date the Icelandic RSFs using a number of relative age criteria, including the degree of vegetation cover, tephrachronology, the degree of weathering, soil development and morphostratigraphic relationships with other landforms. He summarised the relative age data into groups and Whalley et al. (1983) subsequently assigned tentative ages to these. The last authors contend that although Jonsson's relative age data may be criticised they should at least be internally consistent.

The relative age data collected by Jonsson indicate that the majority of slope failures (60%) occurred 3-5,000 years ago and that few RSFs (14%) took place in the early post-glacial (7,000-10,000 years ago). As Whalley et al. (1983) noted, this temporal distribution contradicts the hypothesis that the majority of slope failures occur soon after deglaciation. However, they found that the largest slope failures occurred between 7,000 and 10,000 years ago.

Gardner (1980) attempted to date RSFs in the Rockies using

similar techniques to those employed by Jonsson, including the degree of weathering of rocks, pockets of fines on RSF debris surfaces overlain by a surface organic horizon, overlapping of RSF debris by talus slopes and, in one instance, by a small neoglacial protalus rampart. On the largest RSF (example 1, in Gardner 1980) a deposit of Mazama volcanic ash (c. 6,700 years B.P.) was found, indicating the RSFs minimal age (Gardner pers. comm.). Gardner (1980) stated that all the RSF debris has similar degrees of weathering which suggests that most of the RSFs occurred before c. 6,700 years ago.

A number of researchers have dated RSFs by analysing pollen found within the sediments that overlie topographic features formed during slope failure (e.g. Franks and Johnson 1964, Kujansu 1971, Gil et al. 1974, Tallis and Johnson 1980, Blackham et al. 1981). Tallis and Johnson (1980) used pollen analysis to date the initiation of peat accumulation within hollows on the surface of landslides (including RSFs) in Longdendale, north Derbyshire. Their work indicated that the oldest slope failures occurred over 7,000 years ago though significant slope failures took place between 3,000 and 5,000 years B.P.

Blackham et al. (1981) sought to date a slope failure in N Yorkshire using pollen analysis of lake-floor sediments. The lake was inferred to have been formed by movement of the RSF. They noted that analysis of the basal sediments would provide a minimal age for the slope failure. The lowest recorded sediment yielded a pollen assemblage that they correlated with a pollen zone aged between c. 11,000 and 10,000 years old. The maximum age of the slope failure was thought by them to be 15,000 years B.P., based upon dates for

deglaciation in N Yorkshire. The age of the RSF is thus bracketed between 15,000 and 10,000 years B.P. Unfortunately, the basal sediments in the lake were not recovered by Blackham et al. (1981).

It may be argued that while detailed dating of individual RSFs is both interesting and important, scientific method demands Generality. Following from this and earlier discussion on the potential complexity of RSF occurrence, an absolute age for a single RSF will be of minimal scientific value unless it can be related to other slope failures. Pollen analysis and radiocarbon dating of numerous RSFs must be viewed as an important but long-term aim (cf. Whalley et al. 1983). However, some insight into the chronology of RSF may be gained using techniques suited to a shorter-term study.

9.3 Methodology

Two relative dating techniques are used in this study: (i) rock weathering, which assumes that various quantifiable rock weathering parameters are time-dependent and (ii) morphostratigraphy, which relies upon the positional relationships between landforms.

Rock weathering

Particular care must be paid to the weathering parameters as they may be dependent upon factors other than time (Andrews and Miller 1981). The field area approach however is advantageous in that it minimises the variation in factors such as altitude, aspect and changes in rock type, because of the scale within which the studies are made. This is not to underestimate the subjectivity of the methods used.

The following weathering parameters were measured at the field sites.

Weathering rinds. These are zones of discoloured rock that run parallel with the outer surface of boulders (Dowdeswell 1982). At each site 25 boulders were split open and the zone of discolouration was measured using a micrometer (accurate to 0.1 mm). Rind measurements were not taken from boulder corners but where the rind ran parallel with the boulder surface for a length of at least 2.5 cm. Two weathering rind measures were calculated: (i) the mean thickness of each rind (including zeros) and (ii) the percentage of boulders that had developed rinds.

Surface pitting: A rock is defined as pitted if it has one or more closed depressions. Pitting is probably caused by granular disintegration which, as King (1977) and Ballantyne (1981) have observed, is an important form of weathering in the Scottish Highlands. Fifty boulders were examined for surface pitting at each site and the depth of individual pits was measured using a graduated rod.

Weathered/fresh ratio: A weathered-boulder is rough to the touch and exhibits single-grain mineral relief (Dowdeswell 1982). The number of boulders, out of fifty, that featured single-grain mineral relief on greater than 75% of their surfaces was recorded at each site. Comparison was made between the extent of weathering on the surface of each boulder and the density charts given in Gardiner and Dackombe (1982).

Angularity: It is assumed that boulders will lose their angularity with increasing age. The angularity of fifty boulders was estimated by placing a 2-cm-radius circle on boulders with diameters greater than 0.5 m and less than 1 m. If the boulder edges fell within the circle the boulder was described as being angular.

Rotting. Mica-schist boulders are prone to rotting of their outer surfaces and it is assumed that this process is time-dependent. Pieces of rock can be readily torn from a rotted mica-schist boulder and crushed by hand. The number of boulders, from fifty, with greater than 10% of their surface rotted was recorded at each of the Cowal sites.

Vein relief. Quartz veins in mica-schist boulders appear to be less susceptible to granular disintegration than mica-schist. The relative relief of quartz veins was therefore assumed to be time-dependent and 25 veins were measured (to the nearest 1 mm) normal to the boulder surface.

Evidence for spalling (the periodic loss of the outer layers of boulders) was not observed in the field. It is suggested that the boulders have weathered by granular disintegration and that regeneration of the boulder surfaces has not occurred through spalling.

Dowdeswell (1982) provided a useful means of analysing rock weathering data such as the above, and his scheme has been adopted, with some modification, for this study. There are four stages in the analysis used in this study:

(i) a priori grouping of rock weathering data using theCLUSTAN package (Wishart 1977);

(ii) Principle Components Analysis (PCA) of standardised relative weathering data;

(iii) Cluster Analysis of the sites using the scores on Component 1 from the PCA, to yield a second a priori grouping of sites;

(iv) Discriminant Analysis on both a priori groupings.

This classification process yields statistically significant groupings of sites with similar rock weathering characteristics. To underline the stratigraphic informality of these relative age groupings letter designations are used (Birkeland 1974). The analyses of the rock weathering data will be described in detail during discussion of the Garbh Choire Mór site.

Morphostratigraphy

Three forms of morphostratigraphical relationships were used to attempt to relatively date the RSFs. These are:

(i) periglacial landforms overlapping RSF features such as failure-scarps and obsequent-scarps (e.g. Plate 9.1);

(ii) displacement/truncation of periglacial lardforms (e.g. Plate 9.2);

(iii) accumulation of periglacial debris behind RSF features (e.g. Plate 9.3).

The morphostratigraphic dating technique involved geomorphological mapping at 1:5,000-scale using the mapping symbols devised by Ballantyne (1981). During the mapping programme particular attention was paid to the above three forms of morphostratigraphic relationship and critical sites were mapped.

Plate 9.1: Periglacial debris overlapping the rear-scarp at Sgurr Breac in the Fannichs (A' Chailleach in distance).

Plate 9.2: Disruption of solifluction lobes by the Sgurr na Lapaich RSF. The rock outcrop (centre-right) is part of the rear-scarp.

Plate 9.3: Solifluction lobes/sheet abutting against and overrunning an obsequent-scarp on Mam Sodhail.

Figure 9.1: Garbh Choire Mór, Fannich Mts.

1 = RSF debris

2 = Scree

3 = Morainic ridges/mounds

4 = Rock weathering site

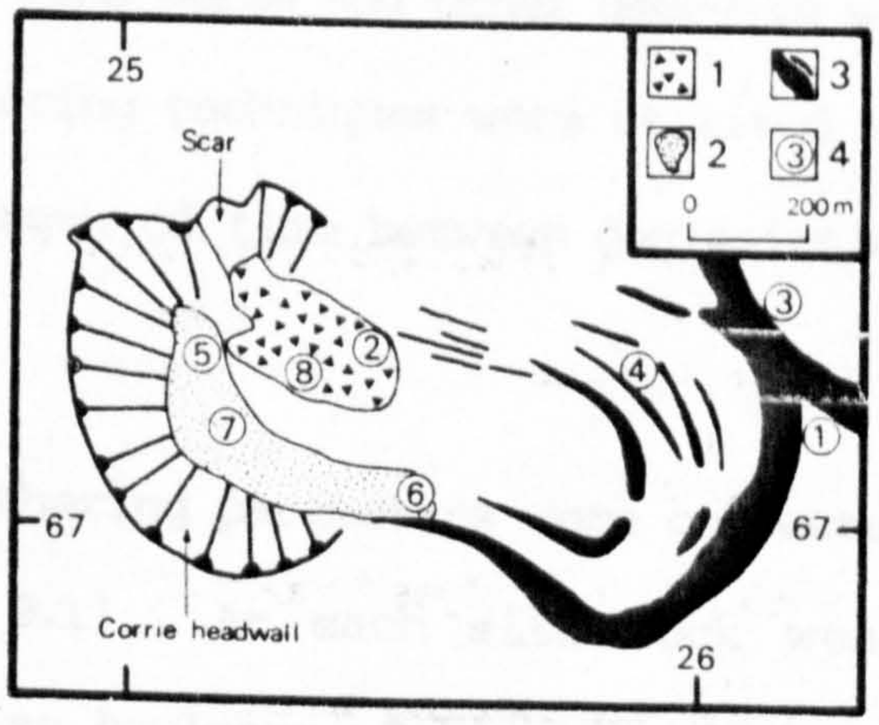
25
Scar
1
3
2
4
0
200 m
5
8
2
3
4
7
1
6
67
67
Corrie headwall
26

The periglacial landforms have been divided into two classes: active and fossil, following Ballantyne's genetic classification. In key areas sections were dug into periglacial landforms to ascertain whether or not fine-grained material (thought to be an indication of the potential mobility of periglacial landforms) was located between clasts. The morphostratigraphic evidence for the Nest of Fannich will be discussed in detail.

9.4 Field data and analyses

The Fannichs

The Garbh Choire Mór RSF debris shows no signs either of disturbance by a glacier or of having formerly fallen onto a glacier surface. This RSF must therefore post-date the last glaciation of the corrie. However, the RSF debris is clearly ancient as its boulder surfaces show a similar degree of weathering to the end moraines. Because end moraines, composed of gneiss boulders, lay in the vicinity of the RSF debris, and scree and other deposits were found within the corrie, rock weathering techniques were utilised to attempt to assess the comparative length of time between deglaciation of the corrie and slope failure.

Five rock weathering parameters were collected at 8 sites within the corrie (Fig. 9.1). At each site rock weathering data were measured from gneiss boulders within 10 x 10-m-squares. The sample plots were located on freely-drained ground usually on topographic highs. These data are summarised in Table 9.1.

Site	Weathering (%) > 75%	Pitting (mm) (%)	mean depth	Rinds (mm) (%)	mean width	Angularity (%)
1	100	90	17.9	100	4.03	8
2	95	82	11.9	95	3.01	12
3	98	90	15.1	100	4.36	10
4	100	88	15.8	100	4.60	10
5	72	53	3.9	82	2.45	36
6	54	55	4.3	90	2.53	38
7	38	50	5.4	92	2.48	38
8	98	83	13.1	100	3.13	18

Table 9.1 Rock weathering data for Garbh Choire Mór. Site locations are given in Figure 9.1.

The rock weathering data were standardised to z-scores and then subjected to Principle Components Analysis (PCA). Standardisation ensures that the variables are equally weighted (having a mean of zero and a variance of one) and overcomes the problems associated with different scales of measurement. Component 1 was found to account for 89.4% of the variability in the original data. Components 2-5, accounting for the remaining 11.6% of the variance in the data, were disgarded at this stage with some loss of original information. The Eigenvectors of Component 1 are of similar magnitude, ranging between -0.42 and 0.43, indicating that Component 1 is an average variable (Davies 1973).

It is not possible to use the scores on Component 1 as a direct measure of time since the analysis merely groups together sites that have similar rock weathering characteristics. It is assumed however that if the weathering parameters are time-dependent, sites of approximate sychroneity should be grouped together.

SITE	SCORES ON COMPONENT 1	DEPOSIT TYPE
1	2.40	end moraine
2	0.68	RSF debris
3	2.21	end moraine
4	2.37	end moraine
5	-2.99	debris cone
6	-2.74	scree
7	-2.95	scree
8	1.02	RSF debris

Table 9.2: Scores on Component 1 for each site within Garbh Choire Mór.

Cluster Analysis places groups (sites) of highest similarity next to one another and also indicates those sites with greatest dissimilarity. The results from a Cluster Analysis are commonly presented in the form of a dendrogram which terminates when all the cases are fused into a single cluster. A subjective choice must be made concerning the 'cut-off' point or the stage in the clustering process at which the classification of groups is imposed.

The point at which the coefficients of dissimilarity necessary to fuse two groups increases rapidly is taken as the cut-off point in this study. Cluster Analysis using Component 1 scores as Euclidean distance coefficients yielded the dendrogram shown in Figure 9.2a and Figure 9.2b gives the clusters computed by the CLUSTAN package using the Wards method. Three groupings emerge: (A) Moraines [sites 1, 3 and 4], (B) RSF debris [sites 2 and 8] and (C) scree deposits [sites 5, 6, and 7].

So far, the analysis has produced only groupings with typological similarities. The significance of the clusters may be tested using

Figure 9.2: (a) Dendrogram of scores on Component 1 (output from PCA) for the Garbh Choire Mór rock weathering data.

(b) Dendrogram output from the CLUSTAN package using Ward's method.

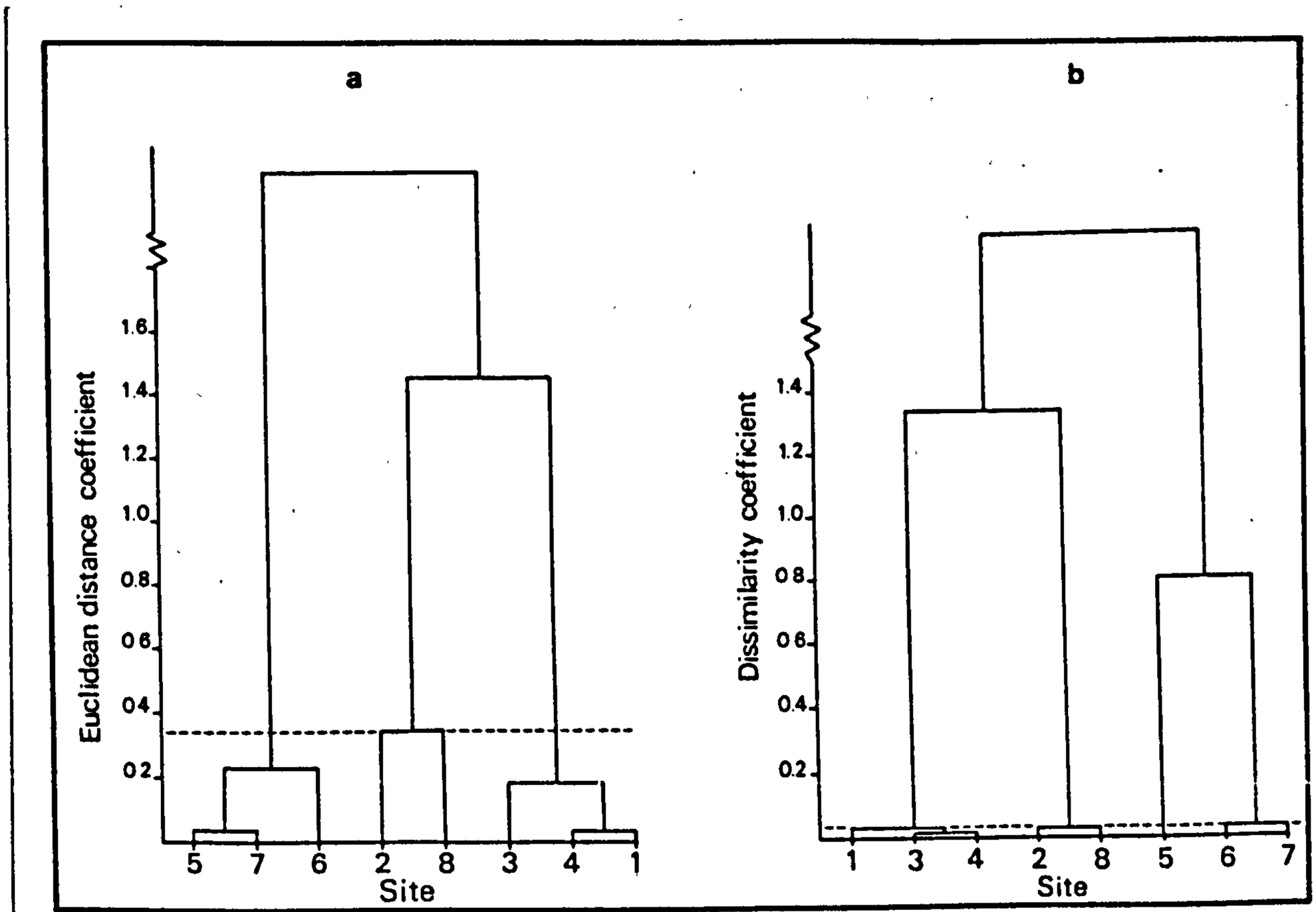

Discriminant Analysis which seeks to find the linear combination of variables that maximises the between-group variations (Davies 1973). This form of analysis is particularly useful because it also provides an F-test on the significance of the groups produced. Discriminant Analyses were performed on both a priori groupings using the original rock weathering data. A significance level of 95% was selected prior to Discriminant Analyses, as the criterion for rejection or acceptance of a classification.

Some delay between the onset of deglaciation and RSF must have occurred otherwise the failed debris would have fallen onto the decaying glacier. It could be suggested that if the Loch Lomond

Stadial intervened between deposition of the end moraines (which pre-date the Loch Lomond Advance) and slope failure then the former deposits would have been subjected to c. 1,000 years of intense periglaciation which should have reduced the apparent similarity between the two landforms. It is not possible to estimate the length of delay between deglaciation of Garbh Choire Mor and RSF but it is tentatively suggested that RSF occurred before the Loch Lomond Stadial and relatively shortly after deglaciation of the corrie.

The diverse periglacial landforms of Sgurr Breac and A' Chailleach were mapped in detail by Ballantyne (1981). It is possible to make some inferences concerning the relative age of the RSFs from his mapping (which was checked in the field), the morphostratigraphic relationships between the RSF and periglacial landforms, and the climatic regimes under which the periglacial forms are thought to have been active.

Debris-sheets were mapped by Ballantyne close to the rear-scarps at both Sgurr Breac and A' Chailleach. The debris sheets were subsequently found to overlap the scarps. According to Ballantyne's (1981) genetic classification of periglacial landforms, debris-sheets were dominantly active during the lateglacial (c. 15,000-10,000 years ago) as they require a climate much more severe than is found at present. Ballantyne cautions however that as a palaeosol was found under a debris lobe on Ben Wyvis movement of the lobe may have occurred during the Flandrian.

At Sgurr Breac, the rear-scarp is intermittantly overlain by a vegetation-covered debris-sheet. The frontal margin of this sheet is

lobate indicating limited flowage after the rear-scarp was formed. The NE margin of A' Chailleach is also partially covered by a debris-sheet. The preservation of the relict periglacial landforms at Sgurr Breac and A' Chailleach indicates that little or no deformation has occurred in the vicinity of the rear-scarps since the periglacial features overrode them.

In addition to the relict periglacial landforms, a range of active periglacial landforms have developed upon the rear-scarp at Sgurr Breac. The active forms include: various types of terraces, ploughing boulders and solifluction lobes (Plate 9.1). Active solifluction lobes have also formed on the S-facing rear-scarp on A' Chailleach.

The fossil forms are particularly important as they indicate that the Sgurr Breac and A' Chailleach RSFs occurred sometime during the Lateglacial. As the upper limit of the Fannich glacier was likely to have been c. 600-650 m O.D. (midway up the Sgurr Breac RSF and below the toe of the A' Chailleach example) in the Nest of Fannich at its Achnasheen Readvance maximum, any higher ground would have been exposed to intense periglacial activity during both deglaciation of this ice mass and later during the Loch Lomond Stadial. The fossil periglacial forms could therefore have overridden the rear-scarps in either period.

Cowal District

If Sutherland's (1981) reconstruction of the Loch Lomond Advance limits in the Cowal are correct, then all the RSFs in this field area lie inside these former glacial limits. As none of the examples shows

any sign of disturbance by former glaciers it is inferred that all postdate the Loch Lomond Advance.

Rock weathering data have been collected at 14 sites on 9 RSFs in this field area (Table 9.3). Site locations are given in Figure 9.3.

Site	Weathering (%) > 75%	Vein relief (mm) mean	Vein relief (mm) maximum	Rotted (%)	Angularity (%)
1	70	11.3	20	10	32
2	100	15.8	32	28	25
3	93	14.0	24	34	22
4	92	18.0	28	31	18
5	3	0.0	0	0	34
6	97	23.0	48	28	14
7	100	24.0	40	24	18
8	95	18.0	36	16	30
9	95	22.2	38	20	26
10	100	18.1	26	26	25
11	75	15.0	20	16	25
12	100	21.3	33	25	30
13	95	23.0	31	25	30
14	58	12.3	24	8	35

Table 9.3: Relative weathering data for the Cowal field area

Because some of the RSFs are complex (e.g. Mullach Choire a' Chuir) and may result from numerous phases of movement, the rock weathering data were collected at more than one location on certain RSFs. This will also provide a further check on the classes produced by the rock weathering parameters as different sites on the same RSF should group together if the RSF debris was the product of one event.

Three of the sites are of particular interest. Sites 6 and 7 are located on a massive accumulation of mica-schist boulders that follows the base of the N-facing crags of Beinn an Lochain (Plate 9.4). Watters (1972) interpreted the boulder feature as being formed by

RSF, inferring that it originated from the steep cliffs further north. It has been suggested however that the feature is a rock glacier (D.G. Sutherland pers. comm.).

During discussion of the Beinn Alligin feature in Wester Ross (Section 3.4), it was noted that rock glaciers and rock avalanches possess similar morphological characteristics. However, unlike the Beinn Alligin feature, no scar can be observed above the Beinn an Lochain debris mass whereas one would surely be expected, given the size of the debris accumulation, if it had originated as a RSF.

Fortuitously, between visits to the feature during May 1983 a large boulder (c. 20 m^3) fell from the cliffs, its origin marked by an area of fresh rock on the cliff some 100 m above the debris mass. The boulder formed a series of craters in the debris mass until it stopped some 200-m-distance from the cliff. If frost wedging released blocks with higher frequency during the Loch Lomond Stadial then the genesis of the feature could be more easily accounted for by rockfall forming a rock glacier rather than a large RSF. The feature lies within Sutherland's reconstruction of the Loch Lomond Advance limits indicating that it must have been active during deglaciation or later.

Despite the above evidence of rockfall, the feature is probably fossil as rock glaciers are not presently active in Scotland (Sissons 1975, Dawson 1977, Ballantyne 1981, Chattopadhyay 1984). As the rock glacier was probably only active during the close of the Loch Lomond Stadial (c. 10,000 years ago) it is important as a morphostratigraphic marker against which the rock weathering data from other sites can be compared.

Plate 9.4: The Beinn Lochain rock glacier (direction of view shown in Fig. 9.3). Note the very large boulders towards the margin of the feature.

Figure 9.3: Location of the rock weathering sites in the Cowal field area.

1 = Rock-slope failure

2 = Location of rock-weathering site (numbers correspond to those given in Table 9.3).

3 = Contours in 200 m intervals.

4 = The Beinn Lochain rock glacier.

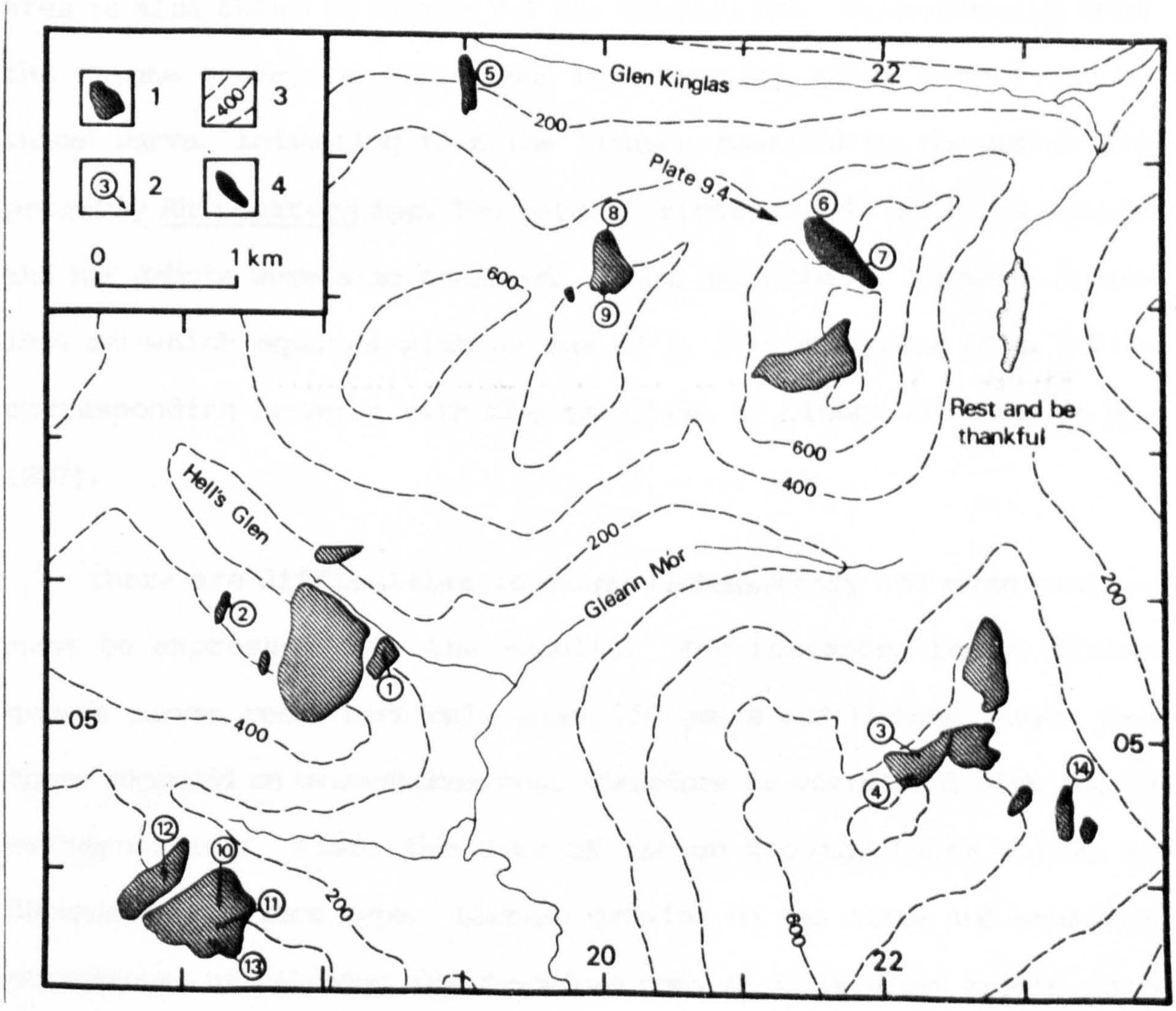
1
2
3
4
0
1 km
Glen Kinglas
22
200
Plate 9.4
600
400
Rest and be thankful
Hell's Glen
Gleann Mór
05
20

Site 5 lies on the RSF that was described by Clough (in Gunn et al. 1897) as having occurred during the 17th Century. Lichenometry was utilised to attempt to date this feature in addition to rock weathering techniques. Measurements were taken of the largest yellow-green lichen thalli (assuming that these are Rhizocarpon spp.) on gravestones at the church in Cairndow village [NN 180 108], sited 1 km NW of the RSF and 200 m below it. Lichen thalli were measured to the nearest 1 mm using a translucent ruler.

These lichen data are plotted against the ages given on the gravestones in Figure 9.4. The growth curve, compiled by Innes (1983), for Rhizocarpon spp. measured on gravestones in the Glencoe area is also shown in Figure 9.4 for comparison. Measurements from the Strone graveyard correspond broadly with those summarised by Innes' curve, indicating that the lichens measured by the author are probably Rhizocarpon spp. The largest lichens on 50 boulders within the RSF debris were also measured. Their mean thalli diameter equals 18.4 mm which equates with an age of c. 250-300 years (Fig. 9.4) - corresponding broadly with the age given by Clough (In Gunn et al. 1897).

There are difficulties in using lichenometry and some caution must be expressed over the results. For instance, Innes' lichen growth curves reach back only about 150 years and lichens larger than those recorded on gravestones must therefore be correlated with age by extrapolation. Also, the rate of lichen growth, Innes warns, is dependent upon rock type. Lichens growing on the slate and sandstone gravestones at Cairndow may therefore possess a different growth curve to those growing on the RSF debris. Despite these reservations, the

Figure 9.4: Growth curve for Rhizocarpon spp. measured in the Strone graveyard.

lichenometric age of the Glen Kinglas RSF is assumed to be reasonably accurate, providing a useful marker for calibration of the rock weathering data from other sites.

The rock weathering data for the Cowal sites are summarised in Table 9.3. The four stages of analysis listed in Section 9.3 were followed. Scores on Component 1 are listed in Table 9.4. Component 1 accounted for 81.4% of the variance of the original data whereas Components 2-5 have eigenvalues less than unity and therefore contained less information than any one of the original variables.

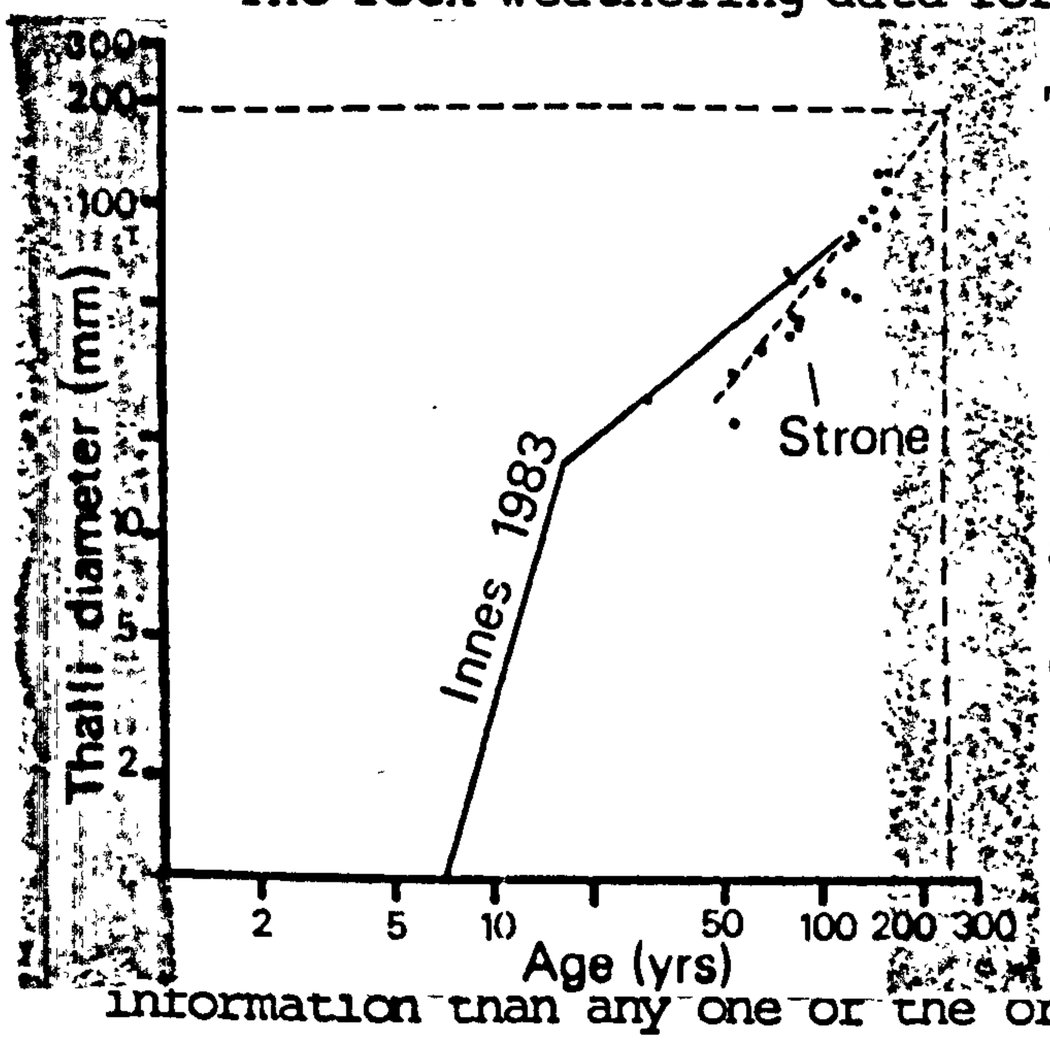

SITE	SCORES ON COMPONENT 1
1	-1.93
2	0.77
3	0.65
4	1.21
5	-5.47
6	2.62
7	1.98
8	0.12
9	0.97
10	0.60
11	-0.82
12	0.77
13	0.72
14	-2.19

Table 9.4: Scores on Component 1 by site for the Cowal RSFs.

They are disgarded for the Cluster Analysis. Eigenvectors on Component 1 ranged between 0.42 and 0.47, indicating that it is an

Figure 9.5: (a) Dendrogram of scores on Component 1 (output from PCA) for the Cowal field area rock weathering data.

(b) Dendrogram output from the CLUSTAN package using the Ward's method.

average variable.

The dendrogram for the clustered Component 1 scores is given in Figure 9.5a and may be compared with the output from the CLUSTAN programme shown in Figure 9.5b. Six groups emerged from Cluster Analysis performed on Component 1 scores (Table 9.5) whilst at the cut-off point of the CLUSTAN analysis only four groups emerged. In the dendrogram output from scores on Component 1, sites 8 and 11 are classified as separate groups while the CLUSTAN method fused them into groups B and C respectively. Discriminant analysis on the a priori

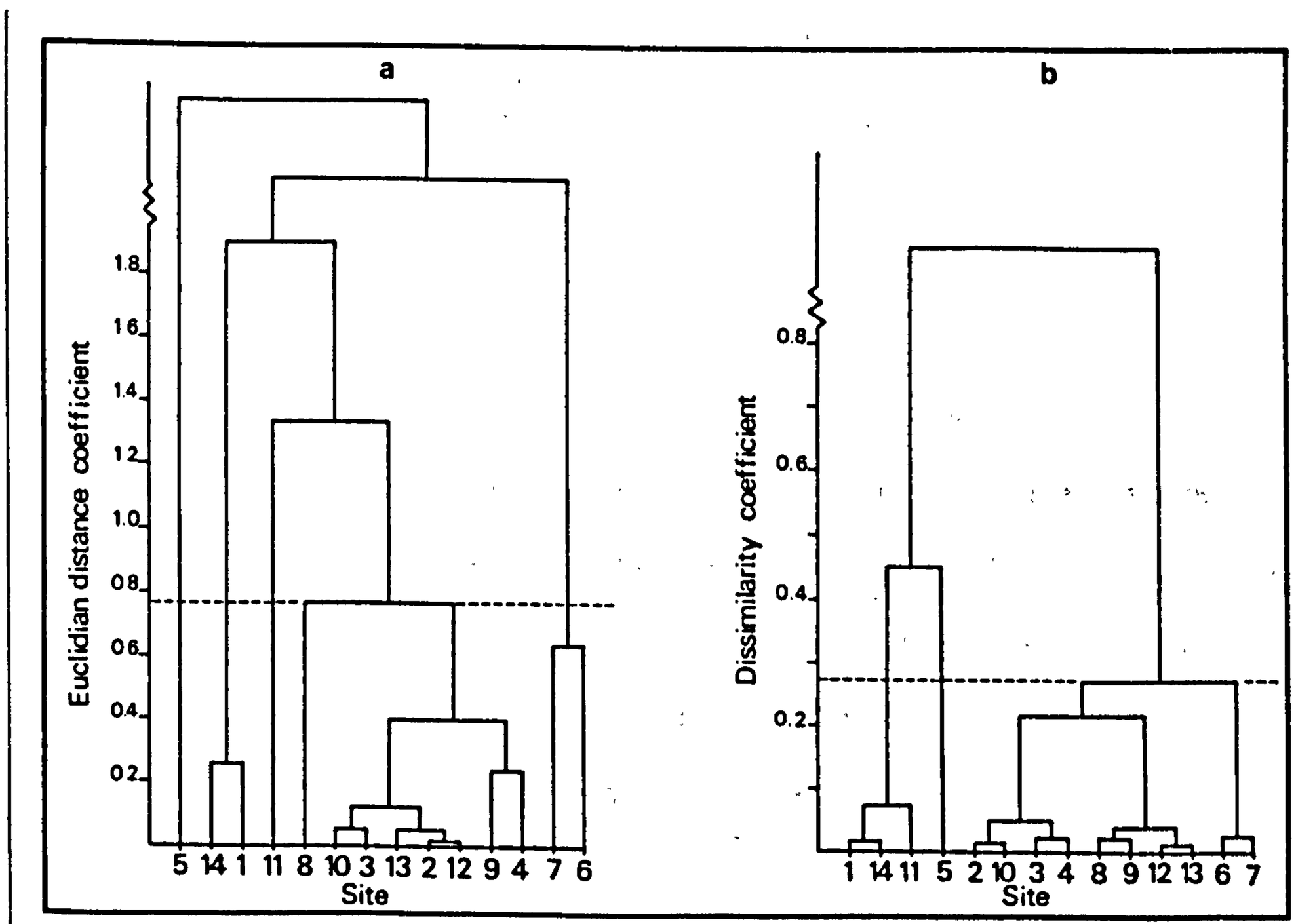

CLUSTERS FROM COMPONENT SCORES						
GROUP	A	B	C	D	E	F
SITES	5	1,14	11	8	2,3,4,9, 10,12,13	6,7

CLUSTERS OUTPUT FROM CLUSTAN				
GROUP	A	B	C	D
SITES	5	1,11,14	2,3,4,9, 8,10,12,13	6,7

Table 9.5: A priori groupings of sites.

groupings revealed that only the CLUSTAN grouping of sites was significant at the 95% confidence level and this fourfold classification of sites is therefore accepted.

Glen Clova

This field area proved to be the most difficult in which to reach inferences concerning RSF chronology. However, even within this area there are marked contrasts in the degree of weathering and vegetation cover of RSFs. For instance, the Corrie of Clova, Glen Effock, Capel Burn and Cairn Inks RSFs are completely vegetation-covered. The rear-scarp of the Corrie of Clova example is overlain by partly-vegetated screes. Boulders found entrapped upslope of the obsequent-scarps at Corrie of Clova and at Cairn Broadlands possess rounded edges and are covered by lichen. In contrast to these sites, the Corrie Brandy RSF features little vegetation on its failure-scarp, the edges of its rear-scarp are sharp and fresh rock exposed by recent rockfall is evident on the slope face (Plate 6.1).

The Corrie of Clova RSF lies within the limits of the Corrie of Clova glacier defined by Sissons (1972). An 8-m-high and 250-m-long ridge composed of large schist boulders lies at the break of slope between the corrie floor and backwall (Plate 7.5). The ridge feature is problematic. It cannot be interpreted as being formed solely by dislocation of blocks from the RSF, since the ridge extends beyond the area of failed slope that could have supplied material to it. The simplest interpretation of the feature is that it is a protalus rampart. If so, the only time when it could have formed would have been during the Lateglacial since these features are now fossil in Scotland (Sissons 1976b, Ballantyne 1981). Unless deglaciation of the Corrie of Clova site occurred comparatively early, perhaps because of its S exposure, the corrie was not glaciated during the Loch Lomond Stadial. It is suggested that the RSF post-dates the formation of the protalus rampart since intensive ice-wedging necessary to form the rampart would have destroyed the obsequent-scarps.

Kintail-Affric area

Most of the RSFs in this area are not amenable to the relative weathering techniques outlined earlier since they did not create boulder debris. Certain of the RSFs however lie within the reconstructed limits of the Loch Lomond Advance. Some slope failures, such as An Sornach, Ben Attow, An Riabhachan and Carn na Con Dhu, possess obsequent-scarps. These essentially delicate features show no signs of ice wedging nor ice-smoothing and, as suggested earlier, would probably not have survived overriding by former glaciers. Similarly, the levees and transverse ridges on Mullach Froach-choire would have been swept away if they were overriden by a glacier.

Morphostratigraphic techniques were used extensively in this field area. For brevity these data are summarised in Table 9.6 though other incidental evidence is discussed below.

At the Mam Sodhail site, relict periglacial landforms have built up behind the obsequent-scarps (Plate 9.3) and cover portions of some obsequent-scarps. This indicates that the obsequent-scarps must either be contemporaneous with formation of the boulder lobes and debris sheets or pre-date them. It was noted in Chapter 9 that the obsequent-scarps are poorly preserved at Mam Sodhail being composed of frost riven blocks. The size of the blocks that have been prised apart is suggestive of macrogelifiaction, a process which is thought to have been restricted to the Lateglacial (Ballantyne 1981, Chattopadhyay 1984). At An Riabhachan, fossilised debris sheets and lobes have buried the obsequent-scarps in many places. Elsewhere the periglacial debris has been dammed behind the scarps, indicating that scarp development was at least contemporaneous with debris sheet/lobe movement.

Holmes and Jarvis (in press) noted that the Ben Attow obsequent-scarp walls are vegetation-covered while relict screes lie upslope of them. Active scree chutes have been dammed by the obsequent-scarps (Plate 8.4) and undisturbed active solifluction lobes have abutted against the uppermost arcuate obsequent-scarp found towards the E of the Ben Attow RSF (Fig. 8.3).

A 1.6-m-deep section was dug beneath the toe of the Mullach

Site	accumulation of F and A periglacial landforms behind RSF features	accumulation of A periglacial landforms behind RSF features	disruption of F periglacial landforms by RSF	disruption of F and A periglacial landforms by RSF	RSF features covered by A and F periglacial landforms	features covered by A periglacial landforms only.
* Sgurr na Lapaich			X			
* Sgurr na Lapaich Ridge			X			X
Mam Sodhail	X					
* Ben Attow		X				
* Mullach Fraoch-choire			X			X
* An Sornach			X			
* Mam Sodhail ridge			X			
* Carn na Con Dhu		X				X
An Riabhachan	X		X			

Table 9.6: Morphostratigraphic data for the Kintail-Affric field area. An asterisk indicates that the RSF lies within the Loch Lomond Advance limits. A = active landforms, F = fossil landforms.

Fraoch-choire RSF to attempt to establish if peat lay beneath it. Only till was uncovered beneath the RSF debris. This is in marked contrast to 1.5-m-deep exposures of peat that occur elsewhere on the corrie floor. It is tentatively suggested that the RSF occurred before formation of peat at the site.

9.5 Interpretation

For economy of discussion the RSFs are tentatively classified into four age groups in Table 9.7. The classification is based upon the morphostratigraphic relationships discussed in Section 9.3, the rock weathering data and the constraints imposed by the Loch Lomond Advance, and earlier glacial limits, in the field areas. "Lateglacial" examples possess RSF features (e.g. rear-scarps or obsequent-scarps) overlapped by both fossil and active periglacial landforms. "Early-Flandrian" (sensu lato) RSFs disrupt fossil periglacial landforms on their surfaces but are overlapped by active landforms. They may also have active periglacial landforms banked up behind RSF features and are usually extensively covered in vegetation. "Late-Flandrian" (sensu lato) RSFs disrupt both fossil and active periglacial landforms, and also possess areas of fresh rock with angular boulder edges. Vegetation cover is not as extensive in comparison with the "early-Flandrian" RSFs. Only one RSF is thought to be "recent", due to its fresh rock boulder surfaces and low vegetation cover.

A major problem in interpreting the relative age data is the assignation of dates to the groupings. Such interpretation must be

TENTATIVE AGE GROUPINGS

LATEGLACIAL (> 10,000 yrs. old)	EARLY-FLANDRIAN (5,000 - 10,000 yrs. old)	LATE-FLANDRIAN (1,000 - 5,000 yrs. old)	RECENT (< 1,000 yrs. old)
A' Chailleach	Mullach Choire a' Chuir (10,12,13)	Corrie Brandy	Glen Kinglas
Sgurr Breac	Hell's Glen S Wedge	Hell's Glen topple	
Garbh Choire Mór	Mullach Fraoch-choire	Ben Donich SE	
An Riabhachan	Ben Attow	Sgurr na Lapaich ridge	
Mam Sodhail	Carn na Con Dhu	Mam Sodhail ridge	
An Riabhachan	Sgurr na Lapaich	Mullach Choire a' Chuir (11)	
	An Sornach		
	Cairn Inks		
	Cairn Broadlands		
	Ben Donich N topple		
	Corrie of Clova		
	Glen Effock		
	Beinn an t' Seilich		
	Sgurr na Lapaich Ridge		
	Hell's Glen N wedge		
	Glen Effock		
	The Steeple		
	Carn na Con Dhu		
	Capel Burn		

Table 9.7: Tentative age groupings of the study sites.

very tentative and the dates allotted to the age groupings are intended to provide ranges of possible age. Significant groupings in the rock weathering data in the Cowal have at least demonstrated that those RSFs have not occurred continuously through time. Allied to this, sufficient variance has been encountered in the morphostratigraphic and rock weathering characteristics of all the RSFs to infer that they have occurred sporadically from the Lateglacial through to the late-Flandrian.

Five RSFs, all of which lie outside the limits of the Loch Lomond Advance, are inferred to be Lateglacial in age. It may be suggested that the degree of coverage by periglacial debris at the Mam Sodhail, An Riabhachan, Sgurr Breac and A' Chailleach slope failures is sufficently small to indicate burial shortly before the termination of the periglacial conditions within which they were active. The depth and extent of periglacial deposits in areas close to these sites is strongly suggestive that had a protracted phase of periglaciation intervened between RSF and the overlapping of the scarps by periglacial landforms then the scarps would have been completely buried.

Despite the 5,000 year period imposed upon the "early Flandrian" RSFs by the classification, the majority of slope failures probably occurred relatively soon after Loch Lomond Advance deglaciation. In the Cowal field area for instance, a group of RSFs are thought to have occurred soon after deglaciation, as a number of sites display similar rock weathering characteristics to a fossil rock glacier. Most of the Glen Clova RSFs occurred at that time.

A second group (C) of slope failures in the Cowal are thought to have occurred in the "late Flandrian". The absolute ages of the group are unknown but are tentatively assumed to be between 5,000 and 1,000 years old. The Corrie Brandy, Mam Sodhail ridge and Sgurr na Lapaich ridge RSFs are also interpreted to have occurred within this period, exhibiting similar degrees of rock weathering and vegetation cover. The examples in the Cowal area retain the 'surface sheen' imparted by fresh muscovite-mica. In contrast the early-Flandrian RSFs in the Cowal have 'dull' boulder surfaces.

The relative dating evidence is suggestive that the RSFs which have moved only slightly (e.g. Ben Attow) are now stable. The morphostratigraphic evidence demonstrates that continuous gravitational deformation has not occurred within the massive RSFs, such as An Riabhachan and Carn na con Dhu, otherwise the periglacial landforms would have been disturbed. It is suggested that the morphostratigraphical record of slope deformation, though not as accurate as that given by detailed surveying and monitoring of the slope, is still valuable because of the length of record.

Previous authors have often cited the need for a "post-glacial" perspective in RSF research (cf. Whalley et al. 1983, Gardner 1980). Where a sequence of advances/readvances has occurred such as in the Highlands the "post-glacial" is diachronous and may vary in length from c. 10,000 to c. 15,000 years or greater. Although RSFs may post-date the deglaciation of their local area, chronology is likely to be complex if the glacial control referred to earlier had acted.

The chronology of RSF in the Highlands is more complex than that implied by the hypothetical model of high activity during deglaciation with decreasing activity through the Flandrian (Sissons 1967, 1976a). Although slope failures are thought to have been more frequent in the early Flandrian, rather than a gradual reduction in the frequency of RSFs, there appears to have been phases of resumed high activity (e.g. Group C in the Cowal). It is not possible to infer whether these were climatically-induced.

9.6 Conclusion

Rock weathering and morphostratigraphic techniques have been used to estimate the ages of twenty-eight RSFs in the four field areas. The rock weathering data have been analysed using Principle Components Analysis, two forms of Cluster Analysis and Discriminant Analysis following the strategy outlined by Dowdeswell (1982). A set of morphostratigraphic criteria involving Ballantyne's (1981) classification of active and fossil periglacial landforms and the positional relationships between RSF features and these periglacial landforms has been detailed.

A tentative classification of the RSFs according to their approximate age is given. The classification distinguishes between RSFs that are thought to be: older than 10,000 years, between 10,000 and 5,000 years old, 5,000 and 1,000 years old and less than 1,000 years old. Rock weathering data are most complete in the Cowal field area where one slope failure is lichenometrically dated to c. 250-300 years. The RSF at Garbh Choire Mór in the Fannichs, in contrast, is thought to have occurred during the Lateglacial (but after before ? p196

? Achnashean

the Loch Lomond Advance. The morphostratigraphic relationships of four other possible Lateglacial age RSFs have been examined.

Most of the RSFs are thought to have occurred in the early-Flandrian when it appears that RSFs occurred more frequently than in any subsequent period. Five RSFs however are thought to have occurred between 1,000 and 5,000 years ago, only one of these (Corrie Brandy) lies outside the Loch Lomond Advance limits. N.S.

This investigation of RSF chronology raises two questions: why should a phase of high RSF frequency have occurred in the early-Flandrian? and why did this control(s) fail to result in RSF at those sites which occurred during the late-Flandrian? Both these questions are addressed in the following chapter.

10: SYNTHESIS

10.1 Introduction

This investigation of rock-slope failure within the Highlands has pursued several related, research themes. Analysis has also been undertaken at a number of geographic scales: from attempted explanation of the distribution of the RSF population to engineering-geology investigations of individual slope failures. One aim of this Chapter is to combine these separate research elements into a model of rock-slope failure for the Scottish Highlands. The model incorporates the possible effects upon rock-slope stability of environmental changes that accompanied deglaciation following the Loch Lomond Advance in the Scottish Highlands. Reports from other glaciated areas of the world are summarised in Section 10.3 for comparison.

The conclusions reached by analyses of the study slopes are extrapolated to the population in Section 10.4, where a possible mechanical explanation for the recorded variability in the response of RSFs to the environmental changes at the close of the Loch Lomond Stadial is given. The Chapter also explores the magnitude-frequency relationships of RSFs in Section 10.5, where an attempt is made to indicate the relative significance of RSF in the denudation of the Highland landscape. Comparisons are again made with studies from other areas of the world.

10.2 Environmental change and rock-slope failure

A spatial correlation between former glaciers and RSFs was inferred in Chapter 4. This relationship extends beyond the mere

occurrence of slope failures in formerly glaciated valleys, as it has been demonstrated that many RSFs occur in close proximity to the upper limits of the Loch Lomond Advance. Although data are most complete for the Advance, it has been established that a correlation also exists between RSFs and the upper limits of some glaciers that predated it. Since, data are most complete for the Advance the following discussion largely concerns rock-slope failures that were controlled by it. An overview of the mechanics of the case studies is provided and the generality of the inferences reached is indicated.

It was noted in discussion of the previous literature that, although glacial oversteepening has often been cited as a cause of RSF in Scotland and elsewhere, the mechanics have not been tested. The glacial oversteepening mechanism is doubted in this study for both rock mechanical and geomorphological reasons. The two forms of evidence are that:

1. Glacial oversteepening cannot account on its own for the occurrence of RSFs close to glacier limits since most of the case study translational RSFs possess failure-planes that are inclined below the lowermost threshold for self-weight sliding: the residual friction angle. The reductions in the effective friction angles required to have caused some translational RSFs was large, in one instance (Hell's Glen N wedge) the $\emptyset'$ would have been less than 14°. As peak friction angles exceed 40° for most of the Highland metamorphics, if glacial oversteepening was the cause of rock-slopes failure then the potential failure-surfaces would need to be inclined at greater than 40° and the slopes inclined greater than the potential failure-planes. Most

slopes in the Highland metamorphics do not exceed 40° (Watters 1972).

The toppling failures discussed in Chapter 7 mostly possess combinations of friction angles, slope angles and discontinuity set orientations that do not satisfy the Goodman and Bray (1976) self-weight toppling criterion. Although glacial oversteepening by a few degrees would narrow the difference between a stable slope and a potential topple by lowering the slope stability, the reductions in the effective friction angles required to initiate toppling at the sites discussed in Chapter 8 are of the order of 10°.

2. Reservations have been expressed by other Quaternary scientists over the efficacy of glacial erosion during the Loch Lomond Advance. Sissons (1981) inferred that part of a protalus rampart in the Cairngorm Mountains had been overridden by an Advance glacier without significant disruption. Work by Hodgson (1982) revealed that the Loch Lomond Advance glaciers, at least in the NW Highlands, succeeded only in redistributing and moulding drift material which already lay within the glens. The implication is that the Advance glaciers achieved little bedrock erosion, though corrie headwalls (cf. Dale 1981) and spurs may be exceptions.

The amount of erosion achieved by the Advance glaciers is critical to the understanding of the mechanics of RSF. Since the volume of material that would need to be removed to cause even a 5° steepening of a valley side would be huge, doubt must now be expressed over glacial oversteepening as a trigger of RSFs, at least following the Loch Lomond Advance. Former glaciers may have created slopes but did not, generally, oversteepen them so as to trigger RSFs.

The climatic change from the Loch Lomond Stadial to the Flandrian triggered a plethora of environmental disturbances. Any mechanical model of RSF must recognise the nature and possible effects of those changes and some, thought to have contributed to rock-slope instability, are discussed below.

It has been noted that the climatic amelioration at the onset of the Flandrian occurred with great rapidity (cf. Bishop and Coope 1977). Two factors would have combined to produce high water-tables within slopes at that time. First, the release of water from, perhaps rapidly melting, glaciers. The thawing of permafrost and snow patches would also have released large volumes of water. Secondly, to excacerbate these effects, the vegetation cover was likely to have been sparse in the early Flandrian and would not have intercepted precipitation as effectively as the present day. Evapotranspiration would also have been reduced. If permafrost still lay beneath slope surfaces it is possible that permeability could have been decreased and overland flow could have occurred. These effects would have been aggravated if tension-cracks had opened within slopes.

Drift limits have often been used by Quaternary scientists to map the limits of former glaciers, particularly the Loch Lomond Advance in Scotland (e.g. Sissons 1972, 1976a). The extent of drift may be of importance in the cleft-water pressure mechanism (Tallis and Johnson 1980). Drift, because of its clay content, may reduce the permeability of the slope and thus impede drainage of a high water-table from it. This may assist explanation of why RSFs occur close to the upper limits of the Loch Lomond Advance. Unfortunately, it is not

known how long it took for the mountain water-tables to return to their present levels.

It is possible that the rapid uplift that followed deglaciation of the last ice sheet and continued after the Loch Lomond Advance created tensional stresses within rock-slopes. Price (1966) has shown that uplift will give rise to tensional forces in the upper crust due to a stretching effect. Although the tensional forces produced by isostatic uplift are likely to be smaller (being related to the amount of vertical displacement that occurred) than those created during orogenic uplift, they may have assisted the opening of tension-cracks within slopes. Wyrwoll (1977) hypothesised that rebound accompanying isostatic recovery may have opened stress-relief joints during the post-glacial.

Rapp (1960) suggested that RSFs would have been most favoured during deglaciation when earthquakes, in addition to high ground-water tables, may have triggered RSFs. The effects of former earthquakes in the Highlands, such as those hypothesised by Sissons and Cornish (1982), on rock-slope stability are unknown. If large earthquakes did occur in Scotland they should theoretically have been most frequent in the early Flandrian when the rates of isostatic uplift were at their greatest. It is perhaps surprising however that few RSFs are found outside the Loch Lomond Advance limits since these areas, it may be hypothesised, should have experienced earthquakes following the deglaciation of the last ice sheet and yet have not been subsequently overridden by glaciers. It is therefore reasoned that earthquakes could have contributed to RSFs in the Highlands rather than acted as a direct cause.

Earthquakes mainly occur in the W Highlands today with the Knoydart-Kintail area suffering the highest seismicity (Burton and Neilson 1980). It is planned to accurately survey selected RSFs within this large area and monitor any minute displacements which may occur in response to the higher-magnitude seismic events.

Mechanical investigations have shown that ground-water tables would have needed to be close to the ground surface to cause rock-slope failure. If the cleft-water pressure hypothesis is accepted, the correlation between RSFs and former glacier limits may appear puzzling since it could be argued that dangerous cleft-water pressures may accumulate anywhere within a slope. The possible weakening mechanism postulated in Chapter 3, involving the repeated seasonal changes in sustained high water-tables, is thought to have lowered the stability of those slopes that lay immediately above the Loch Lomond Advance limits. Since, later accumulation of water during deglaciation would have proved most effective on those components of a slope least able to resist increased shear forces, failure would have been preferred on those weakened joints which lay close to the Advance limit.

The factors that determine the limits of a RSF have received little attention. It may be asked, why a portion of a slope failed in preference to the whole slope. There are two factors of importance here: (i) shear strengths of rock joints vary and (ii) shear forces vary between joints. Chapter 2 concentrated upon certain factors that cause variability in joint shear strength, such as rock type, degree of shear displacement and joint roughness. Joint roughness and

the degree of openness of joints will effect the shear forces mobilised along them. Open joints, for instance, will transmit cleft-water more freely than 'tighter' joints. Asperities or obstructions along joints may also inhibit drainage causing localised build up of cleft-water pressures. The spacing of joints may also be important (Selby 1982).

10.3 Evidence for the delayed-response of RSFs to deglaciation

Few in situ RSFs show any signs of having being disturbed by glaciers. It was noted that deglaciation of the Loch Lomond Advance could have occurred initially under a cold climate and that the occurrence of morainic ridges inside the limits is suggestive that retreat was initially active. After this period of active retreat the Advance glaciers are thought to have stagnated and decayed in situ. This is evidenced by delicate geomorphological structures such as fluted moraines, occasionally found on the crests of hummocky moraine, that would have been destroyed had retreat been active (Hodgson 1982).

If slopes had failed in the Highlands as soon as lowering of Advance glacier surfaces began, their debris would probably have been disturbed as it would have fallen onto decaying (perhaps initially active) glacier surfaces. Also, many of the RSFs reach inside the Advance limits, indicating that the response of slopes was delayed. Some slopes failed well after deglaciation, such as the Glen Kinglas RSF.

There is evidence from other areas of the world for delayed-

response to deglaciation and these data necessitate the movement away from a purely climatic trigger and an explanation unique to the Loch Lomond Advance, towards a model that is both cognizant of the time-dependent mechanical changes within a slope and is applicable to other areas of the world.

Tabor (1971) reported the delayed-response of rock-slope instability to the retreat of the Hoh Glacier, Washingon. Downwasting of this glacier left a rock-slope unsupported and slope failure is known to have occurred sometime after 1952. A slope trench occurs downslope of a 'fresh landslide scarp' (Tabor 1971: 1817). Tension-cracks on the slope are visible on aerial photographs taken in 1939, when the Hoh glacier terminus lay just upvalley of the site. Tabor infers that glacially oversteepened valley walls began to collapse as the Hoh Glacier retreated and that displacements occurred initially by creep, which formed tension-cracks and then by 'landsliding' which formed the slope trenches. Another older slope trench is located downvalley of the site. Glacial oversteepening was not proven by Tabor and he did not consider the possible consequences of high cleft-water pressures and progressive-failure.

At Mount Innstihaus, Iceland, a rock avalanche occurred in mid-January 1967 some 7-8 years after shepherds had noted a deep and narrow crack (probably a tension-crack) close to the summit of the mountain (Kjartansson 1967). The crack widened year by year until in 1966 it was c. 30-cm-wide. Rock-slope failure occurred after a few days of heavy rain and snowmelt, the failed debris falling onto the snout of the Steinholtsjokull, which lay close by but well below the scar.

Wyrwoll (1977) stated that lichen cover on RSFs in the Labrador-Ungava area in Canada is variable, indicating not all slope failures occurred immediately after deglaciation. Whalley et al. (1983) considered that most of the RSFs they examined in Iceland delayed their response to deglaciation, inferring that time-dependent mechanical processes (propogation of cracks through the rock-masses) was responsible for the delay. They found that the smallest RSFs were generally the youngest, the largest oldest and the medium-sized RSFs most numerous in the period 3,000-5,000 years B.P. According to Whalley et al. (1983) climatic changes through the postglacial cannot account for the temporal distribution of RSFs. The Scottish data are too limited and relatively imprecise to enable testing for a correlation between the incidence of RSFs and 'wet' periods in the Flandrian.

10.4 A rock-slope failure model

Two general problems arise from the Scottish RSF data: (i) what caused the delay that prevented failure of most RSFs onto active glaciers? and (ii) why did the duration of this inferred delay vary? Related to the last question is: why did a few slopes remain stable, despite the action of the destabilising factors recognised above, only to fail sometime later?

A possible answer to the first question may be the effects of progressive-failure. Progressive-failure may be conceptualised, after Terzaghi (1950), as a gradually-falling line depicting the factor-of-safety of a slope over time. Muller (1968) also stated that slope

stability was time-dependent. Decreases in the factors-of-safety, due to progressive-failure reducing the cohesion of potential failure-surfaces by shearing through intact rock bridges and asperities, would have caused delayed responses to the removal of glacial support (rather the removal of the physical 'barrier' to RSF) and the hydrological changes which accompanied climatic amelioration. A probabilistic model of progressive-failure may be used to explain the variations in the response time to deglaciation.

The initial stability of a slope (its factor-of-safety) once deglaciation begins, and the nature of increases and decreases of cleft-water pressures over time, are likely to affect the long-term stability of a rock-slope. Figure 10.1 illustrates the progressive-failure of three hypothetical rock-slopes. The factors-of-safety of two curves (B and C) attain unity and these slopes are presumed to have failed completely.

The Ben Attow RSF may be an analoque for slope A. It was inferred in Chapter 8 that this slope has toppled (perhaps slid) sufficiently to mobilise peak shear strength along its toppling layers, the initial movement being a response to high cleft-water pressures associated with deglaciation following the Loch Lomond Advance. Some decrease in the strength of the slope may have been caused by progressive-failure but such changes are thought to have been slight because the normal stresses acting along the steeply inclined layers and, therefore, the ability to shear through asperities is low. It is thought that most of the intact topples accord with this model.

Figure 10.1: Hypothetical decrease in shear strength with time for three rock-slopes.

Slope C in contrast featured a rapid decrease in its factor-of-safety over time culminating in its eventual failure soon after deglaciation. The Mullach Fraoch-choire example may have possessed a stability history similar to this hypothetical example. The factor-of-safety of this hypothetical slope declined markedly towards the end of the Advance perhaps due to the proximity of the upper surface of the glacier. On deglaciation the factor-of-safety of the slope was already low, little further progressive-failure being required to bring the factor-of-safety of the slope close to unity, making the slope highly susceptible to increases in cleft-water pressures.

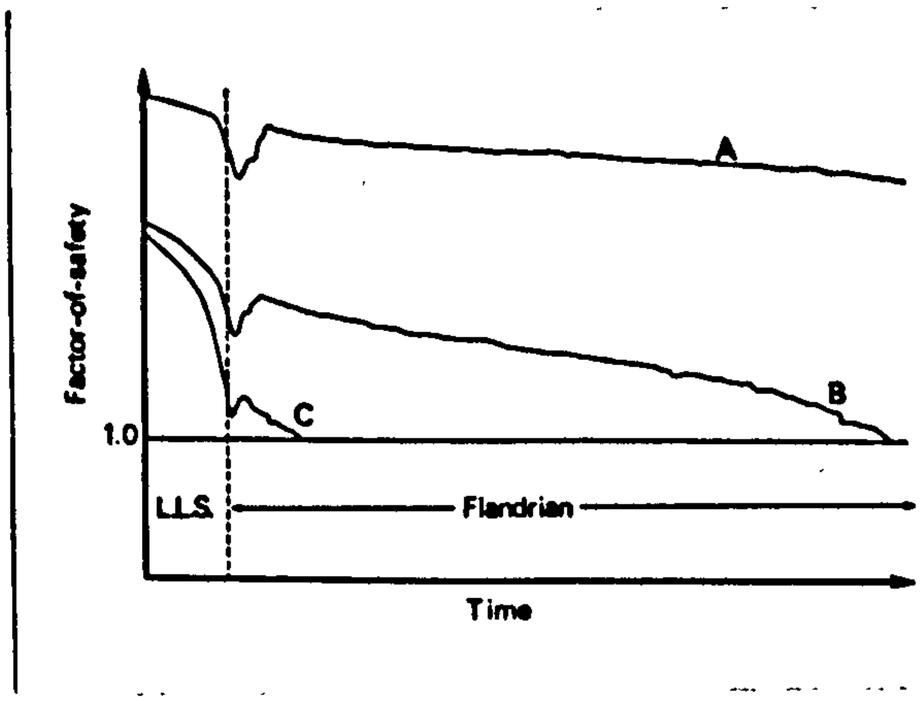

Slope B failed much later than C. It is thought that the Glen Kinglas RSF may accord with this model. Here the portion of the rock-slope that was susceptible to failure lay well inside the Advance limit, being overriden fairly early during the Advance and not suffering the localised weakening experienced by C. Progressive-failure, aided by ephemeral increases in cleft-water pressures, is thought to have been the main weakening mechanism. Failure was probably triggered by high cleft-water pressures within the slope.

The rate of progressive-failure is therefore thought to vary from one slope to another and may also increase or decrease over time due to extrinsic and intrinsic factors. The initial factors-of-safety will also vary for reasons cited earlier. Given these variations it is possible to conceptualise the differences in the delayed response

times to the environmental changes. The model is not predictive, merely indicating that slopes located close to the Advance limits are likely to be weakest, having a higher probability with time of failing. The difficulty becomes that of recognising which slopes are approaching failure and at what rate the probability of failure increases.

10.5 Magnitude/frequency relationships

There is evidence that the majority of slope failures investigated within the field areas probably occurred comparatively soon after deglaciation. This suggests that their factors-of-safety were close to unity and that the cleft-water pressures associated with deglaciation were sufficient to have caused rock-slope failure. During deglaciation high-magnitude RSFs could have occurred with relatively high frequency (cf. Rapp 1960, Gardner 1980).

Figure 10.2 shows the frequency of the 364 *in situ* RSFs occurring in various size (area) classes. The modal size group (less than 0.1 km^2) accounts for 42% of the total. The histogram is negatively skewed with the smallest events being most frequent, the largest most infrequent. These data concur with Wolman and Miller's (1960) magnitude-frequency concept originally developed for fluvial systems. It has been hypothesised that this concept may also be applicable to slope processes (Brunsden and Thornes 1979, Gardner 1980). According to Whalley *et al.* (1983) the Icelandic rock-slope failures do not exhibit this distribution, though their data may be influenced by the restrictions imposed upon the lower size limits of the RSFs and the coarse classification of RSF size.

Figure 10.2: Frequency/size relationship for the Scottish Highland <u>in situ</u> RSFs.

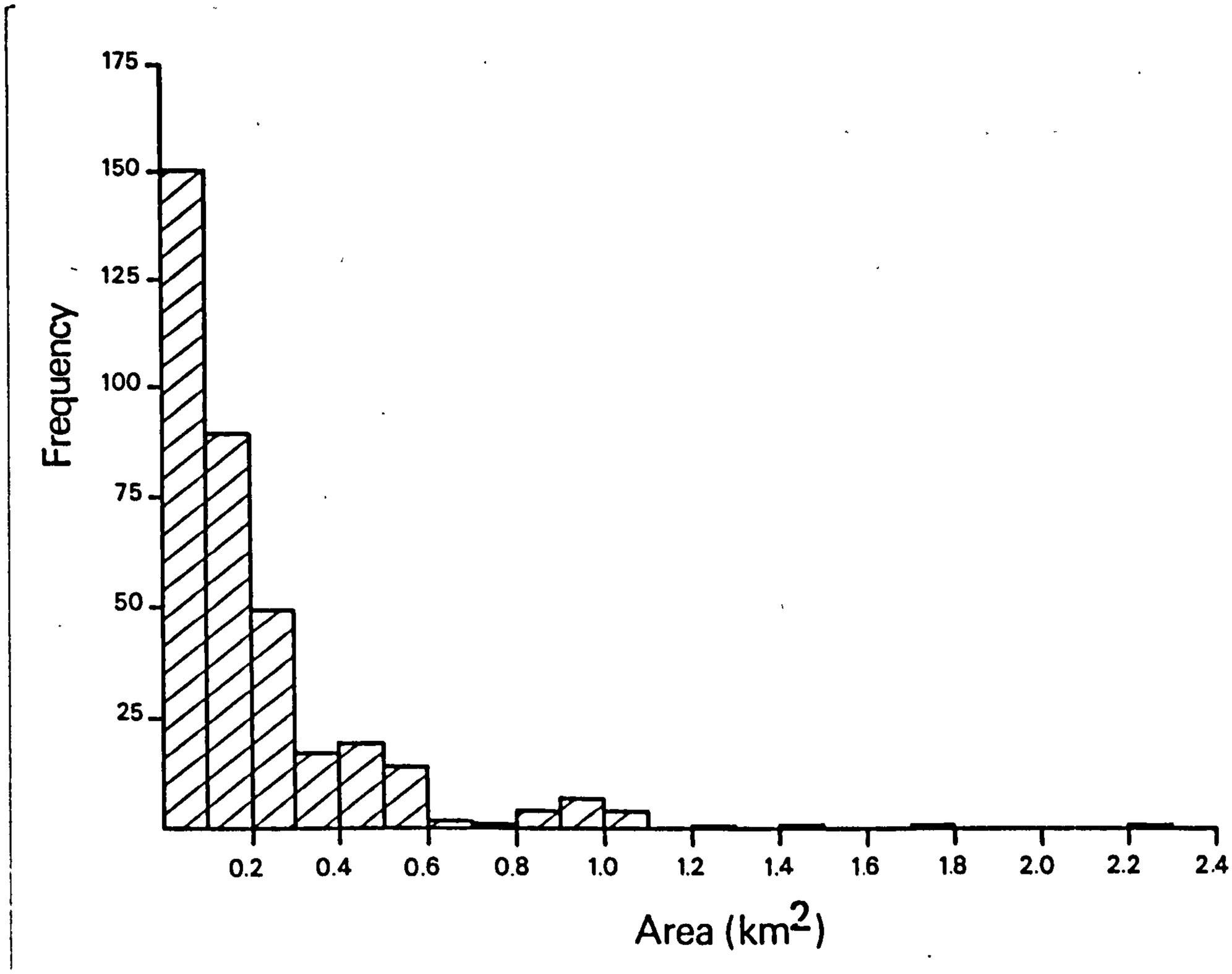

If it is assumed that RSFs occurred evenly over the last 12,500 years (the generally accepted date for final ice-sheet deglaciation of the Highlands), then, given 364 in situ RSFs, one slope-failure should have occurred on average every 34 years. Including debris-less RSFs the average frequency over the same period would equal 29 years. This contrasts with Sissons and Cornish's (1982) statement that no large RSF has occurred in the last 200 years.

For further comparison, the average frequency for each size group may be calculated giving frequencies of approximately one every eighty years for RSFs less than 0.1 km^2 (c. 10^5 m^3) to one in every 12,500 years for RSFs of between 2.2 and 2.3 km^2. Gardner (1980) inferred that rock-slope failures of between 10^2 and 10^5 cubic metres fail on average every 1,000 years. Rock-slope failures of 10^5 to 10^7 cubic metres occurred at an average rate of one every 10,000 years.

However, he examined RSFs which had failed completely and it is not known whether intact RSFs exist. Gretener (1967) emphasised the possible importance of massive RSFs in the Swiss Alps even allowing for their low average frequency of one every 3,000 years.

Clearly, in view of the relative age data from the field areas, RSFs in the Highlands have not occurred with equal frequency through time: rather, the early Flandrian witnessed a comparatively higher frequency of RSF. The amount of erosion achieved by the inferred phase of high RSF incidence during/immediately after deglaciation is of importance and this topic will be considered below.

The volume of material displaced by RSF may be computed from the topographic survey data, providing some estimation of the amount of erosion achieved by the event. Caine (1976) has proposed that geomorphic work should be expressed in power units, but his technique is applicable only if the duration over which the erosion occurred is known. Two techniques are therefore used in this study to compare the geomorphic work achieved by the different forms of RSF. First, to calculate the volume displaced by RSF and multiply this by the amount of vertical and horizontal displacement of the RSF centroid. Figures are given in tonne/metres (volume x 2.65 x displacement). This measure is particularly useful where slopes have not failed completely, having suffered comparatively small displacements. Secondly, the mean value of cliff retreat can be calculated using:

$$\text{mean cliff retreat} = \frac{\text{volume of failed material}}{\text{failed slope area}} \qquad 10.1$$

using: $A_s = w \cdot (H \text{ Cosec}\theta)$

where: A_s = scar area; H = height of scar; θ = angle of former slope surface; w = mean scar width.

Table 10.1 shows the cliff retreat data for all the RSFs studied in the field areas that have failed completely. For comparison mean rates of around 1.0 mm year^{-1} are typical for cliff retreat in high latitude countries such as Spitzbergen and N Sweden (e.g. Poser 1954, Rapp 1960, Gray 1971a,b, Caine 1974) though Kortarba (1983) has computed a mean rate of cliff retreat of up to 3.0 mm year^{-1} in the Tatry Mountains. Even extrapolating this highest rate, 30 metres of cliff retreat is equivalent to 10,000 years of erosion: at the lower rate of 1 mm year $^{-1}$, 30,000 years. Some of the case study rock-slope failures produced localised total cliff retreats of 30 metres (Table 10.1) and therefore instantaneously produced many thousands of years of 'normal' cliff retreat.

The only work done on the relative importance of high magnitude RSF is by Rapp (1960), Whalley (1974), Gardner (1980) and Whalley et al. (1983). Gordon et al. (1978) thought that a RSF in Antarctica was equivalent to 90 years of normal erosion. Rapp (1960) noted that rock-slope failure near Karkevegge, perhaps over a duration of decades or centuries caused cliff retreat of between 10 and 20 m. This, he observed, was greater than ten times the amount of cliff retreat for the whole postglacial period of c. 10,000 years duration. Whalley (1974) considered that high magnitude RSFs could exceed the denudation of smaller but more numerous slope failures.

The importance of RSF is restricted in extent and it is not surprising that localised rates of cliff retreat can be very high.

The measure of displacement against volume moved will allow comparison between those RSFs that transport different volumes of material over variable distances. These data are shown in Table 10.2. It will be noted that although the complete RSFs have achieved high rates of erosion, the most important events are the massive RSFs such as Ben Attow which moved exceedingly large volumes of rock over comparatively small distances.

Unfortunately few comparable data to those given in Table 10.2 are known to the author. The results may be compared with those

Rock-slope failure	Volume (m^3)	Slope area (m^2)	Cliff retreat (m)
Glen Kinglas	89,600	10,500	8.5
Cairn Inks	6,800	675	10.1
Hell's Glen S wedge	8,200	930	8.8
The Steeple	112,500	3,250	34.6
Ben Donich N	288,000	9,600	30.0
Mullach Fraoch-choire	730,000	19,500	37.4
Sgurr na Lapaich ridge	5,600	1,050	5.3
Hell's Glen topple	122,000	15,000	8.1
Garbh Choire Mór	212,000	11,200	19.0

Table 10.1: Estimated volumes, failed slope areas and mean cliff retreat of selected field examples.

collected by Rapp (1960). He found that approximately 20,000 tonne/metres had been transported by rockfalls over a period of 8 years in the glacial trough near Karkevagge. The total transported by all measured processes (including, for example, surface wash and

RSF	Volume (m^3)	Mass displacement vertical (tonne-metres x 10^6)	horizontal
A' Chailleach	5,400,000	280.0	342.0
Garbh Choire Mór	212,500	60.4	123.9
Sgurr Breac	36,160,000	3,353.0	2,874.7
Cairn Broadlands	2,500,000	99.4	132.5
Corrie Brandy	280,000	1.9	2.2
Capel Burn	1,900,000	50.4	75.5
Corrie of Clova	480,000	63.6	50.9
Cairn Inks	7,800	0.03	0.05
Glen Effock	102,000	0.8	0.5
An Riabhachan	6,125,000?	32.5?	113.6?
Mam Sodhail	4,823,000	38.3	102.3
An Sornach	18,000,000	1908.0	945.0
Sgurr na Lapaich	7,200,000	66.8	66.8
Sgurr na Lapaich R.	5,600	0.7	0.9
Mullach Fraoch-choire	710,000	395.0	827.9
Carn na Con Dhu	61,200,000	4,865.0	4,865.0
Ben Attow	112,000,000	26,712.0	29,680.0
Mam Sodhail ridge	1,240,000	32.9	32.9
Carn na Con Dhu summit	2,250,000	26.8	11.9
Ben Donich SE	103,000	0.3	3.6
Hell's Glen topple	122,000	9.7	19.4
Hell's Glen N wedge	1,750,000	21.0	43.8
Ben Donich N	440,000	151.0	198.0
The Steeple	110,000	20.4	34.9
Mullach Choire a' Chuir	9,600,000?	509.0?	636.0?
Glen Kinglas	89,000	22.6	47.6
Hell's Glen S wedge	13,000	1.2	2.4

Table 10.2. Volumes and tonneage (x distance) displaced by the study RSFs. '?' denotes uncertainty caused by lack of sub-surface information

solution) was c. 282,290 tonne/metres over the same period. Extrap-

olating this 8 year rate over 10,000 years yields 3.53 x 10^6 m^3 denudation for the Karkevagge basin: though it is recognised that the denu-dation rate may have been higher in the early post-glacial (cf. Church and Ryder 1972). This extrapolated rate, though conservative, is less than the denudation achieved by the Ben Attow RSF (Table 10.2). Gardner's opinion that high magnitude RSFs, even allowing for their lower frequency, may be responsible for the transport of signif-icantly greater volumes of material than smaller scale rock-slope failures is vindicated by the data given in Table 10.2.

10.5 Conclusion

The scars and deposits of catastrophic rock-slope failures in the field areas have been little modified during the post-glacial. It is therefore difficult to escape the conclusion that many of the Scottish Highland valley slopes are inherited, their morphology having changed little from that incurred by their response to the rapid climatic and environmental changes that accompanied deglaciation. It has been shown that for a comparatively short period of time during/immediately after deglaciation, the erosion achieved by RSFs may have outweighed other geomorphic processes, localised cliff retreat being equal or greater than that attained during the preceding Loch Lomond Stadial (cf. Sissons 1976a, Dawson 1977) and probably much greater than that achieved in the whole post-glacial.

It is likely that numerous glaciations/interglaciations and stadials/interstadials affected the British Isles (including the Scottish Highlands) during the Quaternary (Bowen 1978). Glacial readvances that pre-dated those of the Lateglacial and that failed to

cover rock-slopes completely may have acted as RSF triggers and weakened other slopes, following the model outlined earlier.

No evidence was found in this study to support the notion that the case study RSFs located inside the Loch Lomond Advance limits are older than c. 10,000 years ago and have therefore been overridden by glaciers. Consequently, it is hypothesised that the majority of pre-Lateglacial RSF debris in the field areas (and the Scottish Highlands as a whole) has been transported away during intervening glaciations. The occurrence of debris-less RSFs outside the Loch Lomond Advance limits is proof that glacial transportation of RSF material took place before the Advance.

The extent and distribution of RSFs that occurred in response to earlier valley glaciations, and hence the volume of failed-debris removed, can only be speculated upon. However, assuming that a correlation between RSFs and glacier advances occurred formerly and that earlier valley glaciations originated from the same source areas as the Loch Lomond Advance, then the distribution of rock-slope failures in the past could have been similar to that recorded today.

The role of the Loch Lomond Advance and older valley glaciations in rock-slope failure may have been to raise water tables in slopes, causing fluctuating cleft-water pressures that led to mechanical weakening. Following slope failure, debris was then transported either supraglacially/englacially or during later advances/readvances when other slopes would also have been weakened.

Millions of cubic metres of failed debris, mainly located in the W Highlands, presently awaits glacial transportation. If similar

volumes, to those found today, were created repeatedly in the past, then rock-slope failure combined with glacial transportation must have been a major component of the denudation of the areas of the Highlands where RSF is important.

BIBLIOGRAPHY

ADDISON, K. 1981. The contribution of discontinuous rock-mass failure to glacier erosion. Ann. Glaciol., 2, 3-10.

ANDREWS, J.T. and MILLER, G.H. 1980. Dating Quaternary deposits more than 10,000 years old. In Cullingford, R.A., Davidson, D.A. and Lewin, J., (eds.). Timescales in Geomorphology. Wiley, Chichester, 263-287.

ASHBY, J.P. 1971. Sliding and toppling modes of failure in jointed rock slopes. Univ. London, Imperial College, M.Sc. thesis (unpubl.).

BAILEY, E.B. and MAUFE, H.B. 1916. The geology of Ben Nevis and Glen Coe. Mem. Geol. Surv. Scot.

BALLANTYNE, C.K. 1981. Periglacial landforms and environments on mountains in the northern Highlands of Scotland. Univ. Edinburgh Ph.D. thesis (unpubl.).

BALLANTYNE, C.K. and ECKFORD, J.D. 1984. Characteristics and evolution of two relict talus slopes in Scotland. Scot. Geogr. Mag., 100, 20-33.

BARTON, N.R. 1971a. A model study of the behaviour of steep excavated rock slopes. Univ. London, Imperial College, Ph.D. thesis (unpubl.).

BARTON, N.R. 1971b. Estimation of in-situ shear strength from back analysis of failed slopes. Proc. Rock Fracture Symp., Int. Soc. Rock Mech., Nancy, France, 2-27.

BARTON, N.R. 1972. Progressive failure of excavated rock slopes: Stability of rock slopes. In Cording, E.J., (ed.) Proc. 13th. Symp. Rock Mech., Urbana, Illinois, 139-70.

BARTON, N.R. 1973. Review of a new shear-strength criterion for rock joints. Eng. Geol., 7, 117-36.

BARTON, N.R. 1981. Some size-dependent properties of joints and faults. Geophys. Res. Lett., 8, 667-70.

BARTON, N.R. and CHOUBEY, V. 1977. The shear strength of rock joints in theory and practise. Rock Mech., 10, 1-54.

BECK, A.C. 1968. Gravity faulting as a mechanism of topographic adjustment. N.Z. J. Geol. Geophys., 11, 191-9.

BIRKELAND, P.W. 1973. Use of relative dating methods in a stratigraphic study of rock glacier deposits, Mt. Sopris, Colorado. Arc. Alp. Res., 5, 401-16.

BIRKELAND, P.W. 1974. Pedology, Weathering, and Geomorphological Research. O.U.P., Oxford, 285 pp.

BROWN, E.T. (1981). Rock characterisation, testing and monitoring: I.S.R.M. suggested methods. Commission on testing methods, I.S.R.M. Pergamon, Oxford. 221 pp.

BISHOP, W.W. and COOPE, G.R. 1977. Stratigraphical and faunal evidence for Lateglacial and Early Flandrian environments in south-west Scotland. In Gray, J.M. and Lowe, J.J., (eds.). Studies in the Scottish Lateglacial Environment. Pergamon, Oxford, 61-88.

BJERRUM, L and JØRSTAD, F.A. 1963. Stability of slopes on hard unweathered rock (correspondence on the paper of K. Terzaghi). Géotechnique, 13, 171-3.

BJERRUM, L and JØRSTAD, F.A. 1968. Stability of rock slopes in Norway. Norw. Geotech. Inst. Publ., 79, 1-11.

BLACKHAM, A., DAVIES, C. and FLENLEY, J. 1981. Evidence for Late Devensian landslipping and Late Flandrian forest regeneration at Gomire Lake, north Yorkshire. In Neale, J. and Flenley, J., (eds.). The Quaternary in Britain. Pergamon, Oxford, 184-193.

BOCK, C.G. 1977. Martinez Mountain rock avalanche. In Coates, D.R., (ed.). Reviews in Engineering Geology 3: Landslides. Geol. Soc. Am., Boulder, Colorado, 155-68.

BOULTON, G.S., JONES, A.S., CLAYTON, K.M. and KENNING, M.J. 1977. A British ice sheet model and patterns of glacial erosion and deposition in Britain. In Shotton, F.W., (ed.). British Quaternary Studies. O.U.P., London, 231-46.

BOVIS, M.J. 1982. Uphill-facing (antislope) scarps in the Coast Mountains, south-west British Columbia. Bull. Geol. Soc. Am., 93, 804-12.

BOWEN, D.Q. 1978. Quaternary Geology. Pergamon, Oxford, 221 pp.

BRAY, J.W. 1967. A study of jointed and fractured rock: 1. Rock Mech. Eng. Geol., 5, 117-36.

BROWN, A. 1982. Toppling induced movements in large, relatively flat rock slopes. In Proc. 23rd. U.S. Symp. Rock Mech., Am. Inst. Min. Mettall. Petr. Eng., 1035-47.

BROWN, E.T. and HOEK, E. 1978. Trends in relationships between measured in situ stresses and depth. Int. J. Rock Mech. Sci. Geomech. Abstr., 15, 211-15.

BROWN, I., HITTINGER, M. and GOODMAN, R. 1980. Finite element study of the Nevis Bluff (New Zealand) rock slope failure. Rock Mech., 12, 231-45.

BRUNSDEN, D. and THORNES, J.B. 1979. Landscape sensitivity and change. Trans. Inst. Brit. Geog., NS 4, 463-84.

BURTON, P.W. and NEILSON, G. 1980. Annual catalogues of British earthquakes recorded on LOWNET (1967-1978). Seismol. Bull. Inst. Geol. Sci. No. 7.

CAINE, N. 1974. The geomorphic processes of the alpine environment. In Ives, J.D. and Barry, R.G. (eds.). Arctic and Alpine Environments. Methuen, London, 721-48.

CAINE, N. 1982. Toppling failures from Alpine Cliffs on Ben Lomond, Tasmania. Earth Surf. Processes Landf., 7, 133-52.

CAINE, N. 1976. A uniform measure of subaerial erosion. Bull. Geol. Soc. Am., 87 137-40.

CARRARA, A. and MERENDA, L. 1976. Landslide inventory in northern Calabria, southern Italy. Bull. Geol. Soc. Am., 87, 1153-62.

CARROLL, T. 1974. Relative age dating techniques and a Late Quaternary chronology, Arikaree Cirque, Colorado. Geology, 2, 321-5.

CAWSEY, D.C. and FARRAR, N.S. 1976. A simple sliding apparatus for the measurement of rock joint friction. Géotechnique, 26, 382-6.

CHAPMAN, C.A. 1958. Control of jointing by topography. J. Geol., 66, 552-7.

CHATTOPADHYAY, G.P. 1984. A fossil valley-wall rock glacier in the Cairngorm mountains. Scot. J. Geol., 20, 121-5.

CHOWDHURY, R.N. 1978. Slope Analysis. Developments in Geotechnical Engineering (22). Elsevier, Amsterdam, 433 pp.

CHURCH, M. and RYDER, J.M. 1972. Paraglacial sedimentation: a consideration of fluvial processes conditioned by glaciers. Bull. Geol. Soc. Am., 83, 3059-72.

CLOUGH, C.T. 1913. Notes on the Glencroe landslide. Trans. Edin. Geol. Soc., 10, 243-4

COATES, D.R. 1977. Landslide perspectives. In Coates D.R., (ed.). Reviews in Engineering Geology 3: Landslides. Geol. Soc. Am., Boulder, Colorado, 3-8.

CRUDEN, D.M. 1976. Major rock slides in the Rockies. Can. Geotech. J., 13, 8-20.

CRUDEN, D.M. 1980. The anatomy of landslides. Can. Geotech. J., 17, 295-300.

DALE, M.L. 1981. Rock walls in glacier source areas in parts of the highlands of Scotland. Univ. Edinburgh Ph.D. thesis (unpubl.).

DAVIS, J.C. 1973. Statistics and Data Analysis in Geology. Wiley & Sons, New York, 550 pp.

DAWSON, A.G. 1977. A fossil lobate rock glacier in Jura. Scot. J. Geol., 13, 37-42.

DOWDESWELL, J.A. 1982. Relative dating of Late Quaternary deposits using cluster and discriminant analysis, Audubon Cirque, Mt. Audubon, Colorado Front Range. Boreas, 2, 151-61.

EINSTEIN, H.H. and HIRSCHFELD, R.C. 1973. Model studies on mechanics of jointed rock. J. Soil Mech. Found. Eng., Proc. Am. Soc. Civ. Eng., 99, 229-48.

EISBACHER, G.H. 1979a. Cliff collapse and rock avalanches (sturzstroms) in the Mackenzie Mountains, northwestern Canada. Can. Geotech. J., 16, 309-334.

EISBACHER, G.H. 1979b. First-order regionalisation of landslide characteristics in the Canadian Cordillera. Geoscience Can., 6, 69-79.

EYLES, N. and PAUL, M.A. 1983. Landforms and sediments resulting from former periglacial climates. In Eyles, R.J., (ed.). Glacial Geology. Pergamon, Oxford, 111-39.

FECKER, E. and RENGERS, N. 1971. Measurement of large-scale roughness of rock planes by means of profilograph and geological compass. Proc. Rock Fracture Symp., Int. Soc. Rock Mech. Nancy, France, 1-18.

FRANKS, J.W. and JOHNSON, R.H. (1964). Pollen analytical dating of a Derbyshire landslide. New Phytol., 63, 209-16.

FREITAS de, M.H. and WATTERS, R.J. 1973. Some field examples of toppling failure. Géotechnique, 23, 495-514.

GARDNER, J.S. 1977. High magnitude rockfall-rockslide: frequency and geomorphic significance in the Highwood Pass area, Alberta. Gr. Plains-Rocky Mts. Geogr. J., 6, 228-39.

GARDNER, J.S. 1980. Frequency, magnitude, and spatial distribution of mountain rockfalls and rockslides in the Highwood Pass area, Alberta, Canada. In Coates, D.R. and Vitek, J.D., (eds.). Thresholds in Geomorphology. Allen & Unwin, London, 267-95.

GERBER, E. and SCHEIDEGGER, A.E. 1969. Stress-induced weathering of rock masses. Ecl. geol. Helv., 62, 401-15.

GIL, E., GILOT, E.G., KOTARBA, A., STARKEL, L. and SZCZEPANEK, K. 1974. An early Holocene landslide in the Niski Beskid and its significance for palaeographical reconstructions. Geom. Carpatho., 8, 69-83.

GODARD, A. 1965. Reserches de Géomorphologie en Ecosse du Nord-Ouest. Paris.

GOODMAN, R.E. 1976. Methods of Geological Engineering in Discontinuous Rocks. West Publ. Co., Minnesota.

GOODMAN, R.E. 1981. An Introduction to Rock Mechanics. Wiley & Son, New York, 478 pp.

GOODMAN, R.E. and BRAY, J.W. 1976. Toppling of rock slopes. Proc. Spec. Conf. Am. Soc. Civ. Eng., 2. Boulder, Colorado, 201-234.

GOODMAN, R.E. and DUBOIS, J. 1972. Duplication of dilatancy in analysis of jointed rocks. J. Soil Mech. Found. Div., Am. Soc. Civ. Engs., 98, 399-422.

GORDON, J.E. 1977. Morphometry of cirques in the Kintail-Affric-Cannich area of northwest Scotland. Geogr. Annl., 59A, 177-94.

GORDON, J.E., BIRNIE, R.V. and TIMIS, R. 1978. A major rockfall and debris slide on the Lyell Glacier, South Georgia. Arc. Alp. Res., 10, 49-60.

GRAY, J.M. 1982. The last glaciers (Loch Lomond Advance) in Snowdonia, N. Wales. Geol. J., 17, 111-33.

GRAY, J.M. and LOWE, J.J. 1977. The Scottish Lateglacial environment: a synthesis. In Gray, J.M. and Lowe, J.J., (eds.). Studies in the Scottish Lateglacial Environment. Pergamon, Oxford, 163-81.

GRAY, J.T. 1972a. Postglacial rock wall recession in the Ogilvie and Werneche mountains, central Yukon Territory. In Adams, W.P. and Helleiner, F., (eds.) International Geography. University of Toronto Press, Toronto.

GRAY, J.T. 1972b. Debris accretion on talus slopes in the central Yukon Territory. In Slaymaker, H.O. and McPherson, H.J. (eds.). Mountain Geomorphology: Geomorphological Processes in the Canadian Cordillera. Univ. British Columbia Geographical Series 14, Vancouver, 75-84.

GRETENER, P.E. 1967. The significance of the rare event in geomorphology. Amer. Ass. Petr. Geol. Bull., 51, 2197-2206.

GROVE, J.M. 1972. The incidence of landslides, avalanches and floods in western Norway during the Little Ice Age. Arc. Alp. Res., 4, 131-8.

GUNN, W., CLOUGH, C.T. and HILL, J.B. 1897. The Geology of Cowal. Mem. Geol. Surv. Scot.

HARRISON, J.V. and FALCON, N.L. 1937. The Saidmarreh Landslip, southwest Iran. Geogr. J., 89, 42-7.

HARVEY, D. 1969. Explanation in Geography. Edward Arnold, London, 521 pp.

HAYNES, V.M. 1977. Landslip associated with glacier ice. Scot. J. Geol., 13, 337-8.

HEIM, A. 1882. Der Bergsturz von Elm. Deutsch. Geol. Gesell. Zeits., 34, 74-115.

HEIM, A. 1932. Bergsturze und Menschenleben. Fretz and Wasmuth Verlag, Zurich. 218 pp.

HENSCHER, S.R. 1976. A simple sliding apparatus for the measurement of rock joint friction: discussion. Géotechnique, 26, 641-4.

HITTINGER, M. 1978. Numerical analysis of toppling failures in jointed rock. Univ. California Ph.D. thesis (unpubl.).

HODGSON, D.M. 1982. Hummocky and fluted moraines in part of north-west Scotland. Univ. Edinburgh Ph.D. thesis (unpubl.).

HOEK, E. and BRAY, J.W. 1977. Rock slope engineering. 2nd Ed. Inst. Min. Metall., London.

HOLMES, G. and JARVIS, J.J. in press. Large-scale toppling within a 'sackung' like deformation at Ben Attow, Scotland. Q. J. Eng. Geol.

HSU, K.J. 1975. Catastrophic debris streams (sturzstroms) generated by rockfalls. Bull. Geol. Soc. Am., 86, 129-40.

HUDER, J. 1976. Creep in Bündner Schist. In Janbu, N., Jørstad, F. and Kjaernsli, B., (eds.). Contributions to Soil Mechanics (Laurits Bjerrum Memorial Volume). Norw. Geotech. Inst. Oslo, 125-153.

HUTCHINSON, J.N. 1968. Mass movement. In Fairbridge, F.W., (ed.). Encyclopedia of Geomorphology. Reinhold, New York, 688-96.

INNES, J.L. 1983. Development of lichenometric dating curves for Highland Scotland. Trans. R. Soc. Edinb., Earth Sci., 74, 23-32.

JAEGER, J.C. 1971. Friction of rocks and stability of rock slopes. Géotechnique, 21, 97-134.

JAEGER, C. 1979. Rock Mechanics and Engineering. C.U.P., Cambridge, 523 pp.

JAHN, A. 1964. Slope morphological features resulting from gravitation. Zeits. für Geom., 5, 59-72.

JOHNSTONE, G.S., WRIGHT, J.E., LAWRIE, T.R.M., SMITH, D.I. BERRIDGE, N.G., HARRIS, A.L., MAY, F., PEACOCK, J.D., BISHOP, A.C. and JOHNSON, M.R.W. 1975. Notes accompanying the Drift Edition Sheet 62W (Loch Quoich). I.G.S., Edinburgh.

JONSSON, O. 1976. Bergḧlaup. Raektunar felag Norðurlands, Akureyri, Iceland. 623 pp.

KENT, P.E. 1966. The transport mechanism in catastrophic rock falls. J. Geol., 74, 79-83.

KJARTANSSON, G., 1967. The Steinsholtshlaup, Central-South Iceland on January 15th, 1967. Jökull, 17, 249-62.

KELLY, M. 1980. A prehistoric catastrophic rock avalanche at Holsteinsborg, West Greenland. Bull. Geol. Soc. Denmark, 28, 73-9.

KIERSCH, G.A. 1965. Vaiont reservoir disaster. Geotimes, 9, 9-12.

KING, R.B. 1968. Periglacial features in the Cairngorm Mountains. Univ. Edinburgh Ph. D. thesis (unpubl.).

KIRK, W. and GODWIN, H. 1963. A lateglacial site at Loch Droma, Ross and Cromarty. Trans. R. Soc. Edinb., 65, 225-49.

KOBAYASHI, K. 1956. Periglacial morphology in Japan. Bull. Perigl., 4, 59-72.

KORTARBA, A. 1983. Processes on alpine cliffs in the Polish Tatra Mountains. In Briggs, D.J. and Waters, R.S. (eds.). Studies in Quaternary Geomorphology. Geo Books, Norwich, 223-243.

KUJANSUU, R. 1972. On landslides in Finnish Lapland. Finl. Comm. Geol. Bull., 256, 22 pp.

LADANYI, B. and ARCHAMBOULT, G. 1969. Simulation of shear behaviour of a jointed rock mass. Proc. 11th. Symp. Rock Mech., Berkeley, California, 105-25.

LOWE, J.J. and WALKER, M.J.C. 1977. The reconstruction of the Lateglacial environment in the southern and eastern Grampian Highlands. In Gray, J.M. and Lowe, J.J., (eds.). Studies in the Scottish Lateglacial Environment. Pergamon, Oxford, 101-18.

MAHR, T. 1977. Deep-reaching gravitational deformations of high mountain slopes. Bull. Int. Assoc. Eng. Geol., 16, 121-7.

MAHR, T. and NEMCOK, A. 1977. Deep-seated slope deformations in the crystalline slopes of the Tatry Mountains. Bull. Int. Assoc. Eng. Geol., 16, 104-6.

MARANCUNIC, C. and BULL, C. 1968. The landslide on the Sherman Glacier. In Committee on the Alaska Earthquake, The Great Alaska Earthquake of 1964: Hydrology. National Academy of Sciences, Washington, D.C. Publ. 1603, 383-94.

MOLLARD, J.D. 1977. Some regional landslide types in Canada. In Coates, D.R., (ed.) Reviews in Engineering Geology 3: Landslides, Geol. Soc. Am., Boulder, Colorado, 29-56.

MUDGE, M.R. 1965. Rockfall-avalanche and rockslide-avalanche deposits at Sawtooth Ridge, Montana. Bull. Geol. Soc. Am., 76, 1003-14.

MULLER, L. 1964. The stability of rock bank slopes and the effect of water on the same. J. Rock Mech. Min. Sci., 1, 475-504.

MULLER, L. 1968. New considerations on the Vaiont slide. Fels. Ingeniurgeol., 6, 1-91.

NELSON, R.L. 1954. Glacial geology of the Frying Pan River drainage basin, Colorado. J. Geol., 62, 325-43.

NEMČOK, A. 1972. Gravitational slope deformations in high mountains. Proc. Int. Geol. Congr., 14th Montreal. Section 13, 132-41.

NEMČOK, A. and BALIAK, F. 1977. Gravitational deformations in Mesozoic rocks of the Carpathian Mountains ranges. Bull. Ass. Eng. Geol., 16, 109-11.

NEMČOK, A., PASEK, J and RYBAR, J. 1972. Classification of landslides and other mass movements. Rock Mech., 4, 71-8.

NICHOLS, T.C. 1980. Rebound, its nature and effect on engineering works. Q. J. Eng. Geol. 13, 133-52.

PATTON, F.D. 1966. Multiple modes of shear failure in rock. Proc. 1st Int. Congr. Rock Mech., Lisbon, 509-13.

PATTON, F.D. and DEERE, D.U. 1971. Geologic factors controlling slope stability in open pit mines. In Brawner, C.O. and Milligan, V., (eds.) Stability in Open Pit Mining. American Inst. Min. Metall. and Petr. Eng. New York., 23-48.

PATTON, F.D. and HENDRON, A.J. (1974). General report on "mass movements". In Proc. 2nd Int. Congr. Int. Assoc. Eng. Geol., Paper V-GR, 57 pp.

PEACH, B.N., GUNN, W. CLOUGH, C.T., HINXMAN, L.W., CRAMPTON, C.B. and ANDERSON, E.M. 1912. The geology of Ben Wyvis, Cran Chuirneag, Inchbrae, and the surrounding country. Mem. Geol. Surv. Scot.

PEACH, B.N., HORNE, J., WOODWARD, H.B., CLOUH, C.T., HARKER, A. and WEBB, C.B. 1910. The geology of Glenelg, Lochalsh and the southeastern part of Skye. Mem. Geol. Surv. Scot.

PEACOCK, J.D. 1970. Some aspects of the glacial geology of West Inverness-shire. Bull. Geol. Surv. Gt. Br., 33, 125-45.

PEACOCK, J.D. 1975a. Landslip associated with glacier ice. Scot. J. Geol., 11, 363-4.

PEACOCK, J.D. 1975b. Palaeoclimatic significance of ice-movement directions of Loch Lomond Readvance glaciers in the Glen Moriston and Glen Affric areas, northern Scotland. Bull. Geol. Surv. Gt. Br., 49, 39-42.

PEACOCK, J.D., GRAHAM, D.K. and WILKINSON, I.P. 1978. Late-glacial and Post-glacial marine environments at Ardyne, Scotland, and their significance in the interpretation of the history of the Clyde sea area. Rep. Inst. Geol. Sci., 78/17, 1-24.

PENNINGTON, W., HAWORTH, E.V., BONNY, A.P. and LISHMAN, J.P. 1972. Lake sediments in northern Scotland. Phil. Trans. R. Soc. Lond., B., 264, 191-294.

PENNY, L.F., COOPE, G.R. and CATT, J.A. 1969. Age and insect fauna of the Dimlington Silts, east Yorkshire. Nature, London. 224, 65-7.

PITTY, A.F. 1982. The Nature of Geomorphology. Methuen, London. 161 pp.

POSER, H. 1954. Die Periglazial-Erscheinungen in der Umgebung der Gletscher des Zemmgrundes (Zillertaler Alpen). Gottinger. Geog. Abh., 15, 125-80.

PORTER, S.C. and OROMBELLI, G. 1980a. Catastrophic rockfall of September 12, 1717 on the Italian Flank of the Mont Blanc massif. Z. für Geom., 24, 200-18.

PORTER, S.C. and OROMBELLI, G. 1980b. Alpine rockfall hazards. American Scientist, 69, 67-75.

PRICE, N.J. 1966. Fault and Joint Development in Brittle and Semi-brittle Rock. Pergamon, Oxford. 176 pp.

RADBRUCH-HALL, D.H. 1976. Maps showing areal slope stability in part of the northern Coast Ranges, California. U.S. Geol. Surv. Misc. Investigations Ser., Map I-982.

RADBRUCH-HALL, D.H. 1978. Gravitational creep of rock masses on rock slopes. In Voight, B., (ed.). Rockslides and Avalanches 1: Natural Phenomena. Elsevier, Amsterdam, 607-57.

RADBRUCH-HALL, D.H. and VARNES, D.J. 1976. Landslides - cause and effect. Bull. Int. Assoc. Eng. Geol., 14, 205-16.

RADBRUCH-HALL, D.H., VARNES, D.J. and SAVAGE, W.J. 1976. Gravitational spreading of steep-sided ridges in western U.S. Bull. Int. Assoc. Eng. Geol., 14, 23-35.

RAPP, A. 1960. Recent development of mountain slopes in Karkevagge and surroundings, northern Scandinavia. Geogr. Ann., 42, 65-200.

RENGERS, N. and SOETERS, R. 1982. Two examples of gravitational spreading in the Bohi area, Spanish Pyrenees. ITC J., 283-89.

RICHARDS, K.S. and ANDERSON, M.G. 1978. Slope stability and valley formation in glacial outwash deposits, north Norfolk. Earth Surf. Processes Landf., 3, 301-18.

ROBINSON, M. 1977. Glacial limit, sea-level changes and vegetational development in part of Wester Ross. Univ. Edinburgh Ph.D. thesis (unpubl.).

ROBINSON, M. and BALLANTYNE, C.K. 1979. Evidence for a glacial readvance pre-dating the Loch Lomond Advance in Wester Ross. Scot. J. Geol., 15, 271-7.

RUDDIMAN, W.F., SANCETTA, C.D. and MCINTRE, A. 1977. Glacial/interglacial response rate of subpolar North Atlantic water to climatic change: the record in ocean sediments. Phil. Trans. R. Soc. Lond., B., 280, 119-42.

RYBAR, J. and NEMČOK, A. 1968. Landslide investigations in Czeckoslovakia. Proc. 23rd. Int. Assoc. Eng. Geol., Int. Geol. Congr. Prague, 183-98.

SCHUMM, S.A. and CHORLEY, R.J. 1964. The fall of threatening rock. Am. J. Sci., 262, 1041-54.

SELBY, M.J. 1982. Hillslope Materials and Processes. O.U.P. Oxford. 264 pp.

SHARPE, C.F.S. 1939. Landslides and Related Phenomenon. Cooper Square Publ. New York. 137 pp.

SHREVE, R.L. 1966. Sherman landslide, Alaska. Science, 154, 1639-43.

SHREVE, R.L. 1968. Leakage and fluidisation in air-layer lubricated avalanches. Bull. Geol. Soc. Am., 79, 653-8.

SIJING, W. 1981. On the mechanisms and process of slope deformation in an open pit mine. Rock Mech., 13, 145-56.

SISSONS, J.B. 1967. The Evolution of Scotland's Scenery, Oliver & Boyd, Edinburgh, 259 pp.

SISSONS, J.B. 1972. The last glaciers in part of the south-east Grampians. Scot. Geogr. Mag., 88, 168-81.

SISSONS, J.B. 1975. A fossil rock glacier in Wester Ross. Scot. J. Geol., 11, 83-6.

SISSONS, J.B. 1976a. The Geomorphology of the British Isles: Scotland. Methuen, London. 150 pp.

SISSONS, J.B. 1976b. A remarkable protalus rampart complex in Wester Ross. Scot. Geogr. Mag., 92, 182-90.

SISSONS, J.B. 1977a. The Loch Lomond Readvance in the northern mainland of Scotland. In Gray, J.M. and Lowe, J.J., (eds.). Studies in the Scottish Lateglacial Environment. Pergamon, Oxford, 49-59.

SISSONS, J.B. 1977b. Former ice-dammed lakes in Glen Moriston, Inverness-shire, and their significance in upland Britain. Trans. Inst. Brit. Geog., NS 2, 224-42.

SISSONS, J.B. 1979a. The limit of the Loch Lomond Adance in Glen Roy and vicinity. Scot. J. Geol., 15, 31-42.

SISSONS, J.B. 1979b. The Loch Lomond Advance in the Cairngorm Mountains. Scot. J. Geol., 15, 66-82.

SISSONS, J.B. 1979c. Palaeoclimatic inferences from Loch Lomond Advance glaciers. In Lowe, J.J., Gray, J.M., Robinson, J.E., (eds.). Studies in the Lateglacial of north-west Europe. Pergamon, Oxford, 31-43.

SISSONS, J.B. 1981. The last Scottish ice sheet: facts and speculative discussion. Boreas, 10, 1-17.

SISSONS, J.B. 1982. A former ice-dammed lake and associated glacier limits in the Achnasheen area, central Ross-shire. Trans. Inst. Brit Geog. NS 7, 98-116.

SISSONS, J.B. and CORNISH, R. 1982. Differential isostatic uplift of crustal blocks at Glen Roy, Scotland. Quat. Res., 18, 268-88.

SISSONS, J.B. and DAWSON, A.G. 1981. Former sea-levels and ice limits in part of Wester Ross, northwest Scotland. Proc. Geol. Ass., 92, 115-24.

SISSONS, J.B. and GRANT, A.J.H. 1972. The last glaciers of the Lochnagar area, Aberdeenshire. Scot. J. Geol., 8, 85-93.

SISSONS, J.B. and SUTHERLAND, D.G. 1976. Climatic inferences from former glaciers in the south-east Grampian Highlands, Scotland. J. Glaciol., 17, 325-46.

SISSONS, J.B. and WALKER, M.J.C. 1974. Lateglacial site in the central Grampian Highlands. Nature, London, 249, 822-4.

SKEMPTON, A.W. 1964. Long-term stability of clay slopes. Géotechnique, 20, 320-4.

SKEMPTON, A.W. and DELORY, F.A. 1957. Stability of natural slopes in London Clay. Proc., 4th. Int. Conf. Soil Mech. Found. Eng., 378-81.

SUGDEN, D.E. 1970. Landforms of deglaciation in the Cairngorm mountains, Scotland. Trans. Inst. Brit. Geogr., 51, 201-19.

SUGDEN, D.E. and CLAPPERTON, C.M. 1977. The Late Devensian glaciation of north-east Scotland. In Gray, J.M. and Lowe, J.J., (eds.). Studies in the Scottish Lateglacial Environment. Pergamon, Oxford, 1-13.

SUTHERLAND, D.G. 1980. Problems of radiocarbon dating deposits from newly deglaciated terrain: examples from the Scottish Lateglacial. In Lowe, J.J., Gray, J.M. and Robinson, J.E., (eds.). Studies in the Lateglacial of north-west Europe. Pergamon, Oxford, 139-149.

SUTHERLAND, D.G. 1981. The raised shorelines and deglaciation of the Loch Long/Loch Fyne area, western Scotland. Univ. Edinburgh Ph.D. thesis (unpubl.).

SVATOS, A. 1974. Identification of gravitational slope deformations on aerial photographs. Proc. 2nd. Int. Congr. Ass. Eng. Geol., 13, 1-9.

TABOR, R.W. 1972. Origin of ridge-top depressions by large-scale creep in the Olympic Mountains, Washington. Bull. Geol. Soc. Am., 82, 1811-22.

TALLIS, J.H. and JOHNSON, R.H. 1980. The dating of landslides in Longdendale, north Derbyshire, using pollen-analytical techniques. In Cullingford, R.A., Davidson, D.A. and Lewin, J., (eds.). Timescales in Geomorphology. Wiley, Chichester, 189-205.

TAVENAS, F., TRAK, B. and LE-ROUEIL, S. 1980. Remarks on the validity of stability analyis. Can. Geotech. J., 17, 61-73.

TER-STEPANION, G.E. 1966. Types of depth creep of slopes in rock masses. Proc. 1st. Int. Soc. Rock. Mech., 2, 157-60.

TER-STEPANION, G.E. 1974. Depth creep of slopes. Bull. Int. Assoc. Eng. Geol., 9, 87-102.

TERZAGHI, K. 1950. Mechanisms of landslides. In Paige, S., (ed.). Applications of Geology to Engineering Practise (Berkey volume). Geol. Soc. Am., Colorado, 83-123.

TERZAGHI, K. 1962. Stability of slopes in hard unweathered rock. Géotechnique, 12, 251-70.

TERZAGHI, R.D. 1965. Sources of error in joint surveys. Géotechnique, 15, 287-304.

THOMPSON, K.S.R. 1972. The last glaciers in western Perthshire. Univ. Edinburgh Ph.D. thesis (unpubl.).

THORP, P.W. 1978. The Loch Lomond Readvance in the Glen Nevis and Loch Leven areas of the western Grampians. City London Polytechnic and Polytechnic of North London M.Sc. thesis (unpubl.).

VARNES, D.J. 1958. Landslide types and processes. In Eckel, E.B., (ed.) Landslides and Engineering Practise. Nat. Res. Coun., Highway Res. Board Spec. Rep. Washington, 29, 20-47.

VOIGHT, B. 1978. Rockslides and Avalanches: 2 Engineering Sites. Elsevier, Amsterdam. 632 pp.

VOIGHT, B. and KENNEDY, B.A. 1978. Slope failure of 1967-1969, Chuquicamata, Chile. In Voight, B. Rockslides and Avalanches: 2 Engineering Sites. Elsevier, Amsterdam, 401-32.

VOIGHT, B. and PARISEAU, W.G. 1978. Rockslides and avalanches: an introduction. In Voight, B., (ed.) Rockslides and Avalanches: Natural Phenomena. Elsevier, Amsterdam, 1-67.

WATTERS, R.J. 1972. Slope stability in the metamorphic rocks of the Scottish Highlands. Univ. London, Imperial College, Ph.D. thesis. (unpubl.).

WHALLEY, W.B. 1974. The mechanics of high-magnitude, low-frequency rock failure and its importance in a mountainous area. Univ. Reading Geogr. Pap., 27, 48 pp.

WHALLEY, W.B. 1976. A fossil rock glacier in Wester Ross. Scot. J. Geol., 12, 175-9.

WHALLEY, W.B., DOUGLAS, G.R. and JONSSON, A. 1983. The magnitude and frequency of large rockslides in Iceland in the Postglacial. Geogr. Annl., 65A, 99-110.

WISHART, D. 1977. CLUSTAN User Manual. Program Library Unit, Inter-University Research Council Ser. Rep. 47. 147 pp.

WOLMAN, M.G. and MILLER, J.P. 1960. Magnitude and frequency of forces in geomorphic processes. J. Geol., 68, 54-74.

WYLLIE, D.C. 1980. Toppling rock slope failure examples of analysis and stabilisation. Rock Mech. 13, 89-98.

WYRWOLL, K.H. 1977. Causes of rock slope failure in a cold area: Labrador-Ungava. In Coates, D.R., (ed.). Reviews in Engineering Geology 3: Landslides. Geol. Soc. Am., Boulder, Colorado, 59-67.

YAGI, H. 1981. The origin of uphill-facing scarplets distributed on the high mountain slopes of Japan. Geogr. Rev. Japan, 54, 272-80.

YOUNG, J.A.T. 1974. Ice wastage in Glenmore, upper Spey valley, Inverness-shire. Scot. J. Geol., 10, 147-57.

ZARUBA, Q. and MENCL, V. 1969. Landslides and their Control. Elsevier, Amsterdam. 205 pp.

ZISCHINSKY, U. 1966. On the deformation of high slopes. Proc. 1st. Int. Congr. Soc. Rock Mech., Lisbon. 2, 179-85.

ZISCHINSKY, U. 1969. Uber sackungen. Rock Mech., 1, 30-52.

Figure A.1: Geometry of a plane-sliding failure.

APPENDIX A: LIMIT-EQUILIBRIUM MODELS

PLANE-SLIDING

Plane-sliding failure has the simplest geometry of all the three failure modes identified by Hoek and Bray (1977): involving a triangular or trapezoidal-shaped block in cross-section. Plane-sliding failure geometry is determined by the orientation of the slope face/crest, failure-plane and tension-crack (if present). Although the failure-surface is three-dimensional in nature it can be approximated by a two-dimensional analysis: the 'slice of unit-thickness' approach.

Assuming that the Mohr-Coloumbe criterion is applicable to the example shown in Figure A.1 then the factor of safety of the slope can be calculated using:

$$F = \frac{cL + (W\,\mathrm{Cos}\Theta - U)\,\mathrm{Tan}\phi}{W\,\mathrm{Sin}\Theta + V} \qquad A.1$$

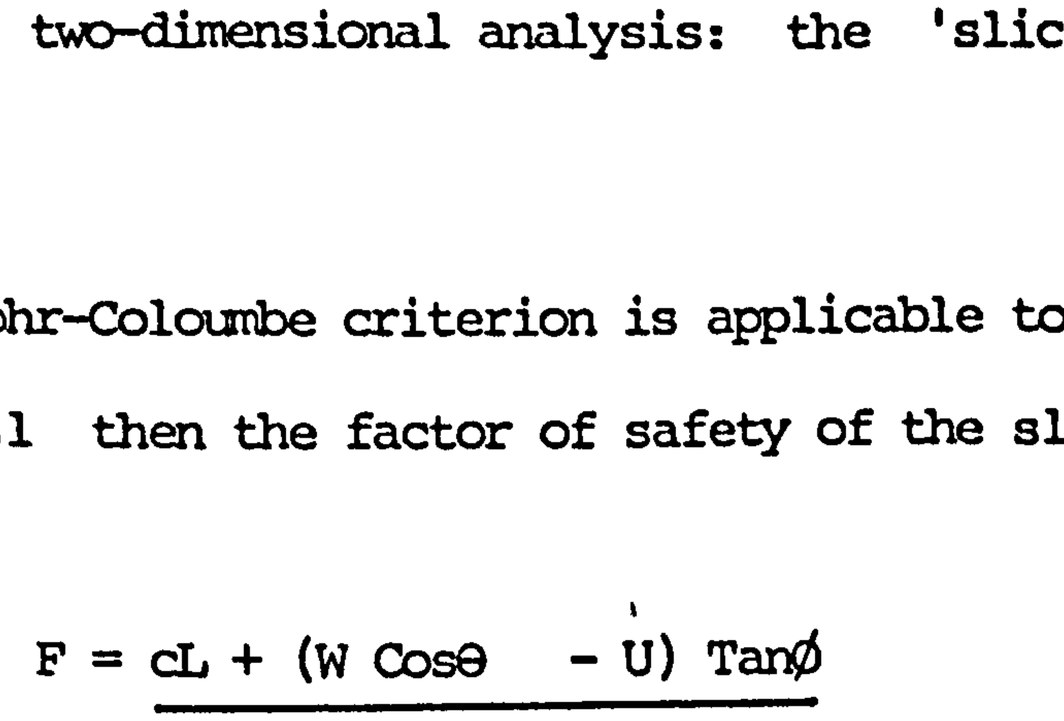

using:

$$W = \gamma H^2\,[(1-(z/H^2))\,\mathrm{Cot}\Theta - \mathrm{Cot}\beta] \qquad L = (H - z)\,\mathrm{Cosec}\Theta$$

$$U = \gamma_w\, z_w\, (H-z)\,\mathrm{Cosec}\,\beta \qquad V = \gamma_w\, z_w^2$$

where: W = weight of the block, H = height of the slope, γ= unit weight of rock, β = inclination of the face, θ = inclination of the failure-plane, z = height of the tension crack, z^w = depth of water in the tension-crack and γw = unit weight of water.

Equation A.1 includes forces U and V which are produced by the cleft-water pressure acting on the failure-plane and the downslope wall of the tension-crack, respectively. Post-failure solution of Equation A.1 assumes that the factor-of-safety (F) at the instant of failure equalled unity.

There are a number of other important assumptions made in this analysis these include:

(i) the Mohr-Coloumbe criterion is applicable to the problem. If the failure-surface upon which translation occurs is rough then the apparent cohesion and apparent ϕ will be defined by a tangent to the shear strength curve. The tangent will touch the curve at a normal stress value which corresponds to that acting upon the failure-surface;

(ii) both the failure-surface and the tension-crack strike parallel with the slope face;

(iii) the tension-crack is vertical and water enters it seeping along the base to escape at atmospheric pressure;

(iv) forces W, U and V all act through the centroid of the block and no moments occur which seek to cause rotation of the block.

WEDGE-SLIDING

A more complex analysis is required to model the limit-equilibrium of a wedge-slide: a block formed by two intersecting failure-surfaces (Hoek and Bray 1977). In the following discussion

Figure A.2: Geometry of a wedge-sliding failure.

the flatter of the two intersecting planes is called A, the steeper B. Hoek and Bray (1977) have shown that the factor of safety for the example in Figure A.2 is given by:

$$F = \frac{3\gamma}{\gamma_H}(cA.X + cB.Y) + (A - \frac{\gamma w}{2\gamma}.X)\text{Tan}\,\phi A + (B - \frac{\gamma w}{2\gamma}.Y)\text{Tan}\,\phi B \qquad A.2$$

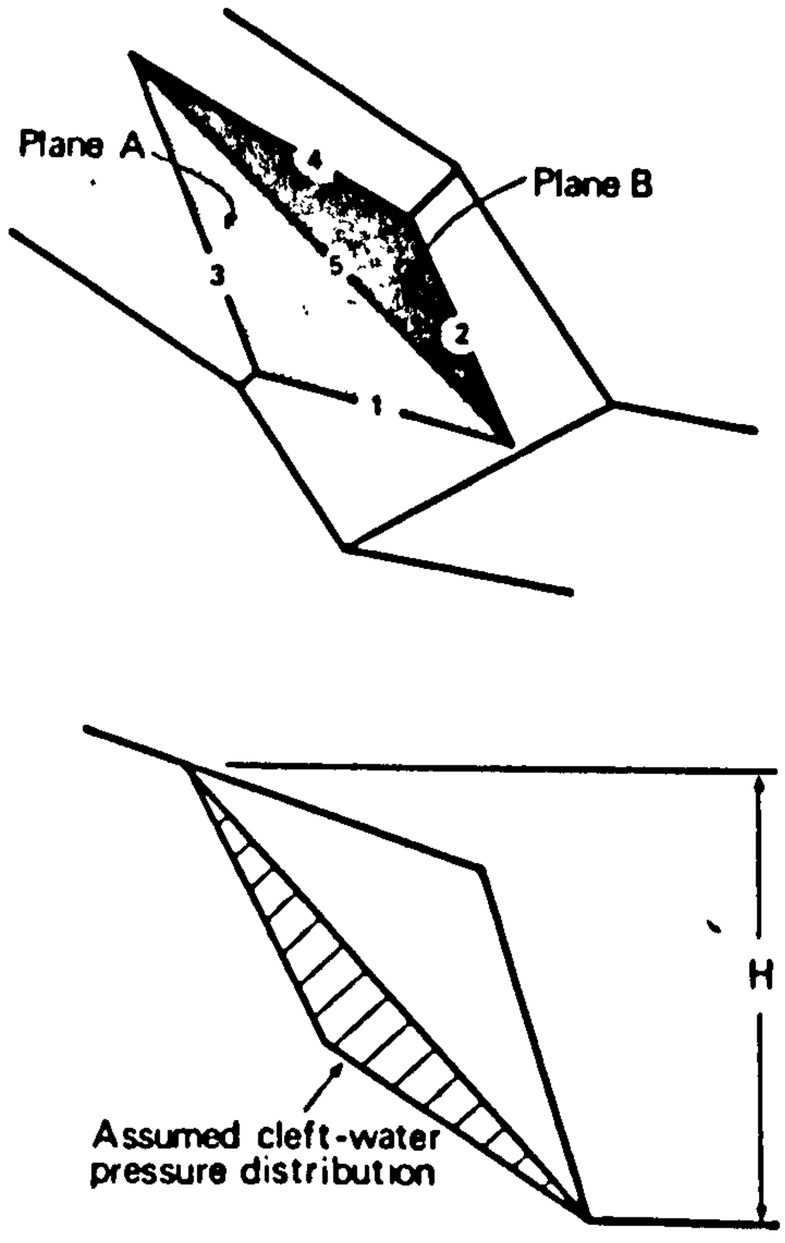

where:

cA and cB = the cohesive strengths of planes A and B respectively,

ϕA and ϕB = the friction angles of planes A and B,

γ = the unit weight of rock,

γw = the unit weight of water,

H = the total height of the wedge,

A, B, X and Y are dimensionless factors which are dependent upon the geometry of the wedge.

Hoek and Bray (1977) have also produced a series of design charts for the analysis of wedge-sliding under friction only. The method preferred here, as the effects of cohesion need to be modelled, was the graphical solution of the parameters A, B, X and Y given in Hoek and Bray (1977): the reader is referred to their book for full explanation of the analysis.

Figure B.1: The area covered by the aerial-photographic survey.

APPENDIX B: ROCK-SLOPE FAILURE INVENTORY

Data collected by an aerial photograph survey of the major upland areas of the Scottish Highlands are given overleaf. Figure B1 shows the area covered by the aerial-photographic survey. The RSF's are grouped into the 10,000 km^2 grid squares (NC, NG etc.) and a six-figure GRID REFERENCE is given for each RSF.

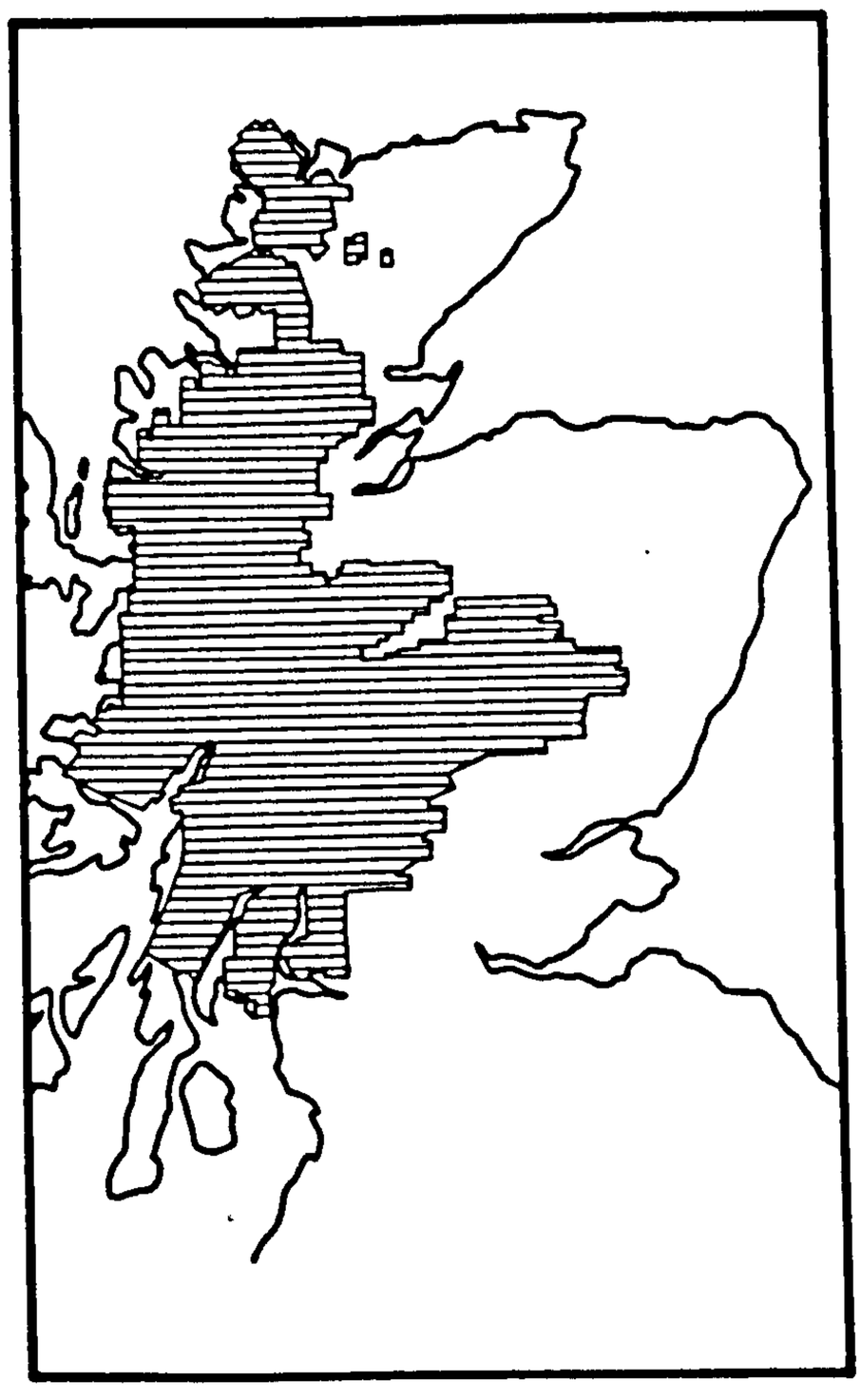

The POSITION of each RSF is summarised in column 2 where; 1 = valley side, 2 = slope crest, 3 = spur, 4 = mountain top and 5 = corrie headwall position, and its ASPECT (in degrees from true north) is given in column 3. AREA is given in km^2 in column 4:where the RSF is a 'DEBRIS-LESS' type the flag 'scarp' indicates its area is unknown.

The horizontal DISTANCE FROM FORMER GLACIAL LIMITS is given in column 5 where; 1-6 are where the RSF centroid occurs inside the limits (in classes of 200 m) with class 1 being within 200-m-inside the limits. Classes 7-12 occur outside the limits (Class 7 being within 200-m-outside the limits). If the slope features OBSEQUENT-SCARPS the flag 'A/S' is printed in column 6. ROCK TYPE, where known, is given in the final column.

10 000 km^2 grid square NC

584	265	1	128	0.28	6	A/S	schist/granite
582	261	1	120	0.02	6		schist/granite
412	364	2	121	0.15	6	A/S	semi-pelite
431	343	5	132	0.36	6	A/S	semi-pelite
440	356	3	073	0.03	1		semi-pelite
442	358	1	083	0.03	7		semi-pelite
443	356	1	071	0.08	7		semi-pelite
447	343	1	093	0.04	6		semi-pelite
398	422	1	182	0.07	3		semi-pelite
387	419	1	159	0.10	1		semi-pelite
485	497	1	123	0.04	7		unknown
347	497	1	118	0.07	7		schist
523	497	2	108	0.18	6	A/S	unknown

10 000 km^2 grid square NG

757	068	1	247	0.05			psammite/pelite
773	057	2	238	0.14			semi-pelite
833	066	1	076	0.34			pelite
837	062	1	045	0.12			pelite
835	017	1	160	1.79		A/S	schist
958	087	2	132	scarp			semi-pelite
986	070	2	051	0.13			unknown
800	005	1	151	0.88			pelitic schist
789	003	1	189	0.04			pelitic schist
880	003	1	125	0.04			pelitic schist
986	066	1	053	scarp			pelite
988	063	1	134	0.08			pelite
985	062	1	160	0.03			pelite
998	073	2	164	0.24			psammite/pelite
862	113	3	123	0.28			gneiss
873	122	4	067	scarp	1		granite/gneiss
930	170	3	093	0.54			pelite/psammite
986	151	2	030	scarp			psammite
987	147	1	159	0.14			psammite/semi-pelite
963	314	1	170	0.19			unknown
804	459	5	127	0.05	1		sandstone
932	496	3	101	0.26	1		sandstone
922	576	5	354	0.03	1		unknown
866	610	5	168	scarp	1		sandstone
976	616	1	097	scarp	1		pipe rock/quartzite
937	766	1	041	0.06	6		unknown
978	771	1	212	0.04	2		unknown
873	127	1	058	scarp	1		granite/gneiss

10 000 km^2 grid square NH

018	093	2	158	scarp			psammite/pelite
035	088	2	092	0.14			psammite
070	090	2	305	0.33			psammite
438	022	1	316	0.13		A/S	unknown
683	043	2	092	scarp			unknown

647	092	2	122	0.13			unknown
665	033	2	299	0.06			unknown
663	031	2	285	0.05			unknown
101	189	1	334	0.20			psammite
115	173	3	092	0.42			psammite/pelite
107	154	2	313	0.17			psammite/pelite
112	158	2	343	scarp			psammite
127	147	1	318	0.12			psammite/semi-pelite
140	120	1	220	0.21	1		quartzite
141	145	1	180	0.22	1		psammite
163	115	1	185	0.14	9		granite
163	184	1	331	0.27			psammite/semi-pelite
168	179	1	200	0.13			psammite/pelite
370	163	1	150	0.48			unknown
010	184	1	221	2.21		A/S	psammite
043	191	2	019	scarp			psammite/pelite
051	192	2	008	scarp			psammite/pelite
019	143	1	188	0.17			pelite
023	140	1	215	0.34			pelite
005	115	1	119	0.46			pelite
047	147	1	109	0.62			psammite
047	157	3	168	scarp			psammite/pelite
031	149	2	095	0.07			psammite
064	128	3	123	scarp			psammite
062	135	2	067	0.11			psammite
058	141	2	075	scarp			psammite/pelite
059	146	3	091	0.03			psammite/pelite
064	155	3	133	0.21			psammite/pelite
063	162	3	145	scarp			psammite/pelite
063	166	2	119	scarp			psammite/pelite
070	173	1	066	0.51		A/S	pelite
090	150	2	250	0.41			psammite/pelite
100	140	3	145	scarp			psammite/pelite
096	167	5	048	scarp			psammite/pelite
098	172	5	159	scarp			psammite/pelite
020	100	2	098	0.49			psammite/pelite
683	149	1	305	0.20			psammite
114	155	2	122	0.54			psammite/pelite
701	154	3	020	scarp			unknown
159	208	1	004	0.03			psammite/pelite
064	257	2	103	0.18	1	A/S	psammite/pelite
073	243	2	308	0.11	1		psammite/pelite
080	242	1	125	1.02	1	A/S	psammite/semi-pelite
101	244	1	314	0.14			semi-pelite
095	214	1	179	0.43			psammite/pelite
114	245	5	156	0.06			psammite/semi-pelite
118	253	4	291	0.17		A/S	pelite
130	249	2	199	0.02			pelite
140	247	2	015	0.09			psammite
152	246	4	005	0.31			psammite/pelite
112	269	1	276	0.04			psammite/pelite

112	282	1	251	0.08			pelite
210	275	1	184	1.22	2	A/S	semi-pelite
056	339	3	005	0.01			schist
055	338	3	347	0.03			schist
095	334	1	291	0.99		A/S	gneiss
116	337	5	189	0.16			gneiss
123	335	5	108	0.07			gneiss
144	339	3	161	0.14			gneiss
148	318	1	201	0.15			pelite
153	314	1	196	scarp			pelite
160	315	1	192	0.32			pelite
162	346	5	130	scarp	1		gneiss
163	349	5	133	scarp	1		gneiss
153	376	1	190	0.05			schist
159	377	1	165	0.04			schist
199	323	1	142	0.15			semi-pelite
289	393	1	183	0.04			schist
076	408	1	036	scarp			gneiss
085	426	1	171	0.21			gneiss
087	429	1	170	0.04			gneiss/schist
106	440	5	137	scarp			schist
211	434	5	116	scarp			schist
208	438	1	311	0.55			gneiss/schist
199	462	1	164	scarp			schist
189	489	1	021	scarp			gneiss/schist
218	458	1	337	0.07			schist
245	480	1	316	0.94		A/S	gneiss/schist
258	423	1	187	0.28			schist
293	424	1	165	0.12			pelite
296	427	1	167	scarp			pelite
092	477	1	170	0.22	3		gneiss
103	487	1	118	0.10	3		gneiss
108	485	1	182	0.24	1		gneiss
111	490	5	124	scarp	3		schist
117	485	1	190	0.16	1		schist
326	408	3	223	0.12			gneiss/schist
363	562	1	159	0.11			unknown
442	664	1	225	0.12			gneiss/psammite
254	673	5	057	0.10			schist
162	623	5	085	scarp			pelite
140	686	3	186	0.58			gneiss
341	751	1	071	0.32		A/S	pelite
088	768	1	307	0.12			unknown
187	715	5	090	0.03			gneiss
150	705	5	206	0.82			gneiss
137	712	5	155	0.23			gneiss
050	737	4	309	scarp	1		unknown
357	792	1	278	0.13			psammite
390	758	1	113	0.06			schist/gneiss

058	734	3	104	scarp	1	unknown
459	833	3	359	scarp		gneiss
457	834	3	338	0.03		gneiss
431	845	1	020	0.11		schist
411	896	2	146	0.02		schist
409	895	2	182	0.03		psammite
392	898	2	036	scarp		psammite
394	893	3	109	scarp		psammite
392	891	1	153	0.07		psammite
373	850	2	132	0.12		psammite
267	861	4	108	0.13		schist
220	848	2	228	0.16		schist
321	839	2	172	0.01		psammite
323	837	1	168	0.02		psammite
325	837	1	163	0.04		psammite
396	905	2	230? 280	0.14		schist
392	907	1	212	0.04		schist

10 000 km^2 grid square NJ

002	014	2	018	0.04		granite

10 000 km^2 grid square NM

695	435	2	175	0.16		basalt/sandstone
706	426	1	232	0.15		basalt/sandstone
723	422	1	196	0.25		basalt/sandstone
632	552	2	033	scarp		basalt/sandstone
639	550	2	035	0.36	A/S	basalt/sandstone
644	545	2	053	scarp		basalt/sandstone
687	563	2	254	0.17		basalt/sandstone
689	553	1	239	0.20		basalt/sandstone
813	536	1	018	scarp		granite
810	666	2	019	scarp		psammitic granulite
783	642	1	305	0.26		psammitic granulite
958	889	2	119	0.17		pelite/psammite
947	860	4/5	170	0.23		pelite
999	862	1	116	scarp		psammite
941	879	4	124	scarp		psammite/pelite
848	894	1	088	0.04	A/S	psammite/pelite
846	842	1	351	0.13		pelite
946	958	2	134	0.12		pelite
988	943	2	081	0.03		pelite/psammite
793	953	1	227	0.11		semi-pelite
856	966	1	153	0.20		semi-pelite
899	946	1	147	0.26		pelite/psammite
910	905	4	172	1.48	A/S	pelite
963	967	1	149	0.19		psammite/pelite
794	954	1	223	0.11		semi-pelite

880	988	1	097	0.04		pelite/semi-pelite
879	995	1	127	0.22		pelite
988	952	1	314	0.05		pelite

10 000 km^2 grid square NN

241	002	1	119	0.50	A/S	schist
162	004	1	214	0.15		schist
159	006	4	200	0.05		schist
160	007	4	312	0.06		schist
143	020	1	337	0.14		schist
251	096	1	279	0.13		schist
252	089	2	279	0.14	A/S	schist
257	056	4	206	0.20		schist
241	086	1	311	0.05		schist
240	080	1	292	0.12	A/S	schist
226	093	1	350	0.01		schist
220	090	1	351	0.15		schist
215	076	1	258	0.21		schist
217	072	3	158	scarp		schist
200	084	1	333	0.18		schist
198	081	1	332	0.02		schist
190	096	1	351	0.07		schist
181	062	1	217	0.03		schist
180	056	1	032	0.49		schist
176	055	1	009	0.02		schist
173	059	1	018	0.02		schist
213	053	1	015	scarp		schist
228	056	1	092	0.09	A/S	schist/schistose grits
233	046	1	042	0.03	A/S	schist
230	045	3	035	0.02		schist
227	048	2	070	0.20		schist
220	048	1	332	0.14	A/S	schist
173	038	4	027	0.32	A/S	schist
168	039	1	037	0.09		schist
166	042	1	042	0.06		schist
245	037	3	359	0.02	A/S	schist
248	035	1	030	0.01		schist
251	032	1	356	0.04		schist
118	099	1	293	0.13		phyllite
387	191	1	336	0.03		schist
390	103	1	158	0.04		schist
385	103	3	165	scarp		schist
123	115	1	284	0.24		phyllite
123	118	1	301	0.08		phyllite
124	121	1	288	0.03		schist
190	113	1	314	0.17		schistose grits
211	140	1	301	0.04	A/S	schist
188	182	1	320	0.07		phyllite

227	105	1	175	0.40			schist
244	117	1	136	0.36			granite
288	132	1	262	0.06		A/S	schist
276	119	1	058	0.09			schist
289	122	1	260	0.06			schist
393	138	1	216	0.43			schist
446	114	1	087	0.21	1		schist
445	122	1	094	0.05	7		schist
446	132	1	091	0.01	1		schist
461	137	1	112	scarp	6		schist
533	125	1	258	0.91	1	A/S	schistose grits/greywackes
553	126	3	346	0.05			schistose grits
566	127	1	034	0.02			schistose grits
573	128	2	029	0.20			schistose grits
627	189	3	312	0.02	2		schistose grits
564	105	1	057	0.21			schistose grits
589	161	2	096	0.47			schistose grits/greywackes
535	125	1	263	0.91	2	A/S	schistose grits/greywackes
553	126	3	244	0.05			schistose grits/greywackes
566	127	1	034	0.02			schistose grits/greywackes
573	128	2	028	0.20			schistose grits/greywackes
564	105	1	051	0.21			schistose grits/greywackes
449	147	1	115	0.01	1		schist
592	140	1	270	0.94	1	A/S	schistose grits/greywackes
589	161	2	100	0.47	1		schistose grits/greywackes
407	140	1	116	0.12			schist
409	133	1	092	scarp			schist
419	196	4	077	0.23			schist
404	213	1	006	0.05			schist
410	212	3	055	0.02			schist
437	212	1	246	0.47		A/S	schist
375	200	2	306	0.28			schist
392	228	2	005	scarp			schist
245	254	1	227	1.08			schist
268	265	2	071	scarp			schist
444	206	1	051	scarp			schist
428	227	1	286	0.08			schist
436	232	1	022	scarp			schist
464	205	2	239	0.13			schist
448	228	1	332	0.15			schist
433	249	1	333	0.22			schist
440	248	1	097	0.03			schist
515	244	3	301	0.01			schist/limestone
583	214	1	310	0.31	1		schistose grits/greywackes
608	200	2	322	0.12	2		schistose grits/greywackes
492	205	2	173	0.04	1		schist
496	206	1	167	0.01	7		schist
497	212	1	058	0.08	1		schist
527	226	1	255	0.23			schist
571	261	1	036	0.03			schist
574	260	1	061	0.08			schist

NN cont.

575	257	1	074	0.03			schist
574	245	1	052	0.03			schist
576	244	1	052	0.05			schist
580	237	3	097	0.15			schist
439	222	3	039	scarp			schist
605	217	1	310	0.14	1		schist
603	214	1	285	0.03	1		schist
689	321	1	118	0.03	3		granite
705	322	1	213	0.10	12		schist
713	345	2	055	0.22	12		schist
730	358	2	060	0.08	1		schist
732	354	2	059	0.03	1		schist
718	378	3	331	0.08	1		schist
577	384	5	349	scarp	1		schist
736	363	1	245	0.06	1		schist
740	360	1	246	0.12	1		schist
059	319	5	024	scarp	1		granite
063	325	5	324	0.05	1		granite
355	325	1	270	0.91		A/S	schist
347	338	1	082	0.20			schist/schistose grits
402	325	1	077	0.09	1		schist
372	436	1	180	0.11	1		schist
399	438	1	272	0.16	9		schist
635	412	4	212	0.25	12		schist
672	423	1	211	0.14	2		schist
647	404	1	154	0.39	2		schist
571	419	1	063	0.10	7		schist
566	443	1	065	0.12	6		schist
615	424	1	024	scarp	1		schist
617	446	1	060	scarp	2		schist
619	449	1	081	0.10	1		schist
598	480	1	199	0.06	7		schist
605	482	1	171	0.49	1		schist
611	499	1	076	scarp	1		schist
091	563	1	284	0.59	7	A/S	schist
080	545	1	164	0.81	1	A/S	schist
137	592	5	315	0.20	1		quartzite
165	556	1	128	0.08	7		quartzite
248	567	1	050	scarp	1		granite
517	538	1	224	scarp	12		schist
494	689	1	224	0.08	7		psammite
147	648	1	190	0.60	1	A/S	quartzite/schist
196	650	3	270	0.49	7	A/S	quartzite/schist
197	642	1	246	0.54	8		quartzite/schist
142	647	1	199	0.57	7		quartzite/schist
226	661	1	308	0.24	7		quartzite
182	611	1	007	scarp	9		quartzite
523	678	2	291	0.26	1		psammitic flaggy gneisses
176	698	1	270	0.04			limestone/schist

200	697	1	180	0.39	9		quartzite/schist
224	698	1	169	0.22	11		quartzite
334	630	3	142	0.02	7		schist
639	710	1	308	0.20	1	A/S	psammite
229	710	1	169	0.10	7		schist
228	714	4	329	0.06	2		quartzite
228	722	1	296	0.08	2		quartzite
223	720	1	301	0.06	1		quartzite
254	726	1	157	0.43	8	A/S	quartzite/schist
242	722	3	113	scarp	1		quartzite
260	720	2	297	0.41	8		quartzite/schist
269	725	1	035	0.05	1		quartzite
266	737	3	114	0.11	7		quartzite
262	735	1	189	0.13	7		quartzite
259	739	5	014	0.04	2		quartzite
514	709	5	113	0.02	6		quartzite
922	738	1	142	0.44			diorite
917	736	1	147	0.05			granite/schist
958	755	1	048	0.20			schist
960	744	1	081	0.19			schist/quartzite
967	745	1	004	0.18			schist/quartzite
335	750	1	103	scarp	8		unknown
322	737	1	153	0.10	1		schist
590	795	1	314	0.24	6	A/S	unknown
210	708	3	098	0.02	7		quartzite
467	738	1	229	0.06	1	A/S	psammite
523	740	3	063	scarp	4		unknown
058	888	1	194	0.13		A/S	psammite
063	885	1	199	0.10			psammite
243	891	1	311	0.56	8		pelite/quartzite
268	887	1	182	0.19	7		psammite/schist
303	865	1	281	0.21	2		unknown
581	808	1	132	0.30	6	A/S	unknown
590	817	1	137	0.56	6	A/S	unknown
712	803	1	293	0.10	8		psammitic schist
716	810	1	304	0.11	7	A/S	psammitic schist
723	811	1	091	0.14	10	A/S	psammitic schist
730	810	1	303	0.53	7	A/S	psammite
752	828	1	294	0.32	1		psammitic schist
511	810	1	112	scarp	6		unknown
317	886	1	332	0.51	6		unknown
231	962	3	048	scarp	1		psammite/granodiorite
311	989	1	311	0.26	8		unknown
219	906	1	142	0.48	1		tonalite
289	916	1	294	0.34	4		unknown
343	912	1	305	0.27	12		unknown
313	900	1	144	1.02	12	A/S	unknown

10 000 km^2 grid square NO

239	627	1	296	0.22			schistose grits
316	621	1	330	0.07			schistose grits
318	718	1	032	0.13	6		schist
313	722	3	073	0.02	6	A/S	schist
273	776	3	076	0.08	6	A/S	schist/diorite
297	781	1	317	0.09	1	A/S	schist
329	758	2	209	0.05	1	A/S	schist
336	758	2	113	0.04	1	A/S	schist
334	754	3	248	0.01	1		schist
329	739	1	177	0.19	6		schist
429	767	2	341	0.04	1		schist
200	748	1	308	0.72		A/S	gneiss
387	883	1	333	0.09			schist
147	818	1	316	0.04			schist/quartzite
139	883	1	117	0.40			schist/quartzite
094	854	1	060	0.21			schist/quartzite
095	846	1	121	0.13			quartzite
069	863	3	084	scarp			schistose grits
062	855	2	138	1.07			schistose grits/schist

10 000 km^2 grid square NS

117	897	1	087	0.05			schist
116	893	1	093	0.04			schist
123	891	1	342	0.03			schist
126	892	1	351	0.09			schist
122	852	1	054	0.09			schist
105	878	1	215	scarp			schist
104	886	1	278	0.04			schist
097	894	3	244	0.03			schist
098	897	1	268	0.01			schist
293	965	3	150	0.06			schist
289	955	2	225	0.86		A/S	schist
277	959	1	174	0.41			schist
272	952	1	036	0.07			schist
134	994	1	280	0.01			schist
237	985	1	098	0.01			schist
093	905	1	297	0.05			schist
102	911	1	296	0.19			schist
109	913	2	037	0.01			schist
112	912	2	004	0.05			schist
116	912	1	083	0.08			schist
127	910	1	031	0.35			schist
131	907	3	079	0.05			schist
176	931	1	067	0.07			schist/quartzite
152	981	1	274	0.06			schist
151	989	3	352	0.04			schist
142	993	1	018	0.07			schist
136	991	2	246	0.06			schist
138	996	1	343	0.16			schist
259	983	1	296	0.56			schist

NS cont.

320	955	1	201	0.18		schist
239	996	3	158	0.29	A/S	schist

APPENDIX C: TILT TESTS

Tilt tests - mica-schist

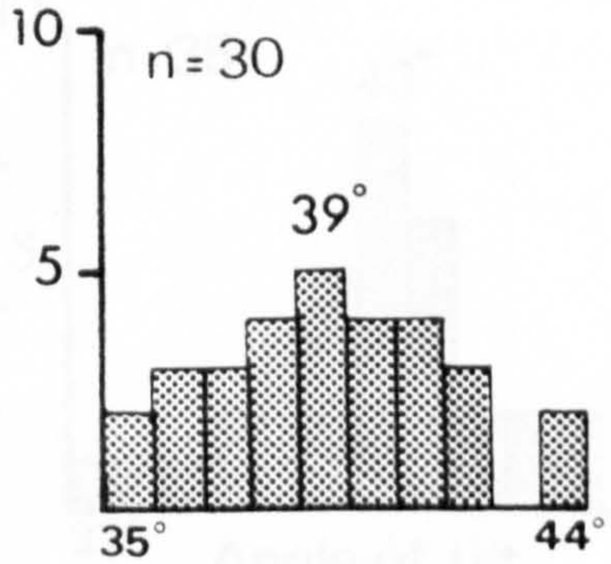

Glen Kinglas

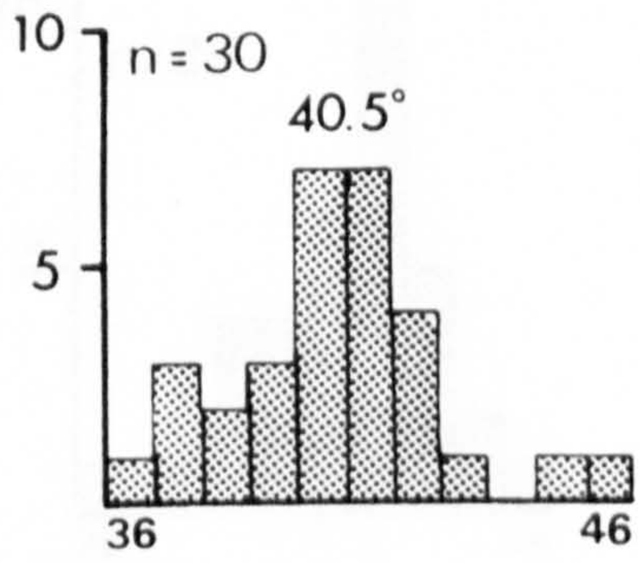

Hell's Glen topple

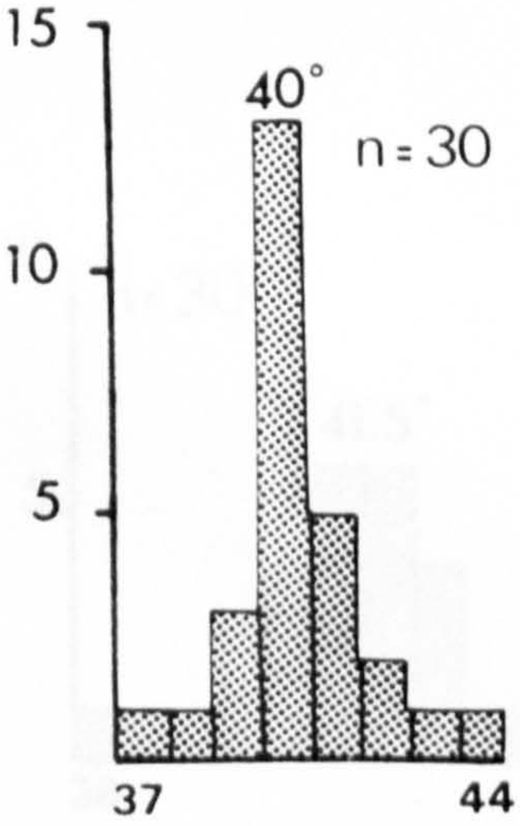

Cairn Broadlands

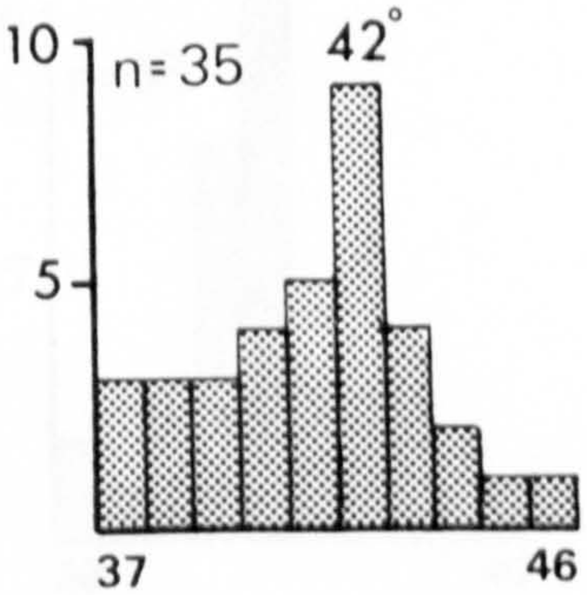

Corrie Brandy

Tilt test - schistose grit

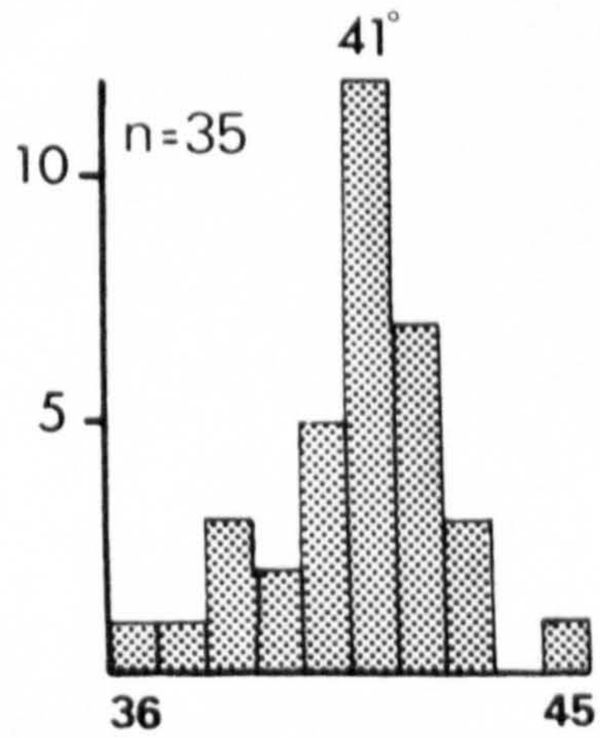

Ben Donich

Tilt tests – psammite

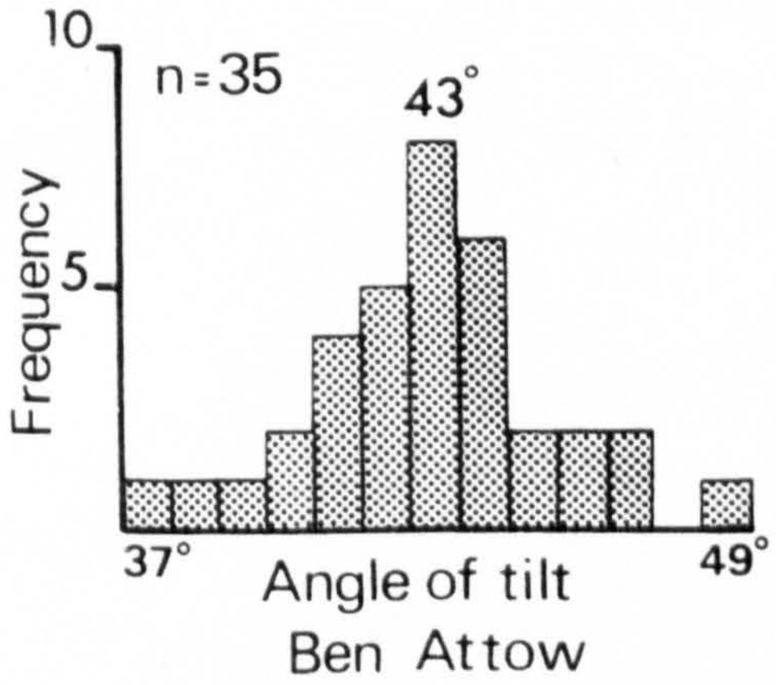

Ben Attow

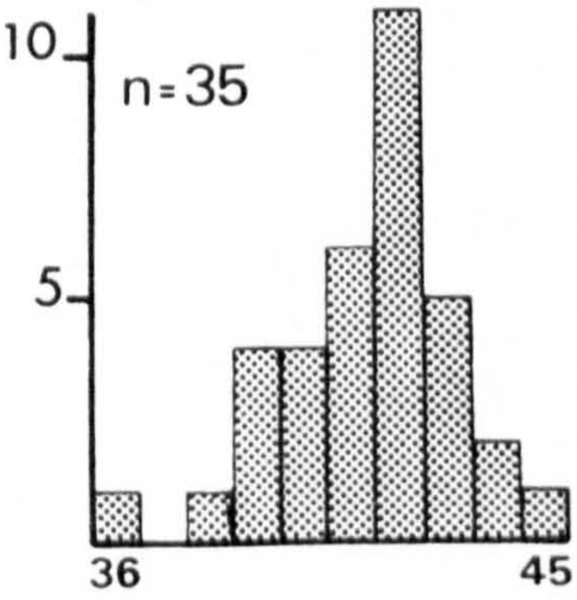

An Sornach

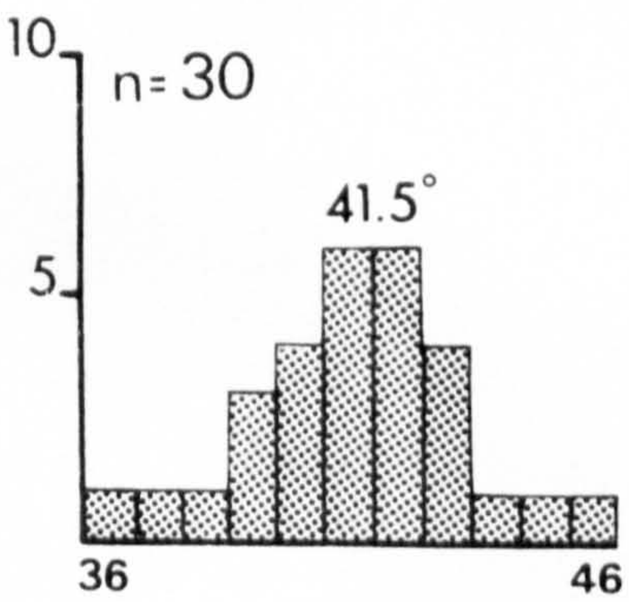

Sgùrr na Lapaich

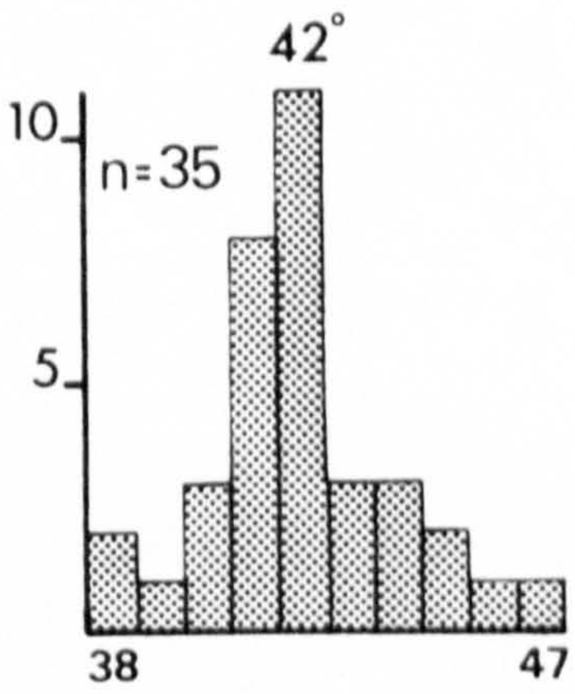

Mullach Fraoch-choire

Tilt tests – gneiss

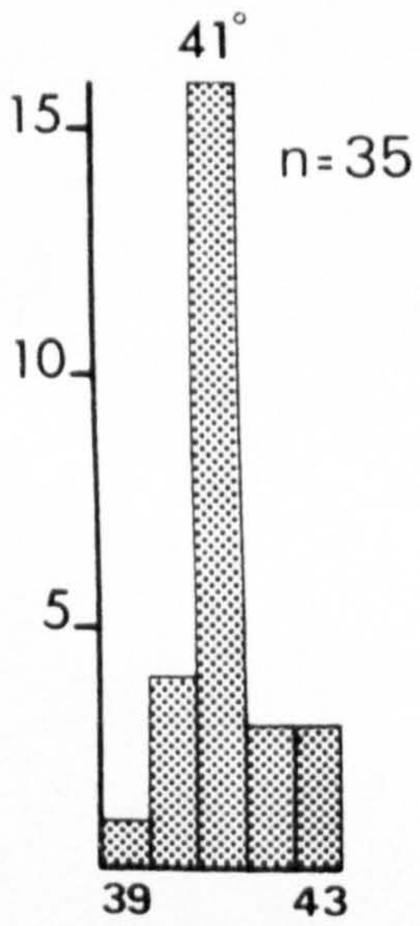

Garbh Choire Mòr

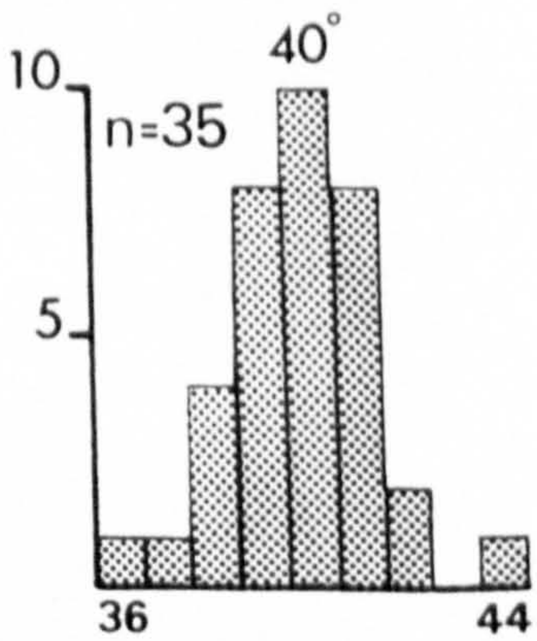

Sgùrr Breac

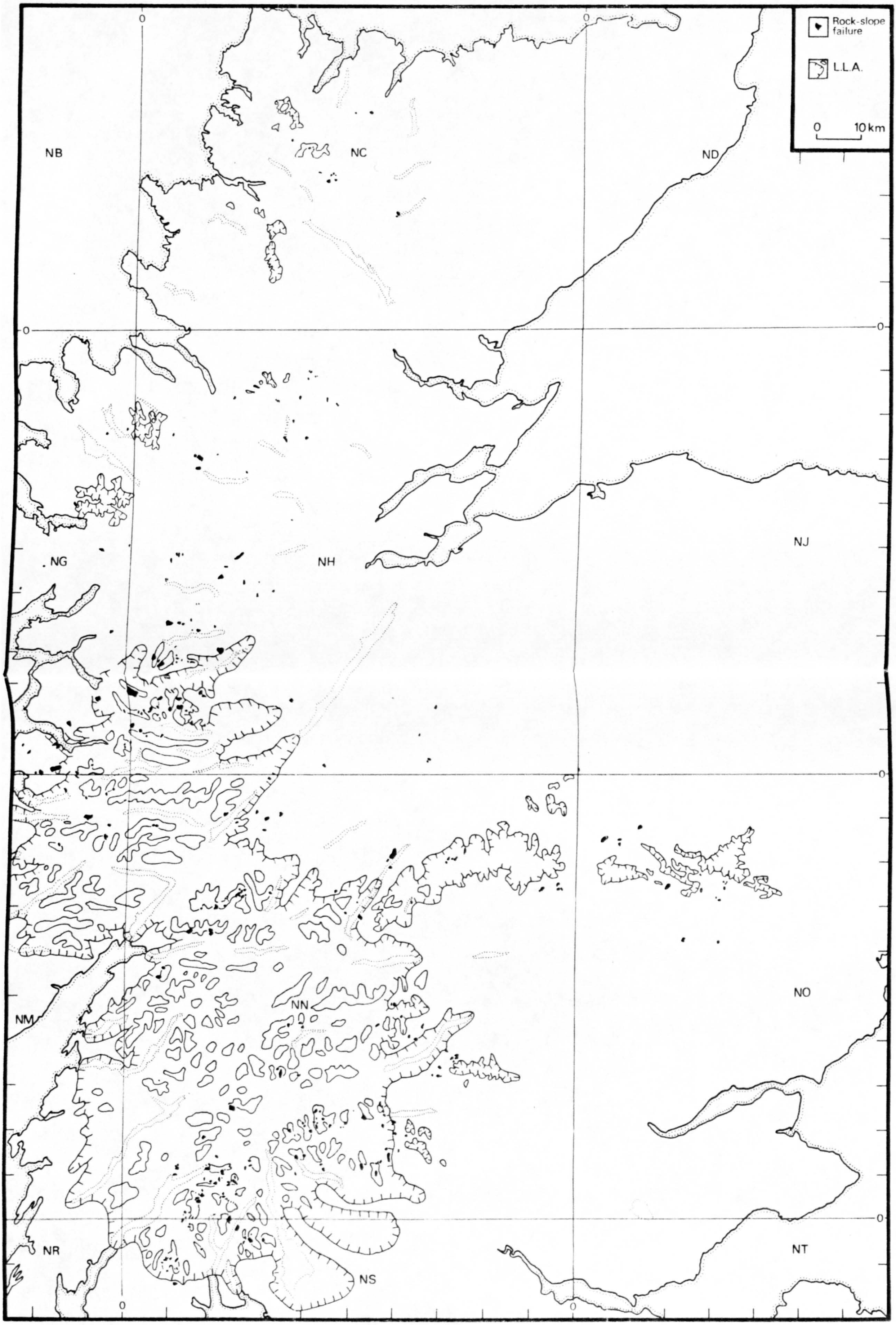

Figure 4.1: Rock-slope failure distribution and Loch Lomond Advance limits